N-Cadherin Juxtacrine Signaling Regulates the Endothelial Barrier

BY

Kevin Kruse

B.S. Illinois Institute of Technology, 2010

THESIS

Submitted as partial fulfillment of the requirements
for the degree of Doctor of Philosophy in Pharmacology
in the Graduate College of the
University of Illinois at Chicago, 2018

Chicago, Illinois

Defense Committee:

Dr. Yulia Komarova, Chair and Advisor

Dr. Dolly Mehta

Dr. Irena Levitan

Dr. Jae-Won Shin

Dr. Leon Tai, Anatomy and Cell Biology

This thesis is dedicated to my family and loved ones.

ACKNOWLEDGEMENTS

There are many people who have helped me throughout my graduate career, and this thesis would not be possible without them. I would first like to thank my advisor, Dr. Yulia Komarova, for her endless support throughout my training. She has spent countless hours helping me perform experiments and interpret data, offering advice, editing and proofreading, and writing letters of recommendation for me. She has always believed in me and encouraged me, defended and supported me, pushed me harder than I thought I could go, and helped me achieve more than I ever thought I could, and for that I am truly grateful. I would also like to thank my committee members, Dr. Dolly Mehta and Dr. Irena Levitan, for their continued support throughout the years, as well as my additional thesis committee members, Dr. Jae-Won Shin and Dr. Leon Tai, for their assistance in helping me complete my thesis, as well as their assistance with experiments and advice. I would additionally like to thank Dr. Asrar Malik and Dr. Deborah Leckband, who have provided additional training, mentoring and advice, and countless letters of recommendation, and have been great sources of support throughout my graduate career.

I am also deeply indebted to all the Komarova and Malik lab members, both past and present, who have helped me finish my graduate studies. I would specifically like to thank Dr. Nathan Sieracki, for helping me develop biomimetic surfaces and perform many experiments. Dr. Melissa Geyer, for her advice and training over the years. Dr. Nazila Daneshjou, who helped me with imaging and analysis. Dr. Ying Sun, for all her assistance with mouse work and cell culture. Dr. Fei Huang, for all his help with biochemistry experiments. Ms. Quinn Lee, for her help in tissue staining and image analysis. Dr. Stephen Vogel, for his help with mouse permeability studies. Dr. Jeff Klomp, for his help analyzing the mass spectrometry data. Dr. Barry Kreutz, for his extensive knowledge and advice. Dr. Xiaoyan Yang, for her mastery of Western blotting. Dr.

ACKNOWLEDGEMENTS (continued)

Peter Toth and Dr. Ke Ma from the UIC imaging core, who have helped me perform many experiments and offered lots of imaging advice.

I would also like to thank everyone in the office of the Department of Pharmacology for their assistance in submitting grants, making sure all my paperwork was in order, and going above and beyond to make sure everything ran smoothly. I am also deeply grateful for Mia Johnson and the GEMS program, GEMS directors, and fellow GEMS students throughout my time at UIC. I am grateful for all the assistance that I've received from my friends both in the GEMS program and the Department of Pharmacology, for advice and help with experiments, reagents and tools they have shared, and for their friendship and understanding. They have been there to share in the fun times and help me through difficult times, and I am lucky to have them as friends.

Finally, I would like to thank my friends and family, who have supported me my entire life. I would like to thank my parents, Jonathan and Diana, my sisters, Caitlin, Lia, and Amy, and my brothers, Stephen and Andy, who have always encouraged me and supported me in whatever I do. Thank you for everything.

CONTRIBUTION OF AUTHORS

Chapter 1 is a literature overview which discusses my research in a broad context. Part of the text comes from a review (Komarova, et. al., 2017) in which I was a second author, and part of it is newly written for this thesis. Chapter 2 discusses all the materials and methods used and includes figures from other publications (cited where used). Chapters 3 – 6 contains work from a manuscript under review of which I was the first author, along with several unpublished experiments. I generated all of the figures, and specific contributions by others to the experiments are noted in each figure legend. I wrote the manuscript along with assistance from my advisor, Yulia Komarova. Chapter 7 is a summary of my conclusions from this work and discusses the implications of the research in a broader context. Chapter 8 contains future directions for this work that may be investigated further in the lab.

TABLE OF CONTENTS

TABLE OF CONTENTS (continued)

TABLE OF CONTENTS (continued)

TABLE OF CONTENTS (continued)

TABLE OF CONTENTS (continued)

LIST OF FIGURES

LIST OF FIGURES (continued)

LIST OF FIGURES (continued)

LIST OF ABBREVIATIONS

AJ
: adherens junction

ARDS
: acute respiratory distress syndrome

BBB
: blood brain barrier

DEP1
: density-enhanced phosphatase-1

ECM
: extracellular matrix

FN
: Fibronectin

GAP
: GTPase-activating protein

GDI
: guanine nucleotide dissociation inhibitors

GDP
: guanosine diphosphate

GEF
: Guanine nucleotide exchange factor

GJ
: gap junction

GPCR
: G protein-coupled receptors

GTP
: guanosine triphosphate

iBRB
: inner blood retinal barrier

JAM
: junctional adhesion molecules

MLC
: myosin light chain

MLCK
: myosin light-chain kinase

MLCP
: myosin light-chain phosphatase

PAK
: p21-activated kinase

PECAM-1
: platelet endothelial cell adhesion molecule 1

PKA
: protein kinase A

PKC
: protein kinase C

LIST OF ABBREVIATIONS (continued)

ROCK
: Rho-associated coiled-coil forming protein kinase

TIRF
: Total Internal Reflection Fluorescence

TJ
: tight junction

TNF
: tumor necrosis factor

VE
: vascular endothelial

VEGF
: vascular endothelial growth factor

VEGFR
: vascular endothelial growth factor receptor

WASP
: Wiskott-Aldrich syndrome protein

WAVE
: WASP-family verprolin-homologous protein

ZO
: zonula occludens

SUMMARY

Vascular Endothelial (VE)-cadherin and Neural (N)-Cadherin are the two major cadherins expressed by endothelial cells. Cadherins are calcium dependent transmembrane molecules that regulate cell-cell adhesions between neighboring cells. VE-cadherin is located between endothelial cells at sites called adherens junctions (AJs), where it acts as the major regulator of the endothelial barrier to control permeability between the blood and the surrounding tissue. N-cadherin is mainly found at the junctions between endothelial cells and mural cells, the layer of cells surrounding endothelial cells in blood vessels (such as smooth muscle cells and pericytes). While the role of VE-cadherin in regulating the endothelial barrier is well understood, the specific contribution of N-cadherin remains mainly unknown.

Pericytes have been shown to be critical in the maintenance of the endothelial barrier, particularly in tissues highly enriched with pericytes, such as the brain. However the specific function of N-cadherin cell-cell signaling between pericytes and endothelial cells remains controversial. Earlier work showed that endothelial specific deletion of the *Cdh2* gene (N-cadherin) results in embryonic lethality at E9.5, showing a very similar phenotype to the *Cdh5* (VE-cadherin) knockout mouse, namely the lack of vasculature formation. It was also thought that N-cadherin regulated VE-cadherin expression, as deletion or knockdown of N-cadherin with siRNA led to a decrease in VE-cadherin levels. More recent work has shown that N-cadherin and VE-cadherin expression levels are either inversely related or not related at all. In this study, I sought to determine if N-cadherin juxtacrine signaling between pericytes and endothelial cells plays a role in regulating the endothelial barrier, and to determine by what mechanism this may occur.

In the first part of this study, I used an endothelial cell specific, inducible knockout model of N-cadherin in order to study the role of N-cadherin juxtacrine signaling in the adult vasculature. I found that deletion of N-cadherin leads to increased permeability both to albumin as well as multiple sizes of dextran tracers in both the lung and the brain, demonstrating that N-cadherin plays a specific role in the maintenance of the endothelial barrier. Interestingly, I found that deletion of N-cadherin had almost no effect on pericyte coverage or number when permeability was increased, suggesting that this effect was specific to N-cadherin juxtacrine signaling between endothelial cells and pericytes.

In the second part of the study, I examined the role of N-cadherin in regulating VE-cadherin adhesions. I found that deletion of N-cadherin led to a loss of VE-cadherin at adherens junctions, thereby leading to an increase in permeability. Additionally, in order to study N-cadherin signaling *in vitro,* I designed biomimetic surfaces which can mimic the interactions between pericytes and endothelial cells. One of the main reasons N-cadherin function in endothelial cells remains elusive is that in most cell culture models, N-cadherin does not form heterotypic adhesions as it would *in vivo,* and is mainly localized diffusely along the plasma membrane. Using these N-cadherin coated biomimetic surfaces, I found that N-cadherin increases VE-cadherin adhesive area at adherens junctions by increasing the rate of VE-cadherin transport to junctions.

In the third part of the study, I sought to identify what molecular mechanisms downstream of N-cadherin are responsible for the increase in VE-cadherin to the membrane. Using a novel approach to isolate N-cadherin complexes, I found a unique binding partner, the Rho guanine nucleotide exchange factor (GEF) Trio. I found that Trio is the main mechanism by which N-

cadherin regulates VE-cadherin localization, as depletion or inhibition of Trio led to a decrease in VE-cadherin localization specifically on N-cadherin biomimetic surfaces.

In the final part of the study, I show that Trio activates both Rac1 and RhoA downstream of N-cadherin adhesions. Rac1 and RhoA are both important regulators of the actin cytoskeleton and endothelial permeability, as VE-cadherin linkage to actin is critical for its proper localization and function. While Rac1 and RhoA generally have antagonistic roles in regulating endothelial permeability, I describe a novel mechanism by which N-cadherin activates both Rac1 and RhoA simultaneously through Trio to control VE-cadherin localization.

1. LITERATURE REVIEW

1.1 Background on endothelium

1.1.1 Basics of endothelial barrier function

The endothelium is composed of a monolayer of endothelial cells which form the innermost lining of all blood vessels (Komarova et al., 2017). It functions as a semi-permeable barrier between blood and the surrounding tissue, restricting the passage of plasma proteins and cells, and thus maintaining tissue-fluid homeostasis (Figure 1). The endothelium has many other functions, including regulating the transport of nutrients and fluids across the endothelial barrier, and allowing for the transmigration of leukocytes in a finely controlled manner. Inter-endothelial junctions are the main structures which regulate the endothelial barrier (Simionescu et al., 1975). Loss of inter-endothelial junctions as the result of an acute or chronic process leads to a flux of proteinaceous fluids into the interstitium causing tissue edema. This is a common cause of a broad range of pathological conditions in humans including systemic capillary leak syndrome (Xie et al., 2012), angioedema (Bouillet et al., 2011), anaphylaxis (Kaplan, 2002), acute respiratory distress syndrome (Herwig et al., 2013; Lee and Slutsky, 2010), age-related and diabetic-associated eye diseases (Aroca et al., 2004; Cheung et al., 2007; Klaassen et al., 2013), and various disorders of the central nervous system (Morganti-Kossmann et al., 2002; Zlokovic, 2006). Hence, elucidating the signaling mechanisms responsible for control of junction integrity is of fundamental importance to developing novel therapeutic strategies for treating edema.

1.1.2 Junction types: Adherens junctions, Tight junctions, and Gap junctions

Inter-endothelial junctions are composed of protein complexes called adherens junctions (AJs), tight junctions (TJs), and gap junctions (GJs) (Firth et al., 1983; Reese and Karnovsky, 1967) (Figure 2). Both AJs and TJs form pericellular zipper-like structures along endothelial cell borders

This page contains text reprinted with permission from Komarova, et. al. 2017.

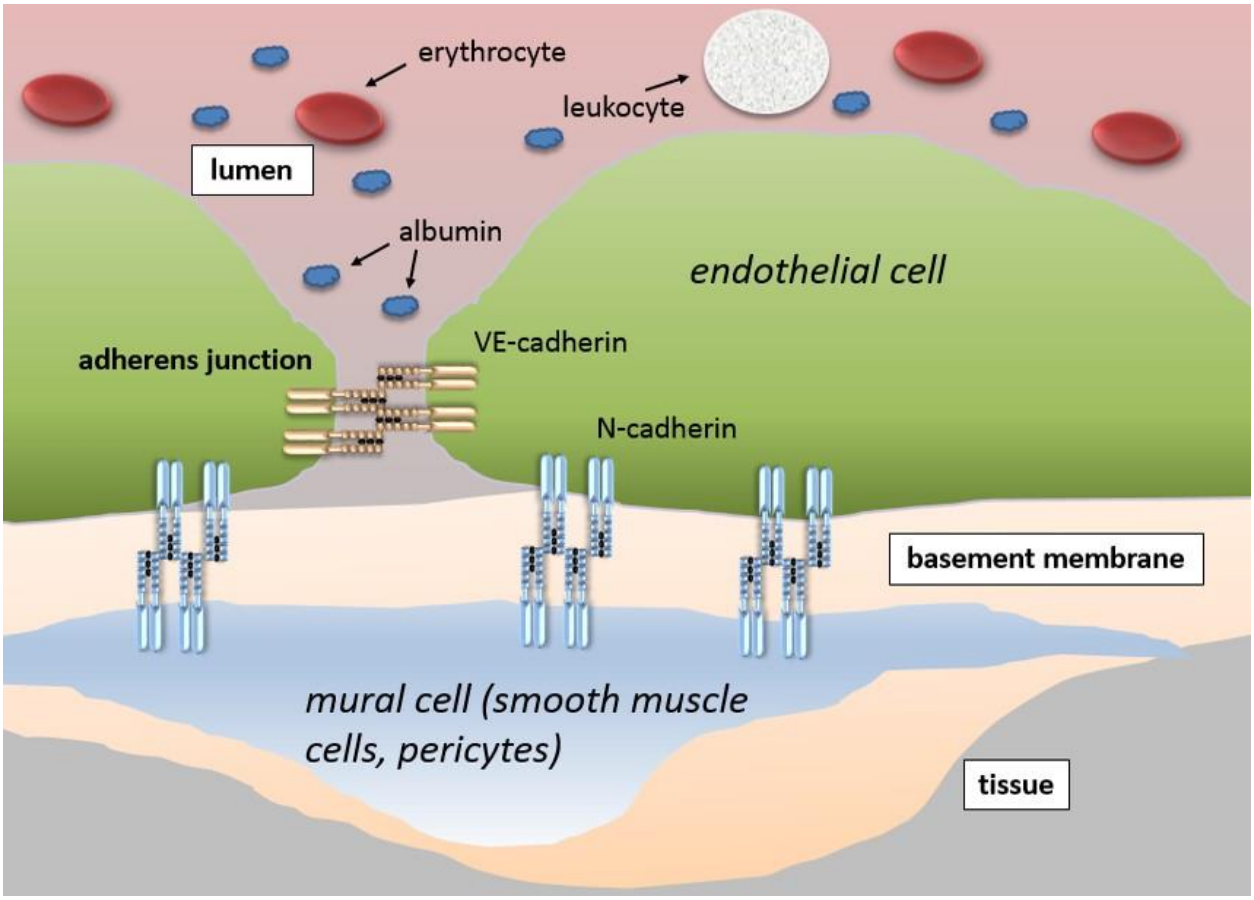

Figure 1. Schematic of the endothelial barrier. VE-cadherin based adherens junctions are formed between endothelial cells to limit vascular permeability. N-cadherin adherens junctions are excluded from inter-endothelial junctions, but instead form interactions with the surrounding mural cells.

This page contains text reprinted with permission from Komarova, et. al. 2017.

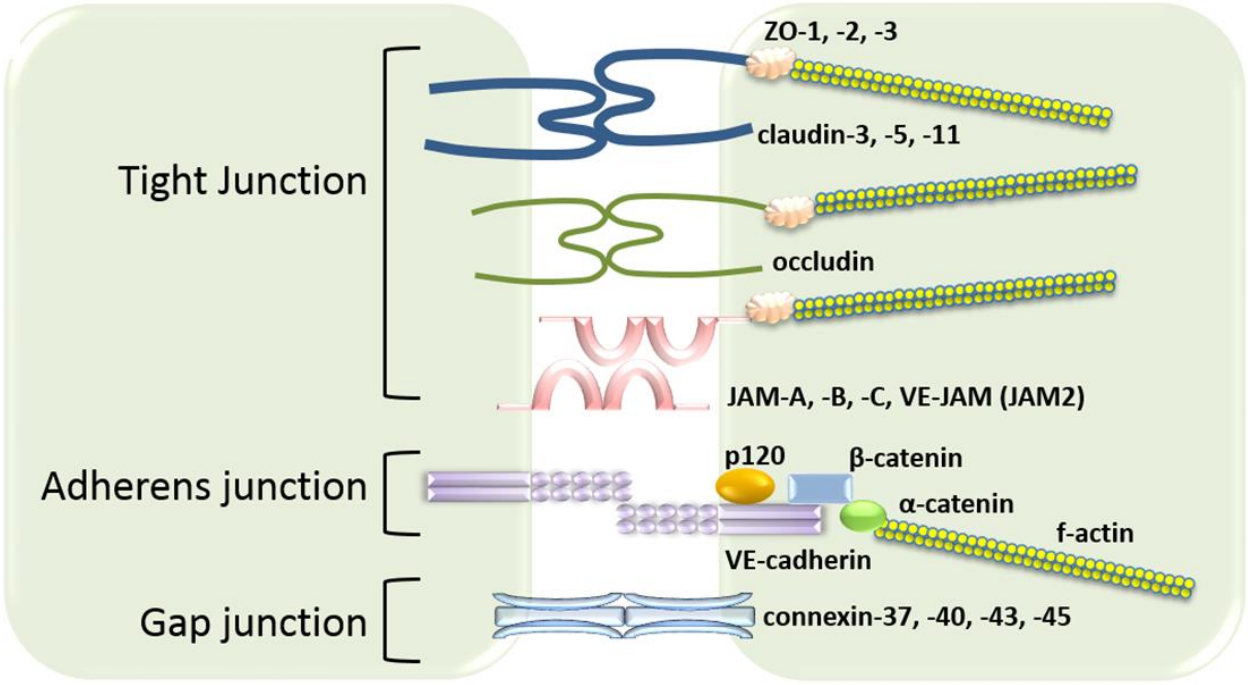

Figure 2: Types of inter-endothelial junctions. Tight junctions and adherens junctions are responsible for endothelial barrier function by preventing the passage of albumin and small molecules. Gap junctions allow for the passage of electrical and chemical messengers directly between endothelial cells. Inter-endothelial adherens junctions are composed of the protein VE-cadherin, which forms cis- (same side of the cell) and trans- (across cell) dimers and are linked to the actin cytoskeleton through β-catenin and α-catenin. Tight junctions limit paracellular permeability and are composed of occludins, claudins, zonula occludens (ZO) proteins, and junctional adhesion molecules (JAMs). Gap junctions are hexameric channels composed of connexins 37, 40, 43, and 45. Reprinted with permission from Komarova, et. al, 2017.

through the linkage of distinct adhesive proteins (Reese and Karnovsky, 1967). In general, AJs restrict permeability by initiating and maintaining cell-cell adhesions, while TJs limit paracellular permeability by regulating the passage of ions and solutes through the paracellular pathway. In contrast, gap junctions are intercellular channels enabling direct electrical and chemical communication between endothelial cells through the passage of ions and signaling molecules with a size of 1kD or less (Qu and Dahl, 2004).

Adherens junctions. AJs are composed of the transmembrane protein Vascular Endothelial (VE)-cadherin and associated α-, β- and p120-catenin adhesion complexes (Lampugnani et al., 1995; Leach et al., 1993) In addition, there is also a variety of other recently described junctional proteins, i.e. vinculin, N-WASP and Arp2/3, which interact with catenins and are involved primarily in stabilizing VE-cadherin-mediated adhesion. Multiple lines of evidence show that VE-cadherin adhesion is the primary adhesion event during vascular development (Breier et al., 1996). VE-cadherin-mediated adhesion promotes activation of forkhead box transcriptional factor FoxO1, which is also required for claudin-5 expression (Giampietro et al., 2012; Taddei et al., 2008). Knockout of β-catenin in endothelial cells leads to disruption of TJs (Tran et al., 2016) indicating the importance of AJs in the assembly and maintenance of TJs. Disassembly of AJs compromised by the integrity of the VE-cadherin adhesion complex is the leading cause of tissue edema associated with a broad range of pathological conditions (Corada et al., 2001; Crosby et al., 2005; Frye et al., 2015; Vittet et al., 1997).

Tight junctions. The architecture and composition of endothelial TJs varies in different vascular beds (Baluk et al., 2007; Simionescu et al., 1975, 1976). For example, TJs are more developed in small arterioles whereas AJs are more predominant in post-capillary venules (Simionescu et al., 1975, 1976). TJs are localized at the outermost part of inter-endothelial

junctions but can also be intermingled with AJs (Liebner et al., 2000b; Liebner et al., 2000c; Lippoldt et al., 2000; Simionescu et al., 1976). In contrast to the peripheral microcirculation, highly specialized vascular beds such as the blood brain barrier (BBB) and the inner blood–retinal barrier (iBRB) where exchange of solutes between microvessel and brain is restricted (Rascher and Wolburg, 1997; Reese and Karnovsky, 1967), TJs are predominant in forming extensive networks at the apical side of inter-endothelial junctions. Disruption of TJs is associated with BBB and iBRB leakage, a characteristic of multiple human diseases including diabetic and oxygen-induced retinopathy (Luo et al., 2011) and disorders of the central nervous system such as stroke (Petito et al., 1982; Yang et al., 2007).

TJs are composed of several adhesive proteins including occludins, claudins, and junctional adhesion molecules (JAMs). Claudin 5 is ubiquitously expressed in all vascular beds whereas claudin 1, 3, and 12 are specific to the brain microvasculature (Liebner et al., 2000a; Nitta et al., 2003). Claudin-1, -2, and -5 are found in TJs of retinal vessels (Luo et al., 2011). Claudins and occludins, in association with cytosolic Zonula occludens (ZO)-1, 2 and 3 proteins assemble "zipper-like" structures along the rim of endothelial cells (Itoh et al., 1999a; Itoh et al., 1999b). JAM-A is a transmembrane protein that is part of the immunoglobulin family and has been shown to be important for leukocyte transmigration (Martin-Padura et al., 1998).

TJs are anchored to the actin cytoskeleton through ZO-1, ZO-2, and ZO-3 (Itoh et al., 1999a; Itoh et al., 1999b). ZO-1 plays a crucial role in the assembly of functional TJs and AJs (Itoh et al., 1999a; Katsuno et al., 2008; Tornavaca et al., 2015). As discussed below, ZO-1 might regulate the cross-interaction between TJs and AJs through control of intracellular tension and assembly of the VE-cadherin mechanosensory complex (Tornavaca et al., 2015). Decreased expression of ZO-1 is associated with severe plasma leakage observed in multiple sclerosis (Kirk

et al., 2003) and diabetic rats (Hawkins et al., 2007a; Hawkins et al., 2007b). ZO-1, -2, and -3 can act as scaffolds for other tight junction proteins and are critical for ZO formation and linkage to the actin cytoskeleton. While knockout of ZO-1 and -2 cause embryonic lethality, ZO-3 does not, suggesting an alternate role for ZO-3 in the regulation of TJs and TJ formation.

Gap junctions. A functional gap junction is composed of two hemichannels aligned in the plasma membrane of adjacent endothelial cells (Hoh et al., 1993). Each hemichannel consists of six connexin molecules, assembled within the ER or *trans*-Golgi (Das Sarma et al., 2001; Smith et al., 2012). The hemichannel can be either homomeric or a heteromeric; i.e., assembled by the same or distinct connexin isoforms, respectively (Barrio et al., 1991). Channels composed of different isoforms might exhibit altered activities in respect to ion selectivity and permeability as compared to homomeric channels (Cottrell and Burt, 2001; Valiunas et al., 2001).

The three major connexin isoforms expressed in systemic arteriolar endothelial cells are Cx37, Cx40, Cx43 (Hakim et al., 2008; Johnson and Nerem, 2007). These gap junctions are responsible for communication between endothelial and endothelial-smooth muscle cells (Dora et al., 2003; Looft-Wilson et al., 2004). In animal models, deletion of Cx43 in endothelial cells causes hypotension (Liao et al., 2001), whereas deletion of Cx40 leads to hypertension associated with dysregulation of the renin system (Krattinger et al., 2007; Wagner et al., 2007). Interestingly, Cx43-mediated gap junctions elicit distinct functions in pulmonary circulation (Parthasarathi et al., 2006). These junctions contribute to conduction of Ca^{2+} between endothelial cells in lung capillaries and induce the expression of P-selectin, the cell surface adhesion molecule involved in the recruitment of leukocytes to sites of injury in post-capillary venules (Parthasarathi et al., 2006). Hence, Cx43-mediated gap junctions are critical for regulation of vascular tone in the systemic

circulation and contribute to the propagation of pro-inflammatory signaling in pulmonary capillary beds.

1.1.3 Regulation of VE-cadherin adhesion

VE-cadherin homophilic dimerization. VE-cadherin is a member of the classical cadherin family that possess a modular structure of five ectodomains, a transmembrane domain, and a cytoplasmic tail (Shapiro et al., 1995). VE-cadherin displays characteristics of both type I and type II cadherins (Brasch et al., 2011). Like type I cadherins, it lacks the hydrophobic non-swapped region that extends the hydrophobicity of the docking surface. Similar to type II cadherins, it contains two conserved tryptophans, Trp2 and Trp4, important for its adhesive property. Anchorage of these tryptophans to a hydrophobic pocket of the partner ectodomain 1 induces "strand-swap" binding mode, resulting in the so-called *trans*-dimerization of VE-cadherin (Harrison et al., 2011; Patel et al., 2006) (Figure 3). *Trans*-interaction reduces the flexibility of the extracellular domain, which enables a secondary adhesion event between ectodomains 1 and 2 of two cadherins on the same side of an endothelial cell (Figure 3). This low-affinity *cis*-interaction is proposed to be responsible for lateral clustering of VE-cadherin, which may increase the strength of adhesive bonds (Harrison et al., 2011; Zhang et al., 2009). Formation of both *trans*- and *cis*-interactions is an intrinsic property of the extracellular moiety of VE-cadherin that does not require the intracellular portion of the protein or assembly of the cadherin-catenin complex (Harrison et al., 2011).

Tethering of VE-cadherin adhesion complex to the actin cytoskeleton. The strength of adhesive bonds, defined specifically as the ability of VE-cadherin adhesion to sustain mechanical stresses from blood flow and pressure, is regulated through attachment of the adhesion complex to the actin cytoskeleton (Nelson and Chen, 2003; Nelson et al., 2004; Shapiro et al., 1995; Wang et al., 2015). The actin cytoskeleton contributes to the strength of AJs by several fundamental mechanisms. It

This page contains text reprinted with permission from Komarova, et. al. 2017.

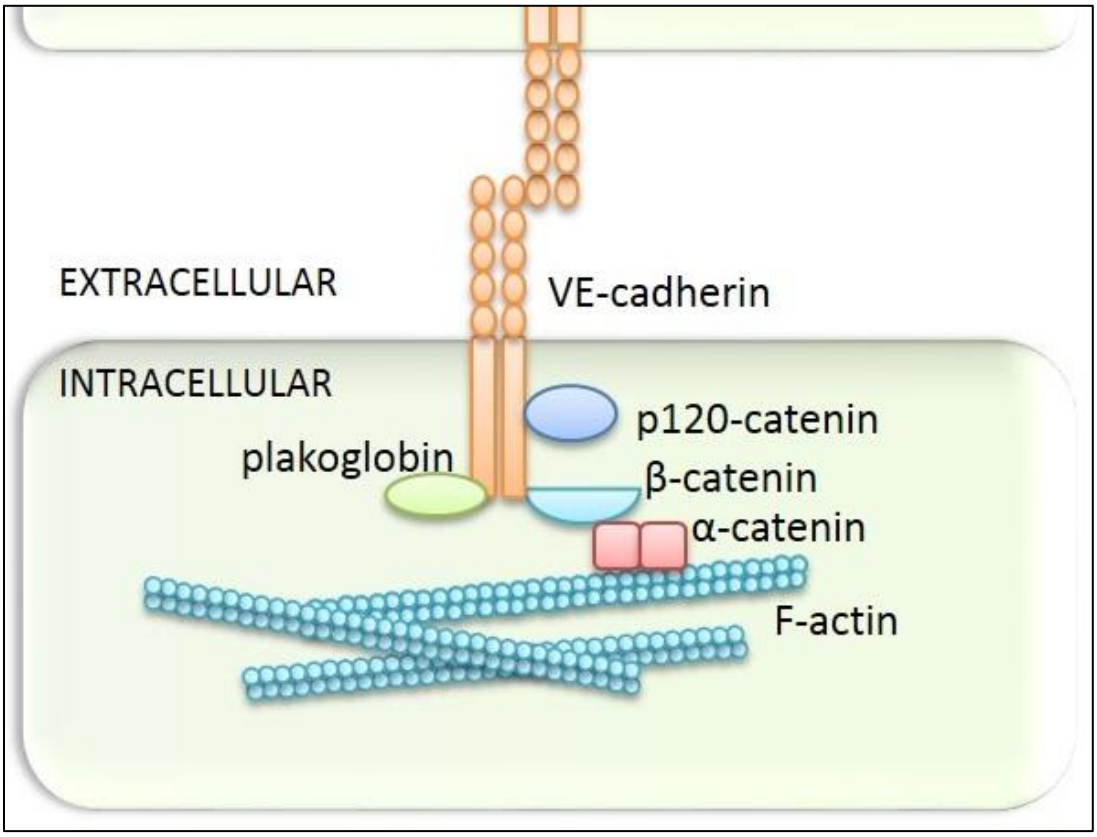

Figure 3. Composition of inter-endothelial adherens junctions. VE-cadherin forms both *trans* (between two cells) and *cis* (on the same side of the cell) interactions to form zipper like adhesions between endothelial cells by binding of the EC1 domain. The intracellular domain of VE-cadherin is linked to the actin cytoskeleton through β-catenin and α-catenin. p120-catenin binds to the juxtamembrane domain, where it blocks a site for adaptor protein 2 (AP2), thereby stabilizing VE-cadherin through preventing its internalization.

generates intracellular tension and clustering of VE-cadherin at AJs (Hong et al., 2013), and facilitates assembly of the VE-cadherin mechanosensory complex (Barry et al., 2015a; Liu et al., 2010; Tornavaca et al., 2015).

α-catenin is the only member of the cadherin-associated catenin proteins that contains an actin-binding domain (Rimm et al., 1995; Wang et al., 2015) enabling the direct association between VE-cadherin adhesion and the actin cytoskeleton (Buckley et al., 2014; Rimm et al., 1995). α-catenin can either tether pre-existing actin filaments to the VE-cadherin complex (Drees et al., 2005), or alternatively, induce *de novo* polymerization of actin filaments at sites of AJs (Drees et al., 2005). The latter mechanism involves recruitment of actin binding proteins such as α-actinin, Epithelial Protein Lost in Neoplasm (EPLIN), and vinculin to VE-cadherin adhesions in the presence of intracellular tension (Drees et al., 2005; Huveneers et al., 2012).

α-catenin and vinculin are allosteric molecules that undergo a rapid and reversible switch between conformational states depending on the applied tension (Craig et al., 1983; Kim et al., 2015; Kolega, 1998; Yao et al., 2014). α-catenin-mediated recruitment of vinculin, along with N-WASP, VASP, and myosin II to AJs enhances the strength of VE-cadherin adhesion by promoting Arp2/3-dependent polymerization of *de novo* actin filaments (Huveneers and de Rooij, 2013; Niederman and Pollard, 1975; Wu et al., 2014). Hence, the strength of VE-cadherin adhesive bonds and therefore integrity of the endothelial barrier is regulated by a complex network involving regulators of actin-polymerization.

Role of intracellular tension in regulating VE-cadherin adhesion. Intracellular tension is a critical component regulating stable anchorage of VE-cadherin to the actin cytoskeleton (Leckband and de Rooij, 2014). Simultaneous binding of α-catenin to both β-catenin and F-actin filament occurs only in the presence of tension (Buckley et al., 2014; Drees et al., 2005; Yamada et al., 2005).

Tension of up to 10 pN induces stable bond formation between the β-catenin/α-catenin complex and F-actin *in vitro* (Buckley et al., 2014). VE-cadherin adhesion at AJs are formed in a tension-dependent manner (Liu et al., 2010) indicating an important role of the acto-myosin apparatus at AJs. Endothelial cell monolayers generate an intercellular tugging force of ~40 nN (Liu et al., 2010) with an average tension on a VE-cadherin molecule from the actin cytoskeleton ranging from 1.8 to 2.4 nN per molecule (Conway et al., 2013). Pro-inflammatory mediators such as α-thrombin increase traction forces and the resultant mechanical stress at AJs (up to ~ 8 nN/μm^2) that uncouples the VE-cadherin complex from the actin cytoskeleton (Liu et al., 2010).

Intracellular tension is generated by the acto-myosin contractile apparatus (Hill, 1968; Liu et al., 2010). The ubiquitously expressed non-muscular actin motor myosin-IIA and B (Kolega, 1998; Simons et al., 1991) are central to control of intracellular tension at endothelial AJs (Liu et al., 2010). Myosin II binds to F-actin filaments and generates tension by sliding these filaments along each other (Craig et al., 1983). The ability of myosin II to assemble antiparallel filaments consisting of 10-30 motors is the main determinant of the magnitude of intracellular tension (Higashi-Fujime, 1982; Niederman and Pollard, 1975).

Phosphorylation of regulatory myosin light chain (MLC) at Thr18 and Ser19 is a prerequisite for motor activity (Craig et al., 1983; Shimokawa et al., 1999). The activity of myosin II in endothelial cells is finely regulated by a variety of intracellular signals (Goeckeler and Wysolmerski, 1995). The canonical pathway involves phosphorylation of MLC by endothelial-specific myosin light-chain kinase (MLCK), which is commonly activated by Ca^{2+}/calmodulin binding (Miller et al., 1983) or Src-dependent phosphorylation at Tyr464 and Tyr471 (Birukov et al., 2001). Myosin light chain phosphatase (MLCP) counteracts MLCK activity by dephosphorylating MLC (Goeckeler and Wysolmerski, 1995). Therefore, a fine balance between

MLCK and MLCP is essential for limiting myosin II phosphorylation and the magnitude of contractile forces at endothelial AJs.

Activity of MLCP (PP1, type 1 protein phosphatase), is downregulated by RhoA signaling (Feng et al., 1999). RhoA activates Rho-associated coiled-coil forming protein kinase (ROCK), which in turn, elicits its effect through phosphorylation of PP1 at Thr-695, Ser-894, and Thr-850 (Feng et al., 1999; van Nieuw Amerongen et al., 2000). The latter inhibits PP1 activity, allowing for myosin II phosphorylation by MLCK and assembly of the acto-myosin apparatus (Feng et al., 1999; van Nieuw Amerongen et al., 2000).

In endothelial monolayers, myosin-II activity is finely tuned at VE-cadherin adhesions by a yet unknown mechanism. A basal level of ROCK activity appears to be essential for the maintenance of endothelial AJs (van Nieuw Amerongen et al., 2007). Recent studies utilizing the RhoA/B/C biosensors show that both RhoA and RhoB are constitutively activated at AJs (Reinhard et al., 2016; Szulcek et al., 2013). It remains unclear, however, how the basal level of Rho activity is maintained at AJs.

VE-cadherin kinetics. The steady-state dynamics of VE-cadherin at AJs is a critical determinant of AJ integrity. This includes several interdependent events concerning both biophysical properties of VE-cadherin adhesive bonds and the integration of intracellular proteins within the VE-cadherin complex. VE-cadherin adhesive bonds undergo continuous assembly, disassembly, and remodeling at AJs; the kinetics of these events are defined by the affinity of *trans*-dimerization (Brasch et al., 2011; Shapiro et al., 1995). This primary adhesion event requires neither energy nor attachment of the VE-cadherin complex to the actin cytoskeleton (Brasch et al., 2011; Shapiro et al., 1995).

In contrast, turnover of VE-cadherin molecules at AJs, specifically the exchange between junctional and intracellular pools, is tightly regulated by the interaction of VE-cadherin with associated catenin proteins and the actin cytoskeleton (Daneshjou et al., 2015; Huveneers et al., 2012; Liu et al., 2010). The steady-state kinetics of VE-cadherin at AJs is controlled through the stability of the cadherin-catenin complex, intracellular tension, and organization of the actin cytoskeleton (Daneshjou et al., 2015; Liu et al., 2010). The disassembly of VE-cadherin adhesion in response to extracellular stimuli is triggered by phosphorylation of VE-cadherin and associated catenins and re-distribution of the actin cytoskeleton to the sites of Focal Adhesions (FAs). Depending on the duration and magnitude of the intracellular response, changes in VE-cadherin dynamics at AJs can lead to weakening or disassembly of AJs, causing either transient or prolonged increases in junctional permeability. For example, tumor vessels represent a case of chronic vascular leakage that is associated with downregulation of VE-cadherin expression (Hashizume et al., 2000).

Multiple lines of evidence suggest that the hyper-permeability response to pro-inflammatory mediators can be mitigated if the integrity of VE-cadherin internalization is preserved. Various strategies have been developed to stabilize VE-cadherin adhesion. They include overexpression of p120-catenin, which blocks clathrin-mediated VE-cadherin internalization (Alcaide et al., 2012; Xiao et al., 2005); expression of a VE-cadherin-α-catenin chimera (Coon et al., 2015), which directly tethers adhesion to the actin cytoskeleton; and artificial bridging of opposing VE-cadherin molecules at AJs with a cyclic peptide (Heupel et al., 2009). This evidence suggests that it is possible to manipulate the integrity of VE-cadherin adhesion, the main gatekeeper of the endothelial barrier.

This page contains text reprinted with permission from Komarova, et. al. 2017.

1.2 Role of N-cadherin in the endothelium

1.2.1 Overview of N-cadherin

Another major cadherin present in endothelial cells, Neural (N)-cadherin (Liaw et al., 1990; Salomon et al., 1992) has been shown to mediate the interaction between endothelial cells and the surrounding mural cells (smooth muscle cells and pericytes), and is critical for endothelial vessel maturation and stabilization (Gerhardt et al., 2000; Tillet et al., 2005). Deletion of the N-cadherin gene *Cdh2* in endothelial cells causes embryonic lethality due to severe vascular defects at E9.5 (Luo and Radice, 2005). Additionally, N-cadherin has been shown to be important for regulating the endothelial barrier *in vitro* through the interaction with pericytes (Alimperti et al., 2017). However, the role of N-cadherin in regulating the endothelial barrier *in vivo* and the molecular signaling mechanisms are not fully understood.

1.2.2 N-cadherin adhesion complex

Similar to VE-cadherin, N-cadherin is composed of five ectodomains, a transmembrane domain, and a cytoplasmic tail which interacts with intracellular binding partners and is linked to the actin cytoskeleton (Figure 4) (Hatta et al., 1985; Shapiro et al., 1995) . N-cadherin is a classical Type I cadherin (like E-cadherin), characterized by the presence of an HAV tripeptide motif in the first extracellular domain (Harrison et al., 2011; Shapiro et al., 1995). While N-cadherin shares an overall 38% sequence homology with VE-cadherin, the intracellular region shares a 47% sequence homology and contains similar binding sites for p120-catenin and β-catenin, and is tightly linked to the actin cytoskeleton (Shapiro et al., 1995). While VE-cadherin is expressed exclusively in endothelial cells, N-cadherin is also widely expressed in fibroblasts, cardiomyocytes, smooth muscle cells, skeletal muscle cells, pericytes, neurons, testis germ cells, and osteoblasts (Hatta et al., 1985).

This page contains text reprinted with permission from Komarova, et. al. 2017.

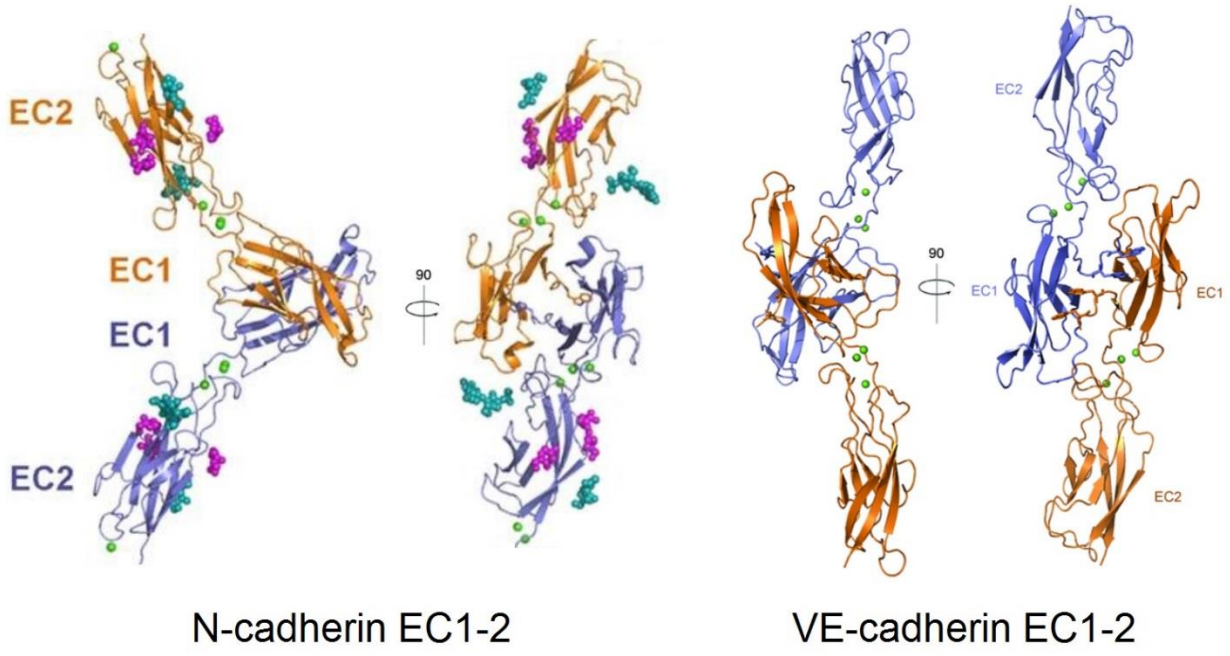

Figure 4. Crystal structure of the extracellular domain 1-2 of N-cadherin and VE-cadherin. Trans adhesions are formed by the interaction of β-strands between cadherins found in the EC1 domain at the N-terminus of the protein. N-cadherin is a Type I classical cadherin, and forms adhesions by insertion of the Trp2 residue into a hydrophobic binding pocket. VE-cadherin is an atypical class II cadherin, lacking the hydrophobic binding region of class II cadherins, but contains an additional tryptophan at Trp4. Reprinted with permission from (Brasch et al., 2011).

This page contains text reprinted with permission from Komarova, et. al. 2017.

1.2.3 N-cadherin localization in the endothelium

Unlike VE-cadherin, N-cadherin is excluded from inter-endothelial cell-cell contacts *in vivo*, where it is instead found at the junctions between endothelial cells and mural cells (Frye et al., 2015; Navarro et al., 1998; Salomon et al., 1992). Here, N-cadherin forms junctions at adhesive sites called myo-endothelial projections, which reach through the basement membrane that surrounds the endothelium and mural cells (Sabatini et al., 2008). Experiments with cultured endothelial cells showed that N-cadherin is excluded from inter-endothelial junctions *in vitro*, however as cells lack the interactions with mural cells, N-cadherin instead is found diffusely distributed along the plasma membrane on the apical side of the cell (Gentil-dit-Maurin et al., 2010; Navarro et al., 1998; Salomon et al., 1992). Knockdown of VE-cadherin using siRNA causes a re-localization of N-cadherin to inter-endothelial junctions suggesting that N-cadherin is capable of forming adhesions, but is excluded specifically by VE-cadherin (Gentil-dit-Maurin et al., 2010; Navarro et al., 1998). Co-transfection of VE-cadherin and N-cadherin in CHO cells (which do not express VE- or N-cadherin) yielded the same distribution as in endothelial cells, where VE-cadherin formed cell-cell adhesions while N-cadherin was localized diffusely on the plasma membrane only in the presence of VE-cadherin (Navarro et al., 1998). Transfection of N-cadherin alone allowed it to localize at cell-cell junctions. This process was found to be dependent on Arg621-Pro702 residues of the VE-cadherin tail cytoplasmic, suggesting that the mechanism is not specific to cell type but is an inherent property of the two cadherins (Navarro et al., 1998). The mechanism for exclusion of N-cadherin from inter-endothelial contacts may be due to the higher binding affinity of VE-cadherin for p120-catenin (Gentil-dit-Maurin et al., 2010). Interestingly, *in vivo*, N-cadherin does not relocate to inter-endothelial junctions after deletion of VE-cadherin

(Frye et al., 2015), suggesting that the regulation of VE-cadherin and N-cadherin may indeed be dependent on the spatial context (e.g. a 2 dimensional monolayer vs a 3 dimensional tissue).

Additionally, it has been suggested that expression levels of VE-cadherin and N-cadherin are inversely related, as they compete for binding to p120-catenin (Gentil-dit-Maurin et al., 2010), which stabilizes cadherins and prevents their internalization and sequential degradation by blocking a β-arresting binding motif. In cells expressing high levels of endogenous N-cadherin, knockdown of N-cadherin led to an increase in VE-cadherin expression (Ferreri et al., 2008). N-cadherin levels have also been shown to decrease *in vitro* as the endothelial monolayer matures (Ferreri et al., 2008), possibly due to the lack of N-cadherin adhesions with other cell types. Conversely, N-cadherin expression can actually be increased when cells are treated with growth factors (Zechariah et al., 2013), which may be related to an angiogenic phenotype, where N-cadherin is needed to recruit pericytes to the newly formed vessel. In ischemic microvessels, Vascular Endothelial Growth Factor (VEGF) signaling increases N-cadherin expression (Zechariah et al., 2013), suggesting that N-cadherin may also be important in vascular repair and remodeling.

1.2.4 Cross-interaction between N-cadherin and VE-cadherin in the endothelium.

Earlier research has indicated that N-cadherin acts upstream of VE-cadherin by controlling both VE-cadherin and p120-catenin protein levels (Ferreri et al., 2008; Luo and Radice, 2005). Endothelial cell specific knockout of *Cdh2* (N-cadherin) led to severe vascular defects and embryonic lethality at E9.5 (Luo and Radice, 2005), displaying a very similar phenotype to the *Cdh5* (VE-cadherin) knockout (Carmeliet et al., 1999) accompanied by a decrease in VE-cadherin levels. Intriguingly, this occurs before investment of pericytes into the endothelium, suggesting a distinct role for N-cadherin besides the formation of endothelial-mural cell interactions. Similarly,

the loss of VE-cadherin after depletion of N-cadherin using siRNA was observed in cell culture studies (Luo and Radice, 2005). However, more recent research has shown that VE-cadherin levels either do not change or even slightly increase when N-cadherin is depleted (Gentil-dit-Maurin et al., 2010; Giampietro et al., 2012). One of the main reasons for this controversy may be related to the fact that N-cadherin does not form cell-cell adhesions *in vitro* (Salomon et al., 1992), thereby leading to its mis-localization and inactivation of downstream signaling pathways.

1.2.5 N-cadherin signaling pathways

N-cadherin and VE-cadherin have some overlapping functions; they bind to β-catenin, α-catenin, and p120 catenin, which are critical for linking cadherin to the actin cytoskeleton as well as preventing cadherin internalization by masking a β-arrestin binding motif. Both N-cadherin and VE-cadherin adhesions activate the (PI3K)-AKT-Forkhead-box protein-O1 (FoxO1) pathway and decrease the transcriptional activity of β-catenin (Giampietro et al., 2012), resulting in inhibition of proliferative and apoptotic pathways. A distinct function of N-cadherin is related to the activation of non-canonical fibroblast growth factor (FGF) signaling and associated endothelial cell motility during angiogenesis, whereas VE-cadherin inhibits this pathway through interaction with the FGF receptor (FGFR) and Density enhanced phosphatase 1 (Dep1) (Giampietro et al., 2012).

N-cadherin may also affect integrin signaling through a cross talk mechanism. For instance, blocking N-cadherin adhesions can modulate integrin signaling by translocation of the non-receptor tyrosine kinase Fer to FAs (Arregui et al., 2000). Additionally, N-cadherin can locally inhibit integrin activity near cell-cell junctions by binding to p120-catenin (Ouyang et al., 2013), leading to inactivation of PI3K and Rac1. This may be due to the inability of the N-cadherin/p120-catenin complex to recruit Rap1, which can activate integrins (Ouyang et al., 2013).

This page contains text reprinted with permission from Komarova, et. al. 2017.

1.3 N-cadherin interaction with pericytes

One of the main functions of N-cadherin is its role in forming heterotypic contacts between endothelial cells and pericytes (Frye et al., 2015; Navarro et al., 1998; Salomon et al., 1992). Pericytes are a specific type of mural cell that wrap around endothelial cells and are encapsulated within the basement membrane (Crocker et al., 1970; Derom et al., 1958), where they form direct contacts with endothelial cells through myoendothelial projections (MEPs) (Moore and Ruska, 1957; Sandow and Hill, 2000). These MEPs cover approximately 30% of the endothelial cell surface area (Armulik et al., 2005). Pericytes act as critical regulators of the endothelium through a variety of different pathways, and pericyte area coverage correlates directly with the relative permeability of the organ (e.g. brain > lung > kidney) (Armulik et al., 2005). Loss of pericytes leads to increased permeability (Alimperti et al., 2017; Armulik et al., 2010; Daneman et al., 2010), but the mechanism is still not well understood. This process could be dependent on N-cadherin juxtacrine signaling as well as through paracrine signaling. Factors secreted by pericytes (for example, Transforming Growth Factor-β) can modify the endothelial barrier directly or through regulating endothelial specific genes (Itoh et al., 2012; Li et al., 2011).

1.3.1 Pericyte recruitment during development

During angiogenesis and vessel formation, pericytes are recruited to stabilize the newly forming vessels (Gerhardt et al., 2000; Tillet et al., 2005). Interestingly, N-cadherin expression is upregulated at the onset of angiogenesis in the developing chick eye and brain (Gerhardt et al., 2000; Hatta and Takeichi, 1986), but expression decreases as the barrier stabilizes, suggesting N-cadherin might be expressed transiently in certain organs. While N-cadherin is not required for angiogenesis, endothelial cell proliferation, or migration, it is required for pericyte coverage of endothelial cell vessel outgrowths (Tillet et al., 2005). Additionally, secretion of platelet derived

growth factor B (PDGFB) by endothelial cells is another critical mediator of pericyte recruitment through binding to the pericyte receptor PDGFR β, and is required for pericyte investment to the endothelium (Lindahl et al., 1997; Wilkinson-Berka et al., 2004). Mice lacking either ligand PDGFB or the receptor PDGFR β show severe cardiovascular disorders due to the lack of pericyte attachment (Armulik et al., 2010; Hall et al., 2016).

1.3.2 Vascular stability

In addition to the recruitment of pericytes during vessel formation, pericytes are critically important for vessel maturation and vascular stability (Gerhardt et al., 1999). Pericytes communicate with endothelial cells both directly through N-cadherin, but also through the secretion of several bioactive factors. Pericytes secrete sphingosine 1 phosphate (S1P), which increases N-cadherin trafficking to the membrane as well as N-cadherin stability by assembling the N-cadherin/catenin/actin complex, and is dependent on activation of the S1P/G_i/Rac1 pathway in endothelial cells (Itoh et al., 2012; Paik et al., 2004). Transforming growth factor-β (TGF-β) is another critical signaling factor involved in vessel maturation (Rivera and Brekken, 2011; Rustenhoven et al., 2016; Sieczkiewicz and Herman, 2003). Pericytes secrete TGF-β, which activates Smad2/3 signaling in endothelial cells, leading to an increase in N-cadherin, VE-cadherin, and S1PR1 expression (Itoh et al., 2012). A similar pathway relies on the activation of Smad4/Notch signaling, which also regulates N-cadherin expression through binding the RBP-J site on the N-cadherin promoter (Li et al., 2011; Winkler et al., 2011). While N-cadherin expression is believed to be critical for the maintenance of pericyte adhesions (Gerhardt et al., 1999; Gerhardt et al., 2000), most studies focus only on N-cadherin levels in endothelial cells, and not the downstream signaling pathways.

1.3.3 Blood brain barrier and inner blood retinal barrier

The BBB and iBRB are two of the tightest endothelial barriers and have the lowest permeability to plasma proteins compared to other organs. This is in part due to the increased number of inter-endothelial tight junctions. Using a PDFGR retention knockout motif mouse model, where pericytes are still present but do not interact with endothelial cells, it was shown that the BBB is specifically maintained through pericyte regulation of BBB-specific protein expression in endothelial cells (Armulik et al., 2010). Lack of pericyte interaction did not affect VE-cadherin levels; however led to altered junction morphology, increased permeability to water, albumin, and small molecular tracers due to increased transcytosis, and a decrease in CD71 (Armulik et al., 2010).

A co-culture of retinal endothelial cells and pericytes demonstrated that pericytes strengthen the iBRB by secreting S1P (McGuire et al., 2011), leading to increased levels of N-cadherin and VE-cadherin and decreased levels of Ang2. N-cadherin was also shown to be essential for the structure of the corneal endothelium, as deletion of N-cadherin in retinal endothelial cells (using floxed N-cadherin and Cre-recombinase expressed under the retinal P0 promoter) leads to increased permeability and edema in the mature eye (Vassilev et al., 2012). While it is clear that pericytes are critical mediators of proper vascular formation and endothelial permeability, the specific signaling events downstream of N-cadherin adhesion in endothelial cells remains unknown. N-cadherin is mainly thought to have a passive role in maintaining the adhesions between endothelial cells and pericytes, but its specific role in endothelial permeability warrants further investigation.

1.4 Other cadherins in the endothelium

T-cadherin (cadherin 13) is also highly expressed in the vasculature (Ivanov et al., 2001). Unlike most cadherins, T-cadherin lacks a transmembrane as well as cytoplasmic region, and is

not involved in cell-cell adhesion or anchorage to the actin cytoskeleton (Dames et al., 2008). T-cadherin is anchored to lipid raft regions via a glycosylphosphatidylinositol anchor, where it acts as a signaling molecule (Ivanov et al., 2004). T-cadherin has been suggested to act as a receptor for LDL, and may play a role in angiogenesis by a yet undefined mechanism (Philippova et al., 2006). Furthermore, T-cadherin enhances endothelial barrier function in monolayers, but appears to negatively regulate the barrier when challenged with thrombin (Andreeva et al., 2010).

Retinal (R)-cadherin is critical for retinal vascular formation, and relies on a similar network pattering as found in neurons (Dorrell et al., 2002). It has also been reported that R-cadherin forms functional, heterotypic interactions with N-cadherin, suggesting a possible role for R-cadherin in endothelial-mural cell interactions (Shan et al., 2000).

VE-cadherin 2 (protocadherin 12, PCDH12) is also localized to endothelial cell-cell junctions, and while sharing a common extracellular cadherin sequence it has a cytosolic region with unknown homology to typical cadherins (Rampon et al., 2005; Telo et al., 1998). VE-cadherin 2 does not bind catenins and is only weakly associated with the cytoskeleton. VE-cadherin 2 does not seem to affect endothelial permeability, and seems to be only involved in cell-cell adhesion (Telo et al., 1998). Transgenic mice deficient in VE-cadherin 2 had no gross morphological defects (Rampon et al., 2005). However recent studies showed that arteries lacking VE-cadherin 2 had increased inner-diameter and circumferential mid-wall stress indicating it is required for both the structure and function of arteries (Philibert et al., 2012).

1.5 N-cadherin and RhoGTPases

Small RhoGTPases at the level of AJs are key molecular switches that play a fundamental role in regulating the plasticity of VE-cadherin adhesion, and hence endothelial permeability (Braga et al., 1997; Daneshjou et al., 2015; van Nieuw Amerongen et al., 2000; Wojciak-Stothard

et al., 2001). They are essential for signaling endothelial responses to both humoral and mechanical stimuli. They are therefore potential drug targets in a variety of inflammatory disorders. The endothelium expresses numerous upstream regulators of RhoGTPases such as guanine nucleotide exchange factors (GEFs), GTPase activating proteins (GAPs), and guanine nucleotide dissociation inhibitors (GDIs) that regulate GTPase activation in space and time.

1.5.1 Function of RhoGTPases

The subfamily of Rho (Ras homologous) GTPases belongs to the Ras-sarcoma (Ras)-related superfamily of low molecular weight monomeric G proteins with highly conserved sequence homology (Andersen et al., 1981; Hillig et al., 2000). RhoA, Rac1, and Cdc42 are the best-studied members of the RhoGTPases sub-family due to their critical role in organization of the actin cytoskeleton as well as profoundly affecting the integrity of AJs (Braga et al., 1997; Timpson et al., 2001; Wojciak-Stothard et al., 1998) .

A fine balance among RhoA, Rac1, and Cdc42 at AJs is regulated by VE-cadherin "outside-in" signaling (Kolega, 1998; Yamada and Nelson, 2007). Formation of nascent VE-cadherin adhesions activates Rac1 (Lampugnani et al., 2002). Rac1, in turn, induces polymerization of actin filaments specifically at sites of VE-cadherin adhesion and contributes to the stabilization of AJs (Lampugnani et al., 2002). Rac1 also stabilizes VE-cadherin *trans*-interaction by counteracting RhoA activity and suppressing acto-myosin tension (Daneshjou et al., 2015). Hence, a subtle balance between RhoA and Rac1 activities is a critical control point of VE-cadherin turnover at AJs (Daneshjou et al., 2015).

RhoGTPases are also involved in destabilization and reannealing of AJs in response to mechanical and humoral stimuli. The net effect of RhoGTPases on barrier integrity depends on the nature of the extracellular stimuli and activation of convergent signaling pathways that are able

to re-wire RhoGTPase signaling to specific intracellular locations and establish their interactions with particular downstream effectors. The complexity of these biological outcomes can be explained by the combinatorial effects of activation of multiple RhoGTPases.

1.5.2 Regulation of RhoGTPases

Monomeric RhoGTPases cycle between active (GTP-bound) and inactive (GDP-bound) states and thus act as binary molecular switches (Vetter and Wittinghofer, 2001). In the GTP-bound state, they interact with the downstream effectors to elicit a physiological response (Alcaide et al., 2012; Ellerbroek et al., 2003; Vetter and Wittinghofer, 2001). RhoGTPases interact with a wide spectrum of downstream effectors that are structurally different from each other (Alcaide et al., 2012; Beckers et al., 2010), and yet the RhoGTPase domain structure itself is highly conserved (Etienne-Manneville and Hall, 2002). All members of the RhoGTPase sub-family contain a G domain structure at the N-terminus, which is composed of 5 sets of G box binding motifs (Etienne-Manneville and Hall, 2002; Vetter and Wittinghofer, 2001). The G domain consists of the nucleotide binding site (also called the p-loop), core effector domain, and switch regions (I and II) forming the interface for interaction with GEFs. The p-loop motif inside the switch I and switch II regions represents the site of GDP to GTP exchange as well as the interface for interaction with downstream effectors upon binding to GTP (Colicelli, 2004). This ability to interact with effectors is lost when the switch region possesses a conformational change due the release of the hydrolyzed phosphate (Vetter and Wittinghofer, 2001).

Because of the high binding affinity of GTPases for both GDP and GTP and slow rate of intrinsic GTP hydrolysis, the GTPase cycle is controlled by upstream regulators; specifically GAPs, GEFs, and GDIs. GAPs accelerate the rate of GTP hydrolysis and switch “off” RhoGTPase activity, whereas GEFs promote GDP to GTP exchange, thus turning RhoGTPases “on” (Bishop

and Hall, 2000; Boguski and McCormick, 1993; Zheng, 2001). The latter is a multi-step process involving formation of a ternary complex between the GTPase, GEF, and nucleotide followed by nucleotide release. Rebinding of GTP, predominantly due to higher concentration in the cell, restores GTPase activity (Bishop and Hall, 2000). GEFs promote GTP exchange by increasing the rate of GDP release (Hart et al., 1991; Hart et al., 1994). Another regulator, GDI interacts with the GDP-bound form and prevents GTP exchange (Sasaki et al., 1990; Ueda et al., 1990). GDIs shield the hydrophobic tail by binding to a prenylated COOH-terminus, and hence sequesters GTPase from the membrane compartment (Hoffman et al., 2000; Scheffzek et al., 2000).

1.5.3 RhoGTPases in the endothelium

Rac1 and Cdc42 signaling pathways regulate the stability of VE-cadherin adhesion. The role of Rac1 and Cdc42 on assembly and maturation of VE-cadherin adhesion is predominantly associated with their ability to induce nucleation, polymerization, and organization of the actin cytoskeleton through interactions with actin binding proteins (Alcaide et al., 2012; Beckers et al., 2010; Wirth et al., 2003). Whereas Rac1 promotes polymerization of branched actin networks within lamellipodia protrusions (Heupel et al., 2009; Komarova et al., 2007; Lampugnani et al., 2002; Vandenbroucke St Amant et al., 2012), Cdc42 facilitates polymerization of linear F-actin filaments into filopodia (Even-Faitelson et al., 2005; Naikawadi et al., 2012). Upon activation, Rac1 interacts with several downstream effectors including the WASP-family verprolin-homologous protein (WAVE), IQRas GTPase-activating proteins (IQGAPs), partitioning-defective polarity protein PAR6, and members of p21 Activated Kinase (Pak) family (Alcaide et al., 2012). Among the members of the Pak family, Pak1 facilitates actin polymerization through activation of Lin1, Isl-1, and Mec-3 Kinase (LIMK) (Edwards et al., 1999). The latter

phosphorylates the actin binding protein cofilin at Ser3 and consequently blocks actin monomer de-polymerization(Yang et al., 1998).

The Cdc42 downstream effectors include Wiskott–Aldrich Syndrome protein (WASP), neuronal (N)-WASP, Diaphanous-related formin-1 (mDia1), IQGAPs, PAR6, and MRCK (Alcaide et al., 2012). Cdc42 induces nucleation and polymerization of actin filaments through WASP and mDia pathways (Barry et al., 2015b). It can also bind to the insulin receptor substrate p53 (IRSp53) that coordinates actin nucleation and polymerization through binding to both WASP and mDia at the plasma membrane (Goh et al., 2012; Riveline et al., 2001). The Cdc42-MRCK pathway activates myosin II and strengthens AJs by generating low magnitude intracellular tension (Wilkinson et al., 2005). Hence, in addition to nucleation, polymerization, and stabilization of the actin cytoskeleton at AJs, the Cdc42 signaling pathway is also capable of generating intracellular tension independent of RhoA signaling.

Cdc42 plays a crucial role in the assembly and maintenance of AJs (Broman et al., 2006). Deletion of Cdc42 in endothelial cells results in loss of apical-basal polarity and disrupted AJs (Barry et al., 2015b). Consistent with the proposed role of Cdc42 in activating both actin polymerization and stabilization, these defects are associated with formation of aberrant filopodia as well as impaired assembly of the acto-myosin apparatus (Barry et al., 2015b). The current model suggests a critical role of Cdc42 signaling in the assembly and maturation of AJs via effectors Pak2, Pak4, and N-WASP (Barry et al., 2015b). Cdc42 signaling thus elicits an endothelial barrier protective effect in inflammatory lung injury (Ramchandran et al., 2008) and also promotes re-annealing of the barrier in inflammatory endothelium through N-WASP-mediated actin polymerization (Broman et al., 2006; Rajput et al., 2013). Moreover, Cdc42 can also act as a

competitive inhibitor of Rac1 and thereby counteract the barrier-disruptive effect of p67phox signaling and ROS production (Birukova et al., 2012; Diebold et al., 2004).

In contrast to Cdc42 that promotes AJ assembly, the outcome of Rac1 signaling on endothelial barrier integrity highly depends on intracellular context (Tan et al., 2008). In some cases, in response to shear stress or the bioactive lipid mediator Sphingosine-1-phosphate (S1P), the activation of Rac1 signaling enhanced endothelial barrier function (Gonzalez et al., 2006; Mehta et al., 2005; Swart-Mataraza et al., 2002; Zhao et al., 2009). In other cases, such as stimulation of endothelial cells with TNFα, Platelet-activating factor (PAF), or VEGF, activation of Rac1 caused disruption of the endothelial barrier (Garrett et al., 2007; Knezevic et al., 2009; Naikawadi et al., 2012; Papaharalambus et al., 2005).Recent work utilizing a photo-activatable Rac1 probe sheds light on the biological outcome of Rac1 signaling at AJs independent of convergent signaling events (Daneshjou et al., 2015). Rac1 counterbalanced RhoA activity at mature AJs and promoted stabilization of VE-cadherin trans-interactions (Daneshjou et al., 2015). This mechanism of RhoA inhibition appears to rely on junctional localization and activity of p190RhoGAP (Wildenberg et al., 2006). Recruitment of p190RhoGAP to AJs is mediated through its direct interaction with p120-catenin, whereas p190RhoGAP activity is regulated by binding to Rac1 as well as Src- and FAK-mediated phosphorylation (Zebda et al., 2013). Rac1 signaling through the effector Pak1 also suppresses MLCK-dependent phosphorylation of myosin II (Wirth et al., 2003). Hence, activation of Rac1 at mature AJs is a pivotal mechanism for balancing the opposing RhoA signaling and suppressing intracellular tension at AJs (Daneshjou et al., 2015).

Rac1 signaling may also cause disassembly of VE-cadherin adhesion and disruption of the endothelial barrier (Gavard and Gutkind, 2006). This is evident by the finding that the pro-inflammatory mediator TNFα leads to a transient and robust increase in Rac1 activity

(Papaharalambus et al., 2005) through phosphatidylinositol (3,4,5)-trisphosphate – dependent Rac exchanger 1 (P-Rex1) (Naikawadi et al., 2012). In this case, Rac1 signals through the p67phox effector leading to production of ROS, and subsequent activation of Src and VE-cadherin phosphorylation (Liu et al., 2013). Another pro-inflammatory mediator PAF also induces Rac1 signaling through T-lymphoma invasion and metastasis-inducing protein 1 (Tiam-1) (Knezevic et al., 2009). PAF-induced activation of Rac1 is associated with profound reorganization of the actin cytoskeleton and vascular leakage (Axelrad et al., 2004; Bussolino et al., 1987). Furthermore, VEGF activates Rac1 through Src-dependent phosphorylation of Vav2 and causes Pak-mediated phosphorylation of VE-cadherin at Serine 665 and subsequent VE-cadherin internalization by β-arrestin (Gavard and Gutkind, 2006; van Wetering et al., 2002). In conclusion, it appears that Rac1 signaling can have divergent effects on AJs ranging from stabilization to disassembly of VE-cadherin adhesions. These responses exemplify the central importance of the intracellular environment, localized signaling, and interaction with specific partners in the net biological outcome of Rac1 signaling.

In contrast to Rac1 and Cdc42, which mediate the assembly, stabilization, and maturation of AJs (Andor et al., 2001; Daneshjou et al., 2015; Petrache et al., 2003; Wojciak-Stothard et al., 2001), RhoA signaling mainly contributes to destabilizing AJs and increasing endothelial permeability (Essler et al., 1998; Nimnual et al., 2003; Sander et al., 1999; Wojciak-Stothard et al., 2005). RhoA promotes the formation of actin stress fibers and acto-myosin contraction through activation of downstream effectors such as ROCK and mDia. The re-organization of the actin cytoskeleton via the mDia pathway and concurrent assembly of the contractile apparatus through activation of ROCK signaling leads to the generation of intracellular tension at junctions that disassembles AJs (van Nieuw Amerongen et al., 2007).

The mDia and ROCK pathways demonstrate a cooperative behavior downstream of RhoA activation (Riveline et al., 2001; Watanabe et al., 1999). mDia promotes the assembly of actin stress fibers, which are re-enforced by ROCK-mediated activation of myosin II (Watanabe et al., 1999). ROCKI and ROCKII are differentially regulated in endothelial cells (Beckers et al., 2015; Mong and Wang, 2009). ROCKI is basally active (Mong and Wang, 2009) and contributes to early responses of endothelial cells to pro-inflammatory mediators such as TNFα and Lipopolysaccharide (LPS) (Han et al., 2013; Joshi et al., 2014). In contrast, activation of ROCKII in response to pro-inflammatory stimuli is required for the long-term effects of LPS and TNFα in disrupting endothelial barrier integrity (Bogatcheva et al., 2011; Mong and Wang, 2009). Evidence also indicates that ROCKII maintains baseline junctional tension and primes the endothelium for hyperpermeability responses such as during thrombin challenge, independent from subsequent ROCKI-mediated contractile stress-fiber formation (Beckers et al., 2015). Both ROCKs maintain MLC in a phosphorylated state through interaction with the PI3K/AKT pathway (Wolfrum et al., 2004). ROCKs also block PI3K/AKT signaling, and thus limit the activation of Rac1 at AJs (Cain et al., 2010). Protracted RhoA signaling leads to persistent disruption of AJs and promotes sustained endothelial leakage (Rabiet et al., 1996), which may be important in the initiation and progression of chronic inflammatory diseases.

Spatial control of RhoGTPases at AJs. VE-cadherin adhesion modulates the organization of the actin cytoskeleton at AJs through the recruitment of signaling and scaffolding proteins such as upstream regulators and downstream effectors of RhoGTPases (Birukova et al., 2012; Braga, 2000; Chen et al., 1997). Engagement of VE-cadherin at cell-cell contacts initiates spatial activation of Rac1 and Cdc42 signaling (Birukova et al., 2012; Noren et al., 2001; Ramchandran et al., 2008). Rac1 signaling is induced through the activation of phosphatidylinositol 3-kinases (PI3K) (Kovacs

et al., 2002) as well as recruitment of the RhoGEFs Tiam1, Vav2, and Triple functional domain protein (Trio) to AJs (Lampugnani et al., 2002; Liu et al., 2013). Tiam1 serves as the scaffold for Rac1 at AJs (Gao et al., 2001) whereas Vav2, a common GEF for RhoA, Rac1, and Cdc42 (Abe et al., 2000) promotes Rac1 GTP loading and hence facilitates activation of Rac1 signaling (Fukuyama et al., 2006; Liu et al., 2013). Some evidence suggests that Trio, a GEF for both RhoA and Rac1, is also recruited to nascent VE-cadherin adhesion where it activates Rac1 signaling and promotes the formation of AJs (Timmerman et al., 2015). IQGAP1, which stabilizes both Cdc42 and Rac1 in the GTP-bound state and protracts the activity of these GTPases (Kurella et al., 2009; Swart-Mataraza et al., 2002), is also recruited to AJs through binding to β-catenin (Kuroda et al., 1998; Swart-Mataraza et al., 2002). Recent data suggest that IQGAP1 is responsible for Rac1 activity at the sites of AJs and hence is an important regulator of AJ integrity and vascular leakage in acute lung injury (Bhattacharya et al., 2012; David et al., 2011).

In contrast to Rac1 and Cdc42, RhoA activity is suppressed at endothelial AJs by multiple convergent pathways (Mammoto et al., 2007; Qiao et al., 2003). RhoA activity is finely counterbalanced by Rac1 signaling (Wojciak-Stothard et al., 2005). Rac1-mediated activation of p190RhoGAP, a RhoA specific GAP, as well as phosphorylation of p190RhoGAP by Src and FAK (Holinstat et al., 2006; Roof et al., 1998; Siddiqui et al., 2011) both play a central role in inhibiting RhoA signaling at endothelial AJs. Whether Cdc42 can also counteract RhoA signaling remains unclear. One tenable mechanism involves Cdc42/MRCK-dependent assembly of myosin-IIB filaments, which can then bind to and suppress activities of Dbl family GEFs containing a DH-PH module at AJs (Lee et al., 2010). It is an attractive possibility that the interaction between myosin-IIB and the RhoGEFs expressed in endothelial cells (Trio, GEF-H1, Dbl, LARG, Tiam1 and Vav2) might provide a mechanism for switching small RhoGTPases ‘on’ and ‘off’ at AJs.

1.5.4 The dual role of Trio GEF in regulating endothelial barrier function

The RhoGEF Trio (Triple functional domain protein) is a unique GEF in that it contains two GEF domains: the GEF1 domain, which is responsible for activation of Rac1 and RhoG, and the GEF2 domain, which activates RhoA (Debant et al., 1996). Trio was first identified in a protein trap assay as a binding partner of the LAR transmembrane protein tyrosine phosphatase and was termed Trio due its two GEF domains as well as a protein serine/threonine kinase domain (Debant et al., 1996). Trio is a large protein, approximately 360 kDa, and is composed of 4 N-terminal spectrin-like repeats, followed by the two Dbl homology (DH) domains, each of which is flanked by pleckstrin homology (PH) and Src homology (SH3) domains, an Ig like domain, and the kinase domain at the C-terminus (Debant et al., 1996). Like many RhoGEFs, Trio is involved in the regulation of many cellular signaling pathways, such as cell morphology (Seipel et al., 2001), cell adhesion (Timmerman et al., 2015), neural outgrowths (van Haren et al., 2014), and cell motility (Marcus-Gueret et al., 2012), depending on the specific context and upstream regulatory mechanisms.

Activities of GEF1 and GEF2 domains are generally regulated by different mechanisms. In neural cells, activation of GEF1 towards Rac1 and RhoG requires binding to Neuronal Navigator 1, while the GEF2 domain is thought to be constitutively active (van Haren et al., 2014). Additionally, Trio can itself be regulated by active RhoA; as RhoA binds to the Ig like domain of Trio it causes the re-localization of Trio to punctate structures at the plasma membrane (Medley et al., 2000). This positive feedback regulation of Trio by RhoA reinforces sustained activity of RhoA at specific microdomains at the plasma membrane (Medley et al., 2000). Another important mechanism for the regulation of Trio GEF2 activity is phosphorylation. Like some other GEFs (for example Vav2), Trio phosphorylation can potentially promote GEF activity (DeGeer et al.,

2013; Medley et al., 2003). While Trio contains multiple tyrosine residues, the effect of phosphorylation on Trio activity is not yet well understood. Trio has been shown to interact with FAK (Medley et al., 2003), but it remains unclear if Trio phosphorylation by FAK is required for Trio to activate RhoGTPase signaling. FAK phosphorylates Trio near the ATP binding site of the Trio kinase domain, and can itself be phosphorylated by Trio (Medley et al., 2003). Hence, the biological significance of Trio phosphorylation by FAK and other kinases remains unclear.

Trio has also been shown to be involved in cadherin mediated juxtacrine signaling. For instance, in epithelial cells, Trio can be found at E-cadherin adherens junctions, where it is linked to the actin cytoskeleton through its binding partner Tara (Trio-associated repeat on actin) (Yano et al., 2011). Knockdown of Tara causes a loss of E-cadherin transcription and expression through the activation of Rac1, suggesting that Tara plays an inhibitory role in the regulation of the Trio GEF1 domain (Yano et al., 2011). Additionally, the Trio GEF1 PH domain was also shown to bind to the actin filament cross linking protein filamin, which was shown to be critical for Trio induced actin based ruffling (Bellanger et al., 2000).

In endothelial cells, Trio is involved in the formation of adherens junction through activation of Rac1. Trio was shown to bind nascent VE-cadherin adhesions through the GEF1 domain, where activation of Rac1 converts radial actin stress fibers into cortical actin bundles which stabilize VE-cadherin adhesions (Timmerman et al., 2015). However, Trio dissociates from adherens junctions as they mature, suggesting that activity of Trio is tightly spatio-temporal regulated in endothelial manolayers (Timmerman et al., 2015). Trio GEF1 domain activity is also critical for leukocyte transmigration across the endothelial barrier (van Rijssel et al., 2012). Leukocyte transmigration is a complex process involving reorganization of the cytoskeleton to allow leukocytes to move through the adherens junctions while maintaining the integrity of the

endothelial barrier (Pawlowski et al., 1988). During leukocyte adhesion to the endothelium, Trio is recruited to leukocyte adhesion sites through interaction with ICAM-1 (van Rijssel et al., 2012). In addition, the interaction of Trio with filamin is required for the activation of both Rac1, which induces ICAM clustering, and RhoG, which initiates membrane protrusive activity (Bellanger et al., 2000).

In neural cells, particularly in development, Trio plays a critical role in both axon guidance and neuronal cell migration, both actin-cytoskeleton-dependent processes (DeGeer et al., 2013; Neubrand et al., 2010; Seipel et al., 2001; Vanderzalm et al., 2009). In cranial neural crest (CNC) cells, binding of Trio to Xenopus cadherin-11 (Xcad-11) causes simultaneous activation of both the Rac1 and RhoA pathways, which is required for filopodia and lamellipodia formation and thereby CNC cell motility (Kashef et al., 2009). One of the main ways that Trio can regulated these actin dependent processes is through p21-activated kinase (PAK), a downstream effector of Rac1 and Cdc42 (Moshfegh et al., 2014). For instance, PAK can induce phosphorylation and activation of MLCK, which results in actin-myosin contractility and cytoskeletal rearrangement, which may regulate growth cone formation or attachment to the extracellular matrix during axon formation and migration (Wirth et al., 2003). My data in endothelial cells demonstrate that engagement of Trio into N-cadherin adhesion complexes leads to activation of both RhoA and Rac1 pathways, which maintains the activity of both RhoA GTPases at homeostatic levels.

In myoblasts, M-cadherin is required for the fusion of myoblasts into myotubes, which occurs via an increase in Rac1 GTPase activity at the time of fusion (Charrasse et al., 2007). Knockdown of Trio blocked the increase in Rac1 activity, suggesting that M-cadherin activates Rac1 through binding of Trio (Charrasse et al., 2007). Trio can also induce complex cytoskeletal arrangements by linking the Rac1 and RhoA pathways downstream of its GEF1 and GEF2

domains (Bellanger et al., 2000; Schmidt and Debant, 2014). *In vivo*, Trio was shown to activate the Mitogen Activated Protein Kinase (MAPK) pathway, causing activation of the Jun kinase pathway and ruffling of the membrane through Rac activation, while simultaneously inducing the formation of stress fibers through activation of the RhoA pathway (Bellanger et al., 1998).

1.6 Statement of Aims

Aim 1. To investigate the role of N-cadherin juxtacrine signaling in the regulation of permeability of the endothelial barrier in adulthood *in vivo*. I will further investigate the role of N-cadherin *in vivo* using a genetic model of inducible, endothelial cell specific deletion of N-cadherin to measure the permeability of the endothelial vessel wall to solutes and plasma proteins in various organs of adult mice as well as investigate the role of N-cadherin on pericyte adhesion *in vivo*.

Aim 2. To investigate the role of N-cadherin juxtacrine signaling on strengthening VE-cadherin adhesion at AJs through activation of both Rac1 and RhoA. My preliminary data suggest that both RhoA and Rac1 signaling is required for VE-cadherin accumulation at AJs downstream of N-cadherin adhesion. Therefore Aim 2 will investigate a postulated signaling mechanism of cross-talk between N-cadherin and VE-cadherin adhesion through RhoGTPase signaling pathways. I will investigate the role of Triple functional domain (Trio) in activation of both Rac1 and RhoA downstream of N-cadherin adhesions.

2. MATERIALS AND METHODS

2.1 **Plasmids, and adenoviruses, purified proteins**

For mammalian expression: Adenoviral particles encoding human wild type VE-cadherin tagged to green fluorescent protein (GFP) was a gift from Dr. F. Luscinkas (Brigham and Women's Hospital, Boston, MA). Adenoviral particles encoding human VE-cadherin-Dendra2 (pCDNA3 and CMV promoter) was generated using PCR and subcloning VE-cadherin and Dendra2 (a gift from S. Troyanovsky, Northwestern University, Chicago, IL), into the pCDNA3 vector (Life Technologies) at restriction sites 5′-KpnI and 3′-EcoRI for VE-cadherin and 5′-EcoRI and 3′-XhoI sites for Dendra2 (Daneshjou et al., 2015). Human peGFP[C1] Trio-FL, peGFP[C1] Trio-N, peGFP[C1] Trio-C mammalian expression vectors were gifts from Dr. J. van Buul (Academic Medical Center at the University of Amsterdam, Netherlands). Human Trio GFP-D1d (GEF1 dead mutant) and Trio GFP-D2d (GEF2 dead mutant) were gifts from Dr. A. Debant (University of Montpellier, Montpellier, France). Photo-activatable (PA)-Rac1 (mCerulean tagged), Light Insensitive (LI)-Rac1 (mCerulean tagged), Rac1-FLARE.dc Biosensor WT, RhoA FLARE.sc Biosensor WT were gifts from Dr. K. Hahn (UNC School of Medicine, Chapel Hill, NC). VE-cadherin FRET tension sensor was a gift From Dr. M. Schwartz (Yale School of Medicine, New Haven, CT).

For bacterial expression: Nucleotide free Rac1 carrying G15A mutation for bacterial expression was gift from Dr. T. Kozasa (University of Illinois at Chicago, Chicago, IL). His-tagged extracellular domain of human N-cadherin (Met 1-Ala 724) was purchased form Sino Biological (Beijing, China).

KEY RESOURCES TABLE

REAGENT or RESOURCE	SOURCE	IDENTIFIER
Antibodies		
Goat monoclonal anti-VE-cadherin	Santa Cruz	sc-6458
Rabbit polyclonal anti-VE-cadherin	Cell Signaling Technology	#2158
Rat monoclonal anti-VE-cadherin	BD Biosciences	555289
Rabbit polyclonal anti-N-cadherin	Abcam	ab12221
Mouse monoclonal anti-N-cadherin	ECM Biosciences	CM-1701
Rabbit polyclonal anti-N-cadherin	Abcam	ab76057
Rabbit polyclonal anti-Desmin	Abcam	ab15200
Rat polyclonal anti-CD31	BD Bioscience	#550274
Rat polyclonal anti-CD31	BD Bioscience	#550274
Rabbit polyclonal anti-CD31	Abcam	ab28364
Alexa Fluor 488 Phalloidin	Invitrogen	A12379
Mouse monoclonal anti-β-tubulin	Sigma Aldrich	T8328
Mouse PDGF R beta Antibody	R & D Systems, Inc.	AF1042
Rabbit polyclonal anti Trio antibody	Bethyl Laboratories	A304-269A-T
Rabbit polyclonal anti Trio antibody	Santa Cruz	sc-28564
Rabbit polyclonal Phospho-Myosin Light Chain 2 (Ser 19) antibody	Cell Signaling Technology	#3671
Bacterial and Virus Strains		
VE-cadherin-Dendra2 adenovirus	Daneshjou, et. al. 2015	N/A
MAX Efficiency™ DH5α™ Competent Cells	Thermo Fischer Scientific	18258012
Chemicals, Peptides, and Recombinant Proteins		
Recombinant human N-cadherin-His	Sino Biological	11039-H08H
Recombinant human N-cadherin-Fc-His	Sino Biological	11039-H03H
EDC	Thermo Fischer Scientific	22980
EDTA	Research Products International	E57020

Imidazole	Sigma Aldrich	I5513
N-Hydroxysuccinimide	Sigma Aldrich	130672
Glymo	Sigma Aldrich	440167
AB-NTA (free acid)	Dojindo	A459-10
10 kDa Dextran, Alexa Fluor 555	Sigma	D34679
70 kDa Dextran, Oregon Green 488	Sigma	D7173
NiCl2	Thermo Fischer Scientific	N53-500
DSP (dithiobis(succinimidyl propionate))	Thermo Fischer Scientific	22585
DL-Dithiotreitol	Sigma Aldrich	D0632
4X Laemmli buffer	BioRad	1610747
RIPA	Sigma Aldrich	R0278
ITX3	Millipore	645890
HisPur Ni-NTA Magnetic Beads	Thermo Fischer Scientific	88831
Fibronectin	Sigma Aldrich	F1141
Glass cover slips	Schott Nexterion	1472309
^{125}I radiolabeled human serum albumin, 10 uCi/ml	Anazao Health	I-125 HSA
Vectashield	Vector Laboratories, Inc.	H-1000
Prolong Gold Antifade	Thermo Fischer Scientific	P36930
Fluoromount	Southern Biotech	0100-01
Rho Kinase Inhibitor III, Rockout	Santa Cruz	sc-203237
Dynabeads™ M-450 Epoxy	Thermo Fischer Scientific	14011
Rho Activator I	Cell Signaling	CN01-A
Rho Activator II	Cell Signaling	CN03-A
Albumin from Bovine Serum (BSA), Alexa Fluor™ 647 conjugate	Thermo Fisher	A34785
PAR-1 agonist peptide, TFLLRNPNDK-NH(2)	The Research Resources Center UIC	custom synthesis
Tamoxifen	Sigma Aldrich	T5648

Corn Oil	Sigma Aldrich	C8267
Critical Commercial Assays		
Basic Endothel. Cells Nucleofector® Kit	Lonza	VPI-1001
GeneSilencer Transfection Reagent	Genlantis	T500020
RhoA G17A Agarose Beads	Abcam	Ab211183
Lipofectamine 2000 Transfection Reagent	Thermo Fisher Scientific	11668019
Experimental Models: Cell Lines		
Human Pulmonary Aortic Endothelial cells	Lonza	CC-2530
Human Lung Microvascular Endothelial cells	Lonza	CC-2527
Experimental Models: Organisms/Strains		
N-cadherin-flox/flox	Jackson	B6.129S6(SJL)-Cdh2tm1Glr/J
end-SCL-CreERT^2	Gothert et al., 2004 Blood. 2004 Sep 15;104(6):1769-77.	available from Jackson, Tg(Tal1-cre/ERT)42-056Jrg
N-cadherin-flox/flox- SCL-CreERT2	This paper	N/A
Oligonucleotides		
Cdh2 ON-TARGETplus siRNA Target Sequence: GUGCAACAGUAUACGUUAA	Dharmacon	J-011605-06
Cdh2 ON-TARGETplus siRNA Target Sequence: GGACCCAGAUCGAUAUAUG	Dharmacon	J-011605-07
Cdh2 ON-TARGETplus siRNA Target Sequence: CAUAGUAGCUAAUCUAACU	Dharmacon	J-011605-08
Cdh2 ON-TARGETplus siRNA Target Sequence: GACAGCCUCUUCUCAAUGU	Dharmacon	J-011605-09
TRIO ON-TARGETplus siRNA Target Sequence: GUAAAGAAGUGAAAGAUUC	Dharmacon	J-005047-05
TRIO ON-TARGETplus siRNA Target Sequence: CGACCUAUCCGUAGCAUUA	Dharmacon	J-005047-06
TRIO ON-TARGETplus siRNA Target Sequence: GGAAUACAACCACGAAGAA	Dharmacon	J-005047-07

TRIO ON-TARGETplus siRNA Target Sequence: AGAACAGGGUAUUGCAUUA	Dharmacon	J-005047-08
ON-TARGETplus Non-targeting siRNA	Dharmacon	D-001810-01-05
Recombinant DNA		
mCerulean-PA-Rac1	Daneshjou, et. al. 2015	N/A
mCerulean-LI-Rac1	Daneshjou, et. al. 2015	N/A
peGFP[C1] Trio-FL	van Rijssel, et. al. 2012	N/A
peGFP[C1] Trio-N	van Rijssel, et. al. 2012	N/A
peGFP[C1] Trio-C	van Rijssel, et. al. 2012	N/A
Rac1-FLARE.dc Biosensor WT	MacNevin, et. al. 2016	N/A
RhoA FLARE.sc Biosensor WT	Pertz, et. al. 2006	Addgene Plasmid #12150
pLPCX-VEcadTS (VE-cadherin Tension Sensor (Mus musculus)	Conway, et. al. 2013	Addgene Plasmid # 45848
pLPCX-VEcadTL (VE-cadherin taillessTension Sensor (Mus musculus)	Conway, et. al. 2013	Addgene Plasmid # 45849
pGEX-4T1-Rac1 G15A	Garcia-Mata et. al. 2006	N/A
Trio-D1d	Bellanger, et. al. 1998	N/A
Trio-D2d	Bellanger, et. al. 1998	N/A
Software and Algorithms		
ImageJ (FIJI)	NIH	https://fiji.sc/
Metamorph	Olympus	https://www.olympus-lifescience.com/en/software/metamorph/
Zen	Carl Zeiss	https://www.zeiss.com/microscopy/us/products/microscope-software/zen-lite.html

Prism 7	GraphPad	https://www.graphpad.com/scientific-software/prism/
Photoshop CS6	Adobe	http://www.adobe.com/products/photoshop.html
R	The R Project for Statistical Computing	https://www.r-project.org/

2.1.1 **The use of VE-cadherin-Dendra2 to study VE-cadherin kinetics**

For studying VE-cadherin dynamics, the photo switchable protein Dendra2 was tagged to the C-terminus of human wild type VE-cadherin. Dendra2 is a genetically encodable photo-convertible protein based on the protein Dendra from octocoral *Dendronephthya* sp. by introducing a single amino acid mutation (A224V). Dendra2 emits photons at a peak of λ=488 nm; however irradiation with a 405 nm laser causes an irreversible shift in the peak emission spectra to λ=543 (Figure 5), which allows the rate of VE-cadherin turnover at AJs to be determined.

2.1.2 **The use of GFP-Trio constructs**

Analysis of Trio (Triple functional domain protein) intracellular localization and co-localization with N-cadherin was performed by using green fluorescent protein (GFP) tagged to the N-terminus of human wild type Trio. Three constructs, GFP-Trio-FL (Full Length, amino acids 60 - 3038), GFP-Trio-N (consisting of the N-terminal portion of Trio with spectrin repeats, the GEF1 domain, and an SH3 domain, amino acids 60 - 1685), and GFP-Trio-C (consisting of the C-terminal portion of Trio with the GEF2 domain and an SH3 domain, amino acids 1861 - 3038) were expressed in endothelial cells (Figure 6).

In addition, human Trio-FL, Trio-D1d (GEF1 dead) and Trio-D2d (GEF2 dead) mutants were used for rescue experiments. These Trio constructs were expressed in endothelial cells depleted of

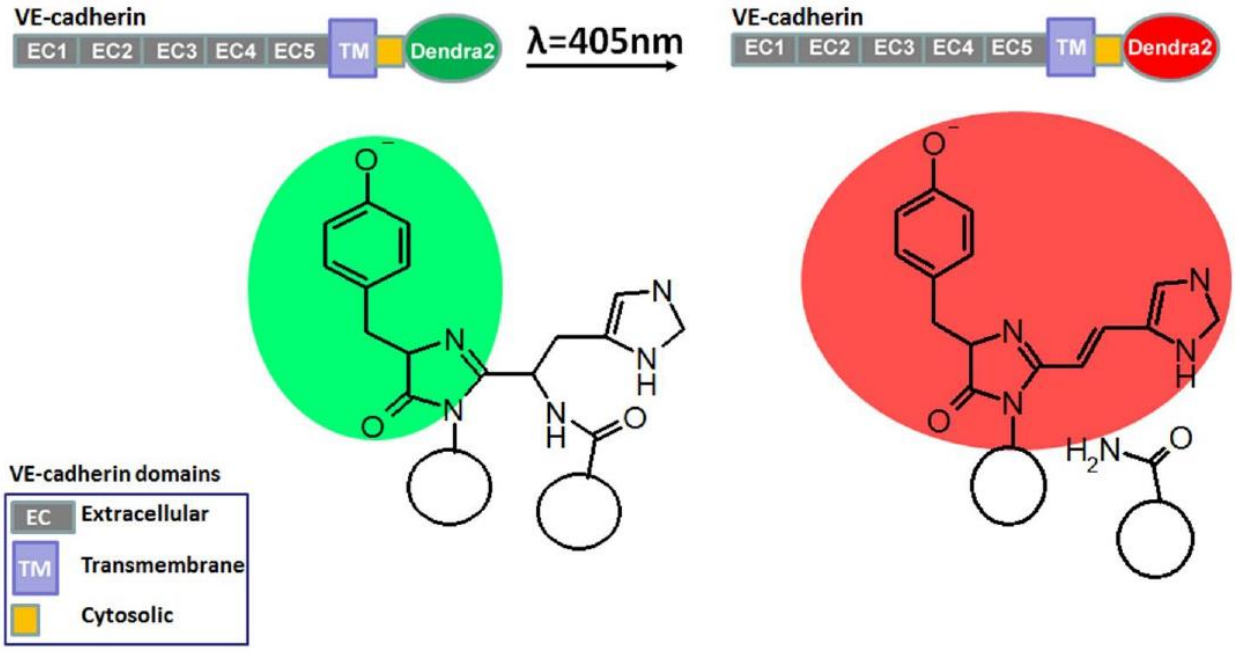

Figure 5. Schematic of VE-cadherin Dendra2. The fluorescent protein Dendra2 is attached to the C-terminus of human VE-cadherin. After irradiation with a 405 nm laser, the protein undergoes an irreversible change in emission from green to red. VE-cadherin association kinetics can be determined from new, unconverted (green) VE-cadherin entering the photo-converted region, while VE-cadherin dissociation kinetics can be determined by tracking the decrease in photo-converted (red) VE-cadherin leaving the region. Reprinted with permission from Daneshjou, PhD thesis, 2014.

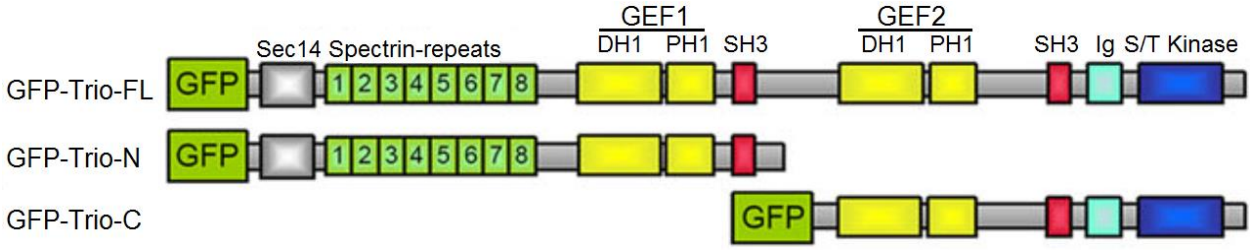

Figure 6. Schematic representation of GFP-Trio constructs. GFP was tagged to the N-terminus of human full length Trio (GFP-Trio-FL, MW 354 kDa) as well as two truncated mutants, GFP-Trio-N (N-terminal portion containing GEF1 domain to activate Rac1/RhoG, MW 221 kDa) and GFP-Trio-C (C-terminal portion containing GEF2 domain to activate RhoA, MW 159 kDa). Reprinted with permission from Timmerman, et. al., 2015.

endogenous Trio and their effects on density and adhesion area for VE-cadherin adhesion were determined as described in 2.6.3.

2.1.3 **The use of photo-activatable Rac1**

Localized activation of Rac1 to rescue VE-cadherin kinetics after knockdown or inhibition of Trio was performed using a genetically encodable photo-activatable Rac1 construct (PA-Rac1) with an mCerulean (CFP) tag. PA-Rac1 contains a photo-sensitive Light Oxygen Voltage (LOV2) domain from *Avena sativa* Phototropin1 with a constitutively active (GTP-bound) $Rac1^{V12}$ mutant. In the dark, the LOV domain is in a closed conformation where Rac1 cannot interact with downstream effectors. Upon local irradiation using a λ=458 nm laser, the LOV domain undergoes a transient conformational change allowing the interaction of GTP-bound Rac1 with its downstream effectors. The half-time of Rac1 activation is about 20 seconds, similar to activation of endogenous Rac1. Therefore, it makes an appropriate tool in studying the effect of Rac1 on VE-cadherin dynamics. As a control, Light Insensitive Rac1 (LI-Rac1, bearing a single point mutation at Cysteine 39 to Alanine [C39A] in the LOV2 domain which prevents conformational change) was used (Figure 7).

2.1.4 **Rac1 FRET biosensor**

To measure Rac1 activity and localization, I used a genetically engineered dual chain Rac1 FRET biosensor (Rac1-FLARE.dc Biosensor WT, Figure 8). This plasmid results in expression of two independent parts of the biosensor. One part contains Rac1 tagged with a yellow fluorescent protein (YFP). The second part is a fragment of Rac1 downstream effector PAK (p21-activated kinase) tagged with a cyan fluorescent protein (CFP) which acts as an affinity reagent and only binds active Rac1. When Rac1 is in the GTP (active) bound form, it binds to the PAK fragment,

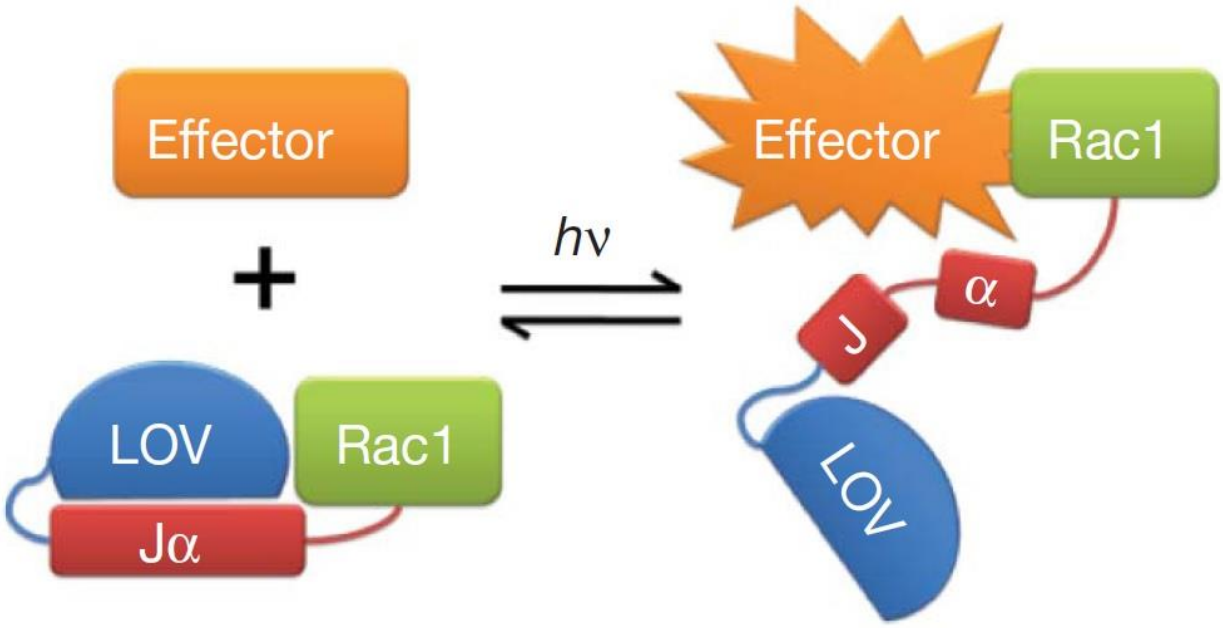

Figure 7. Schematic of photo-activatable Rac1. The LOV2 domain interacts with the carboxy-terminal helical extension (Jα) in the dark, preventing the interaction of Rac1 with downstream effectors. Upon activation with a λ=458 nm laser, the Jα helix unwinds, leading to a conformational change allowing Rac1 to interact with downstream effectors. Reprinted with permission from Wu, et. al., 2009.

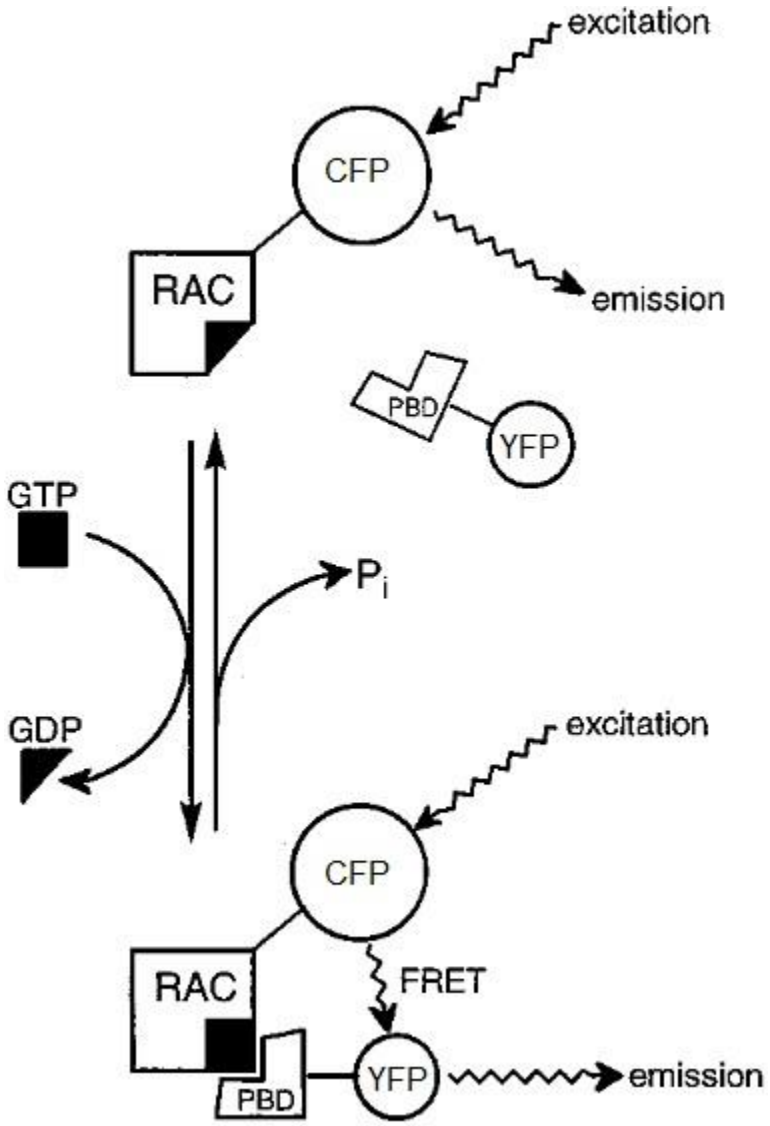

Figure 8. Schematic representation of Rac1 FRET biosensor. A CFP-tagged Rac1 and a YFP-tagged fragment of its downstream effector p21 activated kinase (PAK) binding domain (PBD) are expressed as two engineered proteins. In the GDP bound (inactive) form, Rac1 does not interact with PBD, resulting in no FRET signal between the two fluorophores. In the GTP bound (active) form, Rac1 interacts with PBD, resulting in FRET between the CFP and YFP. Reprinted with permission from Kraynov, et. al., 2000.

bringing the fluorophores close together, resulting in FRET between the CFP and the YFP. By measuring the FRET to CFP ratio, the relative activity of Rac1 was determined.

2.1.5 **RhoA FRET biosensor**

To measure RhoA activity and localization, I used a genetically encodable single chain RhoA FRET biosensor (RhoA FLARE.sc Biosensor WT). This plasmid contains RhoA tagged with a yellow fluorescent protein (YFP) connected to the RBD (Rho Binding Domain) of Rhotekin tagged with a cyan fluorescent protein (CFP) which acts as an affinity reagent and only binds active RhoA. When RhoA is in the GTP (active) bound form, it binds to the RBD, bringing the fluorophores close together, resulting in FRET between the CFP and the YFP. By measuring the FRET to CFP ratio, the relative activity of RhoA was determined (Figure 9).

2.1.6 **VE-cadherin FRET tension sensor**

To measure tension across VE-cadherin adhesions, I used a genetically encodable VE-cadherin FRET tension sensor containing a Venus (YFP) and an mTFP1 (enhanced CFP) inserted between the p120 catenin and β-catenin binding domains of VE-cadherin, separated by an elastic linker protein (Figure 10). When acto-myosin generated tension is high, the fluorophores are pulled apart (due to the linkage of VE-cadherin to the actin cytoskeleton through β-catenin and α-catenin) causing a decrease in FRET efficiency. When acto-myosin generated tension is low, the fluorophores are pulled together due to the elastic linker, resulting in increased FRET efficiency. The relative tension was determined by the FRET to mTFP1 ratio (as tension increases, FRET/mTFP1 decreases).

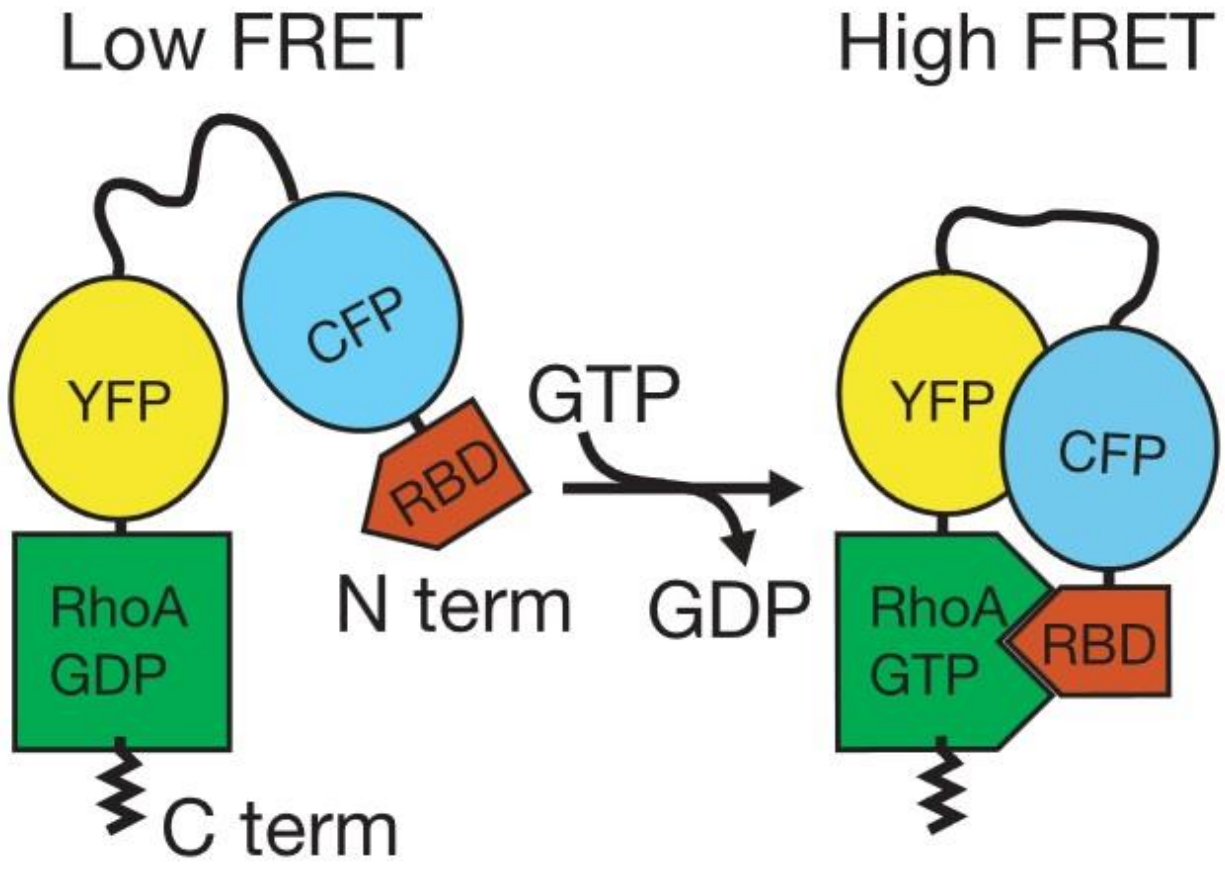

Figure 9. Schematic representation of RhoA FRET biosensor. A CFP-tagged RhoA and a YFP-tagged fragment of the Rho binding domain (RBD) of the RhoA effector Rhotekin are separated by a flexible linker. In the GDP bound (inactive) form, RhoA does not interact with RBD, resulting in low FRET signal between the two fluorophores. In the GTP bound (active) form, RhoA interacts with RBD, resulting in FRET between the CFP and YFP. Reprinted with permission from Pertz, et. al. 2006.

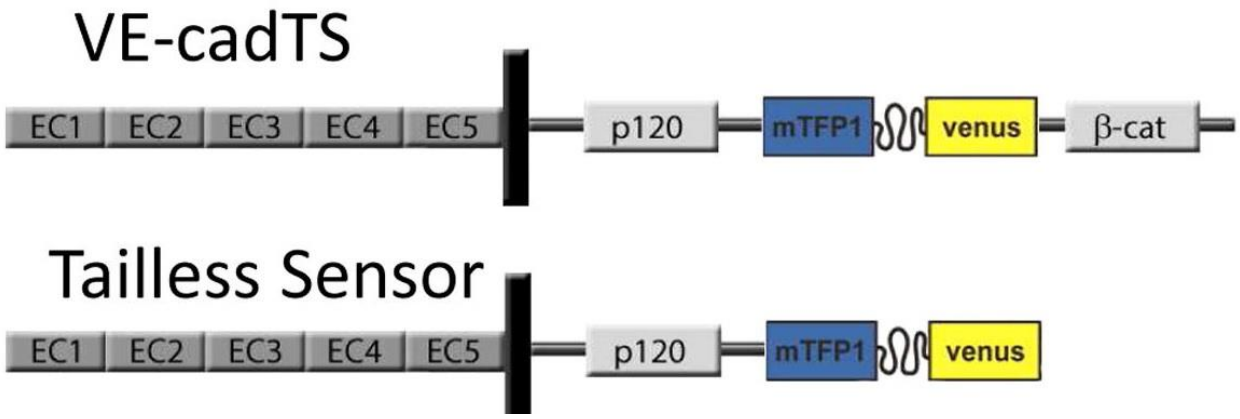

Figure 10. Schematic of VE-cadherin FRET tension sensor. Two fluorescent proteins, mTFP1 (CFP) and venus (YFP) are inserted between the p120 catenin and β-catenin binding domains of VE-cadherin separated by an elastic linker derived from a spider silk protein. Under high acto-myosin tension, the fluorophores are pulled apart, resulting in reduced FRET. When acto-myosin tension is low, the fluorophores are in close proximity, allowing for FRET between the two fluorophores. The relative tension across VE-cadherin can be expressed as the inverse of the ratio of FRET signal to mTFP1 signal. Reprinted with permission from Conway, et. al., 2013.

2.2 **Animal Models**

2.2.1 **Generation of inducible, endothelial cell specific Cdh2 knockout mice**

All mice were maintained on a C57BL/6J genetic background. *Cdh2*-iEC KO (Figure 11) was generated by crossing loxP-flanked *Cdh2* (*Cdh2* $^{flox/flox}$) mice (Jackson, B6.129S6[SJL]-Cdh2tm1Glr/J) with transgenic end-SCL-Cre-ERT mice (Jackson, Tg[Tal1-cre/ERT]42-056Jrg). *Cdh2* $^{flox/flox}$ mice have been bred to F10 generation, authenticated by genotyping and Western blotting for N-cadherin expression in lung endothelial cells. No change in the expression of N-cadherin was observed in *Cdh2* $^{flox/flox}$ as assessed by Western blotting analysis of endothelial-specific fractions. These mice demonstrate no gross change in either behavior or heath. Both 8-12-week-old male and female transgenic Mus/*Cdh2* $^{flox/flox}$-end-SCL-CreER^{T2} and Mus/*Cdh2* $^{flox/flox}$ mice were used in this study. Mice lacking Cre (Mus/*Cdh2* $^{flox/flox}$), labeled as Cre-negative or Cre- in figures, were used as a control. Littermates were randomly assigned to experimental groups.

All animals were housed in the animal facility at The University of Illinois at Chicago, where they were maintained in 12 h light /12 h dark cycle environment with access to water and food. All proposed animal procedures and experiments were approved by the UIC Animal Care Committee. All animal studies were performed under the auspices of the University of Illinois Animal Care and Use Committee.

Sample size was calculated for each experiment using power analysis using JMP release 6 software programs (SAS, Cary NC).

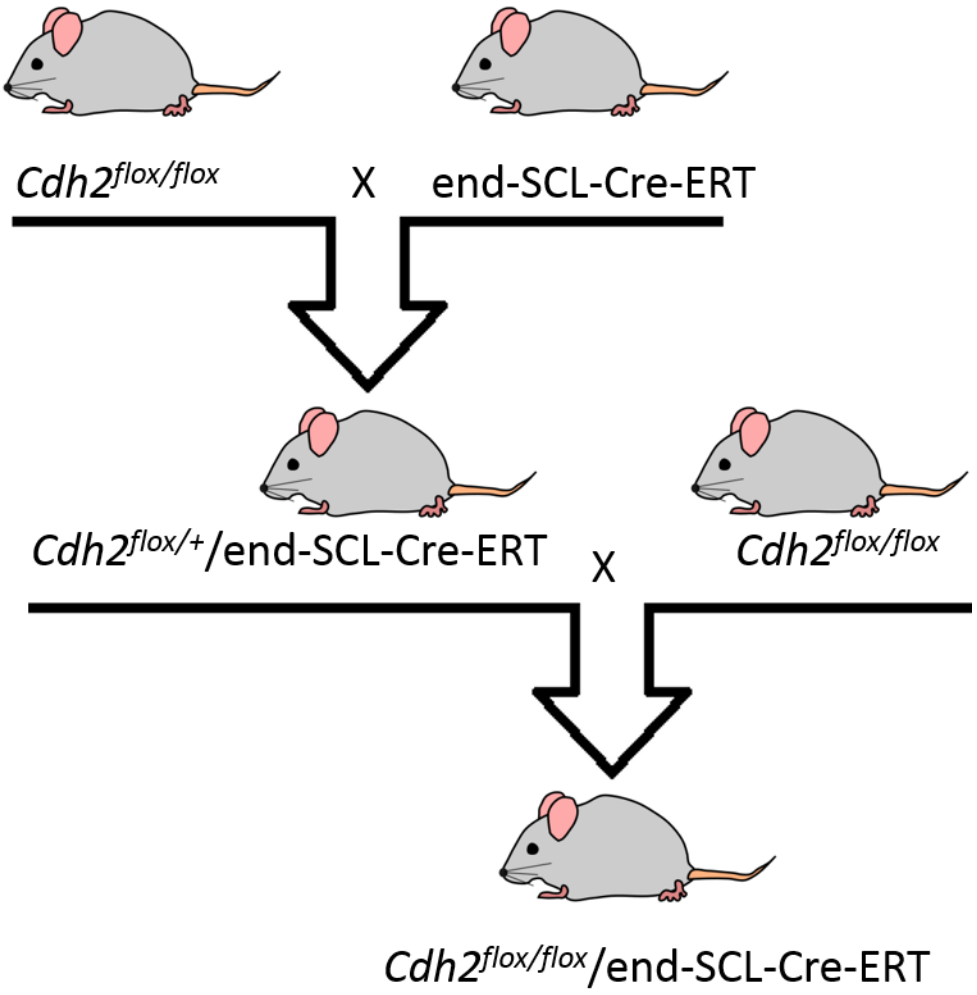

Figure 11. Breeding scheme for generation of *Cdh2*$^{flox/flox}$ /end SCL Cre-ERT mice. *Cdh2*$^{flox/flox}$ were bred with end SCL Cre-ER^{T2} to generate heterozygous *Cdh2*$^{flox/+}$ /end SCL Cre-ER^{T2} mice. These mice were then cross bred with *Cdh2*$^{flox/flox}$ to obtain *Cdh2*$^{flox/flox}$ /end SCL Cre-ER^{T2} mice.

2.2.2 **Deletion of *Cdh2* in endothelial cells**

To delete N-cadherin in endothelial cells (Figure 12), tamoxifen (Sigma Aldrich, T6548) was dissolved in 1 ml of corn oil (Sigma Aldrich, C8267) on shaker at concentration of 20 µg/ml. Solution was passed through a 0.2 um filter and used fresh at 2 µg/mouse. Tamoxifen was injected for 5 continuous days. Mice were used for experiments at day 14 or later after induction. Confirmation of deletion of N-cadherin specifically in endothelial cells was performed by Western blot analysis of cultured endothelial cells isolated from lung tissue as well as endothelial cell specific fractions collected by perfusing the lung with lysate and collecting fractions every 30 seconds. Endothelial cell specific (VE-cadherin) and non-endothelial cell specific (α-Smooth Muscle Actin) markers were used to differentiate between endothelial cells and non-endothelial cells (such as smooth muscle cells).

2.2.3 **Measurement of endothelial permeability to albumin**

150 µl of ^{125}I-human serum albumin containing 2µCi (Anazao Health, I-125 HAS) was intravenously injected via tail vein. 30 minutes later, mice were anesthetized with 2.5% isoflurane. Depth of anesthesia was determined by pinching the toe of the animal. Blood and organs (lung, brain, kidney, and heart) were collected for measurement of radioactivity in whole organ using a gamma counter (Perkin Elmer 2470 Automatic Gamma Counter). Humane euthanasia was carried out by vital organ removal under anesthesia. Given a mean value of 6.8 ± 0.8 µl/min/100 dry lung in Mus/Cdh2flox/flox mice, a population standard deviation of 8, a significance level of 0.05, and power of 0.8 requires a group size of n = 9 as the minimum number of mice required to obtain a significant increase of 50% more than the control. Since the difference between groups were about 2 folds, I limited the animal studies to 5-8 mice per group, which were required to reach statistical significance.

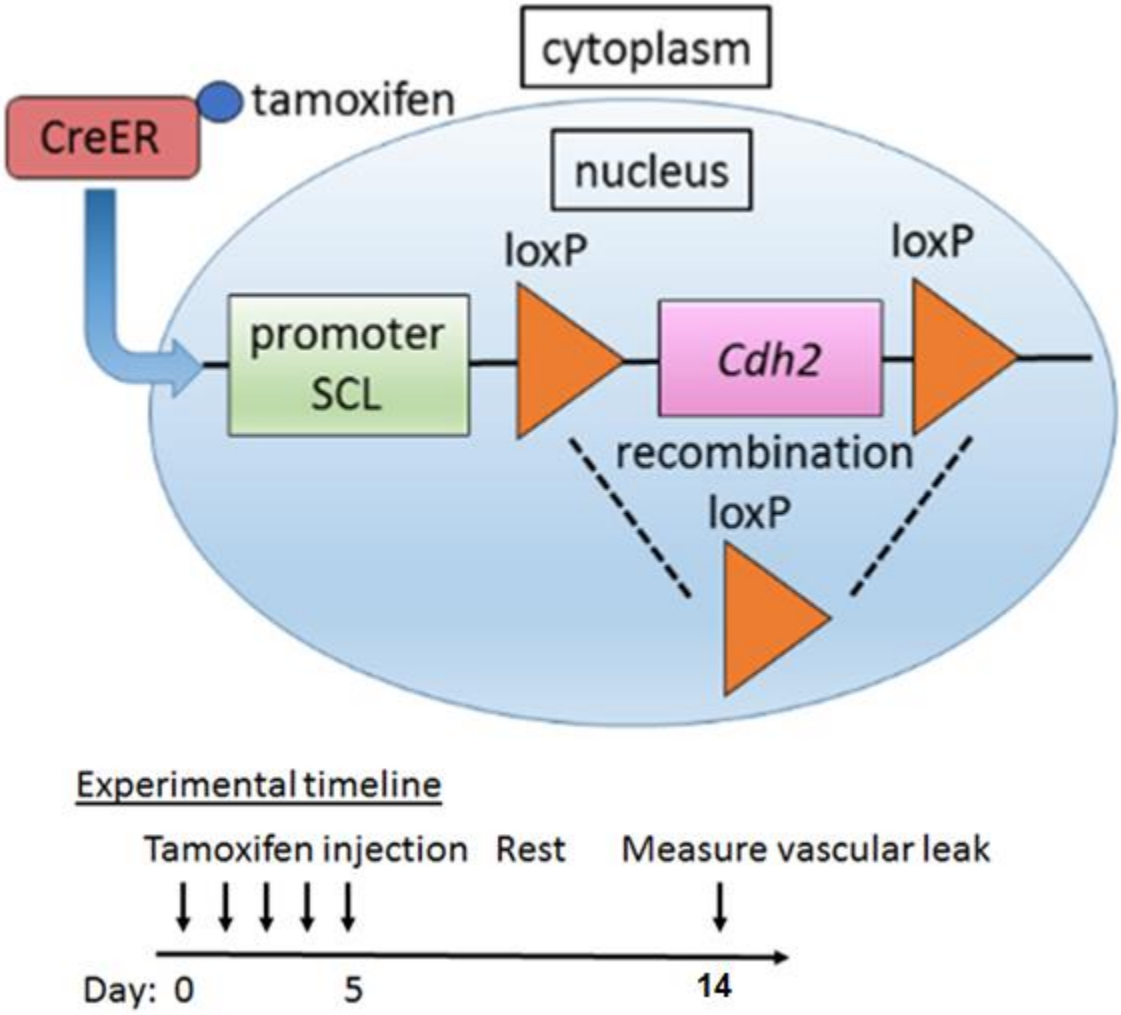

Figure 12. Mechanism of deletion of N-cadherin in endothelial cells. Upon administration of tamoxifen, mice expressing Cre recombinase attached to estrogen receptor (ER) driven by the 5' endothelial enhancer of the stem cell leukemia (SCL) locus will translocate to the nucleus, where it will excise the N-cadherin gene (*Cdh2*) flanked by loxP sites (locus of crossover in phage P1), resulting in recombination and elimination of *Cdh2*. To delete N-cadherin, 12-18-week-old mice were injected with tamoxifen for 5 consecutive days. Measurements of protein expression, permeability, and immunofluorescent staining were performed at day 14 or later after tamoxifen induction.

2.2.4 **Measurement of endothelial permeability to dextran**

10 kDa and 70kDa Dextran tracers conjugated with AlexaFluor 555 (Sigma Aldrich, D34679) or Oregon Green 488 (1 mg/kg; Sigma Aldrich, D34679; D7173) were injected intravenously via retro orbital sinus (100 µl per mouse). In experiments with PAR-1 agonist peptide (TFLLRNPNDK-NH(2)), mice were intravenously (i.v.) injected via retro orbital sinus (100 µl per mouse) with 25 mg/kg body weight PAR-1 agonist peptide into right eye following i.v. injection of fluorescent dextran into left eye. After 30 minutes, mice were euthanized with 2.5% isoflurane. Heparin sodium (Sigma-Aldrich, H3149-25KU; 700 U/kg) was administered intraparietally to prevent clotting. The whole body was perfused through the right ventricle to remove intravascular dye with warm phosphate-buffered saline (PBS) and the right atrium was removed to allow clearance. Lung and brain tissues were collected, fixed, paraffin-imbedded, and sectioned.

2.2.5 **Isolation of primary murine lung microvascular endothelial cells**

The isolation and culture of microvascular endothelial cells from mouse lungs was carried out as follows. Lungs were removed, minced and suspended in 1.0 mg/ml collagenase A (Sigma Aldrich, 10103578001). The released cells were centrifuged, re-suspended and filtered through a 200 mm mesh filter. Platelet-Endothelial Cell Adhesion Molecule (PECAM)-1-positive cells bound to Dynabeads M-450 (Thermo Fischer Scientific 14011) were separated on a magnetic column and grown in EGM-2 MV (Lonza, Cat# CC-3202) culture medium supplemented with 15% FBS (MEDIATECH INC, Cat# 35-015-CVX). Knockout of specific genes was validated with Western Blot analysis. Characterization of endothelial cells was routinely assessed by measuring Dil-Ac-LDL uptake and by immunostaining for endothelial-specific markers, VE-cadherin (Santa

Cruz sc-6458), Von Willebrand factor (vWF; Santa Cruz, sc-14014), and lectins (Thermo Fischer, I32450) as standardized for primary culture.

1 mouse gives ~ 2.5 x 10^5 endothelial cells after several days of culture and reseeding for an experiment. I used 3 mice per group to pool the cells for each individual experiment.

2.2.6 **Staining of lung and brain tissue (histology)**

Whole body was perfused as described above to remove blood; and either pre-fixed in situ by perfusing 4% formaldehyde (Sigma-Aldrich, 433284), or embedded in optimal cutting temperature compound (OCT; Sakura Finetek, 25608-930) and frozen in block. Lung was inflated before fixation or OCT embedding. The frozen tissue was cryosectioned. Pre-fixed samples were fixed in 4% formaldehyde overnight. Tissues were dehydrated using increasing percentages of ethanol and embedded in paraffin. 12 µm sections were sliced and attached to a cover slip. Sections were then dewaxed and rehydrated. Antigen retrieval was performed by boiling samples in sodium citrate (pH 6.0) for 30 minutes using a 100°C water bath and prepared for staining.

2.3 **Generation of N-cadherin biomimetic surfaces**

Glass cover slips (Schott Nexterion 1472309) or dishes (Kimax 23060-10010) were sonicated for 20 mins for each treatment in absolute ethanol, acetone, 2N HCl, and 10N Sodium Hydroxide followed by washing three times with ddH_20 after each treatment, and allowed to dry completely. Glass cover slips or dishes were incubated overnight in toluene vapor containing 2% Glymo (Sigma Aldrich 440167), washed 3 times in ddH_20, and incubated overnight in 2% AB-NTA (Dojindo A459-10) at 60°C, and 10 mM NiCl2 and 5 mM glycine (pH 8.0) for 2 hours followed by washing 3 times in ddH_20. To attach protein, Ni-NTA surfaces were incubated for 1 hour at room temperature with the extracellular domain of N-cadherin fused with a His tag at the

C terminus (Sino Biological, 11039-H03H; Figure 13). Protein was covalently linked to the Ni-NTA glass using 50 mM EDC (Thermo Fischer 22980) and 100 mM NHS (Sigma-Aldrich 130672) in 20 mM HEPES and 100 mM NaCl for 45 minutes at room temperature. Non-covalently linked proteins were eluted by adding 1 M imidazole (Sigma I5513) in 10 mM EDTA (Research Products International E57020).

2.4 **Cell culture, Transfection, and Treatment**

2.4.1 **Cell culture**

2.4.1a **Human primary endothelial cells:**

Human Pulmonary Aortic Endothelial cells (Lonza, Cat# CC-2530) and Human Lung Microvascular Endothelial cells (Lonza, Cat# CC-2527) were grown in Endothelial Basal Media supplemented with Endothelial Growth Medium 2 (Lonza, Cat# CC-3156) or Endothelial Growth Medium 2 – Microvascular (Lonza, Cat# CC-3202) and 10% FBS (MEDIATECH INC, Cat# 35-015-CVX). Cells were used at passages 4–8. All cell lines were maintained at 37°C and 5% CO_2. For all live imaging experiments, cells were imaged in Phenol free red Endothelial Basal Media supplemented with 10% FBS, which contains growth factors such as Vascular Endothelial Growth Factor (VEGF).

2.4.1b **Human Embryonic Kidney cells**

Human Embryonic Kidney (HEK 293) cells were grown in Dulbecco's Modified Eagle's Medium (DMEM) supplemented with 10% FBS and maintained at 37°C and 5% CO2.

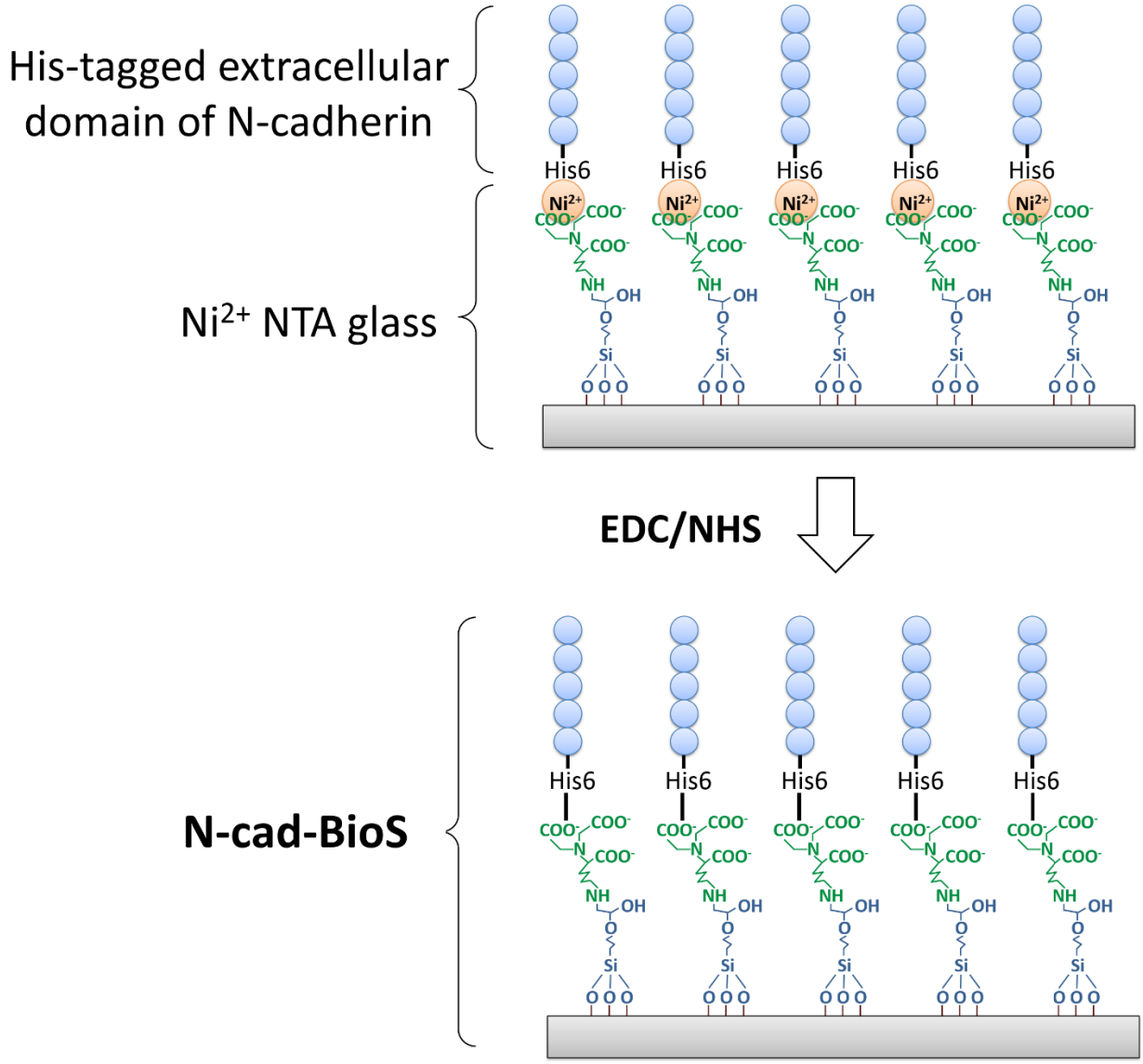

Figure 13. Creation of N-cad-BioS. The His6 tag of recombinant human N-cadherin coordinates with the Ni^{2+}, which is held in place by the NTA moieties. Cross linking via EDC/NHS covalently links N-cadherin to the surface in an oriented manner (with the N-terminus farthest from the glass), which also prevents loss of N-cadherin from the surface over time due to the covalent linkage.

2.4.2 **Transfection**

HEK 293 cells were transfected with Lipofectamine 2000 (Thermo Fischer, 11668019). Human primary cells were electroporated using the Amaxa nucleofector kit (Lonza, VPI-1001) using code M-003 according to the manufacturer's instructions.

2.4.3 **Treatment with siRNA and inhibitors**

Endothelial cells grown to 70% confluence were treated with scrambled control siRNA duplexes or siRNA targeting a specific protein of interest (Dharmacon, *Cdh2*: J-011605-06, -07, -08, -09; *TRIO*: J-005047-05, -06, -07, -08; Scrambled: D-001810-01-05) using GeneSilencer (Genlantis, T500020) according to the manufacturer's instructions. Cell were used for experiments 24 – 48 hrs after treatment. Depletion of the target protein was validated by Western blot analysis.

Confluent monolayers of endothelial cells were treated with 50 µm Rockout for 30 minutes, 10 µm blebbistatin for 10 minutes, or 50 µm ITX3 for 30 minutes where indicated.

2.5 **Western blotting**

Total protein concentrations for each sample were measured using a BCA protein assay kit (Thermo Fischer, 23225) and were adjusted to contain equal protein and volume. Samples were boiled in Laemmli sample buffer (BioRad, 1610747) for 5 minutes and separated using SDS-PAGE. Proteins were transferred to nitrocellulose membranes overnight at 4 degrees and non-specific sites were blocked with 3% milk for 1 hour. Proteins of interest were then detected by probing with the indicated primary antibodies (Santa Cruz sc-6458, sc-7939, ECM Biosciences CM-1701, Bethyl Laboratories A304-269A-T, Sigma T8328, A3854) followed by horseradish peroxidase conjugated secondary antibodies, and the immune-reactivity was developed using the enhanced chemiluminescence (ECL) method.

2.6 **Imaging and image analysis**

2.6.1 **Endothelial permeability to dextran**

To quantify the leak of dextran outside of circulation, samples were imaged using a confocal microscope (Zeiss, LSM880 with Plan-Apochromat 63x/1.40 Oil DIC objective) to obtain a Z-stack of images through the whole tissue using 1 µm thick optical sections. An additional channel (λ = 647 nm) which did not contain any fluorophore was used to capture the tissue architecture through auto-fluorescence. A 3D volume reconstruction for each channel was performed with Imaris (Bitplane) using the surfaces tool and keeping the threshold and surface creation parameters the same for each image. The total volume for each fluorescent tracer was divided by the total volume of tissue to obtain the percentage of leakage area.

2.6.2 **Immunofluorescent staining**

Cells or frozen tissue sections were fixed in 4% formaldehyde for 20 minutes, washed once with PBS, then permeabilized for 15 minutes using 0.1% Triton X-100 (Thermo Fischer, 28313) in PBS. Nonspecific sites were blocked using 3% bovine serum albumin (BSA; Sigma-Aldrich A9418) for 2 hours at room temperature. Cells were incubated with primary antibodies (Santa Cruz sc-6458, sc-7939, sc-1506-R; Abcam ab76057, ab15200, ab12221, ab 11575, ab52235 Cell Signaling Technology #3671; Invitrogen, A12379, BD Biosciences 550274, R and D Systems AF1042) using 1:10 – 1:400 dilution at either 1 hour at room temp or overnight at 4°. Cells were incubated with secondary antibodies using 1:100 dilution (Invitrogen A-21206, A-21202, A-11057, A-31570, A-31572, A-21472, A-31573, A-21469) for 1 hour at room temperature.

2.6.3 **Pericyte coverage area**

Area was calculated by creating a Z-projected image for each channel using only the in-focus frames of a Z-stack. A threshold was used to only include specific fluorescent signal and the total overlapping area of endothelial cells (PECAM1 or Collagen IV) and pericytes (PDGFRβ or desmin) was measured using MetaMorph (Molecular Devices).

2.6.4 **Analysis of VE-cadherin, N-cadherin, phospho-MLC adhesion area**

VE-cadherin, N-cadherin, or phospho-MLC adhesion areas were calculated by creating a Z-projected image for each channel using only the in-focus frames of a Z-stack. The VE-cadherin or N-cadherin adhesion area was found by measuring the number of pixels positive for VE-cadherin or N-cadherin above a certain threshold and converting to square microns.

VE-cadherin adhesion area junction area for cells expressing Trio-FL, Trio-D1d, and Trio-D2d was found by measuring the area of VE-cadherin positive pixels above a certain threshold within the "junction area", which is defined as an 8 pixel wide band going around the perimeter of the cell and extending inward.

2.6.5 **VE-cadherin Dendra2**

Live cells expressing VE-cadherin–Dendra2 alone or co-expressing VE-cadherin-Dendra2 and PA-Rac1-CFP (or LI-Rac1-CFP) were imaged at 5% CO_2 and 37° C with $\lambda = 488$ nm and $\lambda = 543$ nm for green and red states of Dendra2, respectively, and $\lambda = 458$ nm for CFP detection. Dendra2 was photoconverted with $\lambda = 405$-nm laser at 8–12% power. PA-Rac1-mCerulean was photoactivated continuously using 458 nm laser at 8-12% power. Images in green and red channels were simultaneously acquired every 10s using a confocal microscope (Zeiss LSM 710 with Plan-Apochromat 63x/1.40 Oil DIC objective equipped with two Gallium arsenide phosphide

detectors). The changes in mean fluorescent intensities at λ=488- and 543-nm were measured inside the photoconversion zone. For each time point, the percent fluorescent change was calculated by dividing the total fluorescent intensity within the irradiation zone to the total fluorescent intensity of this region immediately after photoconversion. The rate constants for VE-cadherin dissociation (internalization, at λ=543 nm) and association (recruitment, at λ=488 nm) were calculated from decay and recovery kinetics, respectively, after VE-cadherin–Dendra2 photoconversion (Daneshjou et al., 2015). The association and dissociation rate constants (k) were calculated using non-linear regression to fit the values to the one phase association equation $Y=Y_0 + (Plateau-Y_0)*(1^{-exp(-k*t)})$ where Y = fluorescent intensity, Y_0 = initial fluorescent intensity, Plateau is the maximum or minimum fluorescent intensity (recovery or decay) after photoconversion, t = time.

2.6.6 **Trio and N-cadherin co-localization analysis**

Cells expressing GFP-Trio and immunostained for N-cadherin were imaged using a Zeiss LSM 880 microscope equipped with 63X 1.4 NA objective. Colocalization coefficient for GFP-Trio (Trio-FL, Trio-N, and Trio-C) and N-cadherin was determined using projected Z-stack images (using the frames from the abluminal surface) and Zen software (Zeiss) according to the manufacturer's instructions. Thresholded images were used to set the vertical and horizontal crosshairs to separate clusters into four quadrants (Region 1: Trio+/N-cad-, Region 2: Trio-/N-cad+, Region 3: Trio+/N-cad+, Region 4: Trio-/N-cad-). Cross hair threshold values were set using cells only expressing GFP-Trio and not stained for N-cadherin or cells not expressing GFP-Trio and stained for N-cadherin. Colocalization analysis was done on a pixel by pixel basis. The Manders colocalization coefficient was calculated as the sum of GFP-Trio colocalized pixels (with N-cadherin) divided by the total number of GFP-Trio pixels (Region 3/[Region 2 + Region 3]).

2.6.7 **Structured Illumination Microscopy and analysis of lamellipodia area**

3D Super resolution SIM was performed using a Nikon N-SIM using fixed cells stained for f-actin with AlexaFluor 488 conjugated phalloidin. Grating settings were set at 100 EX V-G (100x 405-561) and a 100X objective and 488nm laser were used. SIM reconstruction was done using Nikon Elements software. Images were pseudocolored from 0 nm (basal surface) to 800 nm (apical surface).

The polygon selection tool in ImageJ (NIH) was used to outline the cell borders and the lamellipodia. The fraction between the sum of the lamellipodia area and the total cell area for individual cells was calculated and used as a method of quantitative analysis.

2.6.8 **Analysis of Rac1 and RhoA activities, and tension across VE-cadherin using FRET-based biosensors**

Live cells were imaged using a confocal microscope (Zeiss LSM 710 with Plan-Apochromat 63x/1.40 Oil DIC objective) at 5% CO_2 and 37° C. FRET and CFP images were simultaneously acquired by activating the CFP with a λ=458 nm laser and the subsequent FRET and CFP images were acquired at λ=570 nm and λ=485 nm, respectively. A YFP image was acquired at λ = 514 nm and used for generation of a binary mask. For FRET analysis, the YFP image was used to create a binary mask with a value of 0 outside the cell and a value of 1 inside the cell. To generate a ratio image, the FRET image was first multiplied by a binary mask image and then divided by the CFP image. The ratio images were rescaled to the lower value, and a linear pseudocolor table was applied to generate the color-coded image map (Daneshjou et al., 2015). The integrated intensity for FRET and CFP within this region was measured and the FRET/CFP ratio was calculated. The relative activity of Rac1 and RhoA as well as level of tension across VE-

cadherin adhesions were expressed as mean pixel intensity of FRET/CFP ratio within the entire cell (for RhoA and Rac1) or at AJs (tension sensor).

2.6.9 **Analysis of endothelial permeability to albumin *in vitro***

Live cells expressing VE-cadherin-GFP were grown on either N-cad-BioS or gelatin coated surfaces for 24 hours to form a confluent monolayer. Alexa-647-conjugated albumin was added to the cells at a concentration of 1mg/ml during image acquisition. A z-stack of images was acquired using Zeiss LSM 710 confocal microscope at 5% CO2 and 37° C at λ = 488 nm (VE-cadherin) and λ = 647 nm (albumin) for 30 minutes. To analyze endothelial permeability to albumin, the average fluorescent intensity of the Alexa-647 was measured in an X-Z cross-sectional plane along the VE-cadherin junction. The albumin signal was normalized to the background fluorescence (before albumin was added). The values were plotted as the normalized albumin signal over time. The permeability rate constant (k) was calculated by fitting the data to a non-linear one phase association equation. The junction width was determined using the VE-cadherin cross sectional area. The permeability rate constants were plotted as a function of junction width and a linear fit was applied. (Quadri, et. al. Nat Commun 2009).

2.6.10 **Total Internal Reflection Fluorescence (TIRF) microscopy**

Epifluorescent and TIRF images of endothelial cells stained for VE- and N-cadherin proteins were acquired using a Zeiss Axio Observer Z1 / 7 equipped with an alpha Plan-Fluar 100x/1.45 Oil objective, a Hamamatsu camera, and TIRF adaptor.

2.7 **Identification of novel N-cadherin binding partners**

N-cadherin-His protein (Sino Biological, 11039-H03H) was incubated with magnetic Ni-NTA beads (Thermo Fischer, 88831) at a concentration of 1 μg/μl for 1 hour at room temperature. N-cad-His protein was crosslinked to beads using EDC/NHS for 45 mins at room temperature.

Beads were added directly to the culture of endothelial cells, and allowed to form complexes for 1 hour. Proteins were cross-linked with the reversible crosslinker 50 μM DTSP for 5 minutes. Beads were then collected from cell lysates using a magnetic separator, washed 5 times in PBS, and boiled in sample buffer containing 1mM DTT to break the cross link. Lysates were separated by SDS-PAGE and silver stained to highlight bands of interest. Each lane of the gel was cut into 3 pieces and submitted to The Taplin Biological Mass Spectrometry Facility (Harvard University) for analysis by microcapillary liquid chromatography–tandem mass spectrometry (LC/MS/MS). Non-unique peptides were excluded from the mass spectrometry data. 1,120 unique candidates for constituents of N-cadherin complexes were represented by more than 3 of the 20,607 remaining unique peptides or with arbitrarily chosen $\log_{10}$ mean peptide intensities greater than 6. These candidate proteins were evaluated for known interactions within 10 protein interaction databases, including BioGRID, Bell09, HPRD, IntAct, and MNT as well as other studies via the Human Integrated Protein-Protein Interaction Reference (HIPPIE). Protein interactions were filtered to only include those with confidence scores greater than 0.2. Of the 1,120 interrogated proteins, 1,046 had at least two established interactions, with a maximum of 1,759 (IQGAP1) and median of 77 interactions per protein. An interaction profile was created for each of these proteins using a Euclidean distance comparison with all other protein interaction confidence scores.

I chose to examine the proteins ARHGAP21, ARHGAP31, ARHGEF17, CDH2, IQGAP1, PACSIN2, PECAM1, TJP1, TJP2, TRIO, and TRIOBP for their potential roles related to their physical associations with N-cadherin. Affinity propagation clustering was used to autonomously group proteins into clusters ($N > 3$) based on the protein interaction matrix. Inter-cluster linkages were trimmed to include only those with strong support (>0.7 confidence score). Gene Ontology (GO) terms were obtained from BioMart and associations were computed using the

hypergeometric test (N>5) for each of the nine clusters containing the proteins of interest. Generic cellular structure GO terms such as "cytoplasm", "membrane", "nucleus", etc. were excluded.

R packages used:

biomaRt, igraph, apcluster, parallel, RColorBrewer, RedeR, ggplot2

2.8 **Nucleotide free Rac1 pulldown**

2.8.1 **Purification of GST or GST-Rac1-G15A and attachment to beads**

Transformed DH5α E. coli (Thermo Fischer, 18258012) carrying either GST-Rac1-G15A or GST cDNA were grown overnight. Protein expression was induced by adding IPTG to a final concentration of 100 µM. All following steps were performed at 4° C. Bacteria was spun down, resuspended in lysis buffer, and sonicated for 1 min. Lysates were then spun down at 20,000g for 15 minutes. The supernatant was transferred to a tube containing 500 µl of glutathione-sepharose (Abcam, ab193267) pre-equilibrated in lysis buffer. The tube was rotated at 4° C for 1 hour. Beads were spun down and washed twice with 10 ml lysis buffer and then 2 times with 10 ml HBSS containing 5 mM $MgCl_2$ and 1 mM DTT. Wash buffer was aspirated to reduce initial sepharose volume of 50% slurry, and 0.5 volumes of glycerol was added. Protein concentration directly on beads was estimated by boiling beads in Laemmli buffer and separated by SDS-PAGE, followed by staining with Coomassie blue.

2.8.2 **Pulldown of GEFs**

Cells grown on either 0.2% gelatin/0.1% fibronectin or N-cad-BioS platforms were washed with PBS and lysed in radioimmunoprecipitation assay (RIPA) buffer. Lysates were collected and debris was spun down at 16,000g for 1 minute. Protein concentration was calculated using BCA

protein assay kit and the total amount of protein as well as total volume of each sample was equalized. The lysates were incubated with 10 µg of GST or GST-Rac1-G15A beads or RhoA-G17A beads and rotated for 1 hr at 4°C. Beads were then washed 6 times using lysis buffer. Samples were then boiled in Laemmli buffer at 95° C for 5 minutes and separated by SDS-PAGE. Proteins were transferred to a nitrocellulose membrane overnight at 4 °C and probed with the appropriate antibodies.

2.9 **Statistical analysis**

Statistical significance calculations were performed using GraphPad Prism 7. An unpaired t-test was used for experiments with 2 experimental groups and ANOVA for more than 2 experimental groups. The following notations are used throughout the text: ns, non-significant; *, $p > 0.05$; **, $p < 0.01$; *** $p < 0.001$; **** $p < 0.0001$.

3. N-CADHERIN REGULATES ENDOTHELIAL PERMEABILITY

3.1 **Conditional deletion of N-cadherin increases endothelial permeability**

To determine the role of N-cadherin in the adult microvasculature, I generated a genetic model of inducible deletion of the *Cdh2* gene specifically in endothelial cells (hereinafter iEC-KO, see Methods). Deletion of N-cadherin was validated by Western blot (WB) analyses of both endothelial-specific fractions (Figure 14) and cultured endothelial cells collected from the lungs of transgenic mice (Figure 15) as well as immunofluorescent staining of mouse lung tissue (Figure 16).

Using this transgenic model, I assessed the permeability of the endothelial microvessel wall to albumin in the lung, heart, kidney, and brain (Figure 17). Loss of N-cadherin in endothelial cells led to increased albumin permeability (as determined by the Permeability x Surface Area [PS] product of ^{125}I radiolabeled albumin) in both the lung (basal permeability increased from 6.8 ± 0.8 to 11.2 ± 1.5 µl/min/100 g, p=0.0308) and brain (0.3 ± 0.1 to 1.0 ± 0.4 µl/min/100 g, p=0.0488), however no change in permeability was observed in the heart or kidney.

Additionally, I assessed endothelial permeability to dextran to determine if the leak in lung and brain was through the paracellular route or the transcellular route (as dextran can only cross through the paracellular route). By using two sizes of fluorescently labeled tracers (10 kDa and 70 kDa), I could also assess if the observed leak was size dependent. Loss of N-cadherin in endothelial cells led to increased permeability to both tracers in a size dependent manner (Figure 18). Treatment with PAR-1 agonist to disassemble VE-cadherin adhesions increased leakage in Cre- mice to the same levels as untreated, iEC-KO mice, and caused no further increase in leakage of iEC-KO mice. Together, these data suggest a crucial role of N-cadherin in restricting permeability of the endothelial barrier through the paracellular route in tissues enriched with pericytes.

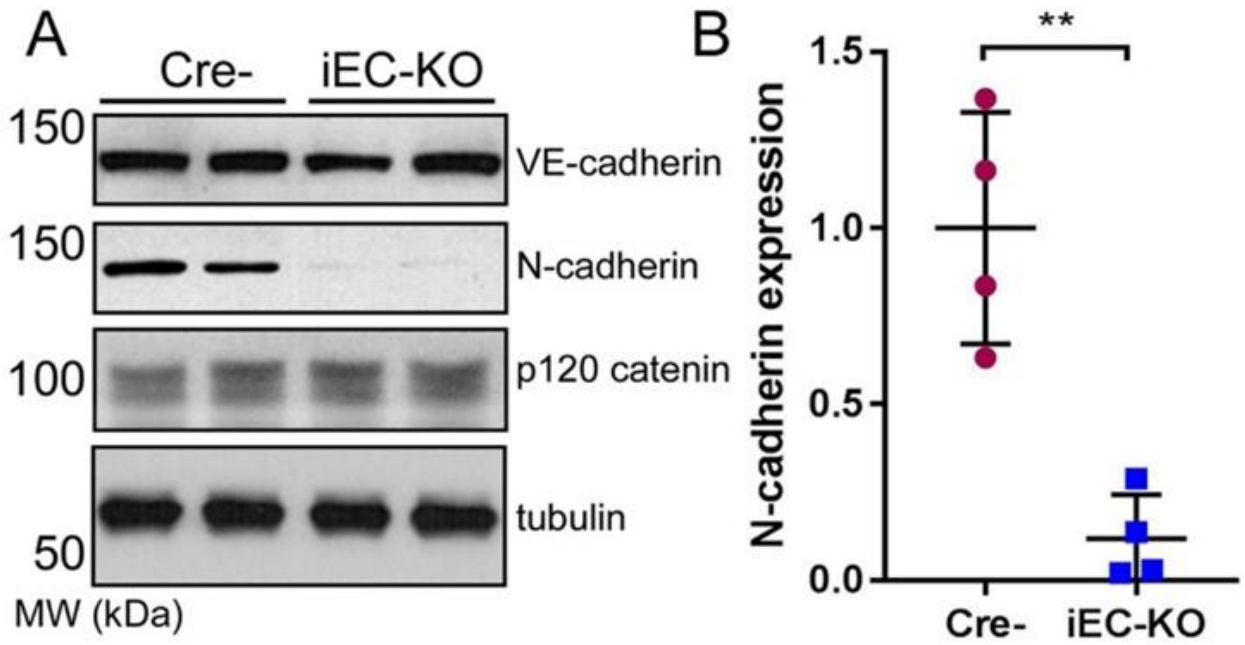

Figure 14. Confirmation of N-cadherin deletion in endothelial cells using endothelial specific lysates collected directly from lungs (A). Quantification of N-cadherin expression normalized to Cre- control mice shown in B. n = 4 mice per condition. Data are presented as mean ± SEM. Collection of cells in A done by Ying Sun.

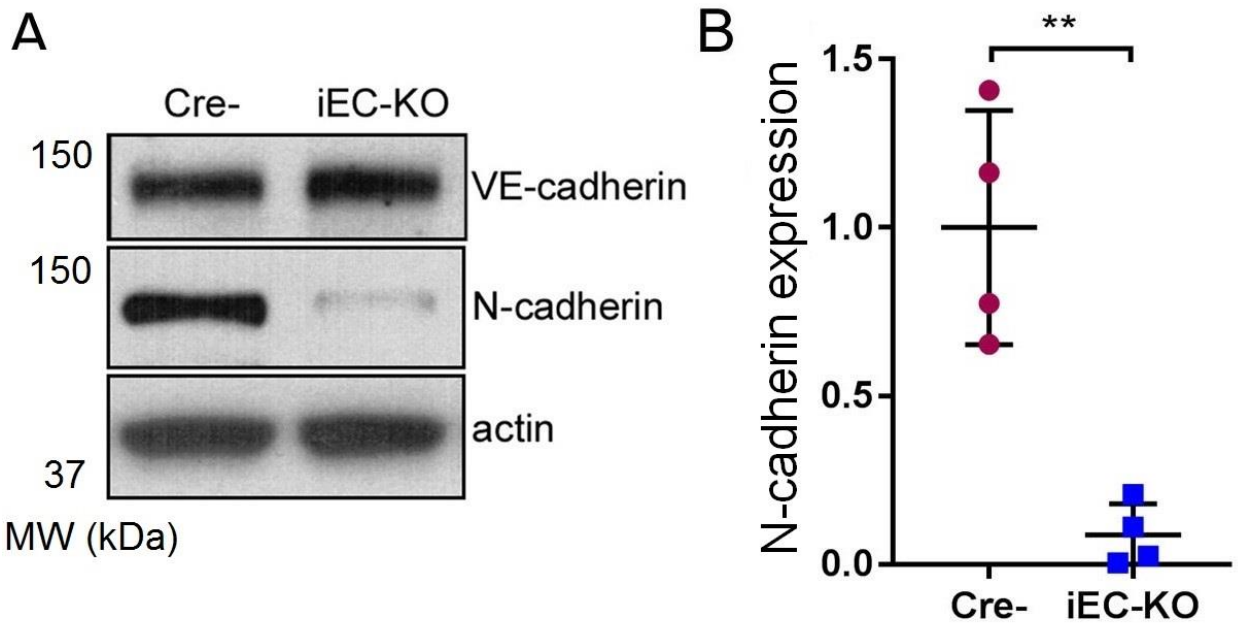

Figure 15. Confirmation of N-cadherin deletion in endothelial cells isolated from lungs and cultured *in vitro* (A). Quantification of N-cadherin expression normalized to Cre- control mice shown in B. n = 4 mice per condition. Data are presented as mean ± SEM. Collection of cells in A done by Ying Sun.

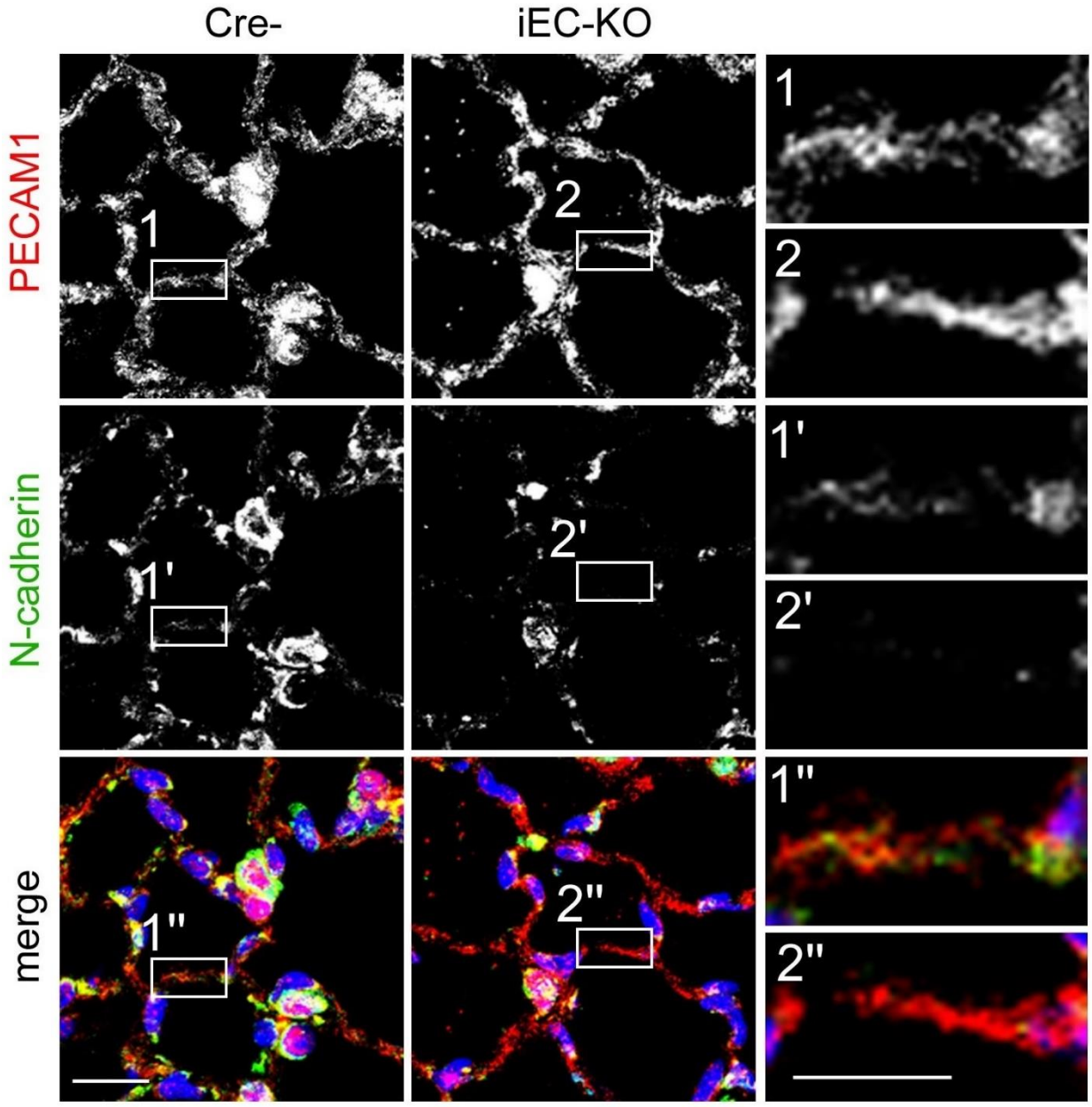

Figure 16. Confirmation of N-cadherin deletion by immunofluorescent staining. Representative confocal images of mouse lung sections from Cre-negative and *Cdh2* iEC-KO mice stained for N-cadherin (green on merged image), PECAM1 (red), and nuclei (DAPI, blue); enlarged inserts are shown. Scale bars, 10 µm, and 5 µm (inserts). Note, reduced expression of N-cadherin in PECAM1-positive cells in Cdh2 iEC-KO mice. N-cadherin expression still observed in mesenchymal cells of *Cdh2* iEC-KO mice. Tissue fixation and sectioning done by Ying Sun.

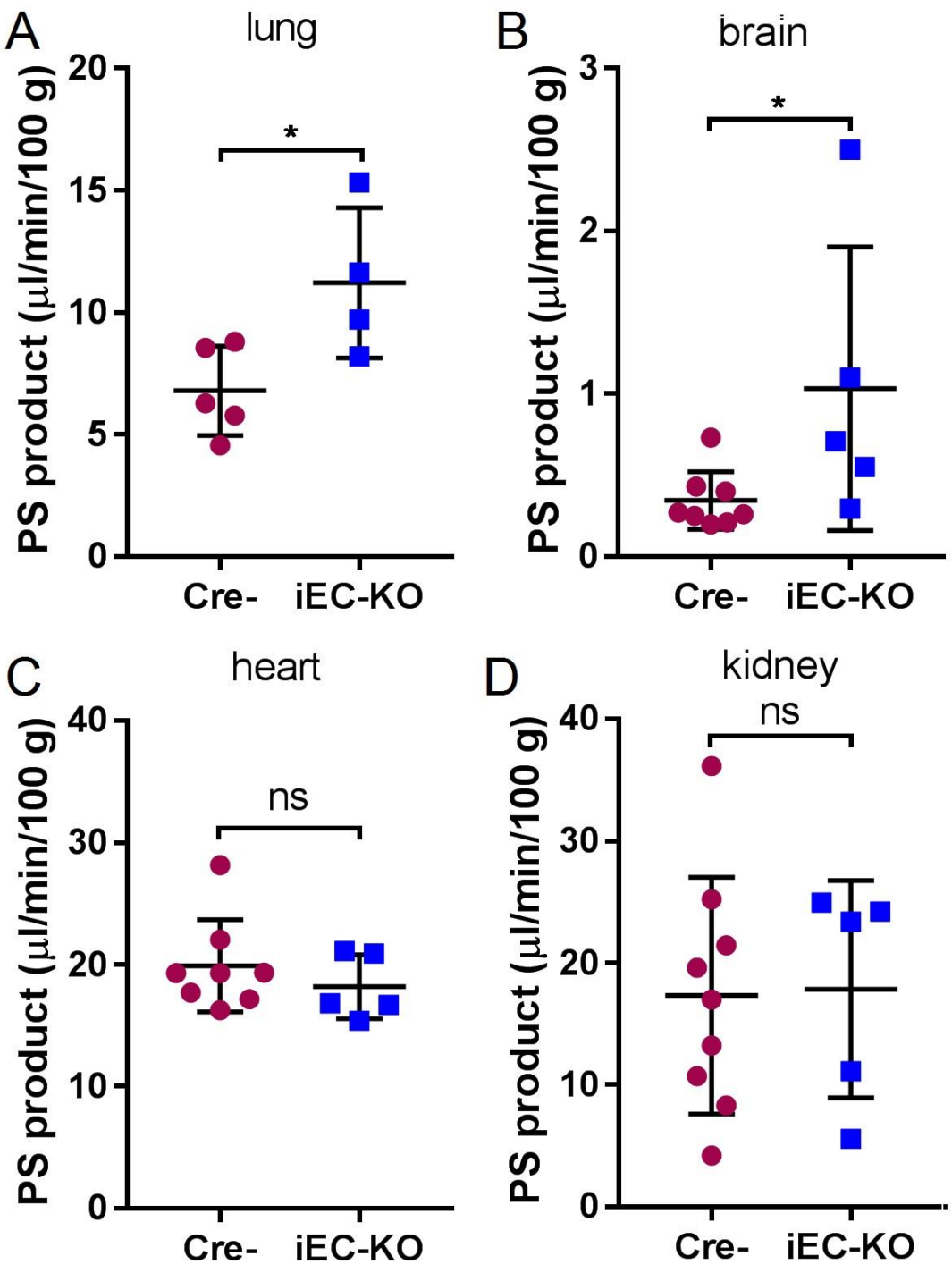

Figure 17. Permeability X Surface Area (PS) Product to ^{125}I radiolabeled albumin in lung (A), brain (B), heart (C), and kidney (D) 30 minutes after injection of albumin. Data are presented as mean ± SEM. Experiment performed with assistance by Stephen Vogel.

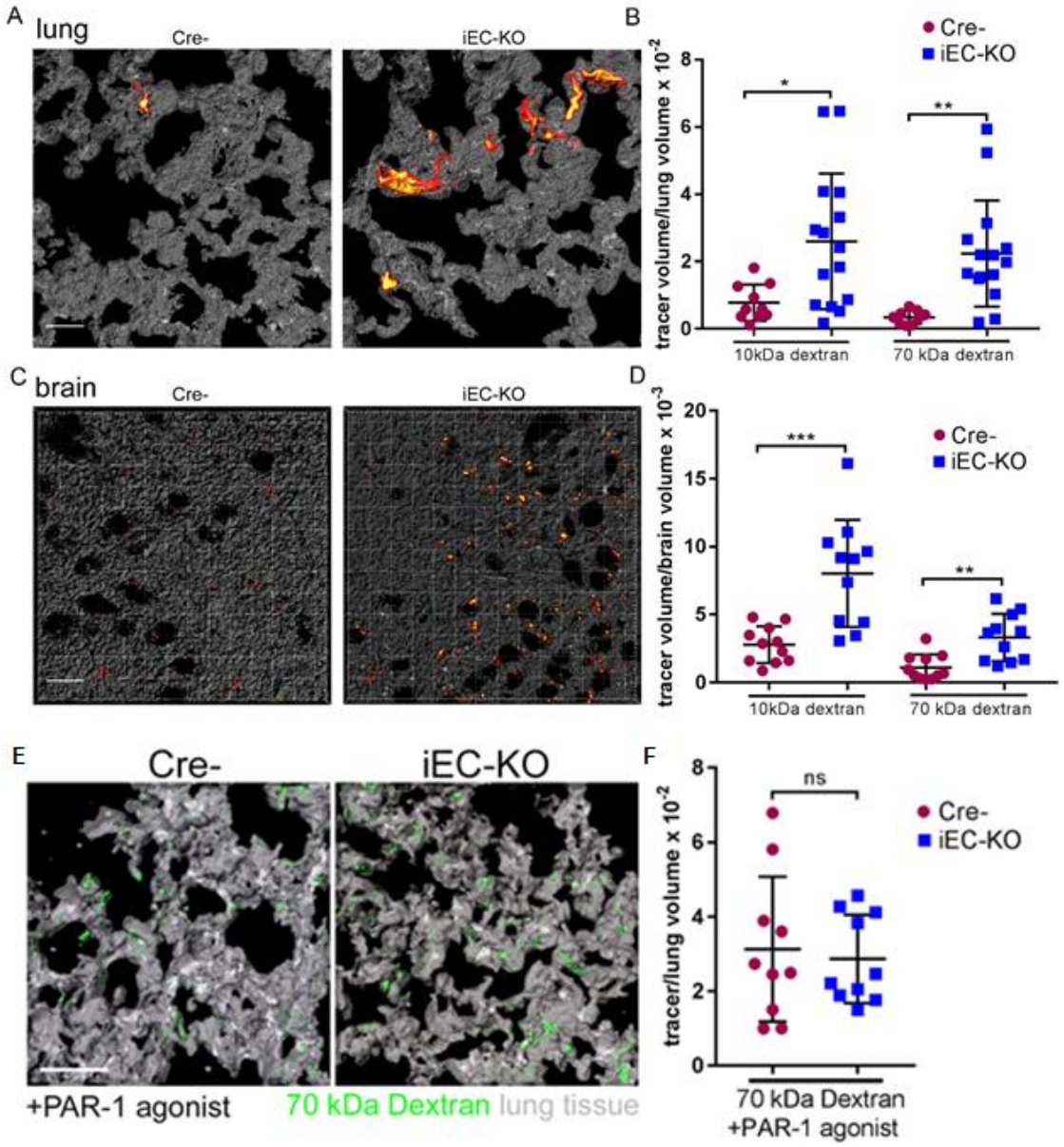

Figure 18. Loss of N-cadherin results in increased permeability to both 10 kD and 70kD dextran. 3D reconstructed volumes of lung (A) and brain (C) tissue after injection with 10 kDa dextran (red) and 70 kDa dextran (green). Quantification of tracer per tissue volume in lung (B) and brain (cerebral cortex) (D). n = 11 sections from 3 mice per group. Data are presented as mean ± SEM. E. 3D reconstructed images of transvascular leakage of 70 kDa Dextran (green) in mouse lung tissue after challenge of Cre- control mice and Cdh2 iEC-KO littermates with 25mg/kg body weight of PAR-1 agonist peptide for 30 min; scale bar, 10 µm. Tissue architecture from autofluorescence is shown in gray. F. Measurement of lung transendothelial permeability from data in E. The data are presented as a ratio of the volume of fluorescent tracer to the volume of lung tissue for Cre-negative (Cre-) control and Cdh2 iEC-KO littermates. n=10 fields from 2-3 mice per group. Injection of fluorescent tracers, tissue fixation and sectioning in A and C done by Ying Sun. Injection of fluorescent tracers and PAR-1 agonist, tissue fixation and sectioning in E done by Shuangping Zhao.

3.2 **Conditional deletion of N-cadherin has no effect on pericyte coverage**

Since heterotypic N-cadherin *trans*-interaction is required for contact between endothelial cells and pericytes (Daneman et al., 2010; Frye et al., 2015; Gerhardt et al., 2000; Li et al., 2011), I next determined whether N-cadherin deficiency in endothelial cells of adult mice induced the loss of pericyte coverage in capillaries. Here I observed normal coverage of pericytes in *Cdh2* iEC-KO mice different times after induction (Figure 19) indicating that increased vascular permeability in *Cdh2* iEC-KO mice is not due to a reduction in the number of pericytes *per se*.

3.3 **N-cadherin controls VE-cadherin localization *in vivo***

The relationship between N- and VE-cadherin in endothelial cells is controversial (Giampietro et al., 2012). This is likely due to the lack of appropriate model systems recapitulating both interactions simultaneously. Some lines of evidence suggest that N-cadherin upregulates VE-cadherin expression during developmental vascular morphogenesis as well as *in vitro* (Luo and Radice, 2005). A more recent study, however, indicates that N-cadherin, through competitive binding to p120-catenin, destabilizes VE-cadherin adhesions by priming VE-cadherin for internalization (Ferreri et al., 2008; Gentil-dit-Maurin et al., 2010). In these studies, I observed no change in VE-cadherin or p120 catenin expression after deletion of *Cdh2* in endothelial cells (Figure 14-15, Figure 20). Analysis of VE-cadherin distribution revealed a 40% reduction in VE-cadherin density at AJs in *Cdh2* iEC-KO lungs (Figure 21) and a 25% reduction in VE-cadherin density at AJs in *Cdh2* iEC-KO cerebral cortex (Figure 22). These data suggest that N-cadherin adhesion at the abluminal side of the endothelium results in increased VE-cadherin localization at AJs as a mechanism to limit the permeability of the endothelial barrier.

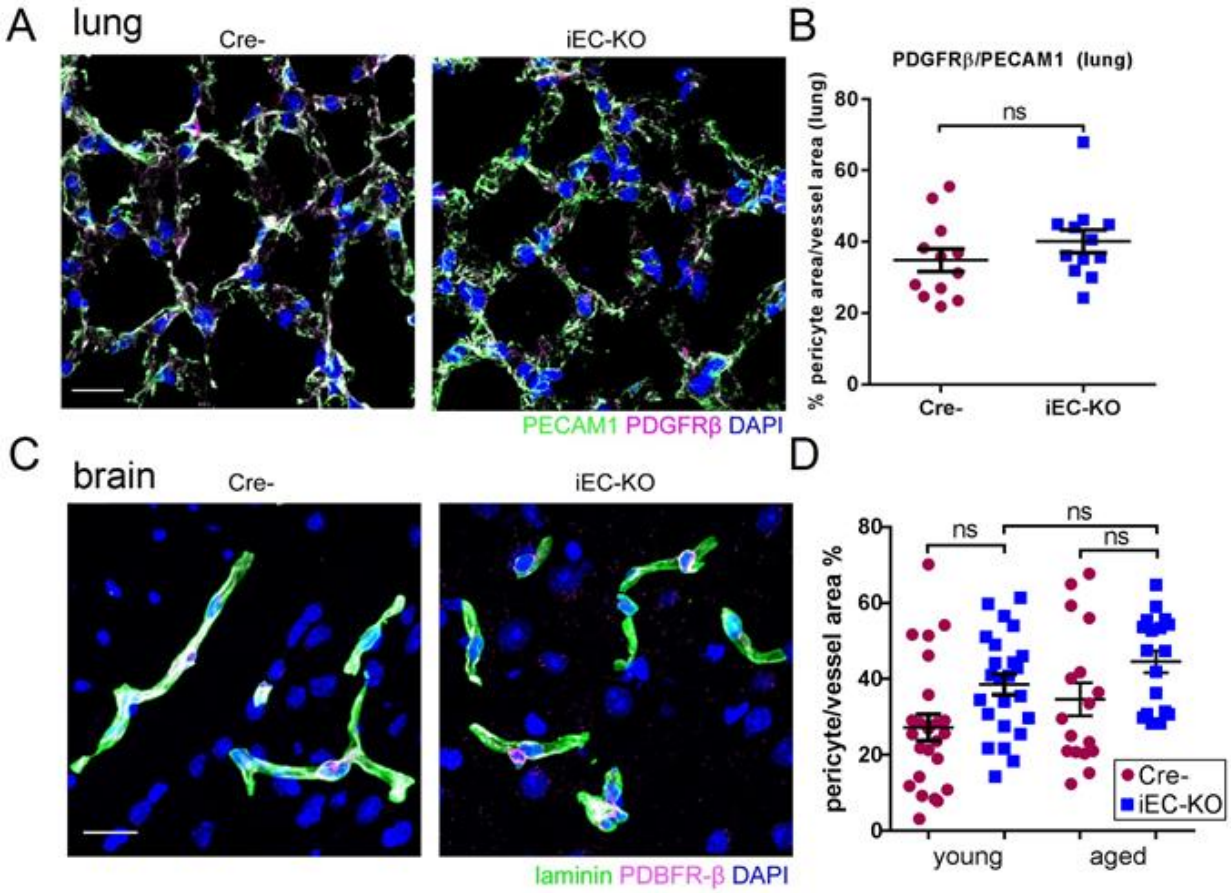

Figure 19. Loss of N-cadherin does not reduce pericyte coverage. Mouse lung (A) and cerebral cortex (A) tissue were stained for the pericyte marker PDGFR-β along with vessel marker (PECAM1, lung; laminin, brain). Quantification of pericyte coverage for lung (C) and cerebral cortex (D). n = 23-24 sections from 3 mice per group. Data are presented as mean ± SEM. Tissue fixation, sectioning, staining, and quantification done with assistance from Quinn Lee.

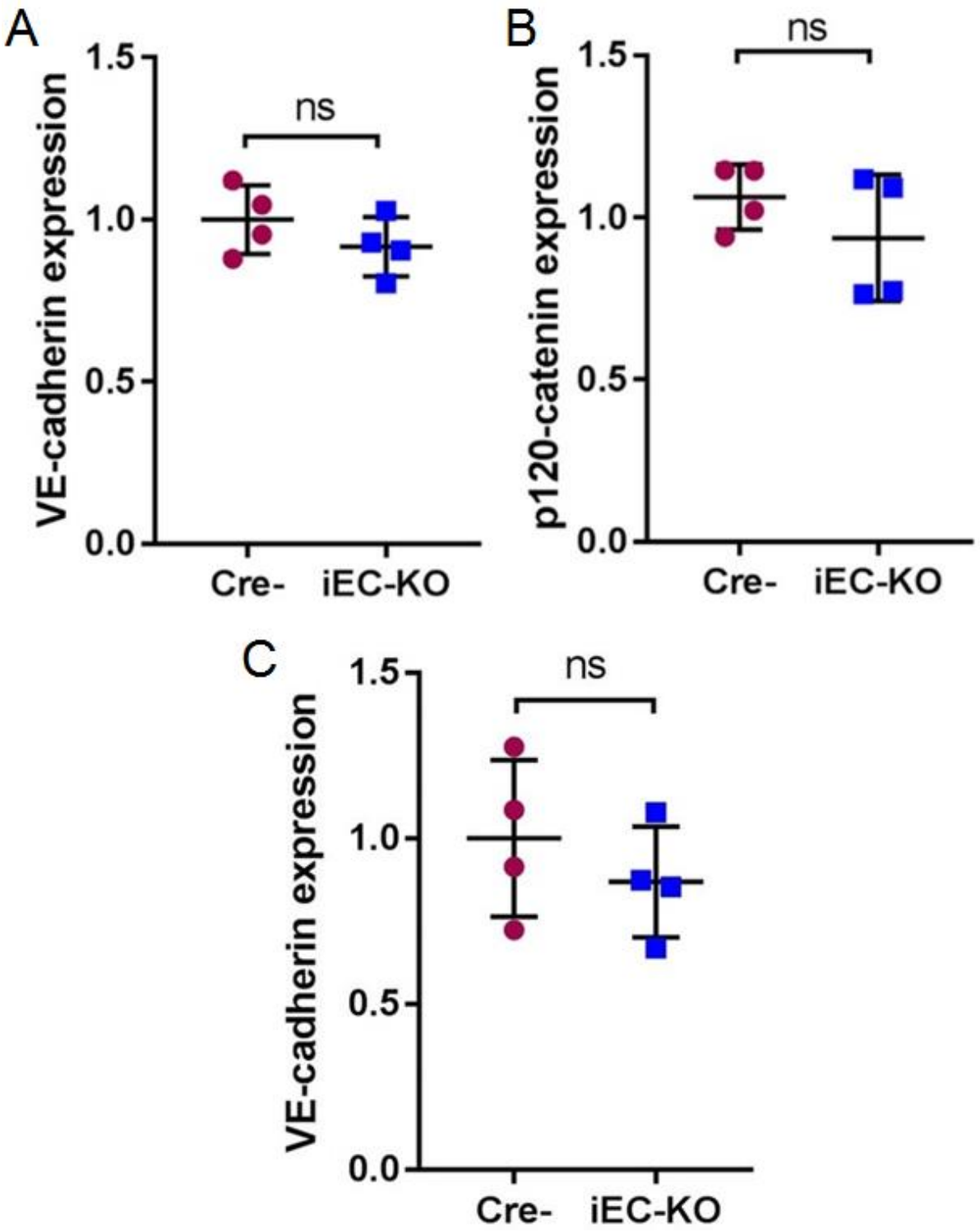

Figure 20. Quantification of VE-cadherin (A) and p120 catenin (B) expression in endothelial cells collected from lung lysates (from Figure 14) or VE-cadherin expression in cultured mouse lung endothelial cells (C, from Figure 15) normalized to expression in Cre- mice; n = 4 mice per group. Data are presented as mean ± SEM.

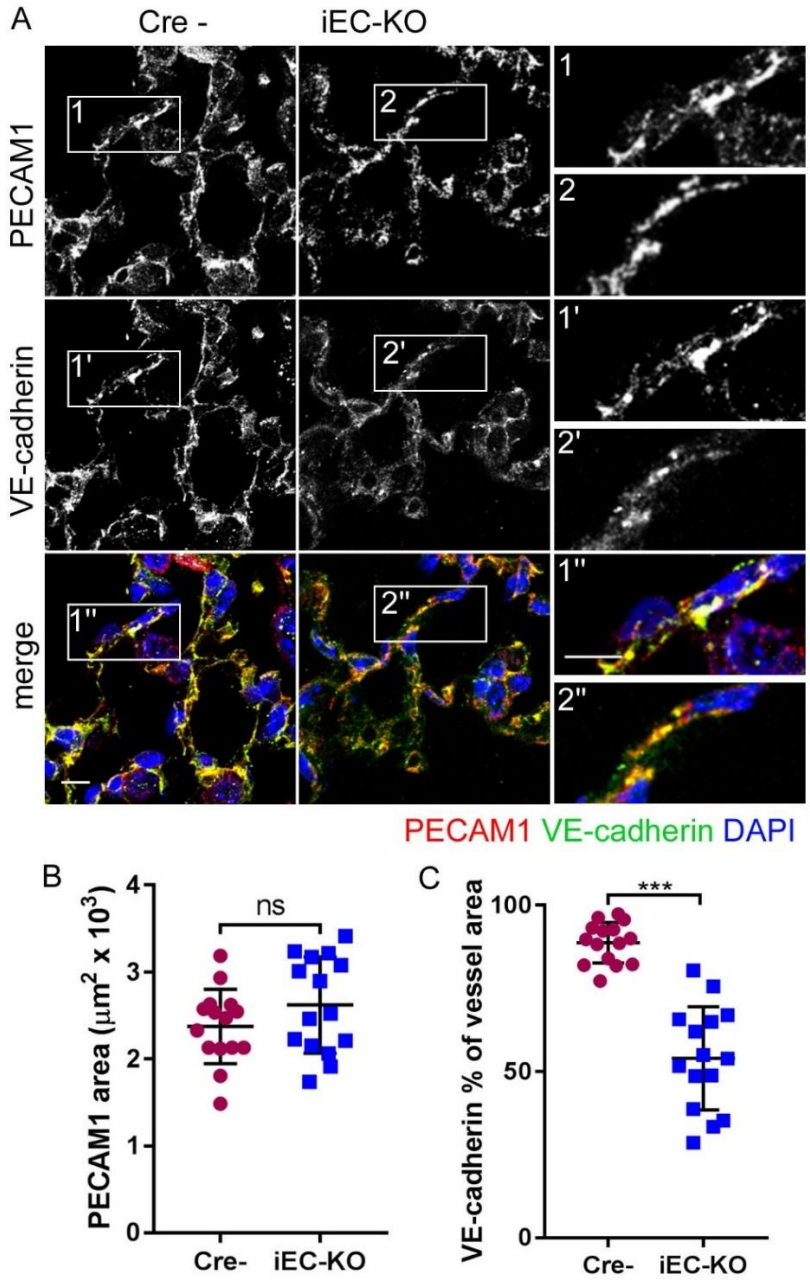

Figure 21: Loss of N-cadherin in ECs leads to decreased VE-cadherin at adherens junctions in lung. A. Representative confocal images of mouse lung sections from Cre- and *Cdh2* iEC-KO mice stained for VE-cadherin (green on merged image), PECAM1 (red), and nuclei (DAPI, blue); enlarged inserts for individual (grayscale) and merged images are shown on right and labeled as indicated. Scale bar, 10 μm, and 5 μm on inserts. VE-cadherin at PECAM1-positive junctions is reduced in *Cdh2* iEC-KO mice as compared to controls. B-C. Quantification of images in A. Vessel area is defined as PECAM1-positive staining (B). VE-cadherin adhesion area normalized to PECAM1 area (C). n = 15 images from 3 mice per group. Data are presented as mean ± SEM. Tissue fixation and sectioning done by Ying Sun.

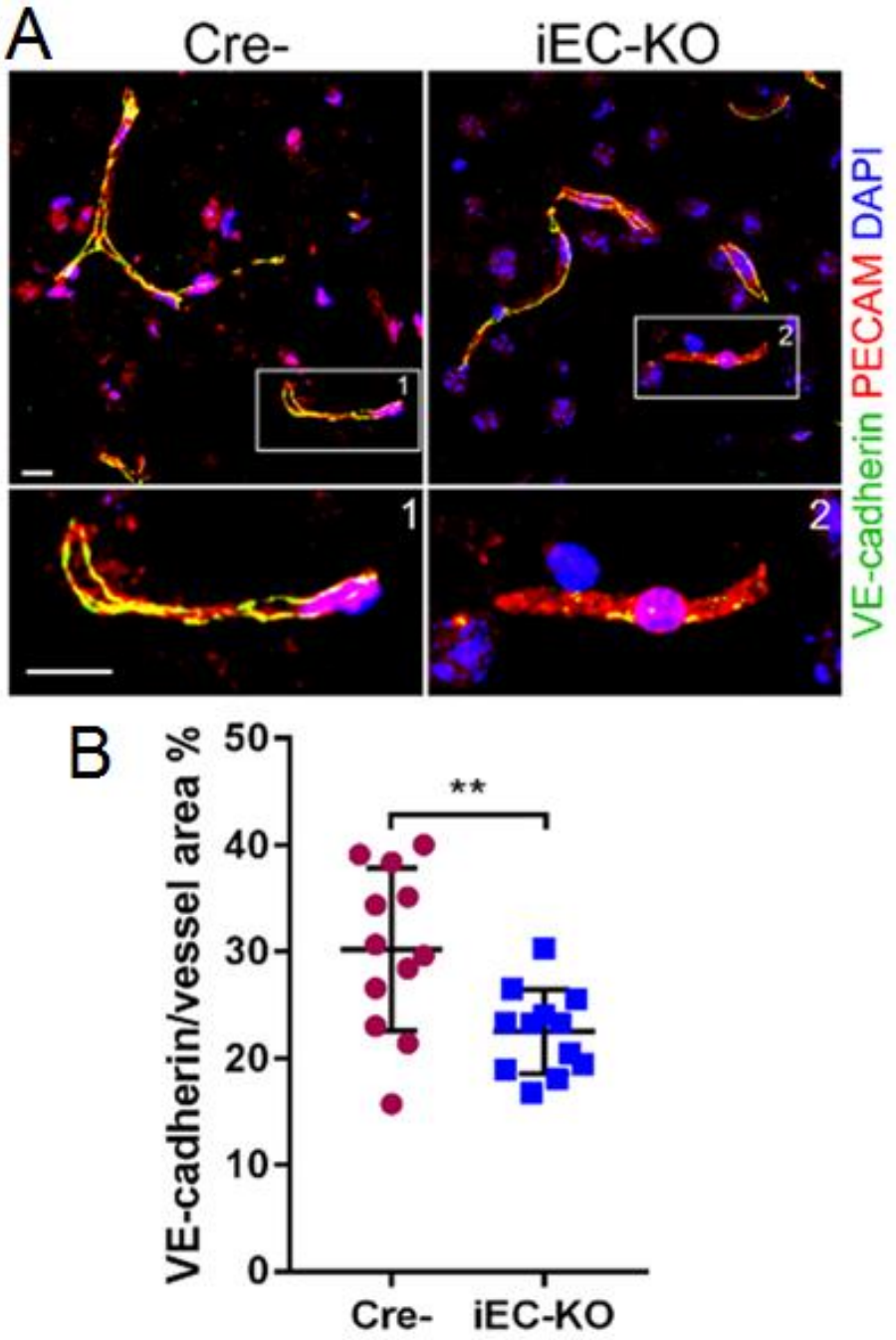

Figure 22: Loss of N-cadherin in ECs leads to decreased VE-cadherin at adherens junctions in cerebral cortex. A. Representative confocal images of mouse brain sections (cerebral cortex) from Cre- and *Cdh2* iEC-KO mice stained for VE-cadherin (green on merged image), PECAM1 (red), and nuclei (DAPI, blue); Scale bar, 10 µm. VE-cadherin at PECAM1-positive junctions is reduced in *Cdh2* iEC-KO mice as compared to controls. B. Quantification of images in A. Vessel area is defined as PECAM1-positive staining. VE-cadherin adhesion area normalized to PECAM1 area (B). n = 12 images from 3 mice per group. Data are presented as mean ± SEM. Tissue fixation and sectioning done by Shuanping Zhao. Tissue staining and imaging done by Quinn Lee.

4. N-CADHERIN REGULATES VE-CADHERIN ASSEMBLY

4.1 **N-cadherin adhesion controls VE-cadherin localization at AJs *in vitro***

In vivo, N-cadherin localizes to the abluminal surface of cells, where it interacts directly with pericytes and smooth muscle cells. However, *in vitro*, N-cadherin is expressed diffusely on the surface, and does not assemble heterotypic adhesions (Figure 23). In order to test whether N-cadherin adhesion activates discrete and heretofore unknown signaling, I have exploited biomimetic surfaces to mimic N-cadherin heterotypic adhesions that occur between endothelial cells and pericytes *in vivo* using an *in vitro* system (hereinafter N-cad-BioS; Figure 13).

To determine whether N-cad-BioS is capable of inducing N-cadherin adhesions in endothelial cells, human pulmonary arterial endothelial (HPAE) cells were grown on either N-cad-BioS or gelatin coated glass cover slips as a control. Epifluorescent microscopy showed a diffuse N-cadherin staining in HPAECs grown on either surface (Figure 24), however Total Internal Reflective Fluorescence (TIRF) microscopy revealed N-cadherin formed adhesions at the "abluminal surface" of the cell (Figure 24) suggesting that this system provides a functional platform capable of recapitulating N-cadherin interactions between pericytes and endothelial cells. Interestingly, cells grown on N-cad-BioS surfaces assembled larger VE-cadherin adhesions (Figure 25), although expression of VE-cadherin remained unchanged (Figure 26). This effect was not observed in primary lung endothelial cells lacking N-cadherin (using knockdown and knockout approaches) or plated on denatured N-cad BioS surfaces (Figure 25-27), suggesting that N-cadherin juxtacrine signaling governs assembly of larger VE-cadherin adhesions than those assembled on gelatin.

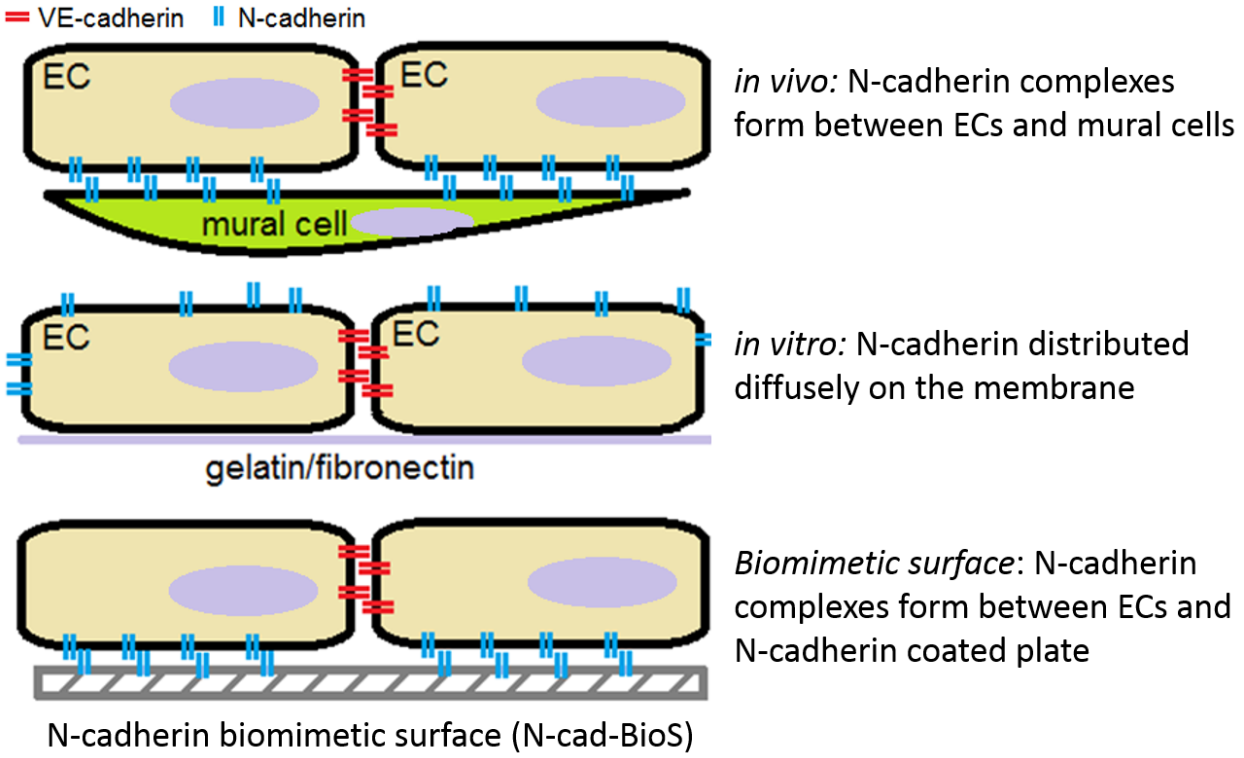

Figure 23. N-cadherin localization *in vivo*, *in vitro*, and *in vitro* using N-cadherin biomimetic surfaces (N-cad-BioS). *In vivo*, VE-cadherin forms homotypic adhesions between endothelial cells (EC), while N-cadherin forms heterotypic adhesions between ECs and mural cells (smooth muscle cells and pericytes). *In vitro*, N-cadherin is distributed diffusely along the plasma membrane and does not form adhesions. On N-cad-BioS, endogenous N-cadherin forms adhesions with the N-cadherin attached to the glass, mimicking the adhesions found between ECs and mural cells *in vivo*, which allows for the study of N-cadherin adhesion mediated signaling in ECs.

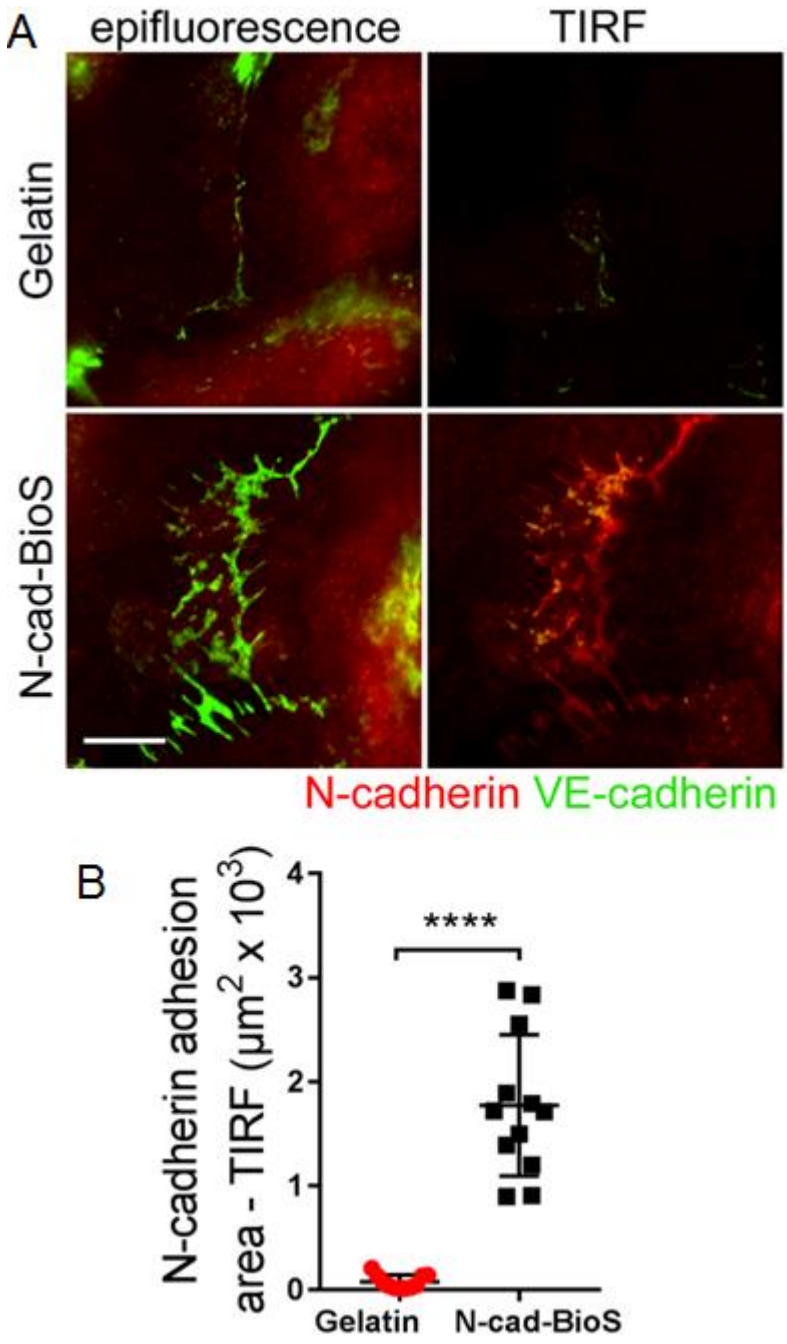

Figure 24: N-cadherin forms adhesions with N-cad-BioS. A. Immunofluorescent staining of HPAEC monolayers for VE- (green) and N-cadherin (red) proteins. Side-by-side comparison of epifluorescent and TIRF images demonstrates clustering of N-cadherin at abluminal side of the cells in HPAECs grown on N-cad-BioS but not on gelatin. Scale bar, 10 μm. Note, the N-cadherin antibody targets the cytosolic domain of N-cadherin to avoid staining of the N-cad-BioS surface. VE-cadherin is excluded from N-cadherin adhesion. B. Quantification of N-cadherin adhesion area from images in A. n = 12-15 images per group from 3 independent experiments.

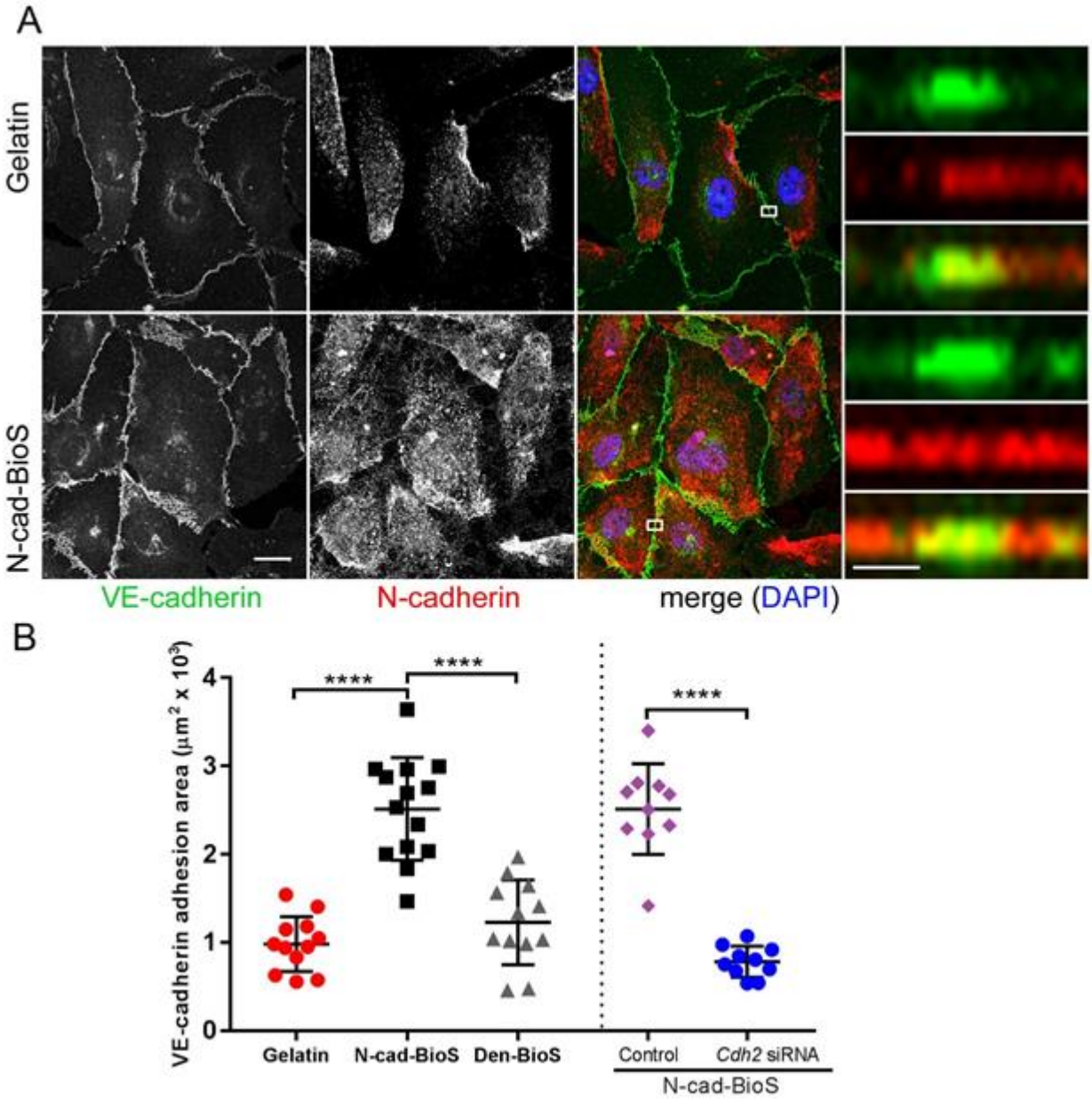

Figure 25. N-cadherin increases VE-cadherin adhesion area. A. Confocal lateral and axial (inserts) projected images of human pulmonary arterial endothelial (HPAE) cells grown on either gelatin-coated glass or N-cad-BioS and stained for VE-cadherin (green), N-cadherin (red), and DAPI (blue). Scale bar, 10 μm and 1 μm (insets). B. Quantification of VE-cadherin adhesion areas from images in A; additional groups included denatured N-cad-BioS or N-cadherin depletion. n = 10-14 images per group from 3 independent experiments. Data are shown as mean ± SEM.

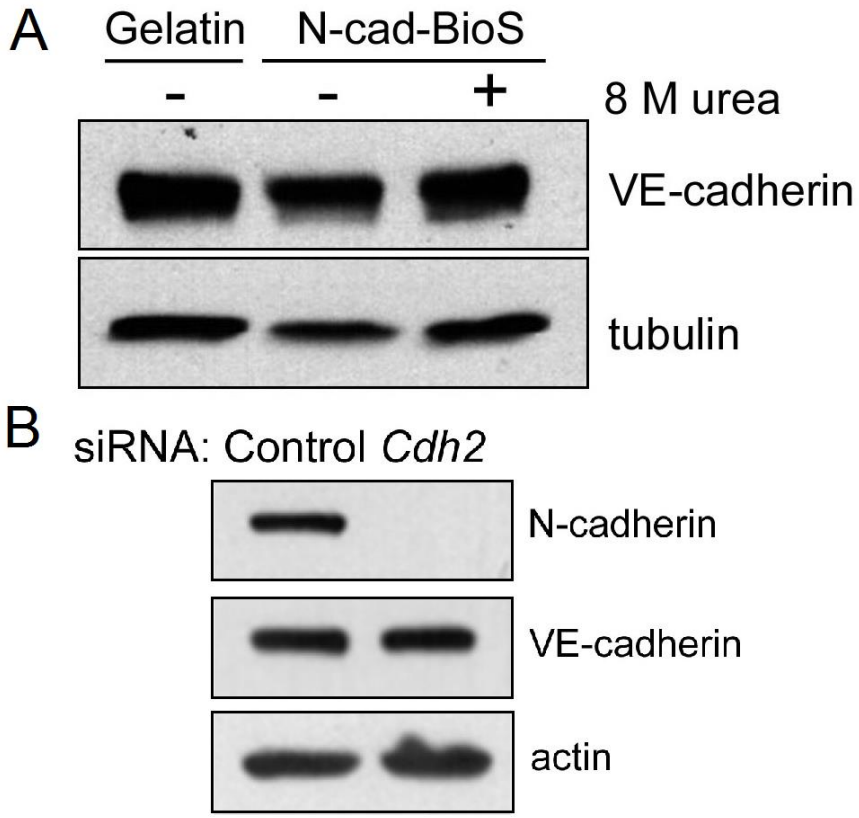

Figure 26. VE-cadherin levels do not change with activation of N-cadherin signaling or depletion of N-cadherin. A. Western blot analysis for VE-cadherin from cells grown on gelatin, N-cad-BioS, or N-cad-BioS denatured with urea. B. Western blot analysis from cells treated with either control siRNA or *Cdh2* siRNA.

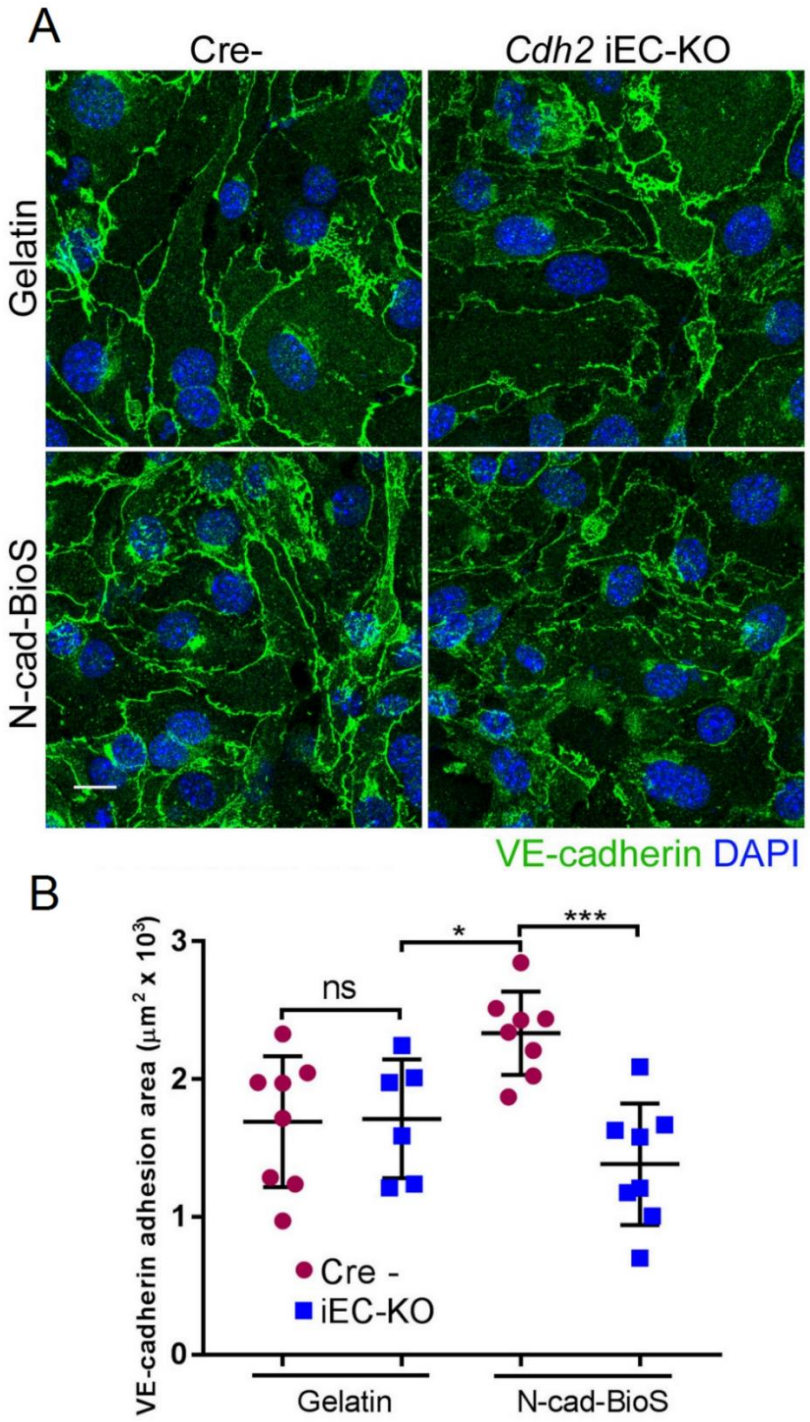

Figure 27. Genetic deletion of N-cadherin disassembles VE-cadherin adhesion. A. Confocal images of VE-cadherin (green) and nuclei (DAPI, blue) in murine endothelial cells isolated from lungs of Cre- or *Cdh2* iEC-KO mice and grown on either gelatin or N-cad-BioS. Scale bar, 10 μm. Quantification of VE-cadherin adhesion area shown in B. n=6-8 images from 2 mice per group. Data are presented as mean ± SEM. Isolation of mouse lung ECs performed by Ying Sun.

4.2 **N-cadherin adhesion controls junctional permeability through the assembly of VE-cadherin junctions**

To determine whether the larger VE-cadherin adhesions observed downstream of N-cadherin signaling correlate with decreased permeability, we added fluorescently labeled albumin to the apical surface of HPAECs expressing VE-cadherin-GFP and recorded the fluorescent intensity in the junction area over time (Figure 28). VE-cadherin junctions in cells grown on N-cadherin biomimetic surfaces showed reduced permeability to albumin over time which correlated with the increased VE-cadherin junctions on N-cadherin biomimetic surfaces, suggesting N-cadherin restricts endothelial permeability by increasing VE-cadherin adhesion area.

4.3 **N-cadherin controls VE-cadherin dynamics *in vitro***

To further interrogate the effect of N-cadherin signaling on AJs, I assessed the rates of VE-cadherin recruitment to, and internalization from, AJs using the photo-convertible fluorescent probe Dendra2 tagged to the C-terminus of VE-cadherin (Figure 29). By photoconverting a region of VE-cadherin from green to red, I can track new VE-cadherin (green) being recruited to adherens junctions while simultaneously tracking VE-cadherin (red) moving away from junctions, which yields the association and dissociation rates, respectively. I observed significantly faster recruitment of VE-cadherin to AJs in endothelial cells grown on N-cad-BioS as compared to gelatin (Figure 29), while the rates of VE-cadherin dissociation from the junction were unchanged. Additionally, the lateral diffusion rate was unchanged (Figure 30), suggesting that only recruitment of VE-cadherin to junctions is the critical factor affecting junction size. Based on these data, I concluded that the steady-state assembly of VE-cadherin adhesion is controlled by N-cadherin juxtacrine signaling.

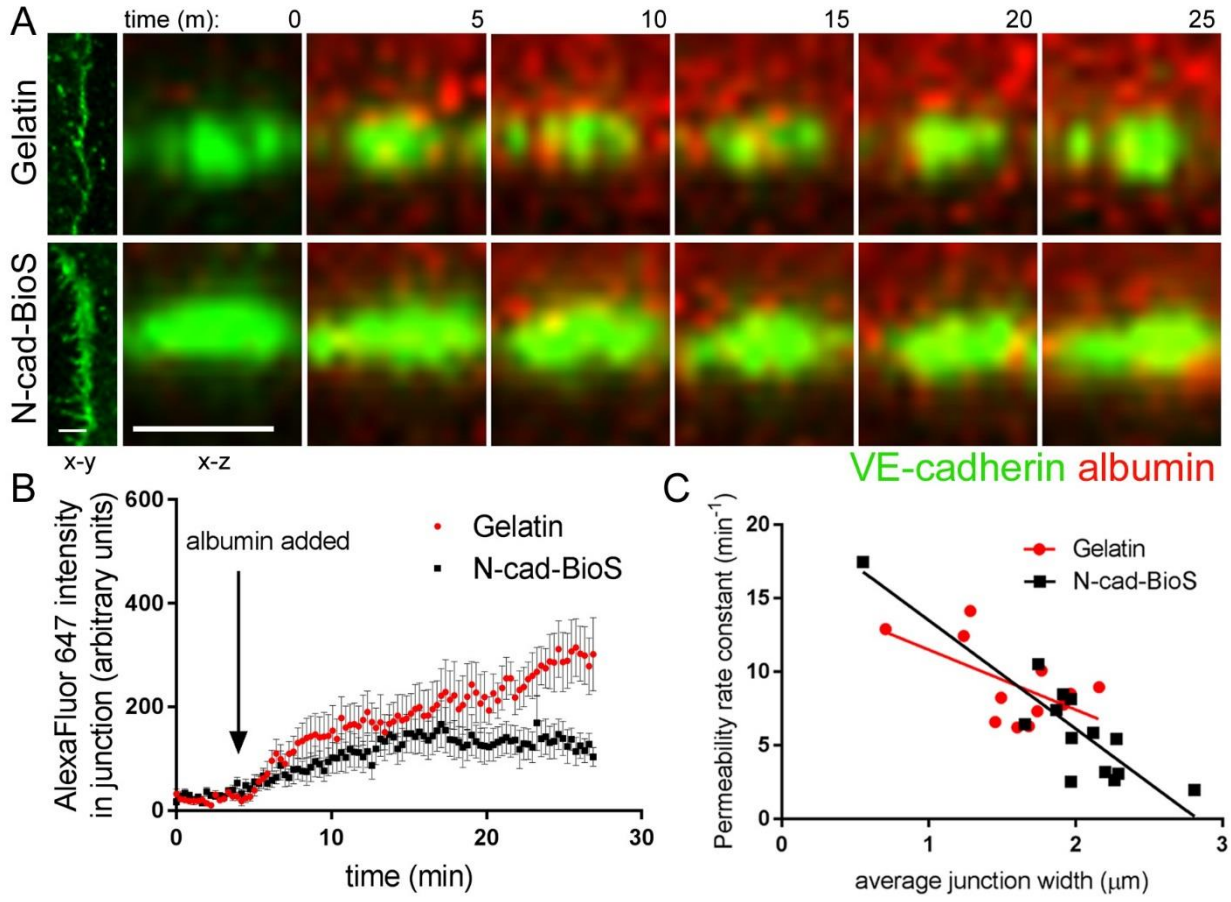

Figure 28. N-cadherin adhesion-mediated signaling restricts permeability of paracellular route to albumin. A. Confocal live cell imaging of HPAECs expressing VE-cadherin-GFP (green) showing albumin-Alexa-Fluor647 (red) permeation across AJs. X-Y (left) and X-Z (enlarged, shown over time) sectional area of VE-cadherin-GFP junction. Albumin-AlexaFluor 647 was apically added at 5 minutes. Time is shown in min; scale bar = 5 μm. B. Measurement of the average fluorescent intensity of albumin-AlexaFluor 647 within VE-cadherin-GFP junction over time. Fluorescence was normalized to the starting fluorescent intensity prior to addition of albumin-AlexaFluor 647. C. Graph showing relationship between junction width (average) and the permeability rate constant from B. The permeability rate constant was found by fitting the data in B to a non-linear one phase association equation (see Methods). Permeability inversely correlated with the junction width. B-C; data are presented as mean ± SEM; n = 12-14 junctions from 3 independent experiments.

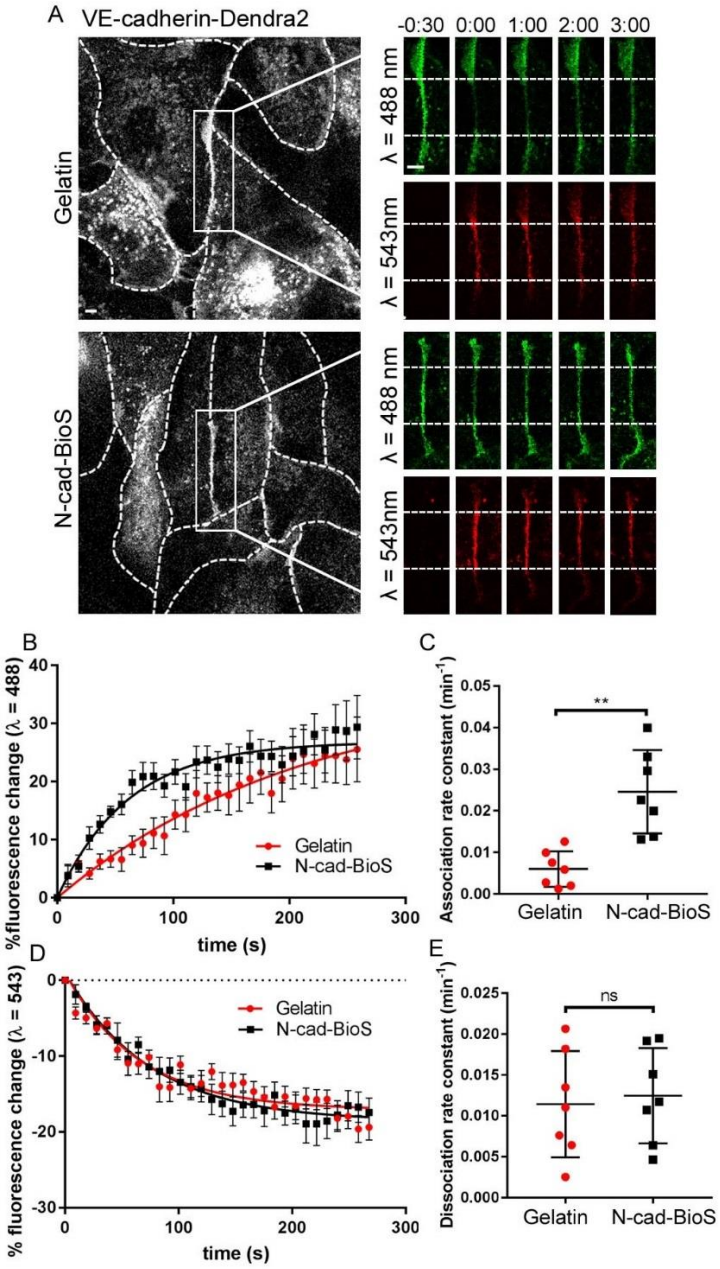

Figure 29. N-cadherin increases VE-cadherin association rate to membrane. A. Time-lapse images of VE-cadherin–Dendra2 before and after photoconversion at t=0 within the irradiation zone (indicated by area between dashed lines on inserts) in HPAECs grown on either gelatin or N-cad-BioS. Images collected at λ=488 nm (green) show unconverted VE-cadherin, and photoconverted VE-cadherin at λ=543 nm (red). Dashed lines of grayscale images outline cell borders. Scale bar, 5 μm; time is shown in minutes. B-C. The rate of VE-cadherin association to AJs (B) and the association rate constant (*k*) was calculated by using non-linear regression (R^2 = 0.404 for gelatin and 0.439 for N-cadherin) (C) in cells grown on gelatin or N-cad-BioS; n = 7 cells per group. D-E. The rate of VE-cadherin dissociation from AJs (D) and the dissociation rate constant (E) in cells grown on gelatin or N-cad-BioS (R^2 = 0.577 for gelatin and 0.573 for N-cadherin); n = 7 cells per group from 3 independent experiments. Data are presented as mean ± SEM.

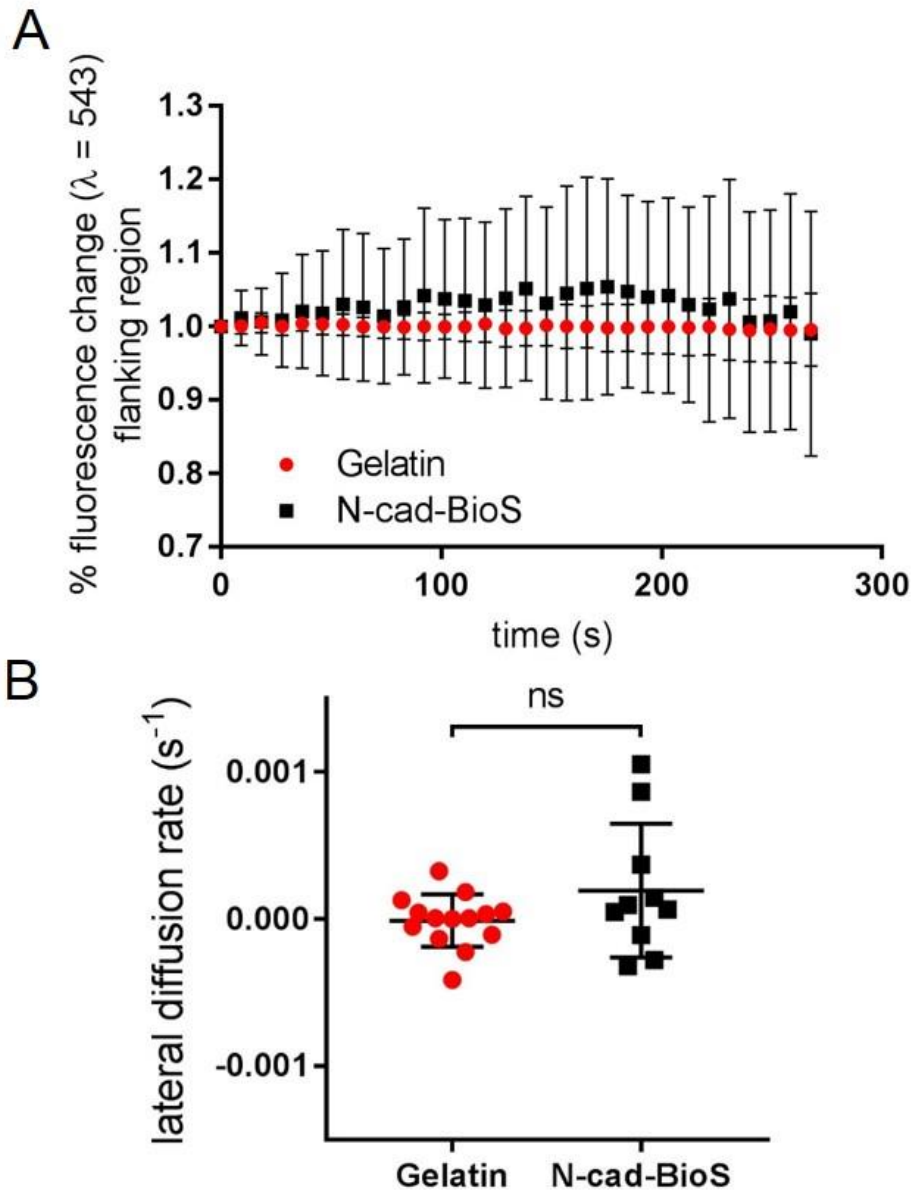

Figure 30. N-cadherin does not change VE-cadherin lateral diffusion. A. The lateral diffusion is the rate at which photoconverted VE-cadherin moves into a flanking region (adjacent to the photoconverted region) after photoconversion, normalized to the initial fluorescence in the flanking region. The lateral diffusion rate is defined as the slope of the fluorescent signal over time. n = 11-14 junctions from 3 independent experiments. Data are presented as mean ± SEM.

5. N-CADHERIN CONTROLS VE-CADHERIN ASSEMBLY THROUGH TRIO

5.1 **Isolation and network analysis of novel N-cadherin binding partners**

To glean a holistic picture of N-cadherin juxtacrine signaling, I isolated N-cadherin adhesion complexes formed in primary human pulmonary endothelial cells using a technique I developed (Figure 31). The His-tagged extracellular domain of N-cadherin was covalently linked to Ni-NTA beads using the cross linker EDC/NHS, which prevents the exogenous protein from contaminating the sample after boiling, allowing for the detection of only endogenous proteins. N-cadherin coated beads were added to endothelial cells in culture, the constituents of N-cadherin adhesion were reversibly crosslinked, and the isolated complexes were analyzed using semi-quantitative mass spectrometry. Denatured N-cadherin beads were used as a control. Analysis of N-cadherin complexes reveled recruitment of α-, β-, β-like, and p120-catenins, canonical members of the "cadhesome", to N-cadherin adhesions (Zaidel-Bar, 2013), thereby validating my method (Figure 32). In addition, I discovered several actin-binding proteins including the members of Arp2/3 complex, coronin, cortactin, capping proteins, Epithelial protein lost in neoplasm (*EPLIN*), α-actinin, myosin IIc, and tropomyosin 1-4 as proteins of the N-cadherin adhesion complex (Figure 32). These data indicate that N-cadherin adhesion complexes are involved in assembly of the actin cytoskeleton at the "abluminal surface" of endothelial cells.

5.2 **N-cadherin forms a complex with Trio**

In addition, several GAPs and GEFs for small RhoGTPases were recruited to the N-cadherin adhesion complex (Figure 32). Gene Ontology analysis of N-cadherin adhesion complexes and known N-cadherin interactions suggested associations with several signal transduction processes including RhoA signal pathways (Figure 33). Both Trio, a Rho guanine

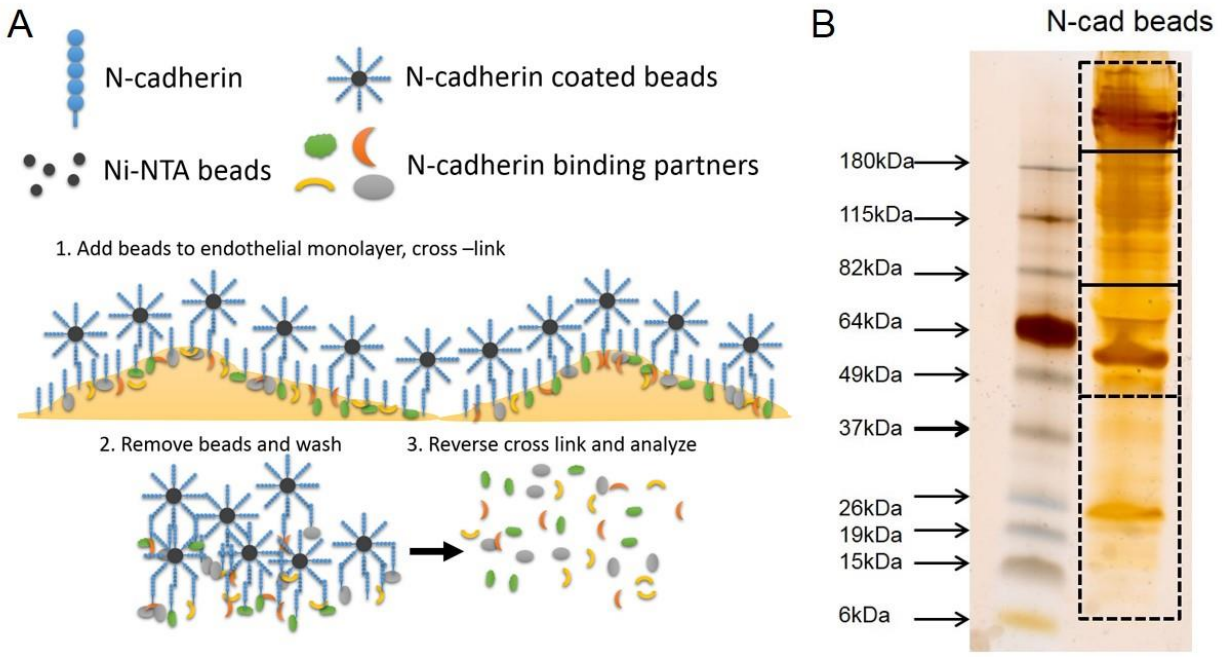

Figure 31. A. Schematic representation of method for isolation of N-cadherin complexes. N-cadherin coated Ni-NTA beads were added to a monolayer of endothelial cells and allowed to form adhesions. N-cadherin adhesions complexes were cross linked to beads using DTSP. Cells were lysed and washed, and the cross link was reversed using dithiothreitol. Samples were separated using SDS-PAGE (B) and were submitted for mass spectrometry analysis. Dashed lanes indicate individual samples used for mass spectrometry. Silver stain gel done by Bao-Shiang Lee.

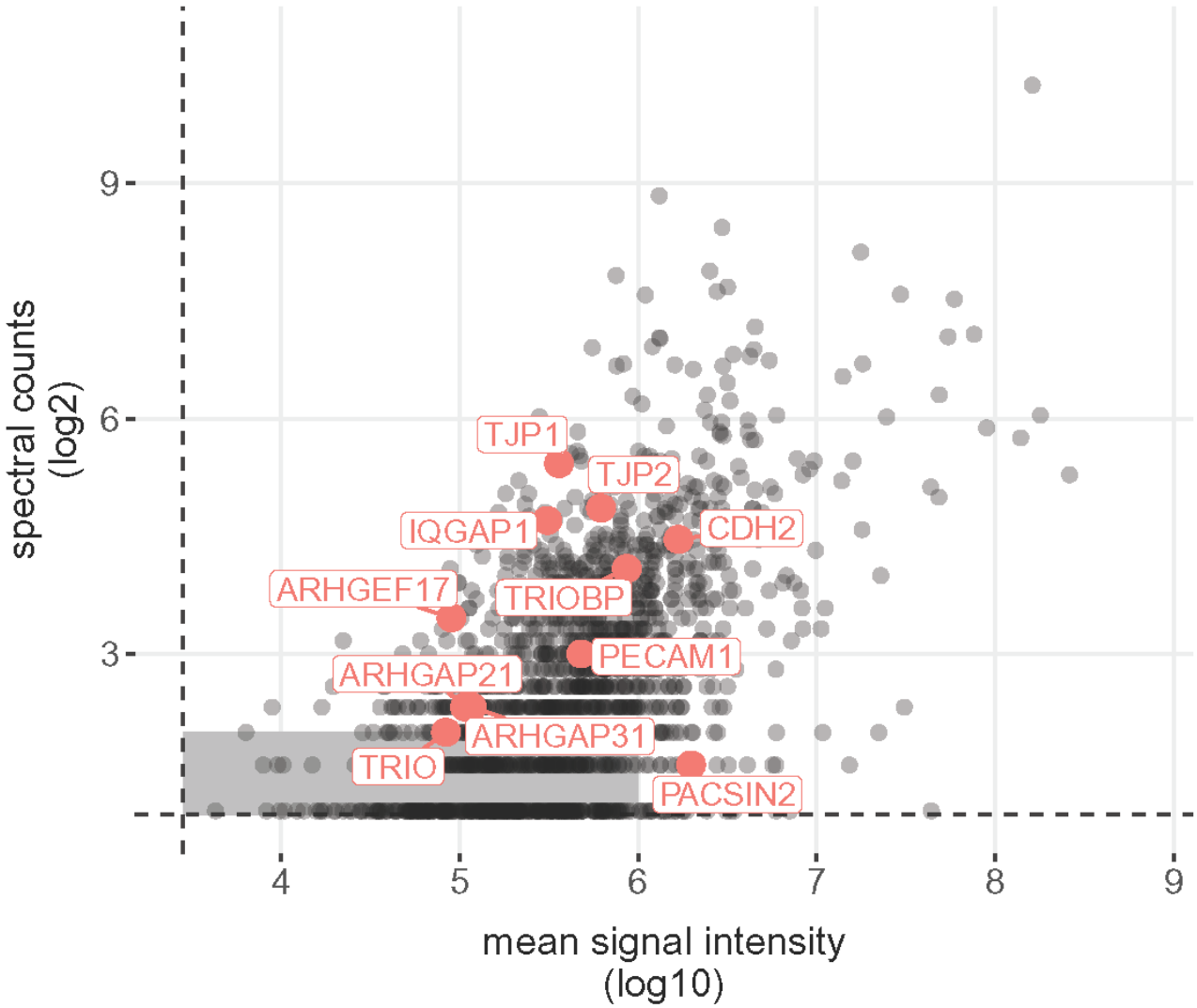

Figure 32. N-cadhesome detected by mass spectrometry assay. A scatter plot of mean intensity vs spectral counts for isolated N-cadherin complexes. Proteins excluded due to low confidence are indicated by the gray box. Analysis of mass spectrometry data performed by Jeff Klomp.

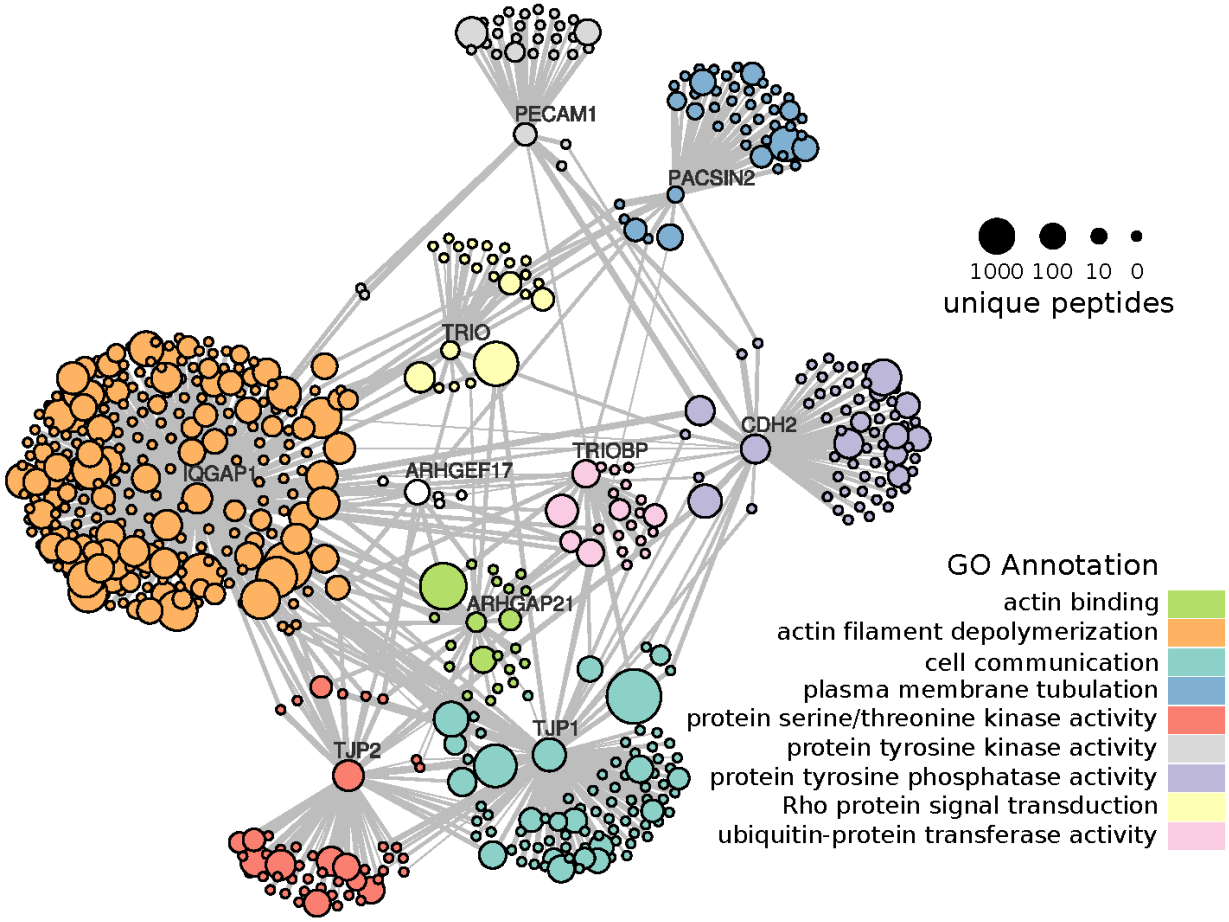

Figure 33. Clustering of N-cadhesome interaction networks detected by mass spectrometry assay. Interaction network for proteins of interest highlighted in Figure 32 with clusters established based on individual protein interaction profiles (see Materials and Methods). Gene Ontology associations were based on a hypergeometric test ($p < 1e^{-12}$). Size of dot indicates number of unique peptides found for each protein. Gene ontology associations performed by Jeff Klomp.

nucleotide exchange factor (GEF) for both Rac1 and RhoA (Debant et al., 1996), and Trio and actin-binding protein (Triobp) were detected as constituents of the N-cadherin adhesion complex (Figure 33). We chose to investigate the role of Trio due to its involvement in formation of VE-cadherin adhesions (Timmerman, et. al. 2015). While Trio has been shown to interact with several cadherins, this is the first recorded interaction between N-cadherin and Trio. As Trio can activate either Rac1 or RhoA, which generally are considered to have opposite effects in endothelial cells, it seemed an interesting candidate to investigate in the context of N-cadherin adhesion mediated signaling. I have validated recruitment of Trio to N-cadherin adhesion complexes using both biochemical and confocal microscopy analyses (Figure 34-35). In my system, both the full-length protein and N-terminus truncated mutant (N-terminal portion of Trio consisting of spectrin-like repeats and GEF1 domain responsible for Rac1 activation) co-localize with N-cadherin adhesion clusters at the "abluminal surface" of endothelial cells (Figure 35). The intracellular domain of VE-cadherin was reported to bind the N-terminal portion of Trio (Timmerman, et. al. 2015), and as N-cadherin shares many of the same binding domains of VE-cadherin, it is likely that a similar site on N-cadherin binds Trio. Additionally, this interaction takes place underneath AJs, suggesting the assembly of a possible compartmentalized signaling complex which may contain N-cadherin, Trio, and VE-cadherin. These data indicate that Trio is a constituent of N-cadherin complexes and is recruited directly or indirectly through interaction with the Trio N-terminus domain.

5.3 **The N-cadherin – Trio complex controls VE-cadherin localization *in vitro***

In order to determine if Trio is required for assembly of VE-cadherin adhesion downstream of N-cadherin juxtacrine signaling *in vitro*, I used an siRNA knockdown approach to deplete Trio in endothelial cells. While Trio depletion had no apparent effect on the adhesion area of VE-cadherin in cells grown on gelatin, it resulted in a significant reduction in VE-cadherin adhesive area in

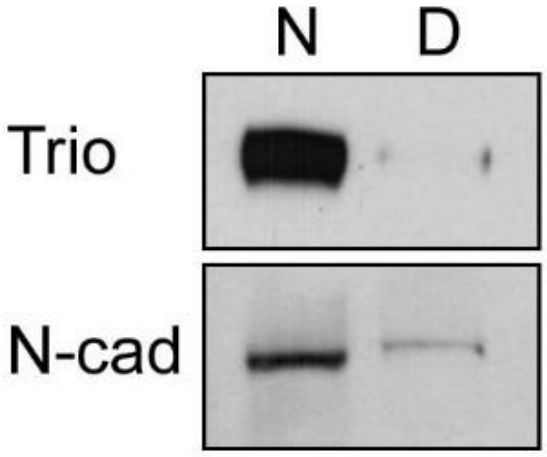

Figure 34. The RhoGEF Trio is recruited to N-cadherin adhesion complexes. Western blot analysis of isolated N-cadherin complexes for endogenous N-cadherin and Trio proteins. HPAE cells were incubated with either N-cad-BioS beads (N) or denatured N-cad-BioS beads (D) for 1 hour; N-cadherin complexes were collected and process as described in Materials and Methods. Western blot done by Fei Huang.

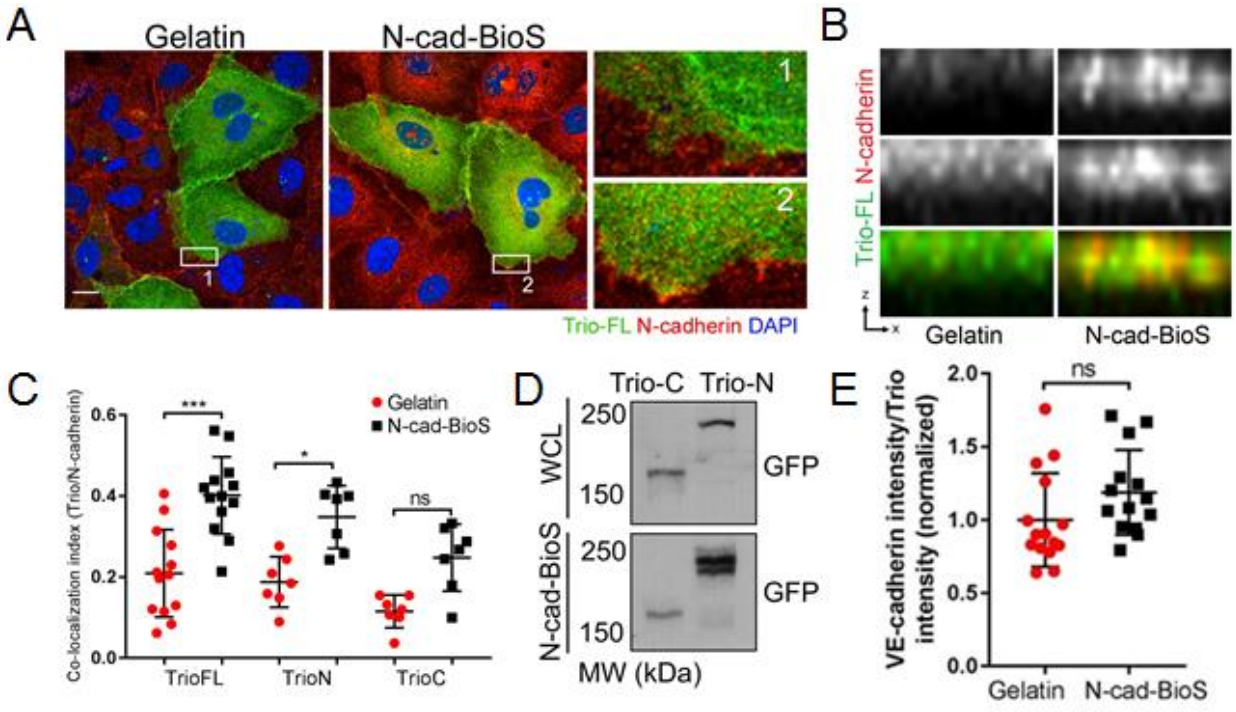

Figure 35. The RhoGEF Trio is recruited to N-cadherin adhesion complexes. Confocal lateral (A, insets) and axial (B) images of exogenously expressed full length (FL) GFP-Trio. Cells were stained for N-cadherin (red) and nuclei (DAPI; blue). Enlarged inserts are shown on right; Scale bar, 10µm. C. Co-localization coefficient of N-cadherin clusters with GFP-Trio-FL (shown in A, MW 354 kDa), GFP-Trio-N (N terminus, MW 221 kDa), and GFP-Trio-C (C-terminus, MW 159 kDa). The colocalization coefficient was calculated as the sum of positive pixels for both N-cadherin and Trio divided by the total number of N-cadherin positive pixels. D. Western blot analysis of GFP-Trio deletion mutants expressed in endothelial cells; whole cell lysates (WCL) and isolated N-cadherin complexes (N-cad-BioS) indicate preferential recruitment of GFP-Trio-N to N-cadherin complexes. E. Trio fluorescent intensity normalized to VE-cadherin fluorescent intensity at AJs in cells expressing GFP-Trio-FL and stained with VE-cadherin. Formation of the Trio-N-cadherin complex did not change the association of Trio with VE-cadherin junctions. n = 15 cells per condition from 3 independent experiments. Data are presented as mean ± SEM.

cells grown on N-cad-BioS (Figure 36), indicating a specific role of Trio in the mechanism of N-cadherin juxtacrine signaling. Additionally, these effects were mirrored by using the small molecule inhibitor ITX3, which specifically blocks the interaction between Rac1 and the GEF1 domain of Trio (Figure 37). Furthermore, overexpression of Trio GEF1 "dead" mutant (Trio-D1d) only partially restored VE-cadherin adhesion area in Trio-depleted cells whereas overexpression of GEF2 "dead" mutant (Trio-D2d) had no effect (Figure 38). However, overexpression of full length GFP-Trio in either control or Trio siRNA-depleted cells significantly increased VE-cadherin adhesion area as compared to cells overexpressing GFP alone. These findings together show that the activities of both GEF1 and GEF2 domains of Trio are essential for assembling VE-cadherin junctions downstream of N-cadherin adhesion-mediated signaling. Cumulatively, these data suggest that GEF1 activity towards Rac1 is required for the observed effect of Trio.

5.4 **The N-cadherin – Trio complex controls assembly of VE-cadherin adhesion *in vitro***

In order to determine if Trio is required downstream of N-cadherin adhesions to increase VE-cadherin association rate to the membrane, I depleted Trio in cells expressing VE-cadherin Dendra2. Loss of Trio significantly reduced the rate of VE-cadherin recruitment to AJs in cells grown on N-cad-BioS platforms (Figure 39) but not in cells grown on gelatin (Figure 40). Interestingly, Trio depletion had no effect on the rate of VE-cadherin internalization in cell grown on either N-cad-BioS platforms or gelatin. Again, the above-mentioned effects of Trio depletion were mirrored by inhibiting the interaction of Trio with Rac1 (Figure 41) using ITX3 (Bouquier et al., 2009). Together, these data indicate a specific role of the N-cadherin – Trio circuit in the assembly of VE-cadherin adhesions and the mechanism of endothelial barrier function.

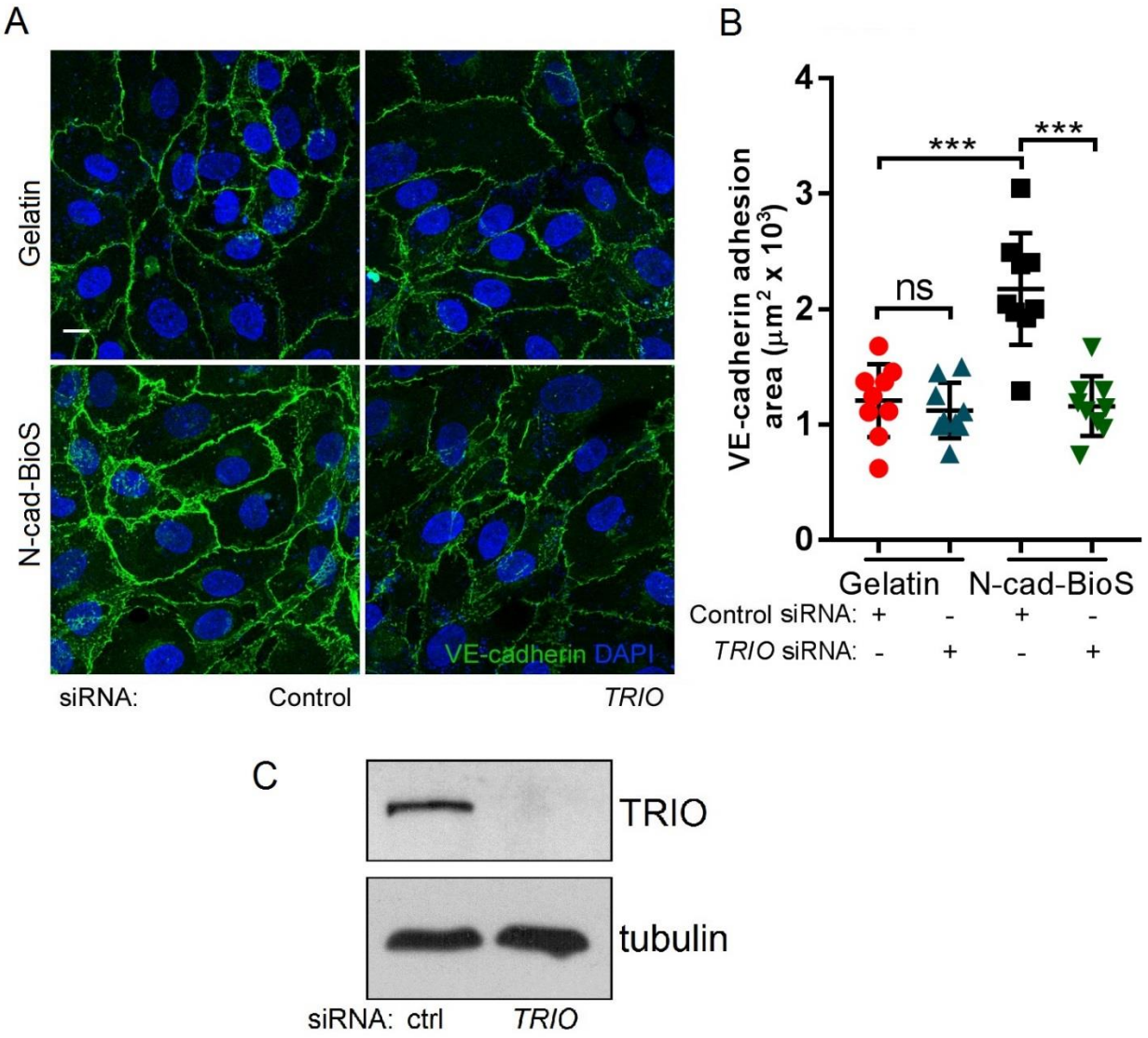

Figure 36. Trio is required for increased VE-cadherin adhesion area downstream of N-cadherin juxtacrine signaling. A. Projected images of HPAECs grown on either gelatin coated glass or N-cad-BioS after depletion of Trio with siRNA or treatment with control siRNA. Cells were stained for VE-cadherin (green) and nuclei (DAPI, blue). Scale bar, 10 μm. B. Quantification of VE-cadherin adhesion area. Note, depletion of Trio significantly reduced VE-cadherin adhesion area only in cells grown on N-cad-BioS. n=9 fields from 3 independent experiments. C. Western blot confirmation of Trio depletion in HPAECs. Data are presented as mean ± SEM.

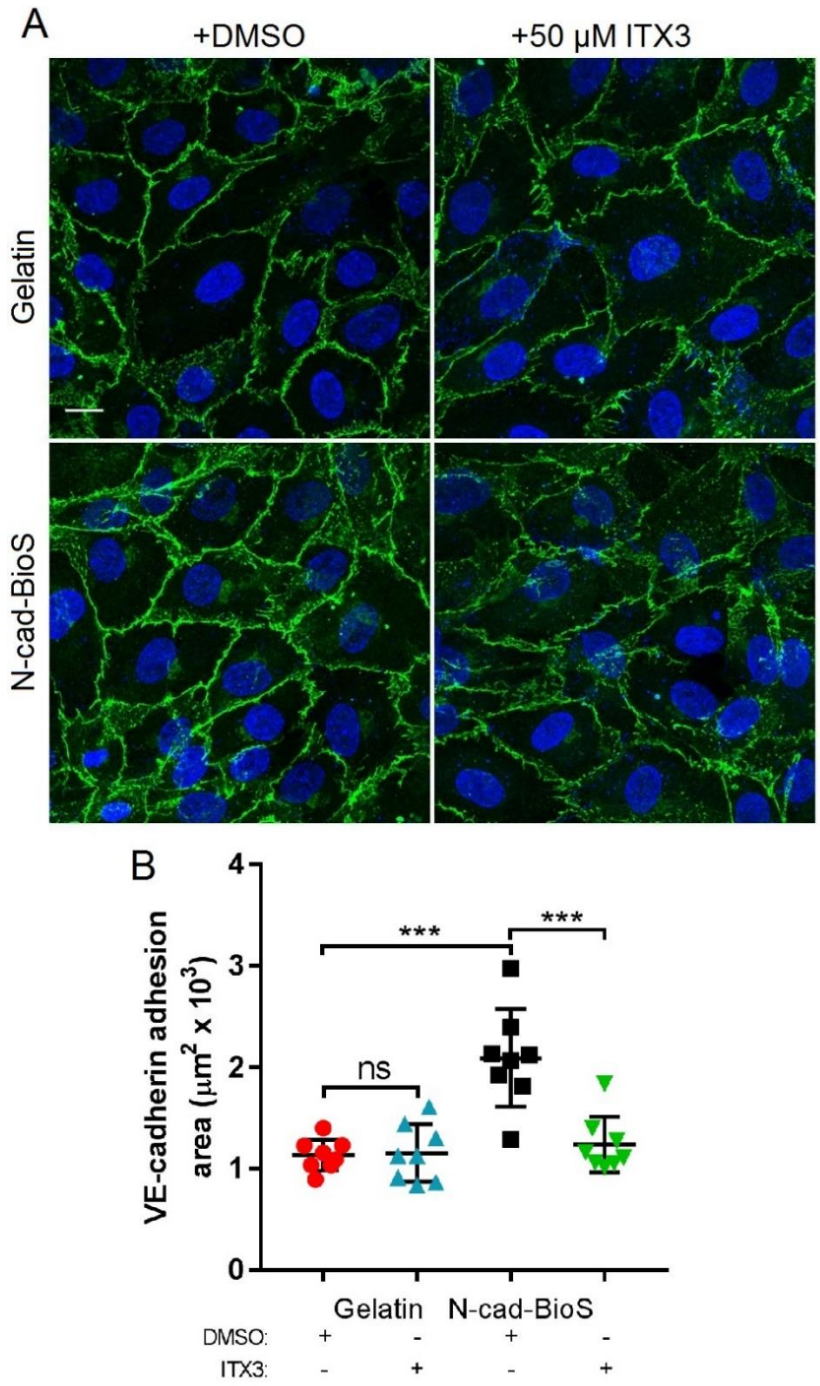

Figure 37. Trio GEF activity is required for increased VE-cadherin adhesion area downstream of N-cadherin juxtacrine signaling. A. Projected images of HPAECs grown on either gelatin coated glass or N-cad-BioS and treated with 50 μm ITX3 or DMSO as a control. Cells were stained for VE-cadherin (green) and nuclei (DAPI, blue). Scale bar, 10 μm. B. Quantification of VE-cadherin adhesion area after treatment with ITX3. Note, inhibition of Trio significantly reduced VE-cadherin adhesion area only in cells grown on N-cad-BioS. n=8 fields from 3 independent experiments. Data are presented as mean ± SEM.

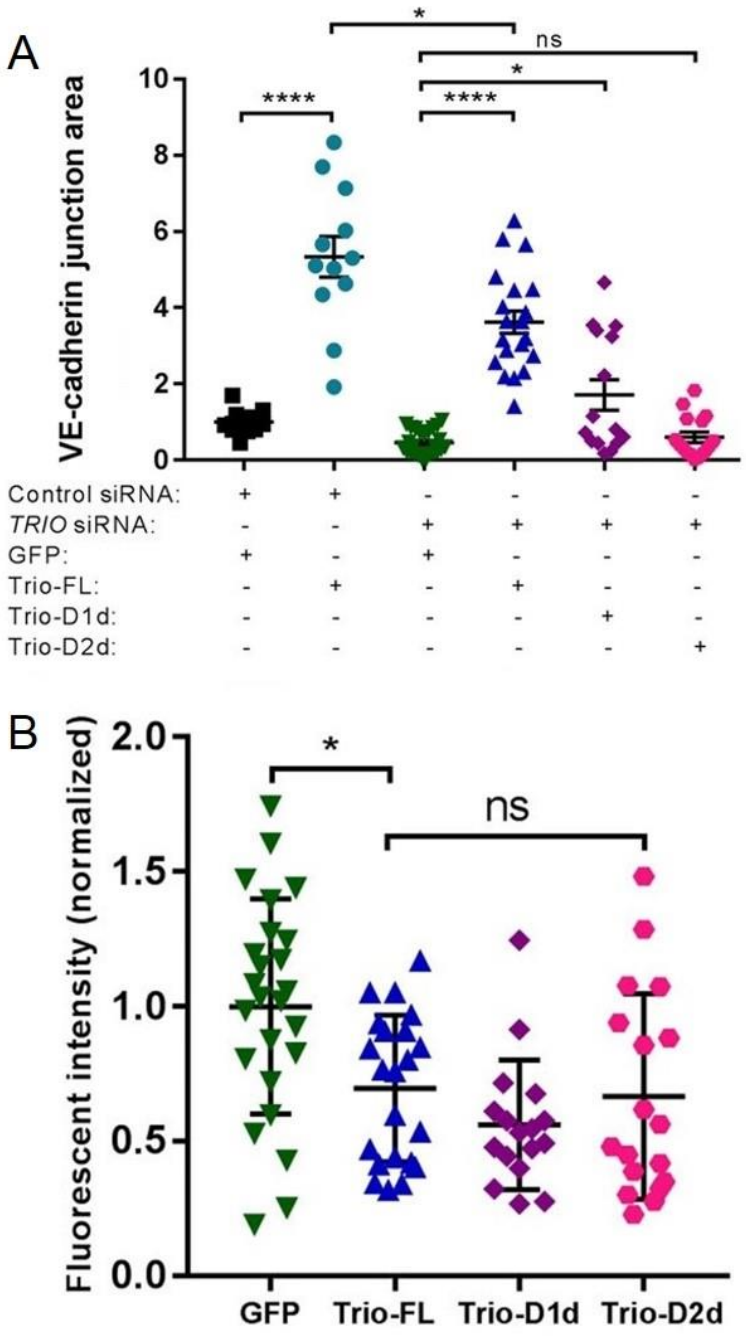

Figure 38. Both Trio domains are required to rescue VE-cadherin adhesion area. A. Quantification of VE-cadherin junction area (for cells expressing GFP or GFP-Trio) following overexpression of GFP alone, full length (FL) GFP-Trio-FL, GEF domain 1 "dead" (Trio-D1d) and GEF domain 2 "dead" (Trio-D2d) mutants. Loss of VE-cadherin after Trio depletion was rescued by overexpressing FL Trio-GFP and partially with GEF1 but not GEF2 "dead" Trio mutants. B. Normalized ratio of GFP fluorescent intensity from cells expressing GFP, GFP-Trio-FL, and GFP-Trio mutants. n= 12 - 25 images per condition from 3 independent experiments. Data are presented as mean ± SEM.

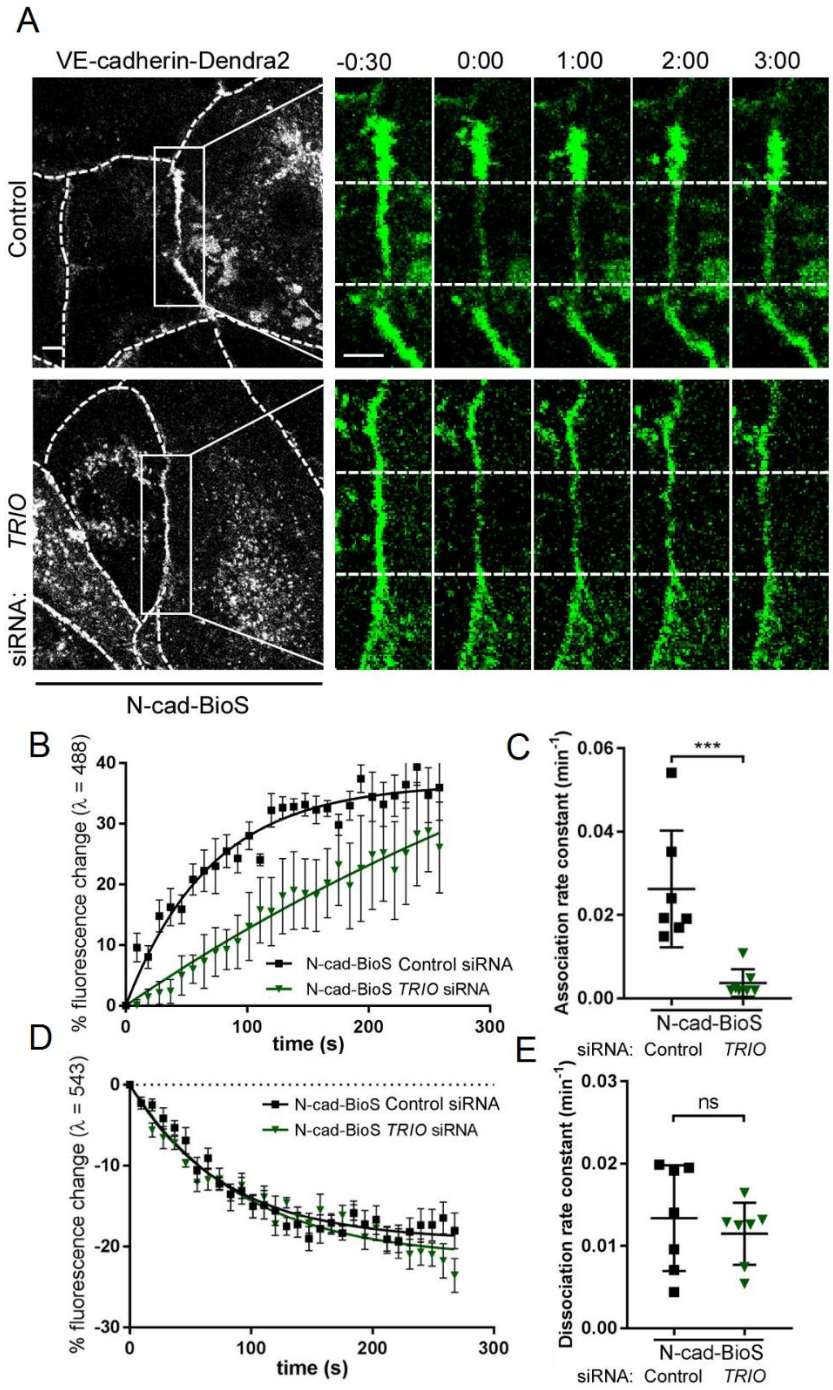

Figure 39. Depletion of Trio decreases VE-cadherin association rate downstream of N-cadherin juxtacrine signaling. Time-lapse images of VE-cadherin–Dendra2 before and after photoconversion at t=0 within in HPAECs grown on N-cad-BioS after depletion of Trio. Dashed lines of grayscale images outline the cell borders. Scale bar, 5 μm; time is shown in minutes. The rate of VE-cadherin association to AJs (B) and the association rate constant (C). n = 7 cells per group. The rate of VE-cadherin dissociation from AJs (D) and the dissociation rate constant (E). n = 7 cells per group from 3 independent experiments. Data are presented as mean ± SEM.

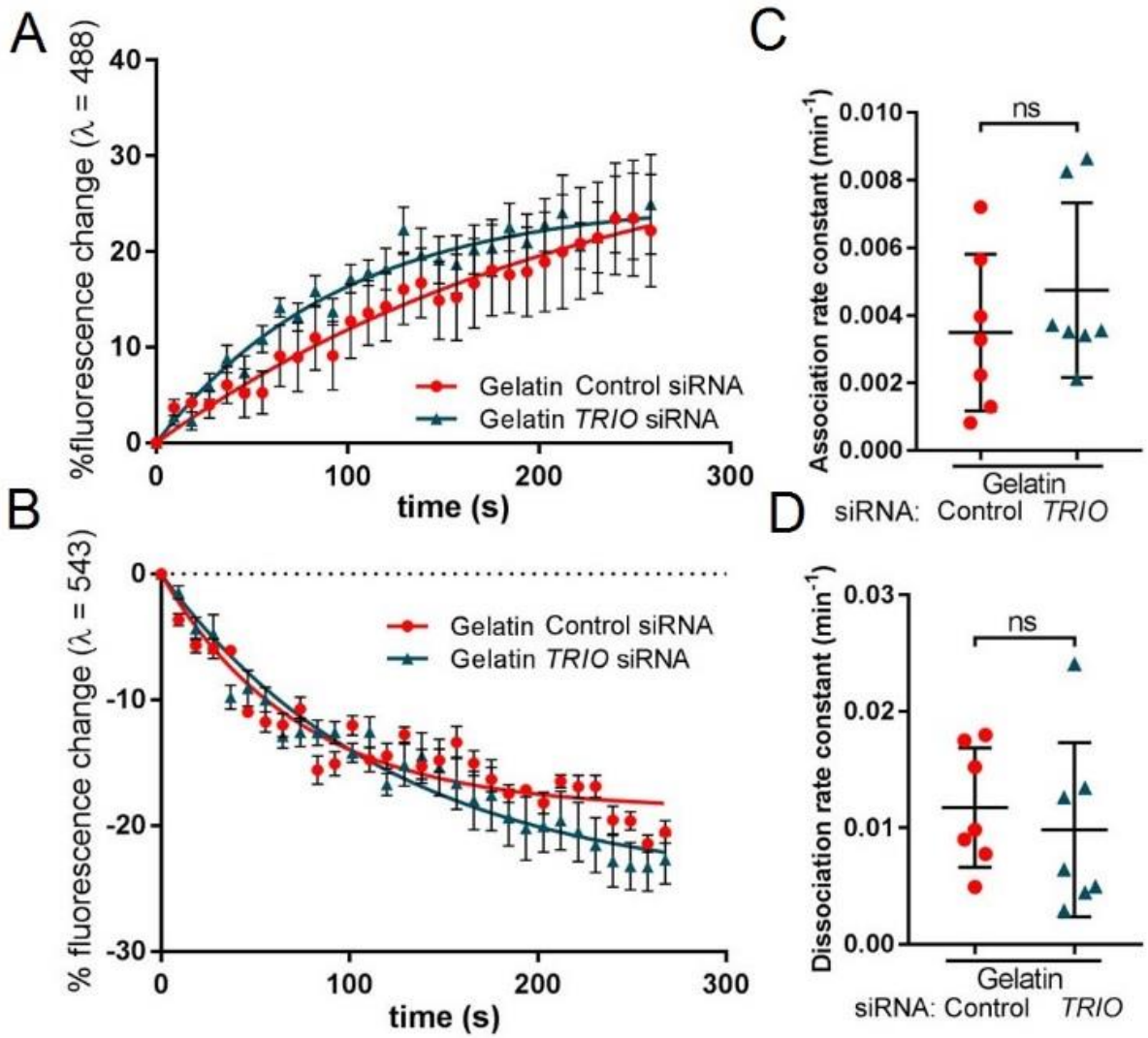

Figure 40. Depletion of Trio has no effect on association or dissociation rates for cells grown on gelatin. A-B. The rate of VE-cadherin association to AJs (A) and the association rate constant (B) in cells grown on gelatin after depletion of Trio or treatment with control siRNA; n = 7 cells per group; ns, non-significant. C-D. The rate of VE-cadherin dissociation from AJs (C) and the dissociation rate constant (D) in cells grown on gelatin after depletion of Trio or treatment with control siRNA. n = 7 cells per group from 3 independent experiments. Data are presented as mean ± SEM.

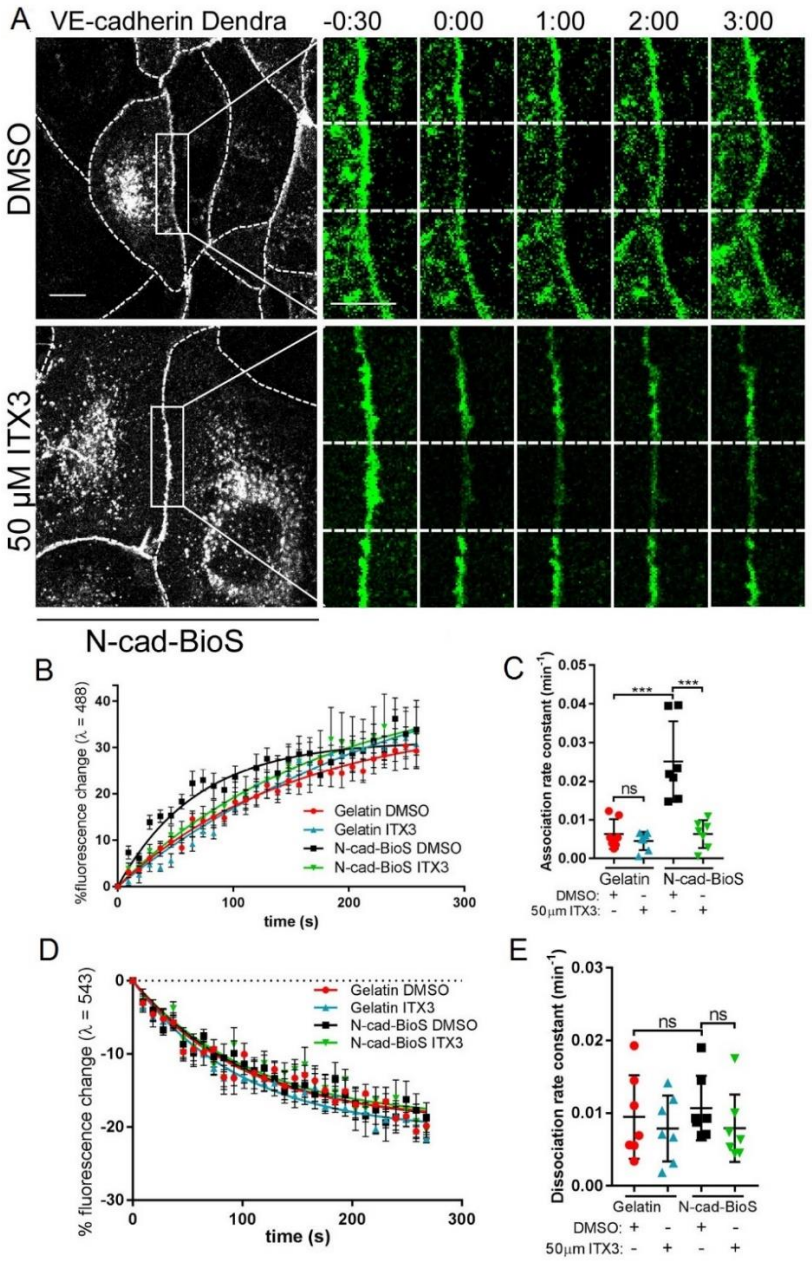

Figure 41. Inhibition of Trio decreases VE-cadherin association rate downstream of N-cadherin juxtacrine signaling. A. Time-lapse images of VE-cadherin–Dendra2 before and after photoconversion at t=0 within the irradiation zone (indicated by area between dashed lines on inserts) in HPAECs grown on N-cad-BioS after treatment with vehicle (DMSO) or 50 μM ITX3. Dashed lines of grayscale images outline the cell borders. Scale bar, 5 μm. B-C. The rate of VE-cadherin association to AJs (B) and the association rate constant (C) in cells grown on gelatin or N-cad-BioS after treatment with vehicle (DMSO) or 50 μM ITX3; n = 7 cells per group; ns, non-significant. D-E. The rate of VE-cadherin dissociation from AJs (D) and the dissociation rate constant (E) in cells grown on gelatin or N-cad-BioS after treatment with vehicle (DMSO) or 50 μM ITX3. n = 7 cells per group from 3 independent experiments. Data are presented as mean ± SEM.

6. N-CADHERIN - TRIO ACTIVATES RAC1 AND RHOA TO CONTROL VE-CADHERIN ASSEMBLY

6.1 **The N-cadherin - Trio complex activates Rac1 at adherens junctions**

Trio is a unique GEF consisting of two GEF domains (Debant et al., 1996). The GEF1 domain is responsible for activation of Rac1 and RhoG, whereas the GEF2 domain is responsible for activation of RhoA (Debant et al., 1996). Interestingly, using structured illumination microscopy, I observed numerous lamellipodia-like structures above established VE-cadherin adhesions, also known as junction associated intermittent lamellipodia (Abu Taha et al., 2014), that were prevalent in endothelial cells grown on N-cad BioS platforms (Figure 42). These data indicate that N-cadherin juxtacrine signaling may promote lamellipodia formation through a Rac1-mediated mechanism. Therefore, I asked whether recruitment of Trio to N-cadherin adhesion complexes activates Rac1 in endothelial cells. Using a FRET-based biosensor for Rac1 (MacNevin et al., 2016), I demonstrated a greater degree of Rac1 activation in cells grown on N-cad-BioS at adherens junctions as compared to gelatin (Figure 43). Interestingly, depletion of Trio reduced Rac1 activity in cells grown on N-cad-BioS but had no apparent effect on Rac1 activity in cells grown on gelatin (Figure 43) indicating a specific role of the N-cadherin – Trio circuit in activating Rac1. These results are consistent with increased interaction of Trio with nucleotide-free Rac1 (a Rac1 mutant *G15A* with the highest affinity for GEFs) in cells grown on N-cad-BioS platforms (Figure 44). Cumulatively, these data support that recruitment of Trio to N-cadherin adhesion complexes primes the GEF1 domain of Trio towards Rac1.

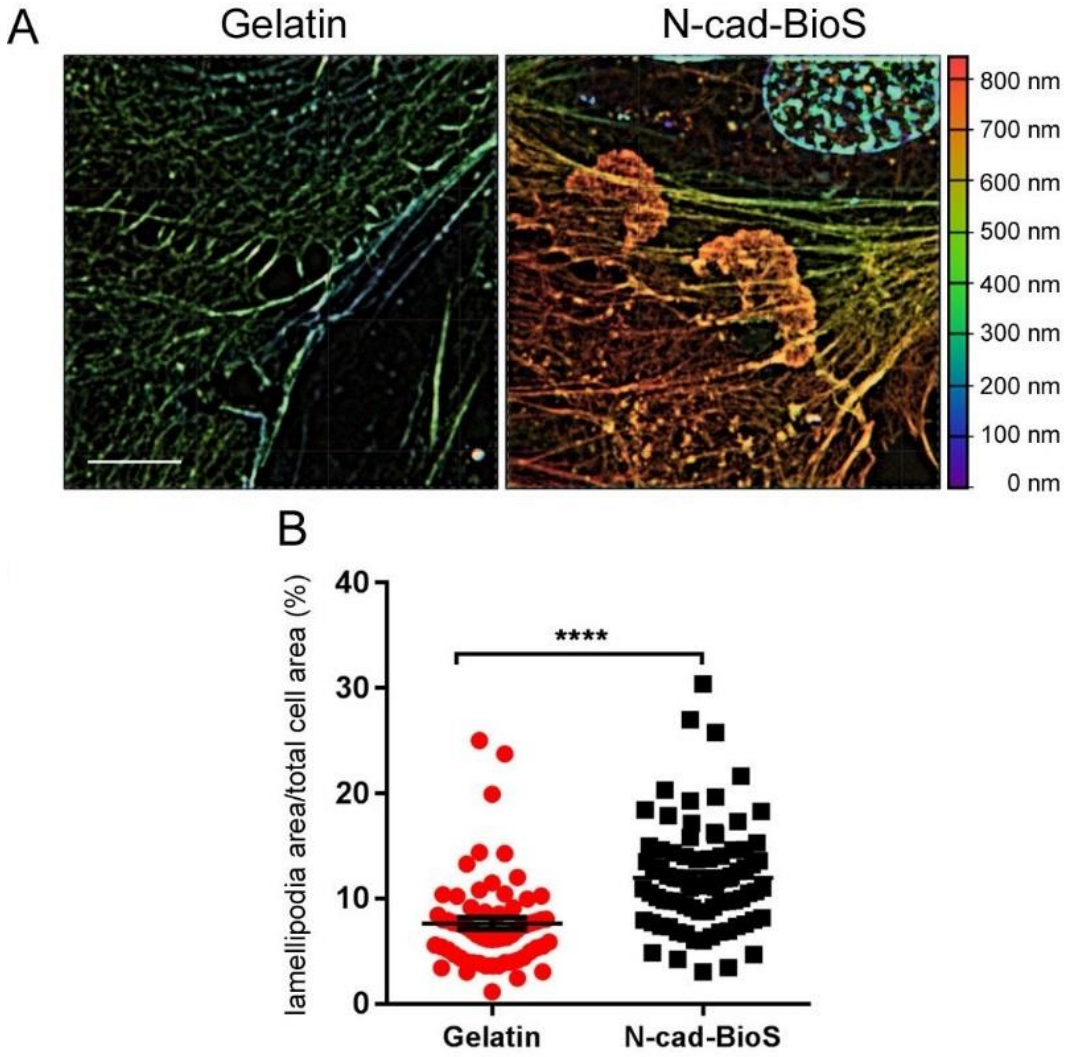

Figure 42. N-cadherin increases lamellipodia area. A. 3D Structure Illumination Microscopy (SIM) images of F-actin (phalloidin) in HPAECs grown on gelatin or N-cad-BioS. The cell depth (0-800nm) is pseudo-colored; cold and warm colors denote basal and apical surfaces of cell, respectively. Scale bar, 10 µm. Note, lamellipodia protrusions above VE-cadherin adhesion in cells grown on N-cad-BioS. B. Analysis of lamellipodia protrusion from data in A. Total lamellipodia area normalized to cell area; n= 65-82 from 3 independent experiments. Data are presented as mean ± SEM. Analysis of lamellipodia done by Quinn Lee.

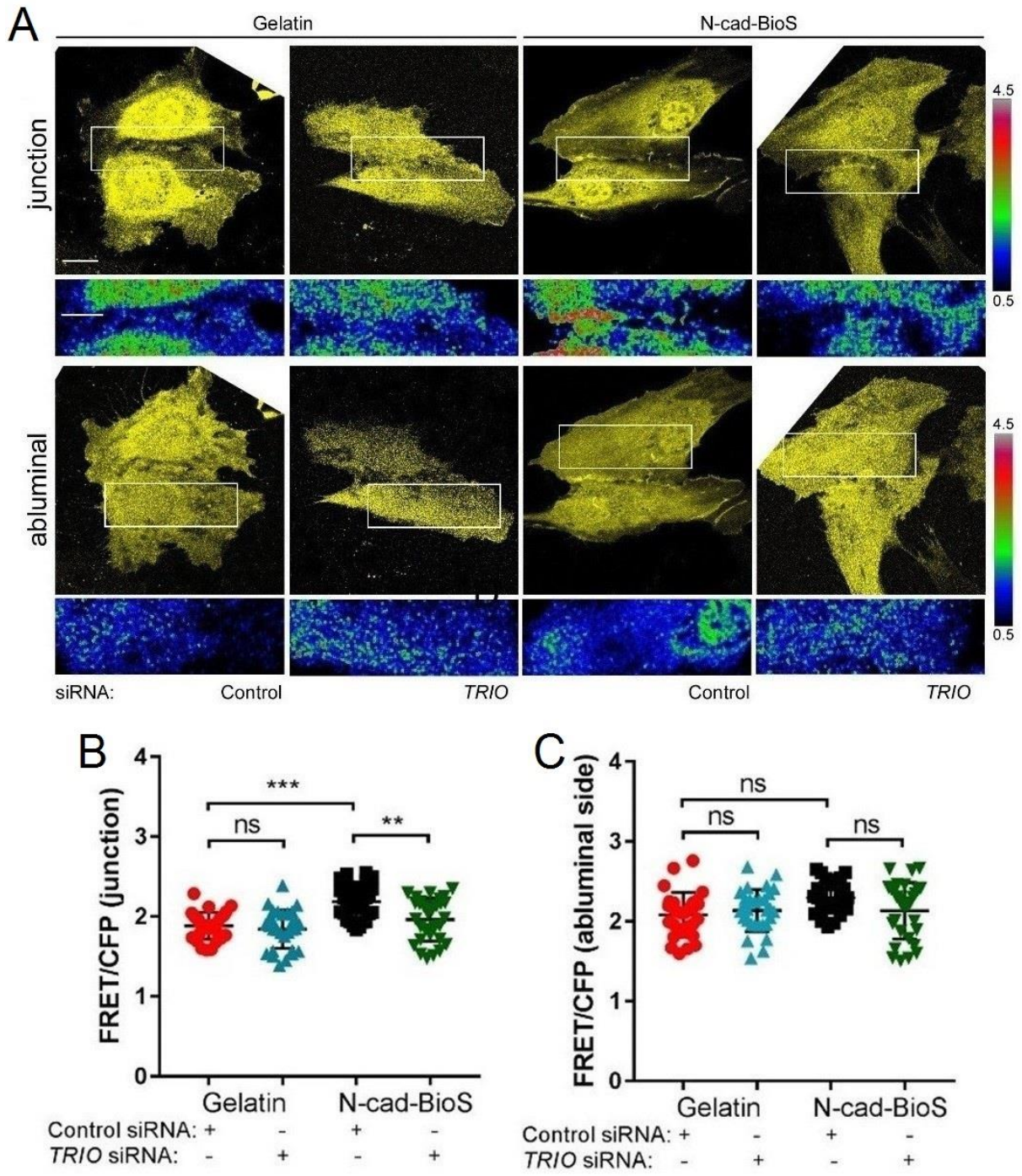

Figure 43. N-cadherin activates Rac1 through Trio. A. Confocal images of Rac1 activity (FRET/CFP) in HPAECs grown on either gelatin or N-cad-BioS and treated with control or *TRIO* siRNA. Ratiometric images were scaled from 0.5 to 4.5 and color coded as indicated on the right. Warmer colors denote higher Rac1 activity. Note, Trio-dependent increase in Rac1 is observed in cells grown on N-cad-BioS. Scale bar, 10 μm. B-C. Quantification of relative Rac1 activity at junctions (B) and abluminal surface (C) presented as FRET/CFP from images in A; n = 5–10 cells per group from 3 independent experiments. Data are presented as mean ± SEM.

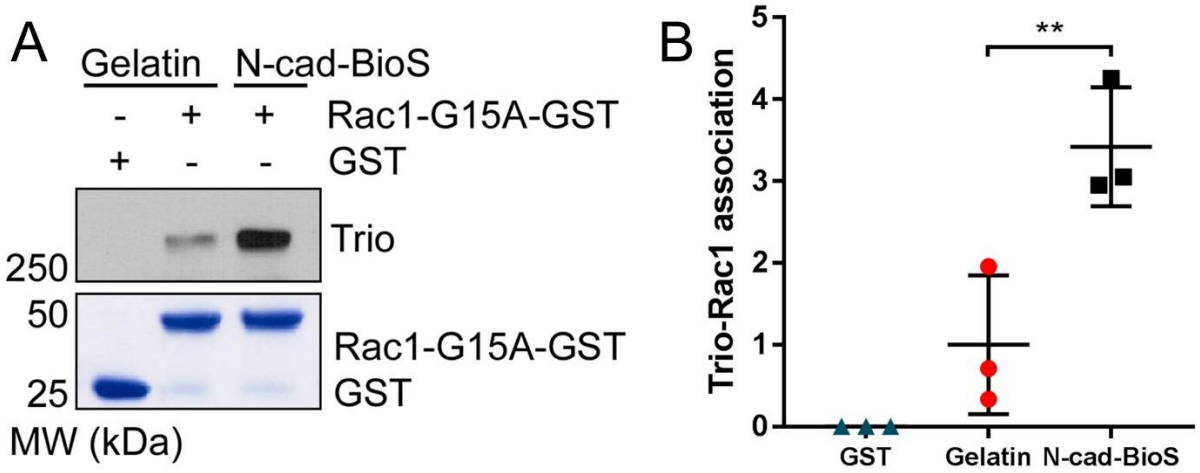

Figure 44. N-cadherin increases activation of Trio GEFs towards Rac1. A. Western blot analysis of Trio pull down with Rac1-G15A-GST from cells grown on gelatin or N-cad-BioS. GST beads alone were used as a control. Coomassie stained loading control gel of GST and Rac1-G15A-GST protein from beads added to cells. B. Quantification of Trio GEF1 activity. n = 3 independent experiments. Data are presented as mean ± SEM. Western blot done by Xiaoyan Yang.

6.2 **Activation of Rac1 rescues VE-cadherin dynamics after Trio depletion or inhibition of Trio GEF1**

Furthermore, I sought to rescue VE-cadherin association kinetics in Trio deficient cells grown on N-cad-BioS platforms using a photo-activatable Rac-1 probe (PA-Rac1) (Wu et al., 2009). Photo-activation of PA-Rac1 but not the light insensitive (LI) Rac1 probe restored the association kinetics of VE-cadherin at AJs in Trio deficient cells from 0.00795 min^{-1} to 0.0304 min^{-1} (Figure 45) as well as in cells treated with ITX3 from 0.0055 min^{-1} to 0.0294 min^{-1} (Figure 46). Together, my data indicate that engagement of Trio to N-cadherin adhesion sites activates Rac1 signaling, which in turn, promotes assembly of VE-cadherin adhesions.

6.3 **The N-cadherin - Trio circuit activates RhoA at adherens junctions and the abluminal side**

Overall, my data indicate that Trio, when engaged by N-cadherin adhesions, activates Rac1 to govern the recruitment of VE-cadherin to AJs. I next addressed the contribution of the Trio GEF2 domain, which activates RhoA (Debant et al., 1996), which may be important for N-cadherin adhesion-mediated signaling and the assembly of VE-cadherin adhesion (Figure 38). I tested the postulate that RhoA mediated intracellular tension enables activation of Trio GEF1 domain leading to Rac1 mediated recruitment of VE-cadherin at AJs. I tested this model first by measuring RhoA activity in endothelial cells grown on N-cad-BioS. I observed that N-cadherin signaling increased RhoA activity at the abluminal surface as well as at AJs in a Trio-dependent manner (Figure 47). Depletion of Trio, however, had no effect on RhoA activity in endothelial cells grown on gelatin, indicating the role of N-cadherin – Trio signaling in the activation of RhoA (Figure 47). Furthermore, we observed increased interaction of Trio with RhoA G17A in cells

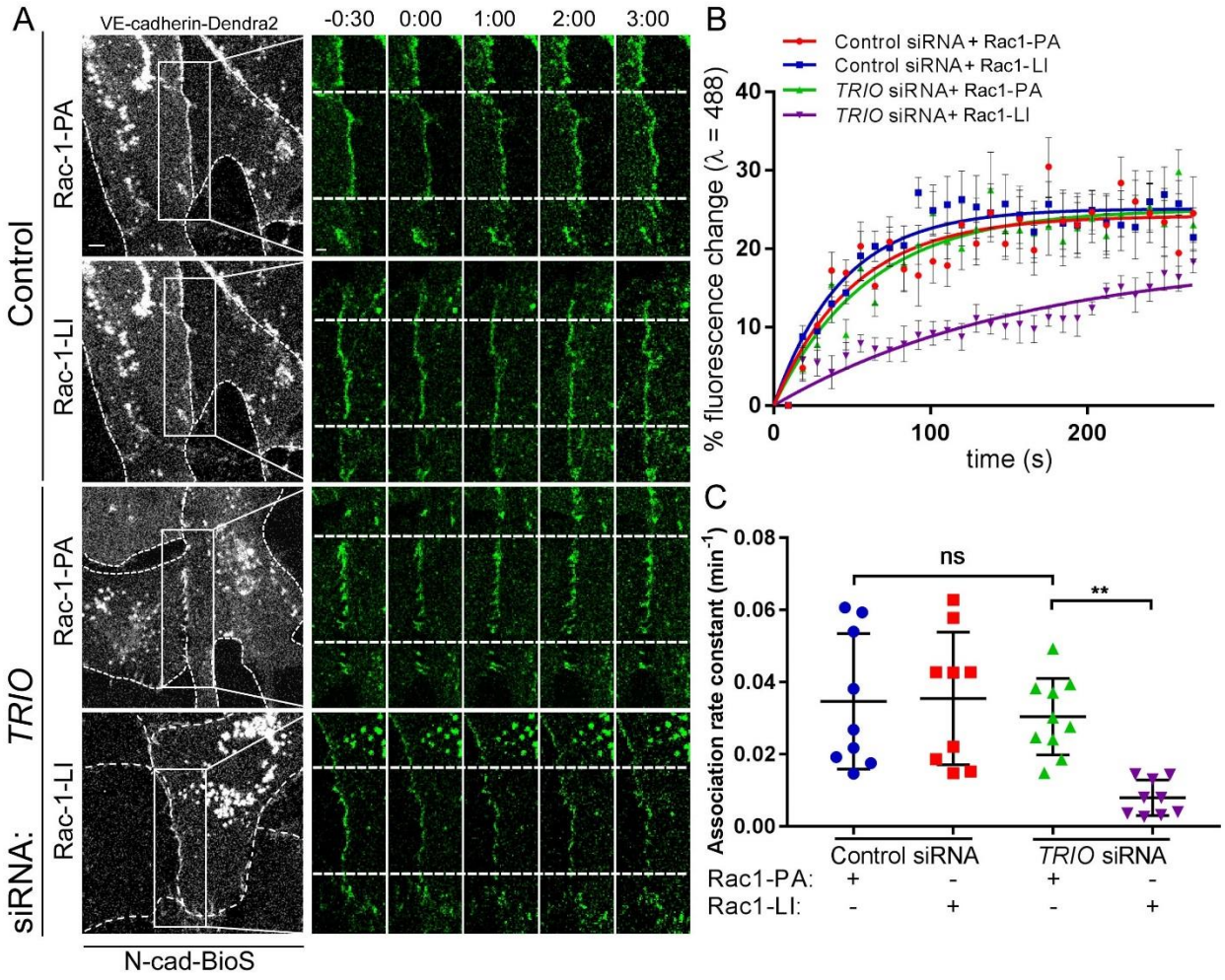

Figure 45. Photo-activatable Rac1 restores VE-cadherin dynamics in Trio deficient cells grown on N-cad-BioS platform. A. Time-lapse images of VE-cadherin–Dendra2 before and after photoconversion at t=0 in HPAECs co-expressing either CFP-Rac1-Photoactivatable (PA) or CFP-Rac1-Light Insensitive mutant (LI) and grown on N-cad-BioS after depletion of Trio or treatment with control siRNA. PA-Rac1 was activated within the photoconversion zone with λ=458 nm. Activation of PA-Rac1 but not LI-Rac1 rescued the VE-cadherin recruitment rate in Trio-depleted cells. Scale bar, 5 μm, and 2 μm on insets; time is shown in minutes. B-C. The rate of VE-cadherin association to AJs (B) and the association rate constant (C) from data in A. n = 9 junctions from 3 independent experiments. Data are presented as mean ± SEM.

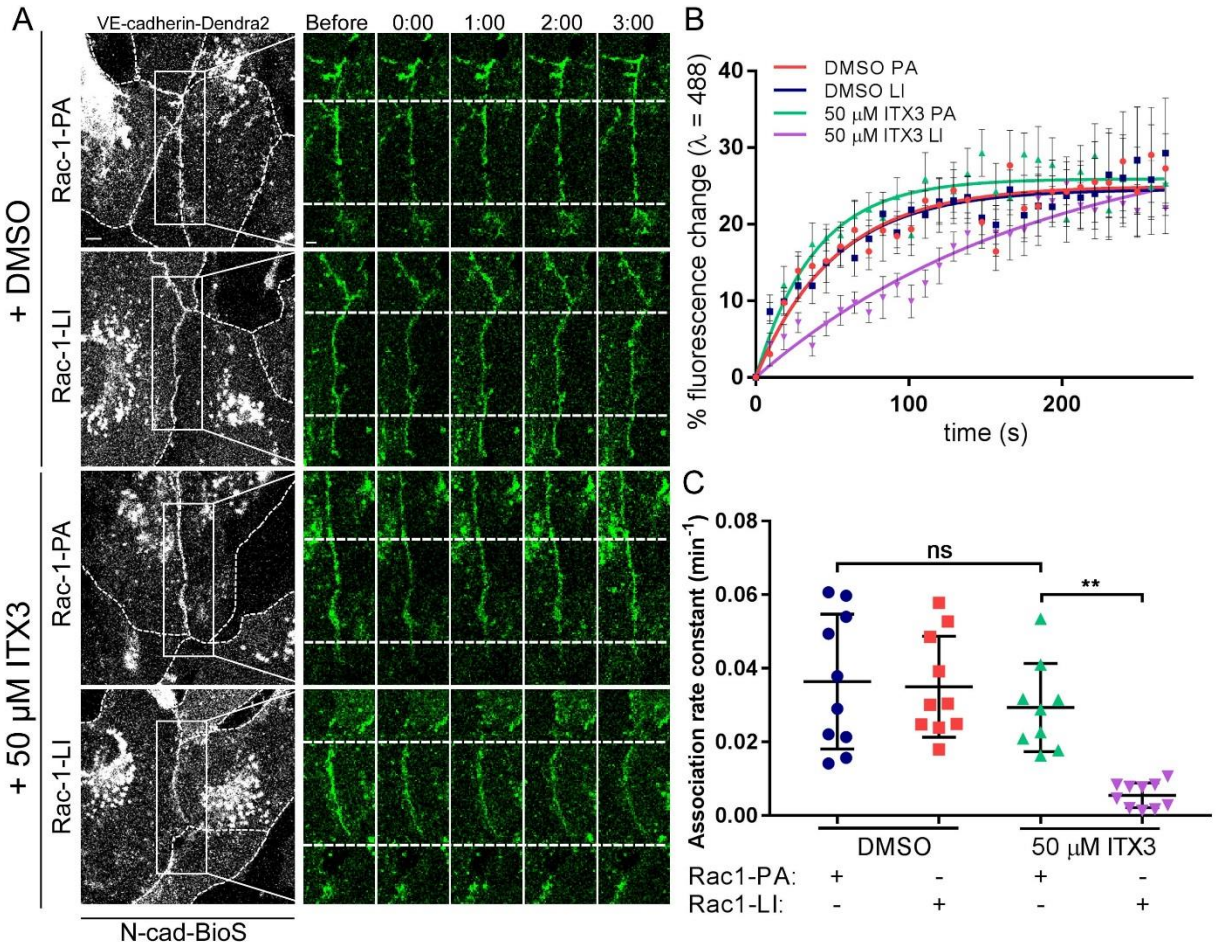

Figure 46. Photo-activatable Rac1 restores VE-cadherin dynamics after inhibition of Trio in cells grown on N-cad-BioS platforms. A. Time-lapse images of VE-cadherin–Dendra2 before and after photoconversion at t=0 within the irradiation zone (indicated by area between dashed lines on inserts) in HPAECs grown on N-cad-BioS after treatment with vehicle (DMSO) or 50 μM ITX3. Dashed lines of grayscale images outline the cell borders. Scale bar, 5 μm. B-C. The rate of VE-cadherin association to AJs (B) and the association rate constant (C) in cells grown on gelatin or N-cad-BioS after treatment with vehicle (DMSO) or 50 μM ITX3. n = 10 junctions from 3 independent experiments. Data are presented as mean ± SEM.

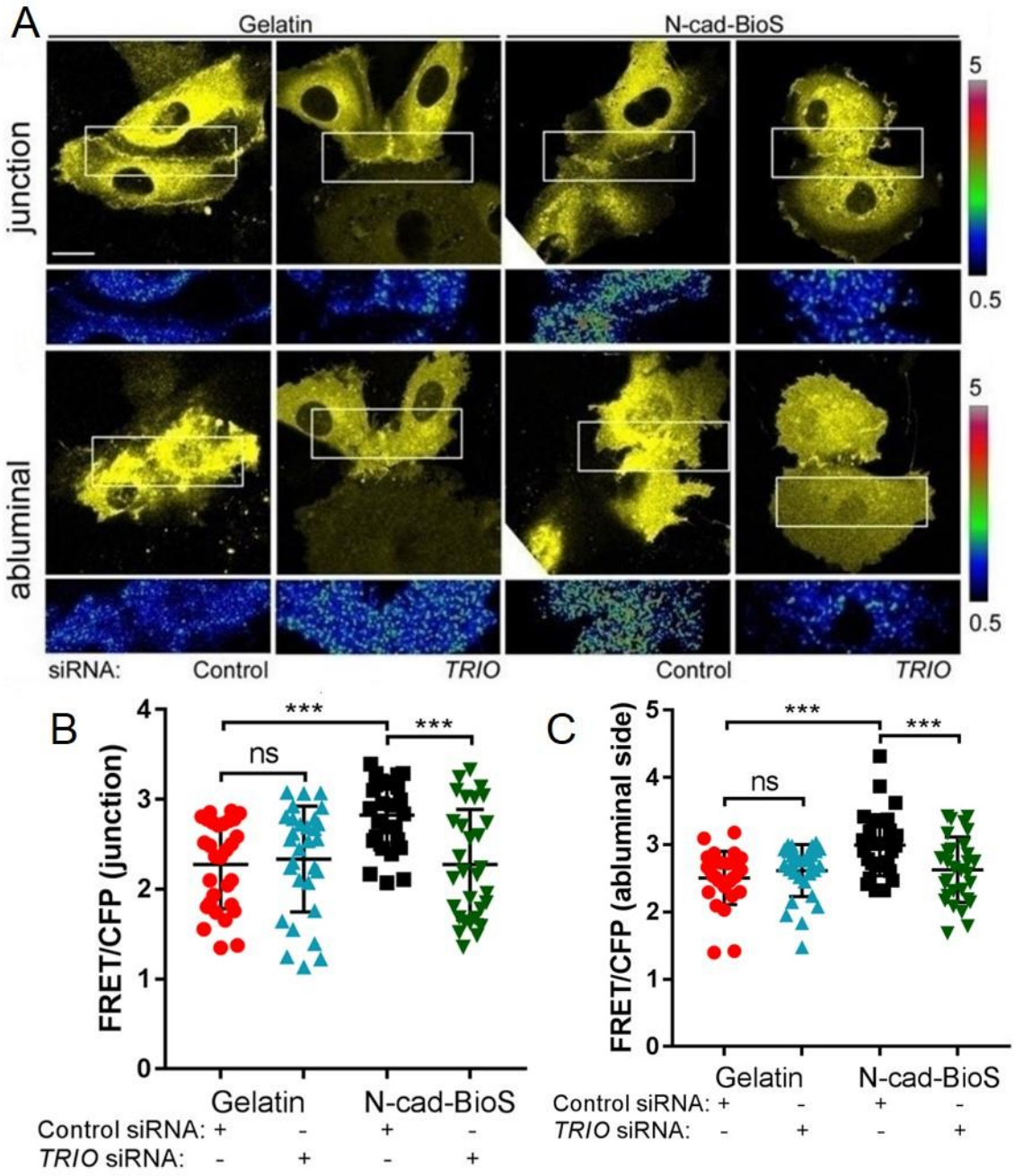

Figure 47. N-cadherin – Trio increases RhoA activity. A. Confocal images of YFP and RhoA activity (FRET/CFP) at AJs and abluminal surface of HPAECs grown on either gelatin or N-cad-BioS and treated with control or TRIO siRNA. Ratiometric images were scaled from 0.5 to 5 and color coded as indicated on the right. Warmer colors denote higher RhoA activity. Trio-dependent increase in RhoA activity is observed at both AJs and abluminal surface of cells grown on N-cad-BioS. Scale bar, 10 µm. B-C. Relative RhoA activity presented as FRET/CFP ratio at AJs (B) and abluminal (C) surface of endothelial cells from images in E; n = 20 cells from 3 independent experiments. Data are presented as mean ± SEM.

grown on N-cad-BioS as compared to gelatin (Figure 48), indicating that Trio GEF2 was also activated towards RhoA downstream of N-cadherin adhesion.

6.4 **Tension is required for assembly of VE-cadherin adhesions downstream of N-cadherin adhesion mediated signaling**

Next to investigate the causal link between RhoA activity and assembly of VE-cadherin junctions, I determined the areas of VE-cadherin junctions in cells treated with Rho kinase inhibitor Rockout. Inhibition of the RhoA pathway reduced both the increased phosphorylation of myosin light chain 2 (MLCII) and VE-cadherin adhesion area of cells grown on N-cad-BioS but not on gelatin (Figure 49). These data suggest a crucial role of intracellular tension development downstream of N-cadherin – Trio-RhoA signaling in mediating the assembly of VE-cadherin junctions. This event was coupled with increased tension across VE-cadherin adhesions as measured by the VE-cadherin tension sensor (Conway et al., 2013). Consistent with my previous observation, VE-cadherin adhesion was under intracellular tension in cells grown on gelatin and the level of tension significantly increased upon engagement of N-cadherin juxtacrine signaling (Figure 50). Depletion of Trio as well as treatment of cells with ROCK inhibitor completely abolished the junctional tension in cells grown on N-cad-BioS platforms, since FRET values were returned to the level of the tailless (under no tension) control.

We next determined whether tension alone was sufficient to increase VE-cadherin adhesion areas. We treated cells grown on gelatin surfaces with two different Rho activators to increase intracellular tension. Activation of intracellular tension in cells grown on gelatin failed to increase VE-cadherin adhesion area (Figure 51), demonstrating that tension alone is not sufficient to increase VE-cadherin assembly, and that simultaneous activation of both RhoA and Rac1 through Trio is required. I further addressed the role of intracellular tension in activation of the Trio GEF1

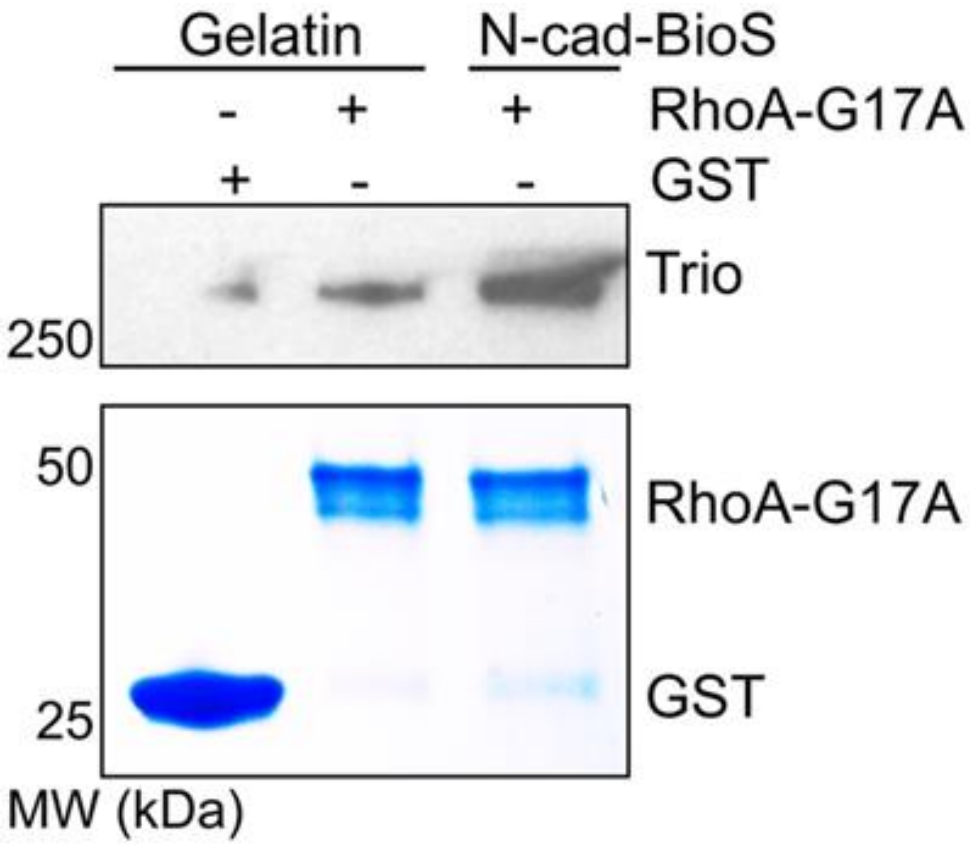

Figure 48. N-cadherin increases activation of Trio GEFs towards RhoA. Western blot analysis of Trio pull down with RhoA-G17A from cells grown on gelatin or N-cad-BioS. GST beads alone were used as a control. Coomassie stained loading control gel of GST and RhoA-G17A protein from beads added to cells.

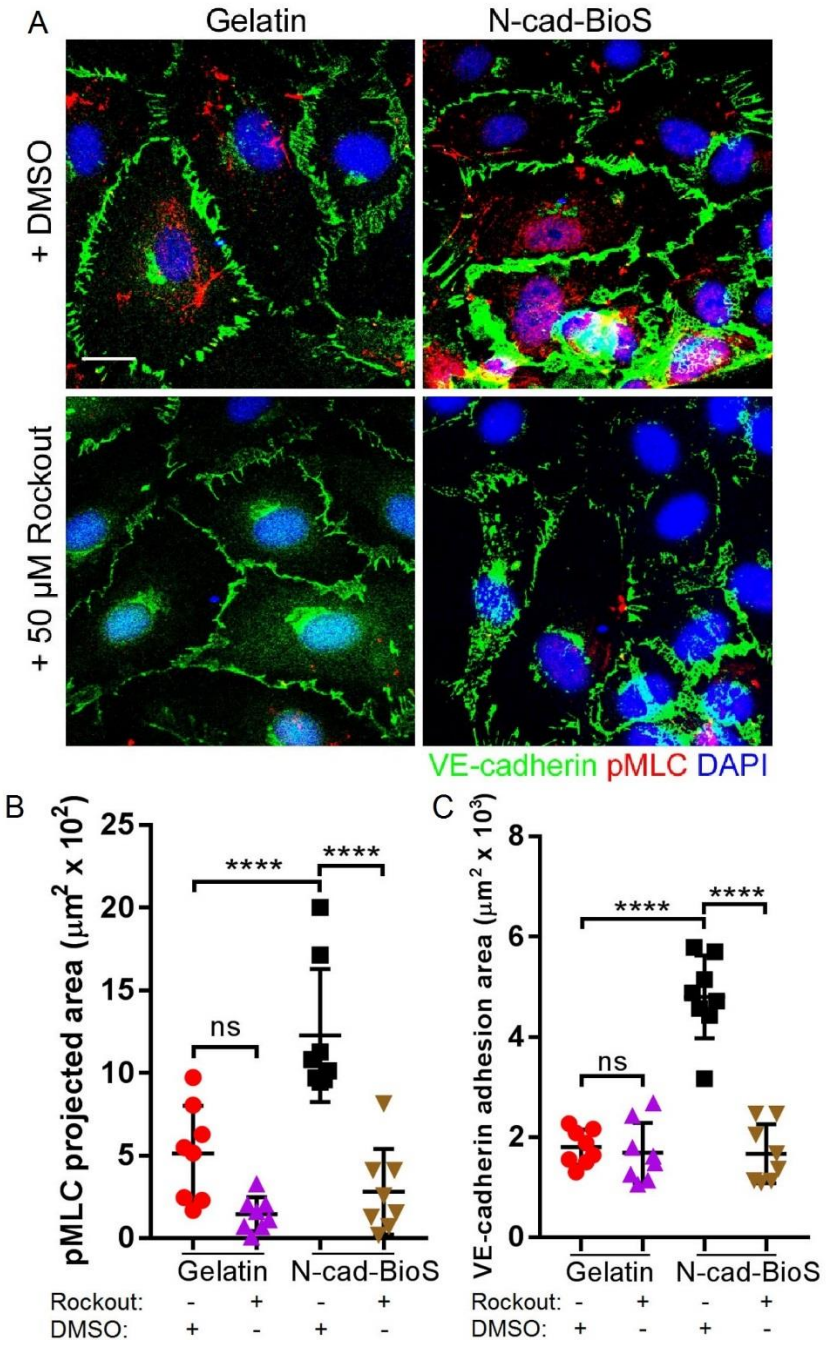

Figure 49. N-cadherin juxtacrine signaling increases VE-cadherin adhesion area in a tension dependent manner. A. Confocal images of HPAECs grown on either gelatin or N-cad-BioS and treated with 50 µM Rockout to inhibit Rho kinase (ROCK) or vehicle (DMSO). Cells were stained for VE-cadherin (green), phosphorylated myosin light chain (pMLC, red) and nuclei (DAPI, blue). Scale bar, 10 µm. B-C. Quantification of phospho-MLC projected area (B) and VE-cadherin adhesion area (C). Note, inhibition of ROCK significantly reduced area of VE-cadherin adhesion only in cells grown on N-cad-BioS. n = 8 images per group from 3 independent experiments. Data are presented as mean ± SEM.

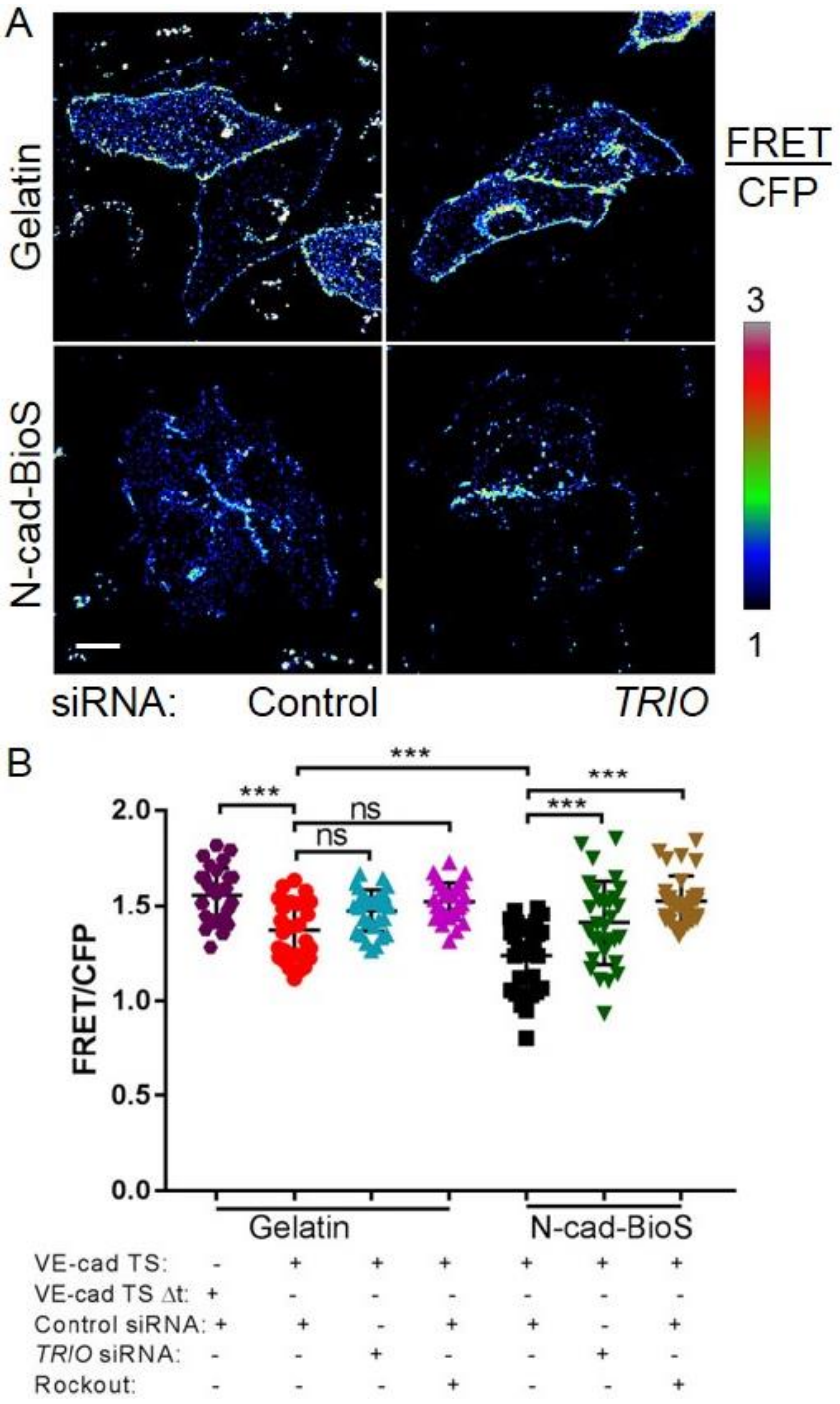

Figure 50. N-cadherin – Trio increases tension across VE-cadherin through activation of RhoA. A. Confocal images of VE-cadherin FRET-based tension sensor (FRET/CFP) in HPAECs grown on either gelatin or N-cad-BioS. Ratiometric images were scaled from 1 to 3 and color coded as indicated on the right. Warmer colors indicate lower tension across VE-cadherin. Scale bar, 10 μm. B. Quantification of tension across VE-cadherin adhesion. Higher FRET/CFP ratio indicates decreased tension across VE-cadherin adhesion. n=11-17 images per group from 3 independent experiments. Data are presented as mean ± SEM.

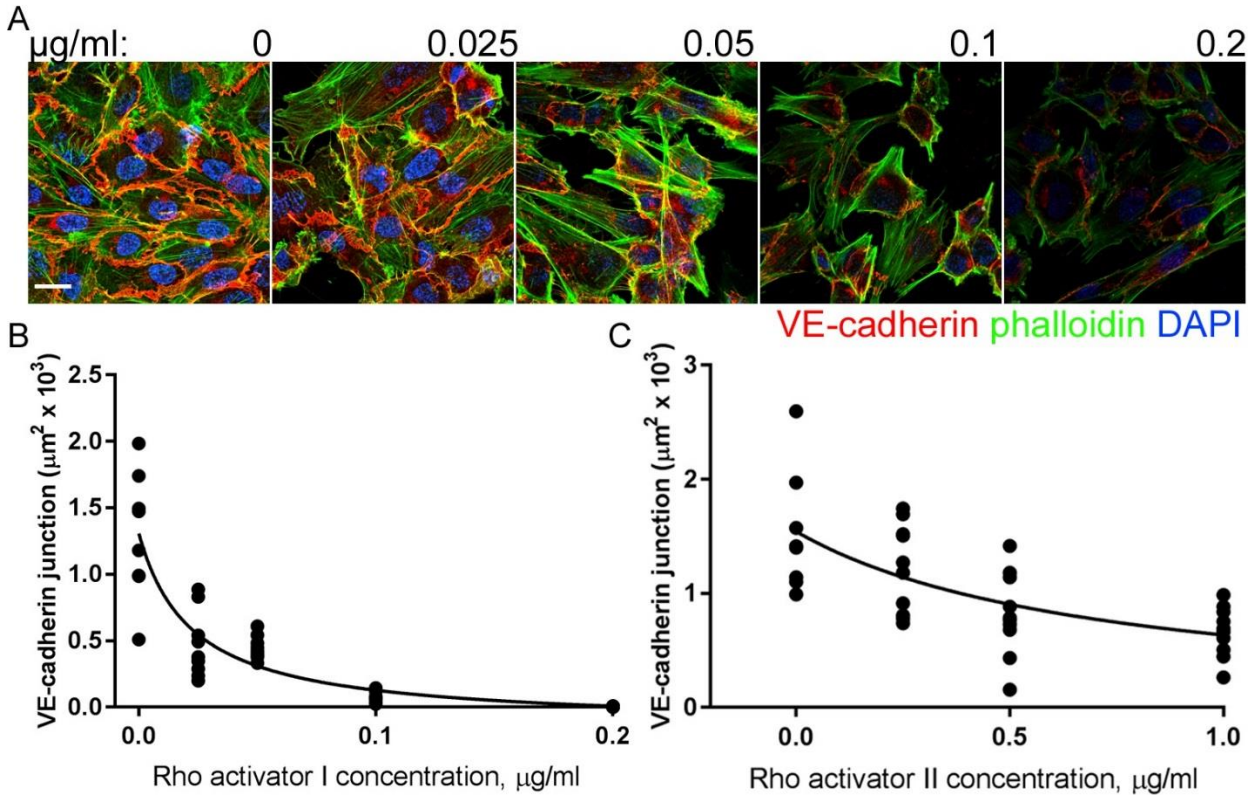

Figure 51. Activation of RhoA and increase in intracellular tension are not sufficient to induce assembly of VE-cadherin junctions. A. Confocal images of HPAECs grown on gelatin and stained for VE-cadherin (red), F-actin (phalloidin, green), and DAPI. Cells were treated with indicated doses of Rho activator I. Scale bar = 10 μm. Note formation of actin stress-fibers and destabilization of VE-cadherin junctions with increased concentration of Rho activator I. B-C. Quantification of VE-cadherin area from images in A for different doses of Rho activator I (B) and Rho activator II (C). n = 8 – 10 fields of view from 2 independent experiments.

domain using the MLCII inhibitor blebbistatin, which inhibits intracellular tension (Straight et al., 2003). Treatment with blebbistatin or Rockout reduced Trio GEF1 activity in cells grown on N-cad-BioS platforms (Figure 52) demonstrating that intracellular tension downstream of N-cadherin mediated signaling is required to activate the Trio GEF1-Rac1 pathway, which is required by which VE-cadherin is recruited to AJs. We therefore describe a mechanism where N-cadherin forms a complex with Trio directly underneath VE-cadherin adhesions (Figure 53). This leads to activation of the Trio GEF2 domain towards RhoA. Increased RhoA activation increases intracellular acto-myosin tension through Rho kinase, which is required for N-cadherin to activate the Trio GEF2 domain towards Rac1 at adherens junctions. Rac1 activation increases the recruitment rate (association) of VE-cadherin to adherens junctions, but does not change the rate of internalization (dissociation) or lateral diffusion of VE-cadherin. The increased recruitment rate of VE-cadherin leads to an accumulation of VE-cadherin at adherens junctions, which decrease paracellular permeability. Therefore we conclude that the main role of endothelial N-cadherin is to regulate the endothelial barrier through increasing VE-cadherin localization to adherens junctions, independent of pericyte adhesion.

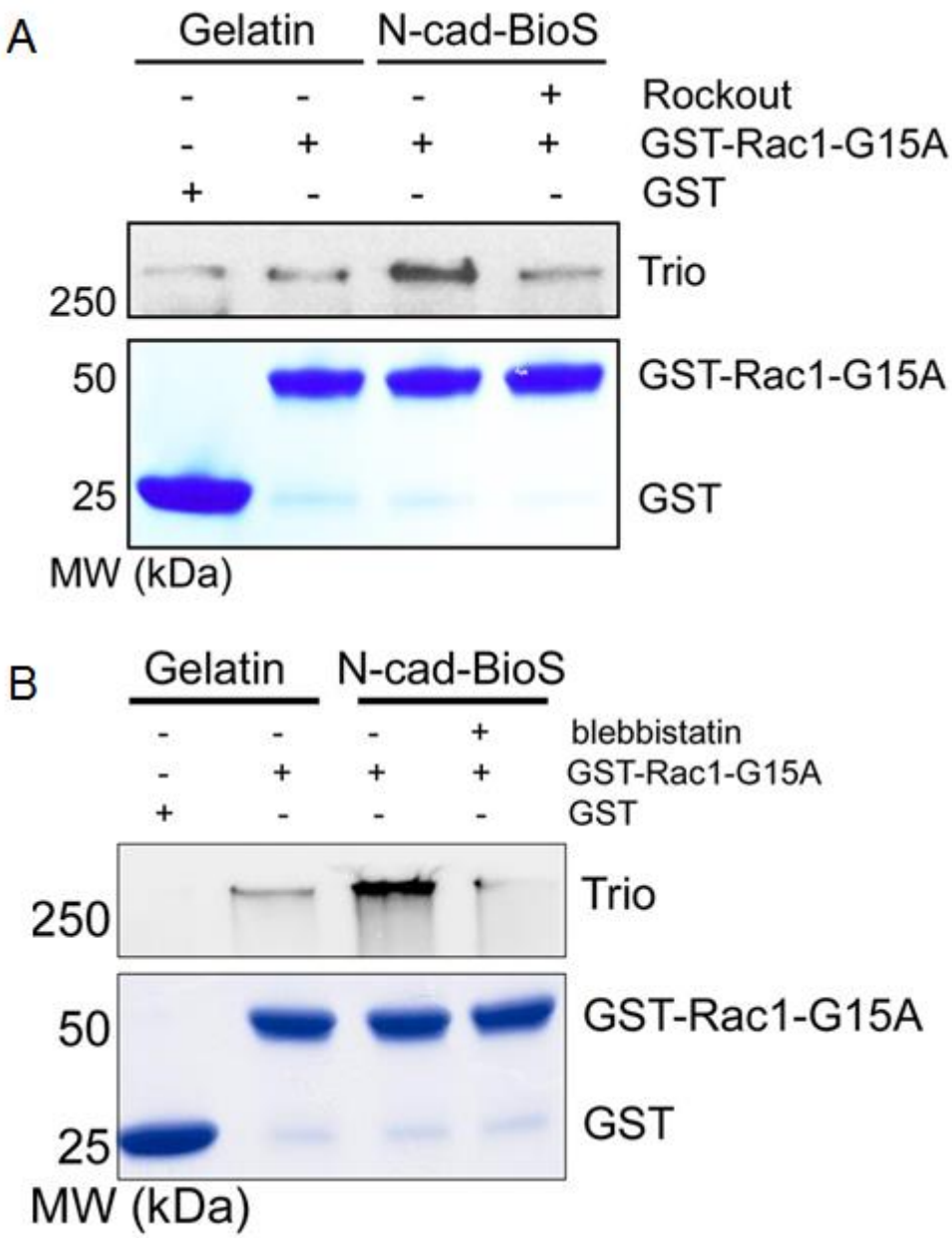

Figure 52. N-cadherin increases activation of Rac1 through Trio in a tension dependent manner. Western blot analysis of Trio levels using Rac1-G15A-GST beads from cells grown on gelatin or N-cad-BioS and treated with the Rho kinase inhibitor Rockout (A) or the myosin II inhibitor blebbistatin (B) or DMSO as a control. GST beads alone were used as an additional control. Coomassie stained loading control gel of GST and Rac1-G15A-GST protein from beads added to cells shown below. Western blot done by Xiaoyan Yang.

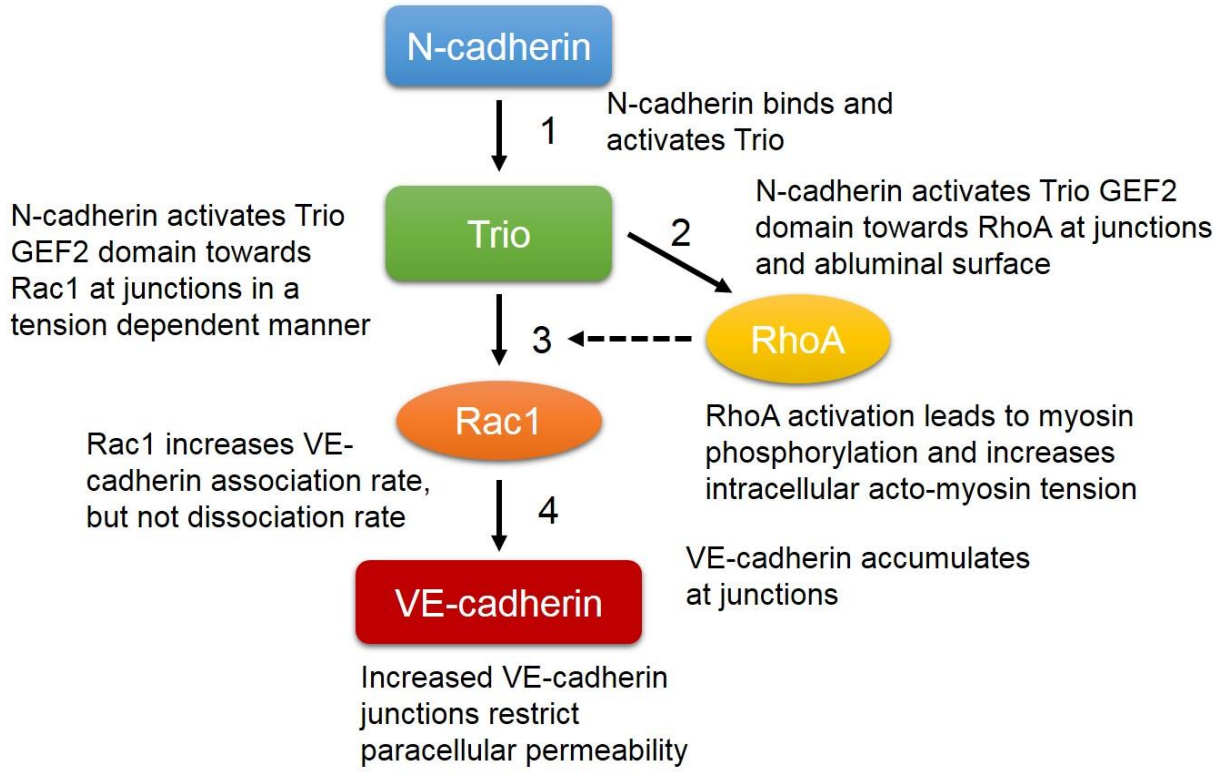

Figure 53. A circuit describing the role of N-cadherin adhesion-mediated signaling in assembling VE-cadherin junctions through Trio mediated activation of both Rac1 and RhoA. 1) N-cadherin forms a complex with Trio; 2) Trio activates RhoA increasing intracellular tension; 3) Increased tension activates Trio GEF1 domain towards Rac1; 4) Rac1 increases VE-cadherin recruitment to AJs and thereby reinforces assembly of AJs.

7. CONCLUSIONS AND DISCUSSION

This study describes a fundamental role of N-cadherin in regulation of the endothelial barrier, in which N-cadherin heterotypic adhesions between pericytes and endothelial cells restricts endothelial permeability through assembly of VE-cadherin adhesions. This process involves formation of an endothelial N-cadherin complex with the dual RhoGEF Trio, which activates RhoA at abluminal and junctional sides of the endothelial monolayer. RhoA activation by the Trio GEF2 domain subsequently increases intracellular tension, allowing the Trio GEF1 domain-dependent activation of Rac1 at AJs, resulting in assembly of VE-cadherin junctions and establishing the restrictive nature of the endothelial barrier.

7.1 **The role of N-cadherin in intercellular communication between endothelial and mural cells**

The endothelium is composed of a monolayer of endothelial cells lining the luminal side of the vessel wall, and forms a physical barrier that restricts the passage of fluids, solutes, and plasma proteins in a size-selective manner (Komarova et al., 2017). This specific property of the endothelium is attributed to adherens and tight junctions between endothelial cells (Simionescu et al., 1975) as well as finely regulated vesicular transport of plasma proteins across the endothelium (Del Vecchio et al., 1987). Previous studies have demonstrated that permeability of the microvascular endothelial barrier to micromolecules is controlled by intercellular communication with pericytes (Armulik et al., 2010; Daneman et al., 2010). In these studies, I describe a novel role of pericytes in regulating endothelial permeability.

Pericytes are the mural cells of blood microvessels that establish the interaction with endothelial cells at the abluminal side of capillaries, postcapillary venules, and terminal arterioles

(Mathiisen et al., 2010; Sims and Westfall, 1983). Pericytes wrap around these blood vessels and are encapsulated within the basement membrane surrounding endothelial cells (Derom et al., 1958). They can interact directly with endothelial cells both physically, such as through forming N-cadherin adhesions (Gerhardt et al., 2000), and through paracrine signaling, such as secretion of S1P (Paik et al., 2004) or PDGF-B (Lindahl et al., 1997). Pericyte coverage of microvessels is organ-specific and is dependent on the endothelial barrier requirements for each tissue (Armulik et al., 2005). For example, pericyte numbers are highest in brain and retinal microvessels, which also have the lowest permeability values (Armulik et al., 2011). Although pericytes have an important role in endothelial permeability regulation (Armulik et al., 2010; Daneman et al., 2010; Lindahl et al., 1997), the underlying signaling mechanisms are not well understood. Reduction in pericyte number in pdgf-b^{ret} (*retention motif knockout*) allele mice is associated with increased endothelial permeability (Alimperti et al., 2017; Armulik et al., 2010; Daneman et al., 2010). This process was shown to be dependent on increased endothelial transcytosis of albumin. Additionally, these pericyte deficient mice display disrupted paracrine signaling, leading to mis-regulation of BBB specific genes in brain endothelial cells, such as Glut1 and CD71 (Armulik et al., 2010). Loss of pericytes due to activation of inflammatory pathways (Alimperti et al., 2017; Zeng et al., 2016) is also implicated in increasing the leakiness of vessels (e.g. in diabetic retinopathy, acute lung injury, septic shock, and brain trauma). Additionally, loss of pericytes in a microfluidic pericyte-endothelial cell co-culture model due to defective N-cadherin adhesions (either through N-cadherin blocking antibodies or deletion of N-cadherin in pericytes) led to increased endothelial permeability (Alimperti et al., 2017).

As N-cadherin adhesion between endothelial cells and pericytes can regulate the endothelial barrier *in vitro* (Alimperti et al., 2017), I tested the hypothesis that N-cadherin signaling

between endothelial cells and pericytes provides the mechanism for regulating microvessel permeability *in vivo*. As endothelial specific deletion of Cdh2 (N-cadherin) causes embryonic lethality at E9.5 due to poorly formed vasculature (Luo and Radice, 2005), I generated a tamoxifen inducible, endothelial specific deletion of *Cdh2* to study the role of N-cadherin in adult mice after the vasculature is formed. Consistent with my hypothesis, my results show that endothelial cell-specific deletion of *Cdh2* in mice leads to increased permeability of the endothelial vessel wall to albumin (Figure 17) as well as low- and high-molecular weight tracers (Figure 18) in tissues with high pericyte coverage (lung and brain), suggesting that endothelial barrier function is greatly compromised without functional N-cadherin adhesions between ECs and pericytes.

Since previous studies support the role of N-cadherin in pericyte recruitment, vascular development, and stability during embryogenesis (Daneman et al., 2010; Gerhardt et al., 1999; Gerhardt et al., 2000; Paik et al., 2004), it is interesting to note that deletion of N-cadherin in adult mice cells had little or no effect on the total number of pericytes or pericyte coverage in a given tissue (Figure 19), demonstrating that N-cadherin is not required for maintenance of physical interaction with pericytes. This may be due to the fact that in mature microvessels, pericytes are tightly encapsulated within the basement membrane (Crocker et al., 1970; Tilton et al., 1981), and N-cadherin may only be important in the recruitment of pericytes, and not for maintaining pericyte adhesion. While it is possible that N-cadherin adhesion could affect EC permeability through other mechanisms (such as PDGFR-β/PDGFB signaling), our current studies focus on the mechanism of VE-cadherin junction assembly due to their importance in restricting endothelial barrier permeability through the paracellular route. We also observed no change in PDGFR-β stained pericytes, suggesting this may not be the mechanism by which N-cadherin regulates permeability. While further research is needed to fully establish the role of N-cadherin adhesion on pericyte

function, the findings here provide the first evidence of the specific function of N-cadherin adhesion in regulating the endothelial barrier *in vivo*.

7.2 **N-cadherin assembles VE-cadherin junctions**

In the first part of this study, I describe how N-cadherin adhesion between endothelial cells and pericytes is required to form a restrictive endothelial barrier. Since VE-cadherin is the primary mechanism by which endothelial cells form a restrictive barrier (Rabiet et al., 1996), and since N-cadherin expression was shown to act upstream of VE-cadherin expression during development (Luo and Radice, 2005), I investigated the role of N-cadherin adhesion mediated signaling on VE-cadherin expression and localization. I found that inducible deletion of N-cadherin does not change in VE-cadherin levels, both in endothelial cells taken directly from lung lysates as well as cultured endothelial cells (Figure 20), suggesting that N-cadherin does not act upstream of VE-cadherin expression, and that the increase in permeability after N-cadherin deletion is not dependent on total VE-cadherin levels. Other studies have shown that VE-cadherin levels are not regulated by N-cadherin *in vitro* (Ferreri et al., 2008; Giampietro et al., 2012), which is consistent with my findings *in vivo*.

Since VE-cadherin levels remained constant after loss of N-cadherin in ECs (Figure 20), I investigated whether deletion of N-cadherin led to a mis-localization of VE-cadherin from adherens junctions. In order to form a restrictive barrier, VE-cadherin must assemble at adherens junctions. Activation of inflammatory pathways, such as with thrombin or TNF-α can cause a loss of VE-cadherin at junctions (Rabiet et al., 1996; Wojciak-Stothard et al., 1998), leading to increased permeability. I found that deletion of N-cadherin in endothelial cells caused a mis-locazliation of VE-cadherin at adherens junctions *in vivo* (Figure 21-22), suggesting that N-cadherin helps form a restrictive endothelial barrier through assembly of VE-cadherin junctions.

Using an N-cadherin coated substrate to mimic N-cadherin interactions (Figure 23-24), I observed that N-cadherin increases VE-cadherin localization to junctions, again with no change in total VE-cadherin expression (Figure 25), which could be blocked by depletion (Figure 25) or deletion (Figure 27) of N-cadherin. The larger VE-cadherin junctions on N-cadherin demonstrated reduced permeability, suggesting that N-cadherin controls endothelial permeability by increasing VE-cadherin junction area (Figure 28). Similarly, I showed that N-cadherin actually increases the rate of VE-cadherin recruitment to junctions, which is the primary mechanism by which VE-cadherin accumulates at junctions (Figure 29). Taken together, these results suggest that N-cadherin plays a specific role in forming a restrictive endothelial barrier by increasing VE-cadherin recruitment to adherens junctions, rather than by controlling VE-cadherin expression.

The current studies describing the mechanism by which N-cadherin can regulate accelerated recruitment of VE-cadherin to AJs suggest that N-cadherin juxtacrine signaling is a critical mechanism by which pericytes regulate endothelial barrier function. This also indicates that paracrine signaling induced by pericytes (Armulik et al., 2010) is not sufficient to explain their role in regulating endothelial permeability, as in my model, pericytes are still present and can signal to endothelial cells in paracrine manner. However, they only fully exert their effect in regulating the endothelial barrier when they can induce signals in endothelial cells through N-cadherin adhesive interactions.

7.3 **N-cadherin forms a complex with Trio at the abluminal surface of endothelial cells**

In this study, I have elucidated for the first time a novel function for heterotypic N-cadherin adhesions between endothelial cells and pericytes *in vivo*, where endothelial N-cadherin adhesion mediated signaling assembles VE-cadherin adhesions to form a restrictive endothelial barrier. To identify the N-cadherin signaling pathway and binding partners responsible for regulating the

assembly of VE-cadherin junctions and restricting endothelial permeability, I carried out mass spectrometric analysis of N-cadherin interacting proteins using a novel method (Figure 31). I observed that N-cadherin assembles a complex consisting of the dual RhoGEF Trio at the abluminal endothelial surface (Figure 35).

Trio is a unique molecule consisting of two distinct GEF domains that can activate both Rac1 and RhoA depending on intracellular context (Debant et al., 1996). Previous studies showed that cadherin proteins can both positively and negatively regulate Trio activity (Debant et al., 1996; Medley et al., 2003; Seipel et al., 1999; van Rijssel et al., 2012). For example, VE-cadherin in endothelial cells (Timmerman et al., 2015) and M-cadherin in myoblasts (Charrasse et al., 2002) preferentially activate the Trio GEF1 domain leading to Rac1 signaling, whereas E-cadherin in epithelial cells inhibits Trio activity through interaction with the Trio binding protein Triobp (Seipel et al., 2001; Yano et al., 2011). In neural crest cells, cadherin-11 activates both Trio GEF1 and GEF2 domains during development (Kashef et al., 2009), similar to how N-cadherin interaction with Trio activates both Rac1 and RhoA in endothelial cells in the present study. The reasons for varying RhoGTPase activation responses induced by the interaction of different cadherins with Trio have not been addressed. The responses may be cell- and cadherin-specific and depend on recruitment of adaptor proteins to the cadherin-Trio complex (Son et al., 2015).

Importantly, my data reveal a specific role of N-cadherin adhesion in activating both RhoA and Rac1 through recruitment of Trio to adhesion sites. Although Trio has been previously defined as a transient partner of VE-cadherin at nascent adhesion sites (Timmerman et al., 2015), its function is ceased upon adhesion maturation, and was shown to only activate Rac1. In contrast to VE-cadherin adhesion, which enables spatial activation of Rac1 and Cdc42 signaling (Wojciak-Stothard et al., 2005), engagement of N-cadherin in endothelial cells triggers both RhoA and Rac1

activities. This specific function of N-cadherin adhesion in activating RhoA signaling has been previously reported in myoblasts (Mary et al., 2002). Although we detected various GTPase Activating Proteins (GAPs) as well as GEFS in association with N-cadherin complexes, IQGAP1, ARHGAP21, and Trio were more abundant. While these upstream regulators of small RhoGTPases might differentially control assembly of N-cadherin adhesion, my data indicate a prerequisite role of Trio signaling upon engagement of N-cadherin.

The mass spectroscopy analysis revealed a broad set of actin binding accessory factors in association with the N-cadherin adhesion complex (Figure 33) indicating that the latter is actively involved in organization and remodeling of the actin cytoskeleton. Given the complex relationship between N-cadherin- and integrin-based signaling networks in other cell types (Arregui et al., 2000; Ouyang et al., 2013; Yano et al., 2004), N-cadherin adhesions might provide a critical hub for organization of the cortical actin cytoskeleton (as opposed to stress fibers) in endothelial cells. N-cadherin adhesion may subsequently function as a site for nucleation and elongation of actin filaments through recruitment of the Arp2/3 nucleation complex and cortactin, which leads to increased VE-cadherin recruitment to adherens junctions.

Aspects of N-cadherin mediated signaling through the actin cytoskeleton have been studied in non-endothelial cells (Comunale et al., 2007; Cosgrove et al., 2016; Mary et al., 2002). N-cadherin adhesion in myoblasts induces reorganization of the actin cytoskeleton leading to myosin-II-dependent maturation of N-cadherin adhesion (Comunale et al., 2007; Yano et al., 2004). This involved recruitment of α-catenin to nascent N-cadherin adhesion sites and consequent attachment of the adhesion complex to the actin cytoskeleton (Leonard et al., 2011). N-cadherin adhesion also activates Rac1 signaling in fibroblasts and mesenchymal stem cells, which restrains cell contractility and modulates the cell's adaptive response to stiffening of the extracellular matrix

(Alimperti et al., 2017; Cosgrove et al., 2016). Since I found that N-cadherin forms a complex with Trio and other actin binding proteins, and can activate both Trio GEF1 and GEF2 domains, I next sought to determine whether the formation of the Trio – N-cadherin complex can activate Rac1 and RhoA signaling to recruit VE-cadherin to adherens junctions.

7.4 **N-cadherin – Trio triggers recruitment of VE-cadherin to cell-cell contacts through RhoA and Rac1**

My data demonstrate that the formation of the N-cadherin – Trio complex is coupled to activation of both Rac1 and RhoA via the Trio GEF1 and GEF2 domains, respectively. Additionally, I showed that Rac1 activation through the GEF1 domain depends on RhoA-mediated intracellular tension via myosin-II. In contrast to N-cadherin, studies have showed that VE-cadherin interaction with Trio only activates Rac1 (Timmerman et al., 2015). The differential signaling function of N-cadherin was confirmed in these studies in which ectopic expression of N-cadherin in Chinese hamster ovary cells, a surrogate model which does not express any cadherins, is also associated with activation of both RhoA and Rac1 whereas expression of VE-cadherin predominantly activates Rac1 while inhibiting RhoA (not shown).

My model explains how the N-cadherin – Trio complex activates both RhoA and Rac1 in endothelial cells (Figure 53). RhoA functions to generate intracellular tension by activating ROCK, which leads to phosphorylation of myosin-II, and consequently allows activation of the Trio GEF1 domain, although it remains to be investigated whether intracellular tension is required for the formation of the N-cadherin – Trio complex or whether tension causes a conformational change to Trio itself, allowing for activation of the GEF1 domain. Rac1 activation leads to an increase in VE-cadherin recruitment to the membrane, leading to an accumulation of VE-cadherin at adherens junctions and subsequent restricted permeability. These results establish for the first

time to our knowledge the causal relationship between intracellular tension and Trio mediated activation of Rac1 signaling in the endothelium.

The signaling steps responsible for the coordinated activation of both GEF1 and GEF2 domains of Trio RhoGTPases are yet unclear. A possibility is that a conformational change in Trio induced by tension activates GEF1. An analogous process of tension induced conformation is shown to regulate GEF-H1 and p115 (Scott et al., 2016). Another possibility is that the activity of GEF1 domain requires binding to other proteins such as neuronal navigator 1 (van Haren et al., 2014). The present results are consistent with the key role of small RhoGTPase signaling in regulating permeability of the endothelial barrier through their effect on organizing AJs and the actin cytoskeleton (Komarova et al., 2017). We demonstrated that N-cadherin adhesion-mediated signaling is essential for the recruitment of VE-cadherin to endothelial cell-cell contacts. These results thus position the N-cadherin – Trio complex as an upstream regulator of Rac1 activity and assembly of VE-cadherin junctions. Rac1 was shown to be a reversible modulator of intracellular tension enabling stabilization of VE-cadherin trans-interactions at mature AJs (Daneshjou et al., 2015). Rac1 activation functioned by reducing the rate of VE-cadherin internalization from AJs and thus promoted assembly of AJs (Daneshjou et al., 2015). These results explained Rac1 dependent re-annealing of AJs in response to barrier-enhancing mediators such as spinghosine-1-phosphate (Itoh et al., 2012; Paik et al., 2004).

My present observations extend these findings in defining N-cadherin signaling as a constitutive mechanism responsible for establishing the restrictive endothelial barrier. In this model (Figure 53), activation of RhoA via N-cadherin – Trio increases intracellular tension, which allows for N-cadherin – Trio activation of Rac1 to promote the recruitment of VE-cadherin to AJs. I can speculate that fast recruitment of VE-cadherin to AJs is achieved through continuous

formation of nascent VE-cadherin adhesions within the junction associated intermittent lamellipodia protrusions (also known as adhesion plaques). Lamellipodia protrusions comprise up to 30% of the cell area upon engagement of the N-cadherin circuit through Rac1, whereas myosin II activation and retrograde flow might deliver these nascent adhesions to the cell borders, where they are incorporated into AJs. Junction associated intermittent lamellipodia, driven by ARP2/3-mediated polymerization of actin filaments, became less frequent and decreased in size upon confluence. Consistent with this model, we have observed that recruitment of VE-cadherin to AJs coincides with activation of both Rac1 and RhoA via Trio. Furthermore, defects in VE-cadherin recruitment to AJs in Trio depleted cells could be rescued by activating Rac1 at AJs using a photoactivable probe. Also, pharmacological inhibition of RhoA or myosin-II activity with blebbistan inhibits the Trio GEF1 domain, and thus prevents the assembly of VE-cadherin junctions.

It has been reported that activation of RhoA destabilizes AJs through generation of tugging forces that pull VE-cadherin adhesions apart (van Nieuw Amerongen et al., 2000) whereas Rac1 stabilizes AJs by counterbalancing RhoA-mediated intracellular tension (Daneshjou et al., 2015). Other experiments have shown that intracellular tension is required for the formation of adherens junctions (Abraham et al., 2009), while activation of Rac1 after stimulation with VEGF can destabilize junctions (Garrett et al., 2007). My data expand upon this conventional view of the antagonistic relationship between RhoA and Rac1, as I demonstrate that both RhoA and Rac1 activities are required to form VE-cadherin adhesions downstream of N-cadherin adhesion mediated signaling, through activation of these RhoGTPases at precise subcellular localizations (Figures 43 and 47). I speculate that fast recruitment of VE-cadherin to AJs is achieved through continuous formation of nascent VE-cadherin adhesions within the junction associated intermittent

lamellipodia protrusions (also known as adhesion plaques). Lamellipodia protrusions comprise up to 30% of the cell area upon engagement of the N-cadherin circuit through Rac 1 (Figure 42), whereas myosin II activation (Figure 49) and retrograde flow might deliver these nascent adhesions to the cell borders, where they are incorporated into AJs. Junction associated intermittent lamellipodia, driven by ARP2/3-mediated polymerization of actin filaments, became less frequent and decreased in size upon confluence. My work indicates that engagement of the N-cadherin – Trio complex promotes assembly of junction associated intermittent lamellipodia in mature confluent monolayers.

The functional role of N-cadherin in regulating RhoGTPase input may have been underplayed due to the lack of N-cadherin adhesion mediated signaling in cell culture models (Figure 23). My findings demonstrate a novel role for N-cadherin-Trio signaling in cooperatively activating both RhoA and Rac1 and assembling VE-cadherin junctions. Because the level of VE-cadherin at AJs correlates with permeability of AJs (Lampugnani et al., 1992), the physiologic consequence of this cooperation is likely to reduce endothelial permeability. This assumption correlated well with our permeability data. It is also possible that the N-cadherin-Trio complex strengthens endothelial AJs in microvessels such that the AJs are more resistant to mechanical forces such as high hydrostatic pressure (Baeyens et al., 2016; Weisberg, 1978). The understanding of N-cadherin mechanobiology may thus lead to therapeutic strategies that limit vascular leakage in inflammatory diseases.

8. FUTURE DIRECTIONS

While this work describes a fundamental novel role of N-cadherin signaling between endothelial cells and pericytes in the regulation of the endothelial barrier, there are still several unanswered questions regarding the biological outcome of N-cadherin signaling on behavior and health. Since loss of N-cadherin leads to increased permeability of the endothelial barrier in both brain and lung, it will be important to determine the short and long-term outcome of vascular leakage in these organs. Currently, permeability was analyzed within several weeks after deletion of *Cdh2* gene in endothelial cells, however it is unclear how chronic vascular leakage in the brain and lung affects the long term physical and mental health of these animals. Since there does not appear to be any change in lifespan or survival of these mice (i.e. they live as long as control mice), further studies focusing on the specialized function of the brain and lung would give greater insight into the role of N-cadherin. Since vascular leakage is known to contribute to pulmonary fibrosis (Mammoto et al., 2013) and memory loss (Sagare et al., 2013), some future studies should aim at understanding whether loss of N-cadherin signaling leads to lung diseases associated with vascular leakage and remodeling such as lung fibrosis or Chronic Obstructive Pulmonary Disease (COPD), and whether chronic vascular leakage in the brain has any effects on cognitive brain function.

Another important area of investigation would be to further examine the effects of endothelial deletion of *Cdh2* in endothelial cell in pericytes behavior and function. What is the long-term effect of deletion of *Cdh2* in endothelial cells on pericyte proliferation, migration, survival, differentiation, and interaction with endothelial cells? Does N-cadherin juxtacrine signaling in pericytes contribute to pericyte survival? Does loss of N-cadherin in endothelial cells leads to pericyte death? In my model, pericyte coverage did not change after deletion of *Cdh2* after 6 months, however over a longer lifespan, pericyte coverage may decrease either due to pericyte

detachment, migration away from vasculature, or pericyte death, which would have further consequences on endothelial permeability and function of the organ in whole. As loss of N-cadherin heterotypic contacts had a drastic effect in endothelial cells, it would be also interesting to see if N-cadherin signaling in pericytes has any effect on pericyte function, which may in turn have a reciprocal effect on endothelial cells. Therefore, it would be critically important to design a pericyte specific, inducible *Cdh2* knockout model to study the effects N-cadherin juxtacrine signaling on both endothelial cells and pericytes. In this respect, it would be interesting to see if *Cdh2* deletion in pericytes mimics the increase in endothelial permeability found when deleting *Cdh2* in endothelial cells, and help further elucidate additional signaling mechanisms between pericytes and endothelial cells.

While endothelial cell specific deletion of N-cadherin results in embryonic lethality at E9.5, it is not clear if or when this would occur with a pericyte specific knockout model, as pericytes are not invested into the endothelium until around E11. Hence, understanding the role of N-cadherin signaling in embryo development will be also important. While several studies have investigated the role of N-cadherin on angiogenesis, it is still unclear how inducible deletion of N-cadherin in endothelial cells of the adult vasculature would affect angiogenesis as well as endothelial barrier recovery after injury. While N-cadherin is thought to mainly control endothelial permeability through recruiting pericytes, I have shown that N-cadherin signaling between endothelial cells and pericytes is the key mechanism responsible for regulating endothelial permeability, leading to further questions regarding the role of N-cadherin in vascular development and stability as well as angiogenesis and vasculogenesis.

Another important question is whether the mechanism presented here is the same for all endothelial cells interacting with pericytes. Do lung and brain endothelial cells have distinct

mechanisms of N-cadherin signaling? For instance, in the Brain Blood Barrier (BBB), tight junctions play a critical role in regulating permeability. Does N-cadherin affect tight junction formation in endothelial cells in the brain microvasculature? While adherens junctions can also influence tight junctions, and vice versa, it is not clear N-cadherin juxtacrine signaling can affect this reciprocal interaction.

In my study, I found a large number of novel proteins interacting with N-cadherin in endothelial cells. This study was specifically interested in function of upstream regulators of RhoA GTPases (RhoGEFs and GAPs), however it is likely that N-cadherin signaling affects many different pathways, which is beyond the scope of this thesis. A thorough analysis of the N-cadherin binding partners presented here may reveal other novel pathways affecting different aspects of endothelial biology.

This work describes a molecular mechanism by which N-cadherin increases VE-cadherin localization and transport to adherens junctions through the RhoGEF Trio. While I show that this occurs through simultaneous activation of Rac1 and RhoA, it is still somewhat unclear how these two cooperate to regulate endothelial permeability. Studies on Rac1 and RhoA have described both barrier enhancing and barrier disrupting properties, depending on the context, therefore a more thorough investigation into the interplay between these two molecules would be critical in understanding the precise mechanism. How does N-cadherin regulate the specific spatio-temporal activation of these RhoGTPases? And how does this lead to an increase in VE-cadherin transport to the membrane? This process likely occurs through a fine balance of Rac1 and RhoA, by polymerizing actin at the membrane while also providing tension for VE-cadherin to properly link to the actin cytoskeleton. A final question on the role of N-cadherin juxtacrine signaling is the distance over which this process occurs. How is Trio activated by N-cadherin adhesions and

brought to the active sites of VE-cadherin adhesions? This transport is likely microtubule dependent, but further work is needed to demonstrate this communication over distance. While this work identifies a novel mechanism by which N-cadherin regulates the endothelial barrier, there are many important aspects of N-cadherin juxtacrine signaling between endothelial cells and pericytes which warrant further investigation.

9. CITED LITERATURE

1. Abe, K., Rossman, K.L., Liu, B., Ritola, K.D., Chiang, D., Campbell, S.L., Burridge, K., and Der, C.J. (2000). Vav2 is an activator of Cdc42, Rac1, and RhoA. J Biol Chem *275*, 10141-10149.
2. Abraham, S., Yeo, M., Montero-Balaguer, M., Paterson, H., Dejana, E., Marshall, C.J., and Mavria, G. (2009). VE-Cadherin-mediated cell-cell interaction suppresses sprouting via signaling to MLC2 phosphorylation. Curr Biol *19*, 668-674.
3. Abu Taha, A., Taha, M., Seebach, J., and Schnittler, H.J. (2014). ARP2/3-mediated junction-associated lamellipodia control VE-cadherin-based cell junction dynamics and maintain monolayer integrity. Mol Biol Cell *25*, 245-256.
4. Alcaide, P., Martinelli, R., Newton, G., Williams, M.R., Adam, A., Vincent, P.A., and Luscinskas, F.W. (2012). p120-Catenin prevents neutrophil transmigration independently of RhoA inhibition by impairing Src dependent VE-cadherin phosphorylation. Am J Physiol Cell Physiol *303*, C385-395.
5. Alimperti, S., Mirabella, T., Bajaj, V., Polacheck, W., Pirone, D.M., Duffield, J., Eyckmans, J., Assoian, R.K., and Chen, C.S. (2017). Three-dimensional biomimetic vascular model reveals a RhoA, Rac1, and N-cadherin balance in mural cell-endothelial cell-regulated barrier function. Proc Natl Acad Sci U S A *114*, 8758-8763.
6. Andersen, P.R., Devare, S.G., Tronick, S.R., Ellis, R.W., Aaronson, S.A., and Scolnick, E.M. (1981). Generation of BALB-MuSV and Ha-MuSC by type C virus transduction of homologous transforming genes from different species. Cell *26*, 129-134.
7. Andor, A., Trulzsch, K., Essler, M., Roggenkamp, A., Wiedemann, A., Heesemann, J., and Aepfelbacher, M. (2001). YopE of Yersinia, a GAP for Rho GTPases, selectively modulates Rac-dependent actin structures in endothelial cells. Cell Microbiol *3*, 301-310.
8. Andreeva, A.V., Han, J., Kutuzov, M.A., Profirovic, J., Tkachuk, V.A., and Voyno-Yasenetskaya, T.A. (2010). T-cadherin modulates endothelial barrier function. J Cell Physiol *223*, 94-102.
9. Armulik, A., Abramsson, A., and Betsholtz, C. (2005). Endothelial/pericyte interactions. Circ Res *97*, 512-523.
10. Armulik, A., Genove, G., and Betsholtz, C. (2011). Pericytes: developmental, physiological, and pathological perspectives, problems, and promises. Dev Cell *21*, 193-215.
11. Armulik, A., Genove, G., Mae, M., Nisancioglu, M.H., Wallgard, E., Niaudet, C., He, L., Norlin, J., Lindblom, P., Strittmatter, K., *et al.* (2010). Pericytes regulate the blood-brain barrier. Nature *468*, 557-561.
12. Aroca, P.R., Salvat, M., Fernandez, J., and Mendez, I. (2004). Risk factors for diffuse and focal macular edema. Journal of diabetes and its complications *18*, 211-215.
13. Arregui, C., Pathre, P., Lilien, J., and Balsamo, J. (2000). The nonreceptor tyrosine kinase fer mediates cross-talk between N-cadherin and beta1-integrins. J Cell Biol *149*, 1263-1274.
14. Axelrad, T.W., Deo, D.D., Ottino, P., Van Kirk, J., Bazan, N.G., Bazan, H.E., and Hunt, J.D. (2004). Platelet-activating factor (PAF) induces activation of matrix metalloproteinase 2 activity and vascular endothelial cell invasion and migration. FASEB J *18*, 568-570.

15. Baeyens, N., Bandyopadhyay, C., Coon, B.G., Yun, S., and Schwartz, M.A. (2016). Endothelial fluid shear stress sensing in vascular health and disease. J Clin Invest *126*, 821-828.
16. Baluk, P., Fuxe, J., Hashizume, H., Romano, T., Lashnits, E., Butz, S., Vestweber, D., Corada, M., Molendini, C., Dejana, E., *et al.* (2007). Functionally specialized junctions between endothelial cells of lymphatic vessels. J Exp Med *204*, 2349-2362.
17. Barrio, L.C., Suchyna, T., Bargiello, T., Xu, L.X., Roginski, R.S., Bennett, M.V., and Nicholson, B.J. (1991). Gap junctions formed by connexins 26 and 32 alone and in combination are differently affected by applied voltage. Proc Natl Acad Sci U S A *88*, 8410-8414.
18. Barry, A.K., Wang, N., and Leckband, D.E. (2015a). Local VE-cadherin mechanotransduction triggers long-ranged remodeling of endothelial monolayers. J Cell Sci *128*, 1341-1351.
19. Barry, D.M., Xu, K., Meadows, S.M., Zheng, Y., Norden, P.R., Davis, G.E., and Cleaver, O. (2015b). Cdc42 is required for cytoskeletal support of endothelial cell adhesion during blood vessel formation in mice. Development *142*, 3058-3070.
20. Beckers, C.M., Knezevic, N., Valent, E.T., Tauseef, M., Krishnan, R., Rajendran, K., Hardin, C.C., Aman, J., van Bezu, J., Sweetnam, P., *et al.* (2015). ROCK2 primes the endothelium for vascular hyperpermeability responses by raising baseline junctional tension. Vascul Pharmacol *70*, 45-54.
21. Beckers, C.M., van Hinsbergh, V.W., and van Nieuw Amerongen, G.P. (2010). Driving Rho GTPase activity in endothelial cells regulates barrier integrity. Thromb Haemost *103*, 40-55.
22. Bellanger, J.M., Astier, C., Sardet, C., Ohta, Y., Stossel, T.P., and Debant, A. (2000). The Rac1- and RhoG-specific GEF domain of Trio targets filamin to remodel cytoskeletal actin. Nat Cell Biol *2*, 888-892.
23. Bellanger, J.M., Lazaro, J.B., Diriong, S., Fernandez, A., Lamb, N., and Debant, A. (1998). The two guanine nucleotide exchange factor domains of Trio link the Rac1 and the RhoA pathways in vivo. Oncogene *16*, 147-152.
24. Bhattacharya, M., Su, G., Su, X., Oses-Prieto, J.A., Li, J.T., Huang, X., Hernandez, H., Atakilit, A., Burlingame, A.L., Matthay, M.A., *et al.* (2012). IQGAP1 is necessary for pulmonary vascular barrier protection in murine acute lung injury and pneumonia. Am J Physiol Lung Cell Mol Physiol *303*, L12-19.
25. Birukov, K.G., Csortos, C., Marzilli, L., Dudek, S., Ma, S.F., Bresnick, A.R., Verin, A.D., Cotter, R.J., and Garcia, J.G. (2001). Differential regulation of alternatively spliced endothelial cell myosin light chain kinase isoforms by p60(Src). J Biol Chem *276*, 8567-8573.
26. Birukova, A.A., Tian, Y., Dubrovskyi, O., Zebda, N., Sarich, N., Tian, X., Wang, Y., and Birukov, K.G. (2012). VE-cadherin trans-interactions modulate Rac activation and enhancement of lung endothelial barrier by iloprost. J Cell Physiol *227*, 3405-3416.
27. Bishop, A.L., and Hall, A. (2000). Rho GTPases and their effector proteins. Biochem J *348 Pt 2*, 241-255.
28. Bogatcheva, N.V., Zemskova, M.A., Gorshkov, B.A., Kim, K.M., Daglis, G.A., Poirier, C., and Verin, A.D. (2011). Ezrin, radixin, and moesin are phosphorylated in response to 2-methoxyestradiol and modulate endothelial hyperpermeability. Am J Respir Cell Mol Biol *45*, 1185-1194.

29. Boguski, M.S., and McCormick, F. (1993). Proteins regulating Ras and its relatives. Nature *366*, 643-654.
30. Bouillet, L., Mannic, T., Arboleas, M., Subileau, M., Massot, C., Drouet, C., Huber, P., and Vilgrain, I. (2011). Hereditary angioedema: key role for kallikrein and bradykinin in vascular endothelial-cadherin cleavage and edema formation. J Allergy Clin Immunol *128*, 232-234.
31. Bouquier, N., Vignal, E., Charrasse, S., Weill, M., Schmidt, S., Leonetti, J.P., Blangy, A., and Fort, P. (2009). A cell active chemical GEF inhibitor selectively targets the Trio/RhoG/Rac1 signaling pathway. Chem Biol *16*, 657-666.
32. Braga, V. (2000). The crossroads between cell-cell adhesion and motility. Nat Cell Biol *2*, E182-184.
33. Braga, V.M., Machesky, L.M., Hall, A., and Hotchin, N.A. (1997). The small GTPases Rho and Rac are required for the establishment of cadherin-dependent cell-cell contacts. J Cell Biol *137*, 1421-1431.
34. Brasch, J., Harrison, O.J., Ahlsen, G., Carnally, S.M., Henderson, R.M., Honig, B., and Shapiro, L. (2011). Structure and binding mechanism of vascular endothelial cadherin: a divergent classical cadherin. J Mol Biol *408*, 57-73.
35. Breier, G., Breviario, F., Caveda, L., Berthier, R., Schnurch, H., Gotsch, U., Vestweber, D., Risau, W., and Dejana, E. (1996). Molecular cloning and expression of murine vascular endothelial-cadherin in early stage development of cardiovascular system. Blood *87*, 630-641.
36. Broman, M.T., Kouklis, P., Gao, X., Ramchandran, R., Neamu, R.F., Minshall, R.D., and Malik, A.B. (2006). Cdc42 regulates adherens junction stability and endothelial permeability by inducing alpha-catenin interaction with the vascular endothelial cadherin complex. Circ Res *98*, 73-80.
37. Buckley, C.D., Tan, J., Anderson, K.L., Hanein, D., Volkmann, N., Weis, W.I., Nelson, W.J., and Dunn, A.R. (2014). Cell adhesion. The minimal cadherin-catenin complex binds to actin filaments under force. Science *346*, 1254211.
38. Bussolino, F., Camussi, G., Aglietta, M., Braquet, P., Bosia, A., Pescarmona, G., Sanavio, F., D'Urso, N., and Marchisio, P.C. (1987). Human endothelial cells are target for platelet-activating factor. I. Platelet-activating factor induces changes in cytoskeleton structures. J Immunol *139*, 2439-2446.
39. Cain, R.J., Vanhaesebroeck, B., and Ridley, A.J. (2010). The PI3K p110alpha isoform regulates endothelial adherens junctions via Pyk2 and Rac1. J Cell Biol *188*, 863-876.
40. Carmeliet, P., Lampugnani, M.G., Moons, L., Breviario, F., Compernolle, V., Bono, F., Balconi, G., Spagnuolo, R., Oosthuyse, B., Dewerchin, M., *et al.* (1999). Targeted deficiency or cytosolic truncation of the VE-cadherin gene in mice impairs VEGF-mediated endothelial survival and angiogenesis. Cell *98*, 147-157.
41. Charrasse, S., Comunale, F., Fortier, M., Portales-Casamar, E., Debant, A., and Gauthier-Rouviere, C. (2007). M-cadherin activates Rac1 GTPase through the Rho-GEF trio during myoblast fusion. Mol Biol Cell *18*, 1734-1743.
42. Charrasse, S., Meriane, M., Comunale, F., Blangy, A., and Gauthier-Rouviere, C. (2002). N-cadherin-dependent cell-cell contact regulates Rho GTPases and beta-catenin localization in mouse C2C12 myoblasts. J Cell Biol *158*, 953-965.

43. Chen, H., Paradies, N.E., Fedor-Chaiken, M., and Brackenbury, R. (1997). E-cadherin mediates adhesion and suppresses cell motility via distinct mechanisms. J Cell Sci *110 (Pt 3)*, 345-356.
44. Cheung, N., Tikellis, G., and Wang, J.J. (2007). Diabetic retinopathy. Ophthalmology *114*, 2098-2099; author reply 2099.
45. Colicelli, J. (2004). Human RAS superfamily proteins and related GTPases. Sci STKE *2004*, RE13.
46. Comunale, F., Causeret, M., Favard, C., Cau, J., Taulet, N., Charrasse, S., and Gauthier-Rouviere, C. (2007). Rac1 and RhoA GTPases have antagonistic functions during N-cadherin-dependent cell-cell contact formation in C2C12 myoblasts. Biol Cell *99*, 503-517.
47. Conway, D.E., Breckenridge, M.T., Hinde, E., Gratton, E., Chen, C.S., and Schwartz, M.A. (2013). Fluid shear stress on endothelial cells modulates mechanical tension across VE-cadherin and PECAM-1. Curr Biol *23*, 1024-1030.
48. Coon, B.G., Baeyens, N., Han, J., Budatha, M., Ross, T.D., Fang, J.S., Yun, S., Thomas, J.L., and Schwartz, M.A. (2015). Intramembrane binding of VE-cadherin to VEGFR2 and VEGFR3 assembles the endothelial mechanosensory complex. J Cell Biol *208*, 975-986.
49. Corada, M., Liao, F., Lindgren, M., Lampugnani, M.G., Breviario, F., Frank, R., Muller, W.A., Hicklin, D.J., Bohlen, P., and Dejana, E. (2001). Monoclonal antibodies directed to different regions of vascular endothelial cadherin extracellular domain affect adhesion and clustering of the protein and modulate endothelial permeability. Blood *97*, 1679-1684.
50. Cosgrove, B.D., Mui, K.L., Driscoll, T.P., Caliari, S.R., Mehta, K.D., Assoian, R.K., Burdick, J.A., and Mauck, R.L. (2016). N-cadherin adhesive interactions modulate matrix mechanosensing and fate commitment of mesenchymal stem cells. Nat Mater *15*, 1297-1306.
51. Cottrell, G.T., and Burt, J.M. (2001). Heterotypic gap junction channel formation between heteromeric and homomeric Cx40 and Cx43 connexons. American journal of physiology Cell physiology *281*, C1559-1567.
52. Craig, R., Smith, R., and Kendrick-Jones, J. (1983). Light-chain phosphorylation controls the conformation of vertebrate non-muscle and smooth muscle myosin molecules. Nature *302*, 436-439.
53. Crocker, D.J., Murad, T.M., and Geer, J.C. (1970). Role of the pericyte in wound healing. An ultrastructural study. Exp Mol Pathol *13*, 51-65.
54. Crosby, C.V., Fleming, P.A., Argraves, W.S., Corada, M., Zanetta, L., Dejana, E., and Drake, C.J. (2005). VE-cadherin is not required for the formation of nascent blood vessels but acts to prevent their disassembly. Blood *105*, 2771-2776.
55. Dames, S.A., Bang, E., Haussinger, D., Ahrens, T., Engel, J., and Grzesiek, S. (2008). Insights into the low adhesive capacity of human T-cadherin from the NMR structure of Its N-terminal extracellular domain. J Biol Chem *283*, 23485-23495.
56. Daneman, R., Zhou, L., Kebede, A.A., and Barres, B.A. (2010). Pericytes are required for blood-brain barrier integrity during embryogenesis. Nature *468*, 562-566.
57. Daneshjou, N., Sieracki, N., van Nieuw Amerongen, G.P., Conway, D.E., Schwartz, M.A., Komarova, Y.A., and Malik, A.B. (2015). Rac1 functions as a reversible tension modulator to stabilize VE-cadherin trans-interaction. J Cell Biol *208*, 23-32.
58. Das Sarma, J., Meyer, R.A., Wang, F., Abraham, V., Lo, C.W., and Koval, M. (2001). Multimeric connexin interactions prior to the trans-Golgi network. J Cell Sci *114*, 4013-4024.

59. David, S., Ghosh, C.C., Mukherjee, A., and Parikh, S.M. (2011). Angiopoietin-1 requires IQ domain GTPase-activating protein 1 to activate Rac1 and promote endothelial barrier defense. Arterioscler Thromb Vasc Biol *31*, 2643-2652.
60. Debant, A., Serra-Pages, C., Seipel, K., O'Brien, S., Tang, M., Park, S.H., and Streuli, M. (1996). The multidomain protein Trio binds the LAR transmembrane tyrosine phosphatase, contains a protein kinase domain, and has separate rac-specific and rho-specific guanine nucleotide exchange factor domains. Proc Natl Acad Sci U S A *93*, 5466-5471.
61. DeGeer, J., Boudeau, J., Schmidt, S., Bedford, F., Lamarche-Vane, N., and Debant, A. (2013). Tyrosine phosphorylation of the Rho guanine nucleotide exchange factor Trio regulates netrin-1/DCC-mediated cortical axon outgrowth. Mol Cell Biol *33*, 739-751.
62. Del Vecchio, P.J., Siflinger-Birnboim, A., Shepard, J.M., Bizios, R., Cooper, J.A., and Malik, A.B. (1987). Endothelial monolayer permeability to macromolecules. Fed Proc *46*, 2511-2515.
63. Derom, F., Sebruyns, M., De Groodt, M., and Lagasse, A. (1958). [Transitional forms, arising from the pericyte and representing a stage in in the development of smooth muscle cells, as seen with the electron microscope]. Pathol Biol *6*, 57-58.
64. Diebold, B.A., Fowler, B., Lu, J., Dinauer, M.C., and Bokoch, G.M. (2004). Antagonistic cross-talk between Rac and Cdc42 GTPases regulates generation of reactive oxygen species. J Biol Chem *279*, 28136-28142.
65. Dora, K.A., Xia, J., and Duling, B.R. (2003). Endothelial cell signaling during conducted vasomotor responses. Am J Physiol Heart Circ Physiol *285*, H119-126.
66. Dorrell, M.I., Aguilar, E., and Friedlander, M. (2002). Retinal vascular development is mediated by endothelial filopodia, a preexisting astrocytic template and specific R-cadherin adhesion. Invest Ophthalmol Vis Sci *43*, 3500-3510.
67. Drees, F., Pokutta, S., Yamada, S., Nelson, W.J., and Weis, W.I. (2005). Alpha-catenin is a molecular switch that binds E-cadherin-beta-catenin and regulates actin-filament assembly. Cell *123*, 903-915.
68. Edwards, D.C., Sanders, L.C., Bokoch, G.M., and Gill, G.N. (1999). Activation of LIM-kinase by Pak1 couples Rac/Cdc42 GTPase signalling to actin cytoskeletal dynamics. Nat Cell Biol *1*, 253-259.
69. Ellerbroek, S.M., Wennerberg, K., and Burridge, K. (2003). Serine phosphorylation negatively regulates RhoA in vivo. J Biol Chem *278*, 19023-19031.
70. Essler, M., Amano, M., Kruse, H.J., Kaibuchi, K., Weber, P.C., and Aepfelbacher, M. (1998). Thrombin inactivates myosin light chain phosphatase via Rho and its target Rho kinase in human endothelial cells. J Biol Chem *273*, 21867-21874.
71. Etienne-Manneville, S., and Hall, A. (2002). Rho GTPases in cell biology. Nature *420*, 629-635.
72. Even-Faitelson, L., Rosenberg, M., and Ravid, S. (2005). PAK1 regulates myosin II-B phosphorylation, filament assembly, localization and cell chemotaxis. Cell Signal *17*, 1137-1148.
73. Feng, J., Ito, M., Ichikawa, K., Isaka, N., Nishikawa, M., Hartshorne, D.J., and Nakano, T. (1999). Inhibitory phosphorylation site for Rho-associated kinase on smooth muscle myosin phosphatase. J Biol Chem *274*, 37385-37390.
74. Ferreri, D.M., Minnear, F.L., Yin, T., Kowalczyk, A.P., and Vincent, P.A. (2008). N-cadherin levels in endothelial cells are regulated by monolayer maturity and p120 availability. Cell Commun Adhes *15*, 333-349.

75. Firth, J.A., Bauman, K.F., and Sibley, C.P. (1983). The intercellular junctions of guinea-pig placental capillaries: a possible structural basis for endothelial solute permeability. J Ultrastruct Res *85*, 45-57.
76. Frye, M., Dierkes, M., Kuppers, V., Vockel, M., Tomm, J., Zeuschner, D., Rossaint, J., Zarbock, A., Koh, G.Y., Peters, K., *et al.* (2015). Interfering with VE-PTP stabilizes endothelial junctions in vivo via Tie-2 in the absence of VE-cadherin. J Exp Med *212*, 2267-2287.
77. Fukuyama, T., Ogita, H., Kawakatsu, T., Inagaki, M., and Takai, Y. (2006). Activation of Rac by cadherin through the c-Src-Rap1-phosphatidylinositol 3-kinase-Vav2 pathway. Oncogene *25*, 8-19.
78. Gao, Y., Xing, J., Streuli, M., Leto, T.L., and Zheng, Y. (2001). Trp(56) of rac1 specifies interaction with a subset of guanine nucleotide exchange factors. J Biol Chem *276*, 47530-47541.
79. Garrett, T.A., Van Buul, J.D., and Burridge, K. (2007). VEGF-induced Rac1 activation in endothelial cells is regulated by the guanine nucleotide exchange factor Vav2. Exp Cell Res *313*, 3285-3297.
80. Gavard, J., and Gutkind, J.S. (2006). VEGF controls endothelial-cell permeability by promoting the beta-arrestin-dependent endocytosis of VE-cadherin. Nat Cell Biol *8*, 1223-1234.
81. Gentil-dit-Maurin, A., Oun, S., Almagro, S., Bouillot, S., Courcon, M., Linnepe, R., Vestweber, D., Huber, P., and Tillet, E. (2010). Unraveling the distinct distributions of VE- and N-cadherins in endothelial cells: a key role for p120-catenin. Exp Cell Res *316*, 2587-2599.
82. Gerhardt, H., Liebner, S., Redies, C., and Wolburg, H. (1999). N-cadherin expression in endothelial cells during early angiogenesis in the eye and brain of the chicken: relation to blood-retina and blood-brain barrier development. Eur J Neurosci *11*, 1191-1201.
83. Gerhardt, H., Wolburg, H., and Redies, C. (2000). N-cadherin mediates pericytic-endothelial interaction during brain angiogenesis in the chicken. Dev Dyn *218*, 472-479.
84. Giampietro, C., Taddei, A., Corada, M., Sarra-Ferraris, G.M., Alcalay, M., Cavallaro, U., Orsenigo, F., Lampugnani, M.G., and Dejana, E. (2012). Overlapping and divergent signaling pathways of N-cadherin and VE-cadherin in endothelial cells. Blood *119*, 2159-2170.
85. Goeckeler, Z.M., and Wysolmerski, R.B. (1995). Myosin light chain kinase-regulated endothelial cell contraction: the relationship between isometric tension, actin polymerization, and myosin phosphorylation. J Cell Biol *130*, 613-627.
86. Goh, W.I., Lim, K.B., Sudhaharan, T., Sem, K.P., Bu, W., Chou, A.M., and Ahmed, S. (2012). mDia1 and WAVE2 proteins interact directly with IRSp53 in filopodia and are involved in filopodium formation. J Biol Chem *287*, 4702-4714.
87. Gonzalez, E., Kou, R., and Michel, T. (2006). Rac1 modulates sphingosine 1-phosphate-mediated activation of phosphoinositide 3-kinase/Akt signaling pathways in vascular endothelial cells. J Biol Chem *281*, 3210-3216.
88. Hakim, C.H., Jackson, W.F., and Segal, S.S. (2008). Connexin isoform expression in smooth muscle cells and endothelial cells of hamster cheek pouch arterioles and retractor feed arteries. Microcirculation *15*, 503-514.

89. Hall, A.P., Ashton, S., Horner, J., Wilson, Z., Reens, J., Richmond, G.H., Barry, S.T., and Wedge, S.R. (2016). PDGFR Inhibition Results in Pericyte Depletion and Hemorrhage into the Corpus Luteum of the Rat Ovary. Toxicol Pathol *44*, 98-111.
90. Han, J., Zhang, G., Welch, E.J., Liang, Y., Fu, J., Vogel, S.M., Lowell, C.A., Du, X., Cheresh, D.A., Malik, A.B., *et al.* (2013). A critical role for Lyn kinase in strengthening endothelial integrity and barrier function. Blood *122*, 4140-4149.
91. Harrison, O.J., Jin, X., Hong, S., Bahna, F., Ahlsen, G., Brasch, J., Wu, Y., Vendome, J., Felsovalyi, K., Hampton, C.M., *et al.* (2011). The extracellular architecture of adherens junctions revealed by crystal structures of type I cadherins. Structure *19*, 244-256.
92. Hart, M.J., Eva, A., Evans, T., Aaronson, S.A., and Cerione, R.A. (1991). Catalysis of guanine nucleotide exchange on the CDC42Hs protein by the dbl oncogene product. Nature *354*, 311-314.
93. Hart, M.J., Eva, A., Zangrilli, D., Aaronson, S.A., Evans, T., Cerione, R.A., and Zheng, Y. (1994). Cellular transformation and guanine nucleotide exchange activity are catalyzed by a common domain on the dbl oncogene product. J Biol Chem *269*, 62-65.
94. Hashizume, H., Baluk, P., Morikawa, S., McLean, J.W., Thurston, G., Roberge, S., Jain, R.K., and McDonald, D.M. (2000). Openings between defective endothelial cells explain tumor vessel leakiness. The American journal of pathology *156*, 1363-1380.
95. Hatta, K., Okada, T.S., and Takeichi, M. (1985). A monoclonal antibody disrupting calcium-dependent cell-cell adhesion of brain tissues: possible role of its target antigen in animal pattern formation. Proc Natl Acad Sci U S A *82*, 2789-2793.
96. Hatta, K., and Takeichi, M. (1986). Expression of N-cadherin adhesion molecules associated with early morphogenetic events in chick development. Nature *320*, 447-449.
97. Hawkins, B.T., Lundeen, T.F., Norwood, K.M., Brooks, H.L., and Egleton, R.D. (2007a). Increased blood-brain barrier permeability and altered tight junctions in experimental diabetes in the rat: contribution of hyperglycaemia and matrix metalloproteinases. Diabetologia *50*, 202-211.
98. Hawkins, B.T., Ocheltree, S.M., Norwood, K.M., and Egleton, R.D. (2007b). Decreased blood-brain barrier permeability to fluorescein in streptozotocin-treated rats. Neuroscience letters *411*, 1-5.
99. Herwig, M.C., Tsokos, M., Hermanns, M.I., Kirkpatrick, C.J., and Muller, A.M. (2013). Vascular endothelial cadherin expression in lung specimens of patients with sepsis-induced acute respiratory distress syndrome and endothelial cell cultures. Pathobiology *80*, 245-251.
100. Heupel, W.M., Efthymiadis, A., Schlegel, N., Muller, T., Baumer, Y., Baumgartner, W., Drenckhahn, D., and Waschke, J. (2009). Endothelial barrier stabilization by a cyclic tandem peptide targeting VE-cadherin transinteraction in vitro and in vivo. J Cell Sci *122*, 1616-1625.
101. Higashi-Fujime, S. (1982). Active movement of bundles of actin and myosin filaments from muscle: a simple model for cell motility. Cold Spring Harb Symp Quant Biol *46 Pt 1*, 69-75.
102. Hill, D.K. (1968). Tension due to interaction between the sliding filaments in resting striated muscle. The effect of stimulation. The Journal of physiology *199*, 637-684.
103. Hillig, R.C., Hanzal-Bayer, M., Linari, M., Becker, J., Wittinghofer, A., and Renault, L. (2000). Structural and biochemical properties show ARL3-GDP as a distinct GTP binding protein. Structure *8*, 1239-1245.

104. Hoffman, G.R., Nassar, N., and Cerione, R.A. (2000). Structure of the Rho family GTP-binding protein Cdc42 in complex with the multifunctional regulator RhoGDI. Cell *100*, 345-356.
105. Hoh, J.H., Sosinsky, G.E., Revel, J.P., and Hansma, P.K. (1993). Structure of the extracellular surface of the gap junction by atomic force microscopy. Biophysical journal *65*, 149-163.
106. Holinstat, M., Knezevic, N., Broman, M., Samarel, A.M., Malik, A.B., and Mehta, D. (2006). Suppression of RhoA activity by focal adhesion kinase-induced activation of p190RhoGAP: role in regulation of endothelial permeability. J Biol Chem *281*, 2296-2305.
107. Hong, S., Troyanovsky, R.B., and Troyanovsky, S.M. (2013). Binding to F-actin guides cadherin cluster assembly, stability, and movement. J Cell Biol *201*, 131-143.
108. Huveneers, S., and de Rooij, J. (2013). Mechanosensitive systems at the cadherin-F-actin interface. J Cell Sci *126*, 403-413.
109. Huveneers, S., Oldenburg, J., Spanjaard, E., van der Krogt, G., Grigoriev, I., Akhmanova, A., Rehmann, H., and de Rooij, J. (2012). Vinculin associates with endothelial VE-cadherin junctions to control force-dependent remodeling. J Cell Biol *196*, 641-652.
110. Itoh, F., Itoh, S., Adachi, T., Ichikawa, K., Matsumura, Y., Takagi, T., Festing, M., Watanabe, T., Weinstein, M., Karlsson, S., *et al.* (2012). Smad2/Smad3 in endothelium is indispensable for vascular stability via S1PR1 and N-cadherin expressions. Blood *119*, 5320-5328.
111. Itoh, M., Furuse, M., Morita, K., Kubota, K., Saitou, M., and Tsukita, S. (1999a). Direct binding of three tight junction-associated MAGUKs, ZO-1, ZO-2, and ZO-3, with the COOH termini of claudins. J Cell Biol *147*, 1351-1363.
112. Itoh, M., Morita, K., and Tsukita, S. (1999b). Characterization of ZO-2 as a MAGUK family member associated with tight as well as adherens junctions with a binding affinity to occludin and alpha catenin. J Biol Chem *274*, 5981-5986.
113. Ivanov, D., Philippova, M., Antropova, J., Gubaeva, F., Iljinskaya, O., Tararak, E., Bochkov, V., Erne, P., Resink, T., and Tkachuk, V. (2001). Expression of cell adhesion molecule T-cadherin in the human vasculature. Histochem Cell Biol *115*, 231-242.
114. Ivanov, D., Philippova, M., Tkachuk, V., Erne, P., and Resink, T. (2004). Cell adhesion molecule T-cadherin regulates vascular cell adhesion, phenotype and motility. Exp Cell Res *293*, 207-218.
115. Johnson, T.L., and Nerem, R.M. (2007). Endothelial connexin 37, connexin 40, and connexin 43 respond uniquely to substrate and shear stress. Endothelium : journal of endothelial cell research *14*, 215-226.
116. Joshi, A.D., Dimitropoulou, C., Thangjam, G., Snead, C., Feldman, S., Barabutis, N., Fulton, D., Hou, Y., Kumar, S., Patel, V., *et al.* (2014). Heat shock protein 90 inhibitors prevent LPS-induced endothelial barrier dysfunction by disrupting RhoA signaling. Am J Respir Cell Mol Biol *50*, 170-179.
117. Kaplan, A.P. (2002). Clinical practice. Chronic urticaria and angioedema. N Engl J Med *346*, 175-179.
118. Kashef, J., Kohler, A., Kuriyama, S., Alfandari, D., Mayor, R., and Wedlich, D. (2009). Cadherin-11 regulates protrusive activity in Xenopus cranial neural crest cells upstream of Trio and the small GTPases. Genes Dev *23*, 1393-1398.

119. Katsuno, T., Umeda, K., Matsui, T., Hata, M., Tamura, A., Itoh, M., Takeuchi, K., Fujimori, T., Nabeshima, Y., Noda, T., *et al.* (2008). Deficiency of zonula occludens-1 causes embryonic lethal phenotype associated with defected yolk sac angiogenesis and apoptosis of embryonic cells. Mol Biol Cell *19*, 2465-2475.
120. Kim, K.R., Sung, C.O., Kwon, T.J., Lee, J., and Robboy, S.J. (2015). Defective pericyte recruitment of villous stromal vessels as the possible etiologic cause of hydropic change in complete hydatidiform mole. PLoS One *10*, e0122266.
121. Kirk, J., Plumb, J., Mirakhur, M., and McQuaid, S. (2003). Tight junctional abnormality in multiple sclerosis white matter affects all calibres of vessel and is associated with blood-brain barrier leakage and active demyelination. The Journal of pathology *201*, 319-327.
122. Klaassen, I., Van Noorden, C.J., and Schlingemann, R.O. (2013). Molecular basis of the inner blood-retinal barrier and its breakdown in diabetic macular edema and other pathological conditions. Prog Retin Eye Res *34*, 19-48.
123. Knezevic, II, Predescu, S.A., Neamu, R.F., Gorovoy, M.S., Knezevic, N.M., Easington, C., Malik, A.B., and Predescu, D.N. (2009). Tiam1 and Rac1 are required for platelet-activating factor-induced endothelial junctional disassembly and increase in vascular permeability. J Biol Chem *284*, 5381-5394.
124. Kolega, J. (1998). Cytoplasmic dynamics of myosin IIA and IIB: spatial 'sorting' of isoforms in locomoting cells. J Cell Sci *111 (Pt 15)*, 2085-2095.
125. Komarova, Y.A., Kruse, K., Mehta, D., and Malik, A.B. (2017). Protein Interactions at Endothelial Junctions and Signaling Mechanisms Regulating Endothelial Permeability. Circ Res *120*, 179-206.
126. Komarova, Y.A., Mehta, D., and Malik, A.B. (2007). Dual regulation of endothelial junctional permeability. Sci STKE *2007*, re8.
127. Kovacs, E.M., Ali, R.G., McCormack, A.J., and Yap, A.S. (2002). E-cadherin homophilic ligation directly signals through Rac and phosphatidylinositol 3-kinase to regulate adhesive contacts. J Biol Chem *277*, 6708-6718.
128. Krattinger, N., Capponi, A., Mazzolai, L., Aubert, J.F., Caille, D., Nicod, P., Waeber, G., Meda, P., and Haefliger, J.A. (2007). Connexin40 regulates renin production and blood pressure. Kidney international *72*, 814-822.
129. Kurella, V.B., Richard, J.M., Parke, C.L., Lecour, L.F., Jr., Bellamy, H.D., and Worthylake, D.K. (2009). Crystal structure of the GTPase-activating protein-related domain from IQGAP1. J Biol Chem *284*, 14857-14865.
130. Kuroda, S., Fukata, M., Nakagawa, M., Fujii, K., Nakamura, T., Ookubo, T., Izawa, I., Nagase, T., Nomura, N., Tani, H., *et al.* (1998). Role of IQGAP1, a target of the small GTPases Cdc42 and Rac1, in regulation of E-cadherin- mediated cell-cell adhesion. Science *281*, 832-835.
131. Lampugnani, M.G., Corada, M., Caveda, L., Breviario, F., Ayalon, O., Geiger, B., and Dejana, E. (1995). The molecular organization of endothelial cell to cell junctions: differential association of plakoglobin, beta-catenin, and alpha-catenin with vascular endothelial cadherin (VE-cadherin). J Cell Biol *129*, 203-217.
132. Lampugnani, M.G., Resnati, M., Raiteri, M., Pigott, R., Pisacane, A., Houen, G., Ruco, L.P., and Dejana, E. (1992). A novel endothelial-specific membrane protein is a marker of cell-cell contacts. J Cell Biol *118*, 1511-1522.

133. Lampugnani, M.G., Zanetti, A., Breviario, F., Balconi, G., Orsenigo, F., Corada, M., Spagnuolo, R., Betson, M., Braga, V., and Dejana, E. (2002). VE-cadherin regulates endothelial actin activating Rac and increasing membrane association of Tiam. Mol Biol Cell *13*, 1175-1189.
134. Leach, L., Clark, P., Lampugnani, M.G., Arroyo, A.G., Dejana, E., and Firth, J.A. (1993). Immunoelectron characterisation of the inter-endothelial junctions of human term placenta. J Cell Sci *104 (Pt 4)*, 1073-1081.
135. Leckband, D.E., and de Rooij, J. (2014). Cadherin adhesion and mechanotransduction. Annual review of cell and developmental biology *30*, 291-315.
136. Lee, C.S., Choi, C.K., Shin, E.Y., Schwartz, M.A., and Kim, E.G. (2010). Myosin II directly binds and inhibits Dbl family guanine nucleotide exchange factors: a possible link to Rho family GTPases. J Cell Biol *190*, 663-674.
137. Lee, W.L., and Slutsky, A.S. (2010). Sepsis and endothelial permeability. N Engl J Med *363*, 689-691.
138. Leonard, M., Zhang, L., Zhai, N., Cader, A., Chan, Y., Nowak, R.B., Fowler, V.M., and Menko, A.S. (2011). Modulation of N-cadherin junctions and their role as epicenters of differentiation-specific actin regulation in the developing lens. Dev Biol *349*, 363-377.
139. Li, F., Lan, Y., Wang, Y., Wang, J., Yang, G., Meng, F., Han, H., Meng, A., Wang, Y., and Yang, X. (2011). Endothelial Smad4 maintains cerebrovascular integrity by activating N-cadherin through cooperation with Notch. Dev Cell *20*, 291-302.
140. Liao, Y., Day, K.H., Damon, D.N., and Duling, B.R. (2001). Endothelial cell-specific knockout of connexin 43 causes hypotension and bradycardia in mice. Proc Natl Acad Sci U S A *98*, 9989-9994.
141. Liaw, C.W., Cannon, C., Power, M.D., Kiboneka, P.K., and Rubin, L.L. (1990). Identification and cloning of two species of cadherins in bovine endothelial cells. EMBO J *9*, 2701-2708.
142. Liebner, S., Fischmann, A., Rascher, G., Duffner, F., Grote, E.H., Kalbacher, H., and Wolburg, H. (2000a). Claudin-1 and claudin-5 expression and tight junction morphology are altered in blood vessels of human glioblastoma multiforme. Acta Neuropathol *100*, 323-331.
143. Liebner, S., Gerhardt, H., and Wolburg, H. (2000b). Differential expression of endothelial beta-catenin and plakoglobin during development and maturation of the blood-brain and blood-retina barrier in the chicken. Dev Dyn *217*, 86-98.
144. Liebner, S., Kniesel, U., Kalbacher, H., and Wolburg, H. (2000c). Correlation of tight junction morphology with the expression of tight junction proteins in blood-brain barrier endothelial cells. European journal of cell biology *79*, 707-717.
145. Lindahl, P., Johansson, B.R., Leveen, P., and Betsholtz, C. (1997). Pericyte loss and microaneurysm formation in PDGF-B-deficient mice. Science *277*, 242-245.
146. Lippoldt, A., Liebner, S., Andbjer, B., Kalbacher, H., Wolburg, H., Haller, H., and Fuxe, K. (2000). Organization of choroid plexus epithelial and endothelial cell tight junctions and regulation of claudin-1, -2 and -5 expression by protein kinase C. Neuroreport *11*, 1427-1431.
147. Liu, Y., Collins, C., Kiosses, W.B., Murray, A.M., Joshi, M., Shepherd, T.R., Fuentes, E.J., and Tzima, E. (2013). A novel pathway spatiotemporally activates Rac1 and redox signaling in response to fluid shear stress. J Cell Biol *201*, 863-873.

148. Liu, Z., Tan, J.L., Cohen, D.M., Yang, M.T., Sniadecki, N.J., Ruiz, S.A., Nelson, C.M., and Chen, C.S. (2010). Mechanical tugging force regulates the size of cell-cell junctions. Proc Natl Acad Sci U S A *107*, 9944-9949.
149. Looft-Wilson, R.C., Payne, G.W., and Segal, S.S. (2004). Connexin expression and conducted vasodilation along arteriolar endothelium in mouse skeletal muscle. J Appl Physiol (1985) *97*, 1152-1158.
150. Luo, Y., and Radice, G.L. (2005). N-cadherin acts upstream of VE-cadherin in controlling vascular morphogenesis. J Cell Biol *169*, 29-34.
151. Luo, Y., Xiao, W., Zhu, X., Mao, Y., Liu, X., Chen, X., Huang, J., Tang, S., and Rizzolo, L.J. (2011). Differential expression of claudins in retinas during normal development and the angiogenesis of oxygen-induced retinopathy. Invest Ophthalmol Vis Sci *52*, 7556-7564.
152. MacNevin, C.J., Toutchkine, A., Marston, D.J., Hsu, C.W., Tsygankov, D., Li, L., Liu, B., Qi, T., Nguyen, D.V., and Hahn, K.M. (2016). Ratiometric Imaging Using a Single Dye Enables Simultaneous Visualization of Rac1 and Cdc42 Activation. J Am Chem Soc *138*, 2571-2575.
153. Mammoto, A., Mammoto, T., Kanapathipillai, M., Wing Yung, C., Jiang, E., Jiang, A., Lofgren, K., Gee, E.P., and Ingber, D.E. (2013). Control of lung vascular permeability and endotoxin-induced pulmonary oedema by changes in extracellular matrix mechanics. Nat Commun *4*, 1759.
154. Mammoto, T., Parikh, S.M., Mammoto, A., Gallagher, D., Chan, B., Mostoslavsky, G., Ingber, D.E., and Sukhatme, V.P. (2007). Angiopoietin-1 requires p190 RhoGAP to protect against vascular leakage in vivo. J Biol Chem *282*, 23910-23918.
155. Marcus-Gueret, N., Schmidt, K.L., and Stringham, E.G. (2012). Distinct cell guidance pathways controlled by the Rac and Rho GEF domains of UNC-73/TRIO in Caenorhabditis elegans. Genetics *190*, 129-142.
156. Martin-Padura, I., Lostaglio, S., Schneemann, M., Williams, L., Romano, M., Fruscella, P., Panzeri, C., Stoppacciaro, A., Ruco, L., Villa, A., *et al.* (1998). Junctional adhesion molecule, a novel member of the immunoglobulin superfamily that distributes at intercellular junctions and modulates monocyte transmigration. J Cell Biol *142*, 117-127.
157. Mary, S., Charrasse, S., Meriane, M., Comunale, F., Travo, P., Blangy, A., and Gauthier-Rouviere, C. (2002). Biogenesis of N-cadherin-dependent cell-cell contacts in living fibroblasts is a microtubule-dependent kinesin-driven mechanism. Mol Biol Cell *13*, 285-301.
158. Mathiisen, T.M., Lehre, K.P., Danbolt, N.C., and Ottersen, O.P. (2010). The perivascular astroglial sheath provides a complete covering of the brain microvessels: an electron microscopic 3D reconstruction. Glia *58*, 1094-1103.
159. McGuire, P.G., Rangasamy, S., Maestas, J., and Das, A. (2011). Pericyte-derived sphingosine 1-phosphate induces the expression of adhesion proteins and modulates the retinal endothelial cell barrier. Arterioscler Thromb Vasc Biol *31*, e107-115.
160. Medley, Q.G., Buchbinder, E.G., Tachibana, K., Ngo, H., Serra-Pages, C., and Streuli, M. (2003). Signaling between focal adhesion kinase and trio. J Biol Chem *278*, 13265-13270.
161. Medley, Q.G., Serra-Pages, C., Iannotti, E., Seipel, K., Tang, M., O'Brien, S.P., and Streuli, M. (2000). The trio guanine nucleotide exchange factor is a RhoA target. Binding of RhoA to the trio immunoglobulin-like domain. J Biol Chem *275*, 36116-36123.

162. Mehta, D., Konstantoulaki, M., Ahmmed, G.U., and Malik, A.B. (2005). Sphingosine 1-phosphate-induced mobilization of intracellular Ca2+ mediates rac activation and adherens junction assembly in endothelial cells. J Biol Chem *280*, 17320-17328.
163. Miller, J.R., Silver, P.J., and Stull, J.T. (1983). The role of myosin light chain kinase phosphorylation in beta-adrenergic relaxation of tracheal smooth muscle. Mol Pharmacol *24*, 235-242.
164. Mong, P.Y., and Wang, Q. (2009). Activation of Rho kinase isoforms in lung endothelial cells during inflammation. J Immunol *182*, 2385-2394.
165. Moore, D.H., and Ruska, H. (1957). The fine structure of capillaries and small arteries. J Biophys Biochem Cytol *3*, 457-462.
166. Morganti-Kossmann, M.C., Rancan, M., Stahel, P.F., and Kossmann, T. (2002). Inflammatory response in acute traumatic brain injury: a double-edged sword. Curr Opin Crit Care *8*, 101-105.
167. Moshfegh, Y., Bravo-Cordero, J.J., Miskolci, V., Condeelis, J., and Hodgson, L. (2014). A Trio-Rac1-Pak1 signalling axis drives invadopodia disassembly. Nat Cell Biol *16*, 574-586.
168. Naikawadi, R.P., Cheng, N., Vogel, S.M., Qian, F., Wu, D., Malik, A.B., and Ye, R.D. (2012). A critical role for phosphatidylinositol (3,4,5)-trisphosphate-dependent Rac exchanger 1 in endothelial junction disruption and vascular hyperpermeability. Circ Res *111*, 1517-1527.
169. Navarro, P., Ruco, L., and Dejana, E. (1998). Differential localization of VE- and N-cadherins in human endothelial cells: VE-cadherin competes with N-cadherin for junctional localization. J Cell Biol *140*, 1475-1484.
170. Nelson, C.M., and Chen, C.S. (2003). VE-cadherin simultaneously stimulates and inhibits cell proliferation by altering cytoskeletal structure and tension. J Cell Sci *116*, 3571-3581.
171. Nelson, C.M., Pirone, D.M., Tan, J.L., and Chen, C.S. (2004). Vascular endothelial-cadherin regulates cytoskeletal tension, cell spreading, and focal adhesions by stimulating RhoA. Mol Biol Cell *15*, 2943-2953.
172. Neubrand, V.E., Thomas, C., Schmidt, S., Debant, A., and Schiavo, G. (2010). Kidins220/ARMS regulates Rac1-dependent neurite outgrowth by direct interaction with the RhoGEF Trio. J Cell Sci *123*, 2111-2123.
173. Niederman, R., and Pollard, T.D. (1975). Human platelet myosin. II. In vitro assembly and structure of myosin filaments. J Cell Biol *67*, 72-92.
174. Nimnual, A.S., Taylor, L.J., and Bar-Sagi, D. (2003). Redox-dependent downregulation of Rho by Rac. Nat Cell Biol *5*, 236-241.
175. Nitta, T., Hata, M., Gotoh, S., Seo, Y., Sasaki, H., Hashimoto, N., Furuse, M., and Tsukita, S. (2003). Size-selective loosening of the blood-brain barrier in claudin-5-deficient mice. J Cell Biol *161*, 653-660.
176. Noren, N.K., Niessen, C.M., Gumbiner, B.M., and Burridge, K. (2001). Cadherin engagement regulates Rho family GTPases. J Biol Chem *276*, 33305-33308.
177. Ouyang, M., Lu, S., Kim, T., Chen, C.E., Seong, J., Leckband, D.E., Wang, F., Reynolds, A.B., Schwartz, M.A., and Wang, Y. (2013). N-cadherin regulates spatially polarized signals through distinct p120ctn and beta-catenin-dependent signalling pathways. Nat Commun *4*, 1589.

178. Paik, J.H., Skoura, A., Chae, S.S., Cowan, A.E., Han, D.K., Proia, R.L., and Hla, T. (2004). Sphingosine 1-phosphate receptor regulation of N-cadherin mediates vascular stabilization. Genes Dev *18*, 2392-2403.
179. Papaharalambus, C., Sajjad, W., Syed, A., Zhang, C., Bergo, M.O., Alexander, R.W., and Ahmad, M. (2005). Tumor necrosis factor alpha stimulation of Rac1 activity. Role of isoprenylcysteine carboxylmethyltransferase. J Biol Chem *280*, 18790-18796.
180. Parthasarathi, K., Ichimura, H., Monma, E., Lindert, J., Quadri, S., Issekutz, A., and Bhattacharya, J. (2006). Connexin 43 mediates spread of Ca2+-dependent proinflammatory responses in lung capillaries. J Clin Invest *116*, 2193-2200.
181. Patel, S.D., Ciatto, C., Chen, C.P., Bahna, F., Rajebhosale, M., Arkus, N., Schieren, I., Jessell, T.M., Honig, B., Price, S.R., *et al.* (2006). Type II cadherin ectodomain structures: implications for classical cadherin specificity. Cell *124*, 1255-1268.
182. Pawlowski, N.A., Kaplan, G., Abraham, E., and Cohn, Z.A. (1988). The selective binding and transmigration of monocytes through the junctional complexes of human endothelium. J Exp Med *168*, 1865-1882.
183. Petito, C.K., Pulsinelli, W.A., Jacobson, G., and Plum, F. (1982). Edema and vascular permeability in cerebral ischemia: comparison between ischemic neuronal damage and infarction. J Neuropathol Exp Neurol *41*, 423-436.
184. Petrache, I., Crow, M.T., Neuss, M., and Garcia, J.G. (2003). Central involvement of Rho family GTPases in TNF-alpha-mediated bovine pulmonary endothelial cell apoptosis. Biochem Biophys Res Commun *306*, 244-249.
185. Philibert, C., Bouillot, S., Huber, P., and Faury, G. (2012). Protocadherin-12 deficiency leads to modifications in the structure and function of arteries in mice. Pathol Biol (Paris) *60*, 34-40.
186. Philippova, M., Banfi, A., Ivanov, D., Gianni-Barrera, R., Allenspach, R., Erne, P., and Resink, T. (2006). Atypical GPI-anchored T-cadherin stimulates angiogenesis in vitro and in vivo. Arterioscler Thromb Vasc Biol *26*, 2222-2230.
187. Qiao, J., Huang, F., and Lum, H. (2003). PKA inhibits RhoA activation: a protection mechanism against endothelial barrier dysfunction. Am J Physiol Lung Cell Mol Physiol *284*, L972-980.
188. Qu, Y., and Dahl, G. (2004). Accessibility of cx46 hemichannels for uncharged molecules and its modulation by voltage. Biophysical journal *86*, 1502-1509.
189. Rabiet, M.J., Plantier, J.L., Rival, Y., Genoux, Y., Lampugnani, M.G., and Dejana, E. (1996). Thrombin-induced increase in endothelial permeability is associated with changes in cell-to-cell junction organization. Arterioscler Thromb Vasc Biol *16*, 488-496.
190. Rajput, C., Kini, V., Smith, M., Yazbeck, P., Chavez, A., Schmidt, T., Zhang, W., Knezevic, N., Komarova, Y., and Mehta, D. (2013). Neural Wiskott-Aldrich syndrome protein (N-WASP)-mediated p120-catenin interaction with Arp2-Actin complex stabilizes endothelial adherens junctions. J Biol Chem *288*, 4241-4250.
191. Ramchandran, R., Mehta, D., Vogel, S.M., Mirza, M.K., Kouklis, P., and Malik, A.B. (2008). Critical role of Cdc42 in mediating endothelial barrier protection in vivo. Am J Physiol Lung Cell Mol Physiol *295*, L363-369.
192. Rampon, C., Prandini, M.H., Bouillot, S., Pointu, H., Tillet, E., Frank, R., Vernet, M., and Huber, P. (2005). Protocadherin 12 (VE-cadherin 2) is expressed in endothelial, trophoblast, and mesangial cells. Exp Cell Res *302*, 48-60.

193. Rascher, G., and Wolburg, H. (1997). The tight junctions of the leptomeningeal blood-cerebrospinal fluid barrier during development. Journal fur Hirnforschung *38*, 525-540.
194. Reese, T.S., and Karnovsky, M.J. (1967). Fine structural localization of a blood-brain barrier to exogenous peroxidase. J Cell Biol *34*, 207-217.
195. Reinhard, N.R., van Helden, S.F., Anthony, E.C., Yin, T., Wu, Y.I., Goedhart, J., Gadella, T.W., and Hordijk, P.L. (2016). Spatiotemporal analysis of RhoA/B/C activation in primary human endothelial cells. Scientific reports *6*, 25502.
196. Rimm, D.L., Koslov, E.R., Kebriaei, P., Cianci, C.D., and Morrow, J.S. (1995). Alpha 1(E)-catenin is an actin-binding and -bundling protein mediating the attachment of F-actin to the membrane adhesion complex. Proc Natl Acad Sci U S A *92*, 8813-8817.
197. Riveline, D., Zamir, E., Balaban, N.Q., Schwarz, U.S., Ishizaki, T., Narumiya, S., Kam, Z., Geiger, B., and Bershadsky, A.D. (2001). Focal contacts as mechanosensors: externally applied local mechanical force induces growth of focal contacts by an mDia1-dependent and ROCK-independent mechanism. J Cell Biol *153*, 1175-1186.
198. Rivera, L.B., and Brekken, R.A. (2011). SPARC promotes pericyte recruitment via inhibition of endoglin-dependent TGF-beta1 activity. J Cell Biol *193*, 1305-1319.
199. Roof, R.W., Haskell, M.D., Dukes, B.D., Sherman, N., Kinter, M., and Parsons, S.J. (1998). Phosphotyrosine (p-Tyr)-dependent and -independent mechanisms of p190 RhoGAP-p120 RasGAP interaction: Tyr 1105 of p190, a substrate for c-Src, is the sole p-Tyr mediator of complex formation. Mol Cell Biol *18*, 7052-7063.
200. Rustenhoven, J., Aalderink, M., Scotter, E.L., Oldfield, R.L., Bergin, P.S., Mee, E.W., Graham, E.S., Faull, R.L., Curtis, M.A., Park, T.I., *et al.* (2016). TGF-beta1 regulates human brain pericyte inflammatory processes involved in neurovasculature function. J Neuroinflammation *13*, 37.
201. Sabatini, P.J., Zhang, M., Silverman-Gavrila, R., Bendeck, M.P., and Langille, B.L. (2008). Homotypic and endothelial cell adhesions via N-cadherin determine polarity and regulate migration of vascular smooth muscle cells. Circ Res *103*, 405-412.
202. Sagare, A.P., Bell, R.D., Zhao, Z., Ma, Q., Winkler, E.A., Ramanathan, A., and Zlokovic, B.V. (2013). Pericyte loss influences Alzheimer-like neurodegeneration in mice. Nat Commun *4*, 2932.
203. Salomon, D., Ayalon, O., Patel-King, R., Hynes, R.O., and Geiger, B. (1992). Extrajunctional distribution of N-cadherin in cultured human endothelial cells. J Cell Sci *102 (Pt 1)*, 7-17.
204. Sander, E.E., ten Klooster, J.P., van Delft, S., van der Kammen, R.A., and Collard, J.G. (1999). Rac downregulates Rho activity: reciprocal balance between both GTPases determines cellular morphology and migratory behavior. J Cell Biol *147*, 1009-1022.
205. Sandow, S.L., and Hill, C.E. (2000). Incidence of myoendothelial gap junctions in the proximal and distal mesenteric arteries of the rat is suggestive of a role in endothelium-derived hyperpolarizing factor-mediated responses. Circ Res *86*, 341-346.
206. Sasaki, T., Kikuchi, A., Araki, S., Hata, Y., Isomura, M., Kuroda, S., and Takai, Y. (1990). Purification and characterization from bovine brain cytosol of a protein that inhibits the dissociation of GDP from and the subsequent binding of GTP to smg p25A, a ras p21-like GTP-binding protein. J Biol Chem *265*, 2333-2337.

207. Scheffzek, K., Stephan, I., Jensen, O.N., Illenberger, D., and Gierschik, P. (2000). The Rac-RhoGDI complex and the structural basis for the regulation of Rho proteins by RhoGDI. Nat Struct Biol *7*, 122-126.
208. Schmidt, S., and Debant, A. (2014). Function and regulation of the Rho guanine nucleotide exchange factor Trio. Small GTPases *5*, e29769.
209. Scott, D.W., Tolbert, C.E., and Burridge, K. (2016). Tension on JAM-A activates RhoA via GEF-H1 and p115 RhoGEF. Mol Biol Cell *27*, 1420-1430.
210. Seipel, K., Medley, Q.G., Kedersha, N.L., Zhang, X.A., O'Brien, S.P., Serra-Pages, C., Hemler, M.E., and Streuli, M. (1999). Trio amino-terminal guanine nucleotide exchange factor domain expression promotes actin cytoskeleton reorganization, cell migration and anchorage-independent cell growth. J Cell Sci *112 (Pt 12)*, 1825-1834.
211. Seipel, K., O'Brien, S.P., Iannotti, E., Medley, Q.G., and Streuli, M. (2001). Tara, a novel F-actin binding protein, associates with the Trio guanine nucleotide exchange factor and regulates actin cytoskeletal organization. J Cell Sci *114*, 389-399.
212. Shan, W.S., Tanaka, H., Phillips, G.R., Arndt, K., Yoshida, M., Colman, D.R., and Shapiro, L. (2000). Functional cis-heterodimers of N- and R-cadherins. J Cell Biol *148*, 579-590.
213. Shapiro, L., Fannon, A.M., Kwong, P.D., Thompson, A., Lehmann, M.S., Grubel, G., Legrand, J.F., Als-Nielsen, J., Colman, D.R., and Hendrickson, W.A. (1995). Structural basis of cell-cell adhesion by cadherins. Nature *374*, 327-337.
214. Shimokawa, H., Seto, M., Katsumata, N., Amano, M., Kozai, T., Yamawaki, T., Kuwata, K., Kandabashi, T., Egashira, K., Ikegaki, I., *et al.* (1999). Rho-kinase-mediated pathway induces enhanced myosin light chain phosphorylations in a swine model of coronary artery spasm. Cardiovasc Res *43*, 1029-1039.
215. Siddiqui, M.R., Komarova, Y.A., Vogel, S.M., Gao, X., Bonini, M.G., Rajasingh, J., Zhao, Y.Y., Brovkovych, V., and Malik, A.B. (2011). Caveolin-1-eNOS signaling promotes p190RhoGAP-A nitration and endothelial permeability. J Cell Biol *193*, 841-850.
216. Sieczkiewicz, G.J., and Herman, I.M. (2003). TGF-beta 1 signaling controls retinal pericyte contractile protein expression. Microvasc Res *66*, 190-196.
217. Simionescu, M., Simionescu, N., and Palade, G.E. (1975). Segmental differentiations of cell junctions in the vascular endothelium. The microvasculature. J Cell Biol *67*, 863-885.
218. Simionescu, M., Simionescu, N., and Palade, G.E. (1976). Segmental differentiations of cell junctions in the vascular endothelium. Arteries and veins. J Cell Biol *68*, 705-723.
219. Simons, M., Wang, M., McBride, O.W., Kawamoto, S., Yamakawa, K., Gdula, D., Adelstein, R.S., and Weir, L. (1991). Human nonmuscle myosin heavy chains are encoded by two genes located on different chromosomes. Circ Res *69*, 530-539.
220. Sims, D.E., and Westfall, J.A. (1983). Analysis of relationships between pericytes and gas exchange capillaries in neonatal and mature bovine lungs. Microvascular research *25*, 333-342.
221. Smith, T.D., Mohankumar, A., Minogue, P.J., Beyer, E.C., Berthoud, V.M., and Koval, M. (2012). Cytoplasmic amino acids within the membrane interface region influence connexin oligomerization. The Journal of membrane biology *245*, 221-230.

222. Son, K., Smith, T.C., and Luna, E.J. (2015). Supervillin binds the Rac/Rho-GEF Trio and increases Trio-mediated Rac1 activation. Cytoskeleton (Hoboken) *72*, 47-64.
223. Straight, A.F., Cheung, A., Limouze, J., Chen, I., Westwood, N.J., Sellers, J.R., and Mitchison, T.J. (2003). Dissecting temporal and spatial control of cytokinesis with a myosin II Inhibitor. Science *299*, 1743-1747.
224. Swart-Mataraza, J.M., Li, Z., and Sacks, D.B. (2002). IQGAP1 is a component of Cdc42 signaling to the cytoskeleton. J Biol Chem *277*, 24753-24763.
225. Szulcek, R., Beckers, C.M., Hodzic, J., de Wit, J., Chen, Z., Grob, T., Musters, R.J., Minshall, R.D., van Hinsbergh, V.W., and van Nieuw Amerongen, G.P. (2013). Localized RhoA GTPase activity regulates dynamics of endothelial monolayer integrity. Cardiovasc Res *99*, 471-482.
226. Taddei, A., Giampietro, C., Conti, A., Orsenigo, F., Breviario, F., Pirazzoli, V., Potente, M., Daly, C., Dimmeler, S., and Dejana, E. (2008). Endothelial adherens junctions control tight junctions by VE-cadherin-mediated upregulation of claudin-5. Nat Cell Biol *10*, 923-934.
227. Tan, W., Palmby, T.R., Gavard, J., Amornphimoltham, P., Zheng, Y., and Gutkind, J.S. (2008). An essential role for Rac1 in endothelial cell function and vascular development. FASEB J *22*, 1829-1838.
228. Telo, P., Breviario, F., Huber, P., Panzeri, C., and Dejana, E. (1998). Identification of a novel cadherin (vascular endothelial cadherin-2) located at intercellular junctions in endothelial cells. J Biol Chem *273*, 17565-17572.
229. Tillet, E., Vittet, D., Feraud, O., Moore, R., Kemler, R., and Huber, P. (2005). N-cadherin deficiency impairs pericyte recruitment, and not endothelial differentiation or sprouting, in embryonic stem cell-derived angiogenesis. Exp Cell Res *310*, 392-400.
230. Tilton, R.G., Hoffmann, P.L., Kilo, C., and Williamson, J.R. (1981). Pericyte degeneration and basement membrane thickening in skeletal muscle capillaries of human diabetics. Diabetes *30*, 326-334.
231. Timmerman, I., Heemskerk, N., Kroon, J., Schaefer, A., van Rijssel, J., Hoogenboezem, M., van Unen, J., Goedhart, J., Gadella, T.W., Jr., Yin, T., *et al.* (2015). A local VE-cadherin and Trio-based signaling complex stabilizes endothelial junctions through Rac1. J Cell Sci *128*, 3041-3054.
232. Timpson, P., Jones, G.E., Frame, M.C., and Brunton, V.G. (2001). Coordination of cell polarization and migration by the Rho family GTPases requires Src tyrosine kinase activity. Curr Biol *11*, 1836-1846.
233. Tornavaca, O., Chia, M., Dufton, N., Almagro, L.O., Conway, D.E., Randi, A.M., Schwartz, M.A., Matter, K., and Balda, M.S. (2015). ZO-1 controls endothelial adherens junctions, cell-cell tension, angiogenesis, and barrier formation. J Cell Biol *208*, 821-838.
234. Tran, K.A., Zhang, X., Predescu, D., Huang, X., Machado, R.F., Gothert, J.R., Malik, A.B., Valyi-Nagy, T., and Zhao, Y.Y. (2016). Endothelial beta-Catenin Signaling Is Required for Maintaining Adult Blood-Brain Barrier Integrity and Central Nervous System Homeostasis. Circulation *133*, 177-186.
235. Ueda, T., Kikuchi, A., Ohga, N., Yamamoto, J., and Takai, Y. (1990). Purification and characterization from bovine brain cytosol of a novel regulatory protein inhibiting the dissociation of GDP from and the subsequent binding of GTP to rhoB p20, a ras p21-like GTP-binding protein. J Biol Chem *265*, 9373-9380.

236. Valiunas, V., Gemel, J., Brink, P.R., and Beyer, E.C. (2001). Gap junction channels formed by coexpressed connexin40 and connexin43. Am J Physiol Heart Circ Physiol *281*, H1675-1689.
237. van Haren, J., Boudeau, J., Schmidt, S., Basu, S., Liu, Z., Lammers, D., Demmers, J., Benhari, J., Grosveld, F., Debant, A., *et al.* (2014). Dynamic microtubules catalyze formation of navigator-TRIO complexes to regulate neurite extension. Curr Biol *24*, 1778-1785.
238. van Nieuw Amerongen, G.P., Beckers, C.M., Achekar, I.D., Zeeman, S., Musters, R.J., and van Hinsbergh, V.W. (2007). Involvement of Rho kinase in endothelial barrier maintenance. Arterioscler Thromb Vasc Biol *27*, 2332-2339.
239. van Nieuw Amerongen, G.P., van Delft, S., Vermeer, M.A., Collard, J.G., and van Hinsbergh, V.W. (2000). Activation of RhoA by thrombin in endothelial hyperpermeability: role of Rho kinase and protein tyrosine kinases. Circ Res *87*, 335-340.
240. van Rijssel, J., Kroon, J., Hoogenboezem, M., van Alphen, F.P., de Jong, R.J., Kostadinova, E., Geerts, D., Hordijk, P.L., and van Buul, J.D. (2012). The Rho-guanine nucleotide exchange factor Trio controls leukocyte transendothelial migration by promoting docking structure formation. Mol Biol Cell *23*, 2831-2844.
241. van Wetering, S., van Buul, J.D., Quik, S., Mul, F.P., Anthony, E.C., ten Klooster, J.P., Collard, J.G., and Hordijk, P.L. (2002). Reactive oxygen species mediate Rac-induced loss of cell-cell adhesion in primary human endothelial cells. J Cell Sci *115*, 1837-1846.
242. Vandenbroucke St Amant, E., Tauseef, M., Vogel, S.M., Gao, X.P., Mehta, D., Komarova, Y.A., and Malik, A.B. (2012). PKCalpha activation of p120-catenin serine 879 phospho-switch disassembles VE-cadherin junctions and disrupts vascular integrity. Circ Res *111*, 739-749.
243. Vanderzalm, P.J., Pandey, A., Hurwitz, M.E., Bloom, L., Horvitz, H.R., and Garriga, G. (2009). C. elegans CARMIL negatively regulates UNC-73/Trio function during neuronal development. Development *136*, 1201-1210.
244. Vassilev, V.S., Mandai, M., Yonemura, S., and Takeichi, M. (2012). Loss of N-cadherin from the endothelium causes stromal edema and epithelial dysgenesis in the mouse cornea. Invest Ophthalmol Vis Sci *53*, 7183-7193.
245. Vetter, I.R., and Wittinghofer, A. (2001). The guanine nucleotide-binding switch in three dimensions. Science *294*, 1299-1304.
246. Vittet, D., Buchou, T., Schweitzer, A., Dejana, E., and Huber, P. (1997). Targeted null-mutation in the vascular endothelial-cadherin gene impairs the organization of vascular-like structures in embryoid bodies. Proc Natl Acad Sci U S A *94*, 6273-6278.
247. Wagner, C., de Wit, C., Kurtz, L., Grunberger, C., Kurtz, A., and Schweda, F. (2007). Connexin40 is essential for the pressure control of renin synthesis and secretion. Circ Res *100*, 556-563.
248. Wang, S., Iring, A., Strilic, B., Albarran Juarez, J., Kaur, H., Troidl, K., Tonack, S., Burbiel, J.C., Muller, C.E., Fleming, I., *et al.* (2015). P2Y(2) and Gq/G(1)(1) control blood pressure by mediating endothelial mechanotransduction. J Clin Invest *125*, 3077-3086.
249. Watanabe, N., Kato, T., Fujita, A., Ishizaki, T., and Narumiya, S. (1999). Cooperation between mDia1 and ROCK in Rho-induced actin reorganization. Nat Cell Biol *1*, 136-143.

250. Weisberg, H.F. (1978). Osmotic pressure of the serum proteins. Ann Clin Lab Sci *8*, 155-164.
251. Wildenberg, G.A., Dohn, M.R., Carnahan, R.H., Davis, M.A., Lobdell, N.A., Settleman, J., and Reynolds, A.B. (2006). p120-catenin and p190RhoGAP regulate cell-cell adhesion by coordinating antagonism between Rac and Rho. Cell *127*, 1027-1039.
252. Wilkinson-Berka, J.L., Babic, S., De Gooyer, T., Stitt, A.W., Jaworski, K., Ong, L.G., Kelly, D.J., and Gilbert, R.E. (2004). Inhibition of platelet-derived growth factor promotes pericyte loss and angiogenesis in ischemic retinopathy. Am J Pathol *164*, 1263-1273.
253. Wilkinson, S., Paterson, H.F., and Marshall, C.J. (2005). Cdc42-MRCK and Rho-ROCK signalling cooperate in myosin phosphorylation and cell invasion. Nat Cell Biol *7*, 255-261.
254. Winkler, E.A., Bell, R.D., and Zlokovic, B.V. (2011). Lack of Smad or Notch leads to a fatal game of brain pericyte hopscotch. Dev Cell *20*, 279-280.
255. Wirth, A., Schroeter, M., Kock-Hauser, C., Manser, E., Chalovich, J.M., De Lanerolle, P., and Pfitzer, G. (2003). Inhibition of contraction and myosin light chain phosphorylation in guinea-pig smooth muscle by p21-activated kinase 1. J Physiol *549*, 489-500.
256. Wojciak-Stothard, B., Entwistle, A., Garg, R., and Ridley, A.J. (1998). Regulation of TNF-alpha-induced reorganization of the actin cytoskeleton and cell-cell junctions by Rho, Rac, and Cdc42 in human endothelial cells. J Cell Physiol *176*, 150-165.
257. Wojciak-Stothard, B., Potempa, S., Eichholtz, T., and Ridley, A.J. (2001). Rho and Rac but not Cdc42 regulate endothelial cell permeability. J Cell Sci *114*, 1343-1355.
258. Wojciak-Stothard, B., Tsang, L.Y., and Haworth, S.G. (2005). Rac and Rho play opposing roles in the regulation of hypoxia/reoxygenation-induced permeability changes in pulmonary artery endothelial cells. Am J Physiol Lung Cell Mol Physiol *288*, L749-760.
259. Wolfrum, S., Dendorfer, A., Rikitake, Y., Stalker, T.J., Gong, Y., Scalia, R., Dominiak, P., and Liao, J.K. (2004). Inhibition of Rho-kinase leads to rapid activation of phosphatidylinositol 3-kinase/protein kinase Akt and cardiovascular protection. Arterioscler Thromb Vasc Biol *24*, 1842-1847.
260. Wu, S.K., Gomez, G.A., Michael, M., Verma, S., Cox, H.L., Lefevre, J.G., Parton, R.G., Hamilton, N.A., Neufeld, Z., and Yap, A.S. (2014). Cortical F-actin stabilization generates apical-lateral patterns of junctional contractility that integrate cells into epithelia. Nat Cell Biol *16*, 167-178.
261. Wu, Y.I., Frey, D., Lungu, O.I., Jaehrig, A., Schlichting, I., Kuhlman, B., and Hahn, K.M. (2009). A genetically encoded photoactivatable Rac controls the motility of living cells. Nature *461*, 104-108.
262. Xiao, K., Garner, J., Buckley, K.M., Vincent, P.A., Chiasson, C.M., Dejana, E., Faundez, V., and Kowalczyk, A.P. (2005). p120-Catenin regulates clathrin-dependent endocytosis of VE-cadherin. Mol Biol Cell *16*, 5141-5151.
263. Xie, Z., Ghosh, C.C., Patel, R., Iwaki, S., Gaskins, D., Nelson, C., Jones, N., Greipp, P.R., Parikh, S.M., and Druey, K.M. (2012). Vascular endothelial hyperpermeability induces the clinical symptoms of Clarkson disease (the systemic capillary leak syndrome). Blood *119*, 4321-4332.
264. Yamada, S., and Nelson, W.J. (2007). Localized zones of Rho and Rac activities drive initiation and expansion of epithelial cell-cell adhesion. J Cell Biol *178*, 517-527.

265. Yamada, S., Pokutta, S., Drees, F., Weis, W.I., and Nelson, W.J. (2005). Deconstructing the cadherin-catenin-actin complex. Cell *123*, 889-901.
266. Yang, N., Higuchi, O., Ohashi, K., Nagata, K., Wada, A., Kangawa, K., Nishida, E., and Mizuno, K. (1998). Cofilin phosphorylation by LIM-kinase 1 and its role in Rac-mediated actin reorganization. Nature *393*, 809-812.
267. Yang, Y., Estrada, E.Y., Thompson, J.F., Liu, W., and Rosenberg, G.A. (2007). Matrix metalloproteinase-mediated disruption of tight junction proteins in cerebral vessels is reversed by synthetic matrix metalloproteinase inhibitor in focal ischemia in rat. Journal of cerebral blood flow and metabolism : official journal of the International Society of Cerebral Blood Flow and Metabolism *27*, 697-709.
268. Yano, H., Mazaki, Y., Kurokawa, K., Hanks, S.K., Matsuda, M., and Sabe, H. (2004). Roles played by a subset of integrin signaling molecules in cadherin-based cell-cell adhesion. J Cell Biol *166*, 283-295.
269. Yano, T., Yamazaki, Y., Adachi, M., Okawa, K., Fort, P., Uji, M., Tsukita, S., and Tsukita, S. (2011). Tara up-regulates E-cadherin transcription by binding to the Trio RhoGEF and inhibiting Rac signaling. J Cell Biol *193*, 319-332.
270. Yao, M., Qiu, W., Liu, R., Efremov, A.K., Cong, P., Seddiki, R., Payre, M., Lim, C.T., Ladoux, B., Mege, R.M., *et al.* (2014). Force-dependent conformational switch of alpha-catenin controls vinculin binding. Nat Commun *5*, 4525.
271. Zaidel-Bar, R. (2013). Cadherin adhesome at a glance. J Cell Sci *126*, 373-378.
272. Zebda, N., Tian, Y., Tian, X., Gawlak, G., Higginbotham, K., Reynolds, A.B., Birukova, A.A., and Birukov, K.G. (2013). Interaction of p190RhoGAP with C-terminal domain of p120-catenin modulates endothelial cytoskeleton and permeability. J Biol Chem *288*, 18290-18299.
273. Zechariah, A., ElAli, A., Doeppner, T.R., Jin, F., Hasan, M.R., Helfrich, I., Mies, G., and Hermann, D.M. (2013). Vascular endothelial growth factor promotes pericyte coverage of brain capillaries, improves cerebral blood flow during subsequent focal cerebral ischemia, and preserves the metabolic penumbra. Stroke *44*, 1690-1697.
274. Zeng, H., He, X., Tuo, Q.H., Liao, D.F., Zhang, G.Q., and Chen, J.X. (2016). LPS causes pericyte loss and microvascular dysfunction via disruption of Sirt3/angiopoietins/Tie-2 and HIF-2alpha/Notch3 pathways. Sci Rep *6*, 20931.
275. Zhang, Y., Sivasankar, S., Nelson, W.J., and Chu, S. (2009). Resolving cadherin interactions and binding cooperativity at the single-molecule level. Proc Natl Acad Sci U S A *106*, 109-114.
276. Zhao, Y.D., Ohkawara, H., Rehman, J., Wary, K.K., Vogel, S.M., Minshall, R.D., Zhao, Y.Y., and Malik, A.B. (2009). Bone marrow progenitor cells induce endothelial adherens junction integrity by sphingosine-1-phosphate-mediated Rac1 and Cdc42 signaling. Circ Res *105*, 696-704, 698 p following 704.
277. Zheng, Y. (2001). Dbl family guanine nucleotide exchange factors. Trends Biochem Sci *26*, 724-732.
278. Zlokovic, B.V. (2006). Remodeling after stroke. Nat Med *12*, 390-391.

10. VITA

NAME	Kevin Kruse
EDUCATION	Ph.D. Pharmacology. University of Illinois at Chicago, Chicago, IL 2018 (expected) B.S. Biomedical Engineering, Illinois Institute of Technology, Chicago, IL 2010
HONORS	American Heart Association Pre-doctoral Fellowship 16PRE27260230 (2016) UIC Department of Pharmacology Woeltjen Award 2nd place (2016) International Vascular Biology Meeting travel award (2016) UIC GEMS Fall Research Symposium 3rd place (2016) UIC College of Medicine Research Forum Honorable Mention (2015, 2016) Chancellor's Graduate Research Award (2015) ASCB Meeting Travel Award (2015) Vasculata Scholarship from North American Vascular Biology Organization NIH R13 HL129717-01 (2015) UIC Dean's Scholar Award (2014) Full fellowship to Quantitative Fluorescent Microscopy course, MDIBL (2014) Lung Biology and Pathobiology Training Program Fellowship NIH T32 HL007829 (2012)

	UIC Student Travel Award, Experimental Biology, San Diego, CA (2014) Camras Heald Scholarship, Illinois Institute of Technology, Chicago, IL (2006-2010)
PUBLICATIONS	**Kruse K**, Klomp J, Sun M, Huang F, Kanabar P., Maienschein-Cline M., Komarova Y. Analysis of biological networks with biomimetic microsystem platform. Current Biology, under preparation. Procter D, Banerjee A, Nukui M, **Kruse K**, Gaponenko V, Murphy EA, Komarova Y, Walsh D. The HCMV Assembly Compartment is a dynamic Golgi-derived MTOC that controls nuclear rotation and virus spread. Under revision in Developmental Cell. **Kruse K**, Lee Q, Sun Y, Klomp J, Yang X, Huang F, Vogel SM, Tai LM, Shin JW, Leckband D, Malik AB, Komarova Y. N-cadherin Signals Assembly of VE-cadherin Junctions to Establish Vascular Barrier Set-Point. Under review in Journal of Cell Biology. Yazbeck P, Tauseef M, **Kruse K**, Amin MR, Sheikh R, Feske S, Komarova Y, Mehta D. STIM1 Phosphorylation at Y361 Recruits Orai1 to STIM1 Puncta and Induces Ca2+ Entry. Sci Rep. 2017. Feb 20;7:42758 Komarova Y, **Kruse K**, Mehta D, and Malik AB. Protein interactions at endothelial junctions and signaling mechanisms regulating endothelial permeability. Circ Res. 2017. Jan 6;120(1):179-206. **Kruse K** and Komarova Y. Tension across Adherens Junctions: When Less is More. Oncotarget. 2015. Oct 13; 6(31):30433-4.
ABSTRACTS	**Kruse K**, Lee Q, Sun Y, Klomp J, Yang X, Huang F, Vogel SM, Tai LM, Malik AB, Shin JW, Komarova Y. N-cadherin Signaling via RhoGEF Trio

	Stabilizes VE-cadherin Junctions and Regulates Vascular Permeability. Featured Topic, Experimental Biology Meeting (2018). **Kruse K**, Huang F, Sun Y, Vogel S, Malik AB, Komarova Y. N-cadherin adhesion modulates RhoGTPase signaling to promote endothelial barrier integrity, Microsymposium talk. Experimental Biology Meeting (2016). **Kruse K**, Huang F, and Komarova Y. The role of N-cadherin in lung endothelium. Chicago Cytoskeleton Meeting, Invited talk (2015). **Kruse K**, Huang F, Sun Y, Vogel S, Malik AB, Komarova Y. The role of N-cadherin signaling on endothelial barrier integrity, Microsymposium talk. American Society for Cell Biology Meeting (2015). **Kruse K**, Sieracki N, and Komarova Y. Role of N-cadherin adhesion mediated signaling in regulating endothelial barrier function. UIC College of Medicine Research Forum (2014). **Kruse K**, Sieracki N, Komarova Y. N-cadherin adhesion mediated signaling stabilizes VE-cadherin-mediated adhesion and strengthens endothelial barrier function (695.3) The FASEB Journal, April 2014 28:695.3

Title: Protein Interactions at Endothelial Junctions and Signaling Mechanisms Regulating Endothelial Permeability

Author: Yulia A. Komarova,Kevin Kruse,Dolly Mehta,Asrar B. Malik

Publication: Circulation Research

Publisher: Wolters Kluwer Health, Inc.

Date: Jan 6, 2017

License Not Required

This request is granted gratis and no formal license is required from Wolters Kluwer. Please note that modifications are not permitted. Please use the following citation format: author(s), title of article, title of journal, volume number, issue number, inclusive pages and website URL to the journal page.

BACK CLOSE WINDOW

ELSEVIER LICENSE
TERMS AND CONDITIONS

Feb 27, 2018

This Agreement between Kevin J Kruse ("You") and Elsevier ("Elsevier") consists of your license details and the terms and conditions provided by Elsevier and Copyright Clearance Center.

License Number	4297220196827
License date	Feb 27, 2018
Licensed Content Publisher	Elsevier
Licensed Content Publication	Trends in Cell Biology
Licensed Content Title	Thinking outside the cell: how cadherins drive adhesion
Licensed Content Author	Julia Brasch,Oliver J. Harrison,Barry Honig,Lawrence Shapiro
Licensed Content Date	Jun 1, 2012
Licensed Content Volume	22
Licensed Content Issue	6
Licensed Content Pages	12
Start Page	299
End Page	310
Type of Use	reuse in a thesis/dissertation
Portion	figures/tables/illustrations
Number of figures/tables /illustrations	1
Format	both print and electronic
Are you the author of this Elsevier article?	No
Will you be translating?	No
Original figure numbers	2a
Title of your thesis/dissertation	N-Cadherin Juxtacrine Signaling Regulates the Endothelial Barrier
Expected completion date	May 2018
Estimated size (number of pages)	160
Requestor Location	Kevin J Kruse 835 S Wolcott Ave MSB E403 CHICAGO, IL 60612 United States Attn: Kevin J Kruse
Publisher Tax ID	98-0397604
Total	0.00 USD

Terms and Conditions

INTRODUCTION

1. The publisher for this copyrighted material is Elsevier. By clicking "accept" in connection with completing this licensing transaction, you agree that the following terms and conditions apply to this transaction (along with the Billing and Payment terms and conditions established by Copyright Clearance Center, Inc. ("CCC"), at the time that you opened your Rightslink account and that are available at any time at http://myaccount.copyright.com).

GENERAL TERMS

2. Elsevier hereby grants you permission to reproduce the aforementioned material subject to the terms and conditions indicated.

3. Acknowledgement: If any part of the material to be used (for example, figures) has appeared in our publication with credit or acknowledgement to another source, permission must also be sought from that source. If such permission is not obtained then that material may not be included in your publication/copies. Suitable acknowledgement to the source must be made, either as a footnote or in a reference list at the end of your publication, as follows:

"Reprinted from Publication title, Vol /edition number, Author(s), Title of article / title of chapter, Pages No., Copyright (Year), with permission from Elsevier [OR APPLICABLE SOCIETY COPYRIGHT OWNER]." Also Lancet special credit - "Reprinted from The Lancet, Vol. number, Author(s), Title of article, Pages No., Copyright (Year), with permission from Elsevier."

4. Reproduction of this material is confined to the purpose and/or media for which permission is hereby given.

5. Altering/Modifying Material: Not Permitted. However figures and illustrations may be altered/adapted minimally to serve your work. Any other abbreviations, additions, deletions and/or any other alterations shall be made only with prior written authorization of Elsevier Ltd. (Please contact Elsevier at permissions@elsevier.com). No modifications can be made to any Lancet figures/tables and they must be reproduced in full.

6. If the permission fee for the requested use of our material is waived in this instance, please be advised that your future requests for Elsevier materials may attract a fee.

7. Reservation of Rights: Publisher reserves all rights not specifically granted in the combination of (i) the license details provided by you and accepted in the course of this licensing transaction, (ii) these terms and conditions and (iii) CCC's Billing and Payment terms and conditions.

8. License Contingent Upon Payment: While you may exercise the rights licensed immediately upon issuance of the license at the end of the licensing process for the transaction, provided that you have disclosed complete and accurate details of your proposed use, no license is finally effective unless and until full payment is received from you (either by publisher or by CCC) as provided in CCC's Billing and Payment terms and conditions. If full payment is not received on a timely basis, then any license preliminarily granted shall be deemed automatically revoked and shall be void as if never granted. Further, in the event that you breach any of these terms and conditions or any of CCC's Billing and Payment terms and conditions, the license is automatically revoked and shall be void as if never granted. Use of materials as described in a revoked license, as well as any use of the materials beyond the scope of an unrevoked license, may constitute copyright infringement and publisher reserves the right to take any and all action to protect its copyright in the

materials.
9. Warranties: Publisher makes no representations or warranties with respect to the licensed material.
10. Indemnity: You hereby indemnify and agree to hold harmless publisher and CCC, and their respective officers, directors, employees and agents, from and against any and all claims arising out of your use of the licensed material other than as specifically authorized pursuant to this license.
11. No Transfer of License: This license is personal to you and may not be sublicensed, assigned, or transferred by you to any other person without publisher's written permission.
12. No Amendment Except in Writing: This license may not be amended except in a writing signed by both parties (or, in the case of publisher, by CCC on publisher's behalf).
13. Objection to Contrary Terms: Publisher hereby objects to any terms contained in any purchase order, acknowledgment, check endorsement or other writing prepared by you, which terms are inconsistent with these terms and conditions or CCC's Billing and Payment terms and conditions. These terms and conditions, together with CCC's Billing and Payment terms and conditions (which are incorporated herein), comprise the entire agreement between you and publisher (and CCC) concerning this licensing transaction. In the event of any conflict between your obligations established by these terms and conditions and those established by CCC's Billing and Payment terms and conditions, these terms and conditions shall control.
14. Revocation: Elsevier or Copyright Clearance Center may deny the permissions described in this License at their sole discretion, for any reason or no reason, with a full refund payable to you. Notice of such denial will be made using the contact information provided by you. Failure to receive such notice will not alter or invalidate the denial. In no event will Elsevier or Copyright Clearance Center be responsible or liable for any costs, expenses or damage incurred by you as a result of a denial of your permission request, other than a refund of the amount(s) paid by you to Elsevier and/or Copyright Clearance Center for denied permissions.

LIMITED LICENSE

The following terms and conditions apply only to specific license types:
15. **Translation**: This permission is granted for non-exclusive world **English** rights only unless your license was granted for translation rights. If you licensed translation rights you may only translate this content into the languages you requested. A professional translator must perform all translations and reproduce the content word for word preserving the integrity of the article.
16. **Posting licensed content on any Website**: The following terms and conditions apply as follows: Licensing material from an Elsevier journal: All content posted to the web site must maintain the copyright information line on the bottom of each image; A hyper-text must be included to the Homepage of the journal from which you are licensing at http://www.sciencedirect.com/science/journal/xxxxx or the Elsevier homepage for books at http://www.elsevier.com; Central Storage: This license does not include permission for a scanned version of the material to be stored in a central repository such as that provided by Heron/XanEdu.
Licensing material from an Elsevier book: A hyper-text link must be included to the Elsevier homepage at http://www.elsevier.com . All content posted to the web site must maintain the copyright information line on the bottom of each image.

Posting licensed content on Electronic reserve: In addition to the above the following clauses are applicable: The web site must be password-protected and made available only to bona fide students registered on a relevant course. This permission is granted for 1 year only. You may obtain a new license for future website posting.
17. **For journal authors:** the following clauses are applicable in addition to the above:
Preprints:
A preprint is an author's own write-up of research results and analysis, it has not been peer-reviewed, nor has it had any other value added to it by a publisher (such as formatting, copyright, technical enhancement etc.).
Authors can share their preprints anywhere at any time. Preprints should not be added to or enhanced in any way in order to appear more like, or to substitute for, the final versions of articles however authors can update their preprints on arXiv or RePEc with their Accepted Author Manuscript (see below).
If accepted for publication, we encourage authors to link from the preprint to their formal publication via its DOI. Millions of researchers have access to the formal publications on ScienceDirect, and so links will help users to find, access, cite and use the best available version. Please note that Cell Press, The Lancet and some society-owned have different preprint policies. Information on these policies is available on the journal homepage.
Accepted Author Manuscripts: An accepted author manuscript is the manuscript of an article that has been accepted for publication and which typically includes author-incorporated changes suggested during submission, peer review and editor-author communications.
Authors can share their accepted author manuscript:

- immediately
    - via their non-commercial person homepage or blog
    - by updating a preprint in arXiv or RePEc with the accepted manuscript
    - via their research institute or institutional repository for internal institutional uses or as part of an invitation-only research collaboration work-group
    - directly by providing copies to their students or to research collaborators for their personal use
    - for private scholarly sharing as part of an invitation-only work group on commercial sites with which Elsevier has an agreement
- After the embargo period
    - via non-commercial hosting platforms such as their institutional repository
    - via commercial sites with which Elsevier has an agreement

In all cases accepted manuscripts should:

- link to the formal publication via its DOI
- bear a CC-BY-NC-ND license - this is easy to do
- if aggregated with other manuscripts, for example in a repository or other site, be shared in alignment with our hosting policy not be added to or enhanced in any way to appear more like, or to substitute for, the published journal article.

Published journal article (JPA): A published journal article (PJA) is the definitive final record of published research that appears or will appear in the journal and embodies all value-adding publishing activities including peer review co-ordination, copy-editing,

formatting, (if relevant) pagination and online enrichment.
Policies for sharing publishing journal articles differ for subscription and gold open access articles:
Subscription Articles: If you are an author, please share a link to your article rather than the full-text. Millions of researchers have access to the formal publications on ScienceDirect, and so links will help your users to find, access, cite, and use the best available version.
Theses and dissertations which contain embedded PJAs as part of the formal submission can be posted publicly by the awarding institution with DOI links back to the formal publications on ScienceDirect.
If you are affiliated with a library that subscribes to ScienceDirect you have additional private sharing rights for others' research accessed under that agreement. This includes use for classroom teaching and internal training at the institution (including use in course packs and courseware programs), and inclusion of the article for grant funding purposes.
Gold Open Access Articles: May be shared according to the author-selected end-user license and should contain a CrossMark logo, the end user license, and a DOI link to the formal publication on ScienceDirect.
Please refer to Elsevier's posting policy for further information.
18. **For book authors** the following clauses are applicable in addition to the above:
Authors are permitted to place a brief summary of their work online only. You are not allowed to download and post the published electronic version of your chapter, nor may you scan the printed edition to create an electronic version. **Posting to a repository:** Authors are permitted to post a summary of their chapter only in their institution's repository.
19. **Thesis/Dissertation**: If your license is for use in a thesis/dissertation your thesis may be submitted to your institution in either print or electronic form. Should your thesis be published commercially, please reapply for permission. These requirements include permission for the Library and Archives of Canada to supply single copies, on demand, of the complete thesis and include permission for Proquest/UMI to supply single copies, on demand, of the complete thesis. Should your thesis be published commercially, please reapply for permission. Theses and dissertations which contain embedded PJAs as part of the formal submission can be posted publicly by the awarding institution with DOI links back to the formal publications on ScienceDirect.

Elsevier Open Access Terms and Conditions
You can publish open access with Elsevier in hundreds of open access journals or in nearly 2000 established subscription journals that support open access publishing. Permitted third party re-use of these open access articles is defined by the author's choice of Creative Commons user license. See our open access license policy for more information.
Terms & Conditions applicable to all Open Access articles published with Elsevier:
Any reuse of the article must not represent the author as endorsing the adaptation of the article nor should the article be modified in such a way as to damage the author's honour or reputation. If any changes have been made, such changes must be clearly indicated.
The author(s) must be appropriately credited and we ask that you include the end user license and a DOI link to the formal publication on ScienceDirect.
If any part of the material to be used (for example, figures) has appeared in our publication with credit or acknowledgement to another source it is the responsibility of the user to ensure their reuse complies with the terms and conditions determined by the rights holder.
Additional Terms & Conditions applicable to each Creative Commons user license:

CC BY: The CC-BY license allows users to copy, to create extracts, abstracts and new works from the Article, to alter and revise the Article and to make commercial use of the Article (including reuse and/or resale of the Article by commercial entities), provided the user gives appropriate credit (with a link to the formal publication through the relevant DOI), provides a link to the license, indicates if changes were made and the licensor is not represented as endorsing the use made of the work. The full details of the license are available at http://creativecommons.org/licenses/by/4.0.
CC BY NC SA: The CC BY-NC-SA license allows users to copy, to create extracts, abstracts and new works from the Article, to alter and revise the Article, provided this is not done for commercial purposes, and that the user gives appropriate credit (with a link to the formal publication through the relevant DOI), provides a link to the license, indicates if changes were made and the licensor is not represented as endorsing the use made of the work. Further, any new works must be made available on the same conditions. The full details of the license are available at http://creativecommons.org/licenses/by-nc-sa/4.0.
CC BY NC ND: The CC BY-NC-ND license allows users to copy and distribute the Article, provided this is not done for commercial purposes and further does not permit distribution of the Article if it is changed or edited in any way, and provided the user gives appropriate credit (with a link to the formal publication through the relevant DOI), provides a link to the license, and that the licensor is not represented as endorsing the use made of the work. The full details of the license are available at http://creativecommons.org/licenses/by-nc-nd/4.0.
Any commercial reuse of Open Access articles published with a CC BY NC SA or CC BY NC ND license requires permission from Elsevier and will be subject to a fee.
Commercial reuse includes:

- Associating advertising with the full text of the Article
- Charging fees for document delivery or access
- Article aggregation
- Systematic distribution via e-mail lists or share buttons

Posting or linking by commercial companies for use by customers of those companies.

20. **Other Conditions**:

v1.9

Copyright Clearance Center

Note: Copyright.com supplies permissions but not the copyrighted content itself.

1 PAYMENT 2 REVIEW 3 CONFIRMATION

Step 3: Order Confirmation

Thank you for your order! A confirmation for your order will be sent to your account email address. If you have questions about your order, you can call us 24 hrs/day, M-F at +1.855.239.3415 Toll Free, or write to us at info@copyright.com. This is not an invoice.

Confirmation Number: 11701619
Order Date: 02/27/2018

If you paid by credit card, your order will be finalized and your card will be charged within 24 hours. If you choose to be invoiced, you can change or cancel your order until the invoice is generated.

Payment Information

Kevin Kruse
kkruse2@uic.edu
+1 (312) 996-1332
Payment Method: CC ending in 0917

Order Details

Journal of cell science

Order detail ID:	71043859
Order License Id:	4297230344171
ISSN:	1477-9137
Publication Type:	e-Journal
Volume:	
Issue:	
Start page:	
Publisher:	COMPANY OF BIOLOGISTS LTD.
Author/Editor:	Company of Biologists

Permission Status: Granted
Permission type: Republish or display content
Type of use: Republish in a thesis/dissertation

Requestor type	Academic institution
Format	Print, Electronic
Portion	chart/graph/table/figure
Number of charts/graphs/tables/figures	1
The requesting person/organization	Kevin Kruse
Title or numeric reference of the portion(s)	Figure 1D
Title of the article or chapter the portion is from	A local VE-cadherin and Trio-based signaling complex stabilizes endothelial junctions

Note: This item will be invoiced or charged separately through CCC's **RightsLink** service. More info **$ 3.50**

This is not an invoice.

Total order items: 1

Order Total: 3.50 USD

Confirmation Number: 11701619

Special Rightsholder Terms & Conditions

The following terms & conditions apply to the specific publication under which they are listed

Journal of cell science
Permission type: Republish or display content
Type of use: Republish in a thesis/dissertation

TERMS AND CONDITIONS

The following terms are individual to this publisher:

The acknowledgement should state "Reproduced / adapted with permission" and give the source journal name. The acknowledgement should either provide full citation details or refer to the relevant citation in the article reference list. The full citation details should include authors, journal, year, volume, issue and page citation.

Where appearing online or in other electronic media, a link should be provided to the original article (e.g. via DOI):

Development: dev.biologists.org

Disease Models & Mechanisms: dmm.biologists.org

Journal of Cell Science: jcs.biologists.org

The Journal of Experimental Biology: jeb.biologists.org

Other Terms and Conditions:

STANDARD TERMS AND CONDITIONS

1. Description of Service; Defined Terms. This Republication License enables the User to obtain licenses for republication of one or more copyrighted works as described in detail on the relevant Order Confirmation (the “Work(s)”). Copyright Clearance Center, Inc. (“CCC”) grants licenses through the Service on behalf of the rightsholder identified on the Order Confirmation (the “Rightsholder”). “Republication”, as used herein, generally means the inclusion of a Work, in whole or in part, in a new work or works, also as described on the Order Confirmation. “User”, as used herein, means the person or entity making such republication.

2. The terms set forth in the relevant Order Confirmation, and any terms set by the Rightsholder with respect to a particular Work, govern the terms of use of Works in connection with the Service. By using the Service, the person transacting for a republication license on behalf of the User represents and warrants that he/she/it (a) has been duly authorized by the User to accept, and hereby does accept, all such terms and conditions on behalf of User, and (b) shall inform User of all such terms and conditions. In the event such person is a “freelancer” or other third party independent of User and CCC, such party shall be deemed jointly a “User” for purposes of these terms and conditions. In any event, User shall be deemed to have accepted and agreed to all such terms and conditions if User republishes the Work in any fashion.

3. Scope of License; Limitations and Obligations.

3.1 All Works and all rights therein, including copyright rights, remain the sole and exclusive property of the Rightsholder. The license created by the exchange of an Order Confirmation (and/or any invoice) and payment by User of the full amount set forth on that document includes only those rights expressly set forth in the Order Confirmation and in these terms and conditions, and conveys no other rights in the Work(s) to User. All rights not expressly granted are hereby reserved.

3.2 General Payment Terms: You may pay by credit card or through an account with us payable at the end of the month. If you and we agree that you may establish a standing account with CCC, then the following terms apply: Remit Payment to: Copyright Clearance Center, 29118 Network Place, Chicago, IL 60673-1291. Payments Due: Invoices are payable upon their delivery to you (or upon our notice to you that they are available to you for downloading). After 30 days, outstanding amounts will be subject to a service charge of 1-1/2% per month or, if less, the maximum rate allowed by applicable law. Unless otherwise specifically set forth in the Order Confirmation or in a separate written agreement signed by CCC, invoices are due and payable on “net 30” terms. While User may exercise the rights licensed immediately upon issuance of the Order Confirmation, the license is automatically revoked and is null and void, as if it had never been issued, if complete payment for the license is not received on a timely basis either from User directly or through a payment agent, such as a credit card company.

3.3 Unless otherwise provided in the Order Confirmation, any grant of rights to User (i) is "one-time" (including the editions and product family specified in the license), (ii) is non-exclusive and non-transferable and (iii) is subject to any and all limitations and restrictions (such as, but not limited to, limitations on duration of use or circulation) included in the Order Confirmation or invoice and/or in these terms and conditions. Upon completion of the licensed use, User shall either secure a new permission for further use of the Work(s) or immediately cease any new use of the Work(s) and shall render inaccessible (such as by deleting or by removing or severing links or other locators) any further copies of the Work (except for copies printed on paper in accordance with this license and still in User's stock at the end of such period).

3.4 In the event that the material for which a republication license is sought includes third party materials (such as photographs, illustrations, graphs, inserts and similar materials) which are identified in such material as having been used by permission, User is responsible for identifying, and seeking separate licenses (under this Service or otherwise) for, any of such third party materials; without a separate license, such third party materials may not be used.

3.5 Use of proper copyright notice for a Work is required as a condition of any license granted under the Service. Unless otherwise provided in the Order Confirmation, a proper copyright notice will read substantially as follows: "Republished with permission of [Rightsholder's name], from [Work's title, author, volume, edition number and year of copyright]; permission conveyed through Copyright Clearance Center, Inc. " Such notice must be provided in a reasonably legible font size and must be placed either immediately adjacent to the Work as used (for example, as part of a by-line or footnote but not as a separate electronic link) or in the place where substantially all other credits or notices for the new work containing the republished Work are located. Failure to include the required notice results in loss to the Rightsholder and CCC, and the User shall be liable to pay liquidated damages for each such failure equal to twice the use fee specified in the Order Confirmation, in addition to the use fee itself and any other fees and charges specified.

3.6 User may only make alterations to the Work if and as expressly set forth in the Order Confirmation. No Work may be used in any way that is defamatory, violates the rights of third parties (including such third parties' rights of copyright, privacy, publicity, or other tangible or intangible property), or is otherwise illegal, sexually explicit or obscene. In addition, User may not conjoin a Work with any other material that may result in damage to the reputation of the Rightsholder. User agrees to inform CCC if it becomes aware of any infringement of any rights in a Work and to cooperate with any reasonable request of CCC or the Rightsholder in connection therewith.

4. Indemnity. User hereby indemnifies and agrees to defend the Rightsholder and CCC, and their respective employees and directors, against all claims, liability, damages, costs and expenses, including legal fees and expenses, arising out of any use of a Work beyond the scope of the rights granted herein, or any use of a Work which has been altered in any unauthorized way by User, including claims of defamation or infringement of rights of copyright, publicity, privacy or other tangible or intangible property.

5. Limitation of Liability. UNDER NO CIRCUMSTANCES WILL CCC OR THE RIGHTSHOLDER BE LIABLE FOR ANY DIRECT, INDIRECT, CONSEQUENTIAL OR INCIDENTAL DAMAGES (INCLUDING WITHOUT LIMITATION DAMAGES FOR LOSS OF BUSINESS PROFITS OR INFORMATION, OR FOR BUSINESS INTERRUPTION) ARISING OUT OF THE USE OR INABILITY TO USE A WORK, EVEN IF ONE OF THEM HAS BEEN ADVISED OF THE POSSIBILITY OF SUCH DAMAGES. In any event, the total liability of the Rightsholder and CCC (including their respective employees and directors) shall not exceed the total amount actually paid by User for this license. User assumes full liability for the actions and omissions of its principals, employees, agents, affiliates, successors and assigns.

6. Limited Warranties. THE WORK(S) AND RIGHT(S) ARE PROVIDED "AS IS". CCC HAS THE RIGHT TO GRANT TO USER THE RIGHTS GRANTED IN THE ORDER CONFIRMATION DOCUMENT. CCC AND THE RIGHTSHOLDER DISCLAIM ALL OTHER WARRANTIES RELATING TO THE WORK(S) AND RIGHT(S), EITHER EXPRESS OR IMPLIED, INCLUDING WITHOUT LIMITATION IMPLIED WARRANTIES OF MERCHANTABILITY OR FITNESS FOR A PARTICULAR PURPOSE. ADDITIONAL RIGHTS MAY BE REQUIRED TO USE ILLUSTRATIONS, GRAPHS, PHOTOGRAPHS, ABSTRACTS, INSERTS OR OTHER PORTIONS OF THE WORK (AS OPPOSED TO THE ENTIRE WORK) IN A MANNER CONTEMPLATED BY USER; USER UNDERSTANDS AND AGREES THAT NEITHER CCC NOR THE RIGHTSHOLDER MAY HAVE SUCH ADDITIONAL RIGHTS TO GRANT.

7. Effect of Breach. Any failure by User to pay any amount when due, or any use by User of a Work beyond the scope of the license set forth in the Order Confirmation and/or these terms and conditions, shall be a material breach of the license created by the Order Confirmation and these terms and conditions. Any breach not cured within 30 days of written notice thereof shall result in immediate termination of such license without further notice. Any unauthorized (but licensable) use of a Work that is terminated immediately upon notice thereof may be liquidated by payment of the Rightsholder's ordinary license price therefor; any unauthorized (and unlicensable) use that is not terminated immediately for any reason (including, for example, because materials containing the Work cannot reasonably be recalled) will be subject to all remedies available at law or in equity, but in no event to a payment of less than three times the Rightsholder's ordinary license price for the most closely analogous licensable use plus Rightsholder's and/or CCC's costs and expenses incurred in collecting such payment.

8. **Miscellaneous.**

8.1 User acknowledges that CCC may, from time to time, make changes or additions to the Service or to these terms and conditions, and CCC reserves the right to send notice to the User by electronic mail or otherwise for the purposes of notifying User of such changes or additions; provided that any such changes or additions shall not apply to permissions already secured and paid for.

8.2 Use of User-related information collected through the Service is governed by CCC's privacy policy, available online here: http://www.copyright.com/content/cc3/en/tools/footer/privacypolicy.html.

8.3 The licensing transaction described in the Order Confirmation is personal to User. Therefore, User may not assign or transfer to any other person (whether a natural person or an organization of any kind) the license created by the Order Confirmation and these terms and conditions or any rights granted hereunder; provided, however, that User may assign such license in its entirety on written notice to CCC in the event of a transfer of all or substantially all of User's rights in the new material which includes the Work(s) licensed under this Service.

8.4 No amendment or waiver of any terms is binding unless set forth in writing and signed by the parties. The Rightsholder and CCC hereby object to any terms contained in any writing prepared by the User or its principals, employees, agents or affiliates and purporting to govern or otherwise relate to the licensing transaction described in the Order Confirmation, which terms are in any way inconsistent with any terms set forth in the Order Confirmation and/or in these terms and conditions or CCC's standard operating procedures, whether such writing is prepared prior to, simultaneously with or subsequent to the Order Confirmation, and whether such writing appears on a copy of the Order Confirmation or in a separate instrument.

8.5 The licensing transaction described in the Order Confirmation document shall be governed by and construed under the law of the State of New York, USA, without regard to the principles thereof of conflicts of law. Any case, controversy, suit, action, or proceeding arising out of, in connection with, or related to such licensing transaction shall be brought, at CCC's sole discretion, in any federal or state court located in the County of New York, State of New York, USA, or in any federal or state court whose geographical jurisdiction covers the location of the Rightsholder set forth in the Order Confirmation. The parties expressly submit to the personal jurisdiction and venue of each such federal or state court.If you have any comments or questions about the Service or Copyright Clearance Center, please contact us at 978-750-8400 or send an e-mail to info@copyright.com.

v 1.1

Close

Confirmation Number: 11701619

Citation Information

Order Detail ID: 71043859

Journal of cell science by Company of Biologists Reproduced with permission of COMPANY OF BIOLOGISTS LTD. in the format Republish in a thesis / dissertation via Copyright Clearance Center.

Close

SPRINGER NATURE LICENSE TERMS AND CONDITIONS

Feb 27, 2018

This Agreement between Kevin J Kruse ("You") and Springer Nature ("Springer Nature") consists of your license details and the terms and conditions provided by Springer Nature and Copyright Clearance Center.

License Number	4297230690072
License date	Feb 27, 2018
Licensed Content Publisher	Springer Nature
Licensed Content Publication	Nature
Licensed Content Title	A genetically encoded photoactivatable Rac controls the motility of living cells
Licensed Content Author	Yi I. Wu, Daniel Frey, Oana I. Lungu, Angelika Jaehrig, Ilme Schlichting et al.
Licensed Content Date	Aug 19, 2009
Licensed Content Volume	461
Licensed Content Issue	7260
Type of Use	Thesis/Dissertation
Requestor type	academic/university or research institute
Format	print
Portion	figures/tables/illustrations
Number of figures/tables /illustrations	1
High-res required	no
Will you be translating?	no
Circulation/distribution	<501
Author of this Springer Nature content	no
Title	N-Cadherin Juxtacrine Signaling Regulates the Endothelial Barrier
Instructor name	n/a
Institution name	n/a
Expected presentation date	May 2018
Portions	1A
Requestor Location	Kevin J Kruse 835 S Wolcott Ave MSB E403 CHICAGO, IL 60612 United States Attn: Kevin J Kruse
Billing Type	Invoice

Billing Address	Kevin J Kruse 835 S Wolcott Ave MSB E403 CHICAGO, IL 60612 United States Attn: Kevin J Kruse
Total	0.00 USD

Terms and Conditions

Springer Nature Terms and Conditions for RightsLink Permissions

Springer Customer Service Centre GmbH (the Licensor) hereby grants you a non-exclusive, world-wide licence to reproduce the material and for the purpose and requirements specified in the attached copy of your order form, and for no other use, subject to the conditions below:

1. The Licensor warrants that it has, to the best of its knowledge, the rights to license reuse of this material. However, you should ensure that the material you are requesting is original to the Licensor and does not carry the copyright of another entity (as credited in the published version).

   If the credit line on any part of the material you have requested indicates that it was reprinted or adapted with permission from another source, then you should also seek permission from that source to reuse the material.

2. Where **print only** permission has been granted for a fee, separate permission must be obtained for any additional electronic re-use.

3. Permission granted **free of charge** for material in print is also usually granted for any electronic version of that work, provided that the material is incidental to your work as a whole and that the electronic version is essentially equivalent to, or substitutes for, the print version.

4. A licence for 'post on a website' is valid for 12 months from the licence date. This licence does not cover use of full text articles on websites.

5. Where **'reuse in a dissertation / thesis'** has been selected the following terms apply: Print rights for up to 100 copies, electronic rights for use only on a personal website or institutional repository as defined by the Sherpa guideline (www.sherpa.ac.uk/romeo/).

6. Permission granted for books and journals is granted for the lifetime of the first edition and does not apply to second and subsequent editions (except where the first edition permission was granted free of charge or for signatories to the STM Permissions Guidelines http://www.stm-assoc.org/copyright-legal-affairs/permissions/permissions-guidelines/), and does not apply for editions in other languages unless additional translation rights have been granted separately in the licence.

7. Rights for additional components such as custom editions and derivatives require additional permission and may be subject to an additional fee. Please apply to Journalpermissions@springernature.com/bookpermissions@springernature.com for these rights.

8. The Licensor's permission must be acknowledged next to the licensed material in print. In electronic form, this acknowledgement must be visible at the same time as the figures/tables/illustrations or abstract, and must be hyperlinked to the journal/book's homepage. Our required acknowledgement format is in the Appendix below.

9. Use of the material for incidental promotional use, minor editing privileges (this does not include cropping, adapting, omitting material or any other changes that affect the meaning,

intention or moral rights of the author) and copies for the disabled are permitted under this licence.

10. Minor adaptations of single figures (changes of format, colour and style) do not require the Licensor's approval. However, the adaptation should be credited as shown in Appendix below.

Appendix — Acknowledgements:

For Journal Content:
Reprinted by permission from [**the Licensor**]: [**Journal Publisher** (e.g. Nature/Springer/Palgrave)] [**JOURNAL NAME**] [**REFERENCE CITATION** (Article name, Author(s) Name), [**COPYRIGHT**] (year of publication)

For **Advance Online Publication papers:**
Reprinted by permission from [**the Licensor**]: [**Journal Publisher** (e.g. Nature/Springer/Palgrave)] [**JOURNAL NAME**] [**REFERENCE CITATION** (Article name, Author(s) Name), [**COPYRIGHT**] (year of publication), advance online publication, day month year (doi: 10.1038/sj.[JOURNAL ACRONYM].)

For Adaptations/Translations:
Adapted/Translated by permission from [**the Licensor**]: [**Journal Publisher** (e.g. Nature/Springer/Palgrave)] [**JOURNAL NAME**] [**REFERENCE CITATION** (Article name, Author(s) Name), [**COPYRIGHT**] (year of publication)

Note: For any republication from the British Journal of Cancer, the following credit line style applies:

Reprinted/adapted/translated by permission from [**the Licensor**]: on behalf of Cancer Research UK: : [**Journal Publisher** (e.g. Nature/Springer/Palgrave)] [**JOURNAL NAME**] [**REFERENCE CITATION** (Article name, Author(s) Name), [**COPYRIGHT]** (year of publication)

For **Advance Online Publication** papers:
Reprinted by permission from The [**the Licensor**]: on behalf of Cancer Research UK: [**Journal Publisher** (e.g. Nature/Springer/Palgrave)] [**JOURNAL NAME**] [**REFERENCE CITATION** (Article name, Author(s) Name), [**COPYRIGHT**] (year of publication), advance online publication, day month year (doi: 10.1038/sj.[JOURNAL ACRONYM])

For Book content:
Reprinted/adapted by permission from [**the Licensor**]: [**Book Publisher** (e.g. Palgrave Macmillan, Springer etc) [**Book Title**] by [**Book author**(s)] [**COPYRIGHT**] (year of publication)

Other Conditions:

Version 1.0

THE AMERICAN ASSOCIATION FOR THE ADVANCEMENT OF SCIENCE LICENSE TERMS AND CONDITIONS

Feb 27, 2018

This Agreement between Kevin J Kruse ("You") and The American Association for the Advancement of Science ("The American Association for the Advancement of Science") consists of your license details and the terms and conditions provided by The American Association for the Advancement of Science and Copyright Clearance Center.

License Number	4297230830041
License date	Feb 27, 2018
Licensed Content Publisher	The American Association for the Advancement of Science
Licensed Content Publication	Science
Licensed Content Title	Localized Rac Activation Dynamics Visualized in Living Cells
Licensed Content Author	Vadim S. Kraynov,Chester Chamberlain,Gary M. Bokoch,Martin A. Schwartz,Sarah Slabaugh,Klaus M. Hahn
Licensed Content Date	Oct 13, 2000
Licensed Content Volume	290
Licensed Content Issue	5490
Volume number	290
Issue number	5490
Type of Use	Thesis / Dissertation
Requestor type	Scientist/individual at a research institution
Format	Print
Portion	Text Excerpt
Number of pages requested	1
Order reference number	
Title of your thesis / dissertation	N-Cadherin Juxtacrine Signaling Regulates the Endothelial Barrier
Expected completion date	May 2018
Estimated size(pages)	160
Requestor Location	Kevin J Kruse 835 S Wolcott Ave MSB E403 CHICAGO, IL 60612 United States Attn: Kevin J Kruse
Billing Type	Invoice
Billing Address	Kevin J Kruse 835 S Wolcott Ave MSB E403 CHICAGO, IL 60612

United States
Attn: Kevin J Kruse

Total 0.00 USD

Terms and Conditions

American Association for the Advancement of Science TERMS AND CONDITIONS
Regarding your request, we are pleased to grant you non-exclusive, non-transferable permission, to republish the AAAS material identified above in your work identified above, subject to the terms and conditions herein. We must be contacted for permission for any uses other than those specifically identified in your request above.
The following credit line must be printed along with the AAAS material: "From [Full Reference Citation]. Reprinted with permission from AAAS."
All required credit lines and notices must be visible any time a user accesses any part of the AAAS material and must appear on any printed copies and authorized user might make.
This permission does not apply to figures / photos / artwork or any other content or materials included in your work that are credited to non-AAAS sources. If the requested material is sourced to or references non-AAAS sources, you must obtain authorization from that source as well before using that material. You agree to hold harmless and indemnify AAAS against any claims arising from your use of any content in your work that is credited to non-AAAS sources.
If the AAAS material covered by this permission was published in Science during the years 1974 - 1994, you must also obtain permission from the author, who may grant or withhold permission, and who may or may not charge a fee if permission is granted. See original article for author's address. This condition does not apply to news articles.
The AAAS material may not be modified or altered except that figures and tables may be modified with permission from the author. Author permission for any such changes must be secured prior to your use.
Whenever possible, we ask that electronic uses of the AAAS material permitted herein include a hyperlink to the original work on AAAS's website (hyperlink may be embedded in the reference citation).
AAAS material reproduced in your work identified herein must not account for more than 30% of the total contents of that work.
AAAS must publish the full paper prior to use of any text.
AAAS material must not imply any endorsement by the American Association for the Advancement of Science.
This permission is not valid for the use of the AAAS and/or Science logos.
AAAS makes no representations or warranties as to the accuracy of any information contained in the AAAS material covered by this permission, including any warranties of merchantability or fitness for a particular purpose.
If permission fees for this use are waived, please note that AAAS reserves the right to charge for reproduction of this material in the future.
Permission is not valid unless payment is received within sixty (60) days of the issuance of this permission. If payment is not received within this time period then all rights granted herein shall be revoked and this permission will be considered null and void.
In the event of breach of any of the terms and conditions herein or any of CCC's Billing and Payment terms and conditions, all rights granted herein shall be revoked and this permission will be considered null and void.
AAAS reserves the right to terminate this permission and all rights granted herein at its

discretion, for any purpose, at any time. In the event that AAAS elects to terminate this permission, you will have no further right to publish, publicly perform, publicly display, distribute or otherwise use any matter in which the AAAS content had been included, and all fees paid hereunder shall be fully refunded to you. Notification of termination will be sent to the contact information as supplied by you during the request process and termination shall be immediate upon sending the notice. Neither AAAS nor CCC shall be liable for any costs, expenses, or damages you may incur as a result of the termination of this permission, beyond the refund noted above.

This Permission may not be amended except by written document signed by both parties. The terms above are applicable to all permissions granted for the use of AAAS material. Below you will find additional conditions that apply to your particular type of use.

FOR A THESIS OR DISSERTATION

If you are using figure(s)/table(s), permission is granted for use in print and electronic versions of your dissertation or thesis. A full text article may be used in print versions only of a dissertation or thesis.

Permission covers the distribution of your dissertation or thesis on demand by ProQuest / UMI, provided the AAAS material covered by this permission remains in situ.

If you are an Original Author on the AAAS article being reproduced, please refer to your License to Publish for rules on reproducing your paper in a dissertation or thesis.

FOR JOURNALS:

Permission covers both print and electronic versions of your journal article, however the AAAS material may not be used in any manner other than within the context of your article.

FOR BOOKS/TEXTBOOKS:

If this license is to reuse figures/tables, then permission is granted for non-exclusive world rights in all languages in both print and electronic formats (electronic formats are defined below).

If this license is to reuse a text excerpt or a full text article, then permission is granted for non-exclusive world rights in English only. You have the option of securing either print or electronic rights or both, but electronic rights are not automatically granted and do garner additional fees. Permission for translations of text excerpts or full text articles into other languages must be obtained separately.

Licenses granted for use of AAAS material in electronic format books/textbooks are valid only in cases where the electronic version is equivalent to or substitutes for the print version of the book/textbook. The AAAS material reproduced as permitted herein must remain in situ and must not be exploited separately (for example, if permission covers the use of a full text article, the article may not be offered for access or for purchase as a stand-alone unit), except in the case of permitted textbook companions as noted below.

You must include the following notice in any electronic versions, either adjacent to the reprinted AAAS material or in the terms and conditions for use of your electronic products: "Readers may view, browse, and/or download material for temporary copying purposes only, provided these uses are for noncommercial personal purposes. Except as provided by law, this material may not be further reproduced, distributed, transmitted, modified, adapted, performed, displayed, published, or sold in whole or in part, without prior written permission from the publisher."

If your book is an academic textbook, permission covers the following companions to your textbook, provided such companions are distributed only in conjunction with your textbook at no additional cost to the user:

- Password-protected website
- Instructor's image CD/DVD and/or PowerPoint resource
- Student CD/DVD

All companions must contain instructions to users that the AAAS material may be used for non-commercial, classroom purposes only. Any other uses require the prior written permission from AAAS.

If your license is for the use of AAAS Figures/Tables, then the electronic rights granted herein permit use of the Licensed Material in any Custom Databases that you distribute the electronic versions of your textbook through, so long as the Licensed Material remains within the context of a chapter of the title identified in your request and cannot be downloaded by a user as an independent image file.

Rights also extend to copies/files of your Work (as described above) that you are required to provide for use by the visually and/or print disabled in compliance with state and federal laws.

This permission only covers a single edition of your work as identified in your request.

FOR NEWSLETTERS:

Permission covers print and/or electronic versions, provided the AAAS material reproduced as permitted herein remains in situ and is not exploited separately (for example, if permission covers the use of a full text article, the article may not be offered for access or for purchase as a stand-alone unit)

FOR ANNUAL REPORTS:

Permission covers print and electronic versions provided the AAAS material reproduced as permitted herein remains in situ and is not exploited separately (for example, if permission covers the use of a full text article, the article may not be offered for access or for purchase as a stand-alone unit)

FOR PROMOTIONAL/MARKETING USES:

Permission covers the use of AAAS material in promotional or marketing pieces such as information packets, media kits, product slide kits, brochures, or flyers limited to a single print run. The AAAS Material may not be used in any manner which implies endorsement or promotion by the American Association for the Advancement of Science (AAAS) or Science of any product or service. AAAS does not permit the reproduction of its name, logo or text on promotional literature.

If permission to use a full text article is permitted, The Science article covered by this permission must not be altered in any way. No additional printing may be set onto an article copy other than the copyright credit line required above. Any alterations must be approved in advance and in writing by AAAS. This includes, but is not limited to, the placement of sponsorship identifiers, trademarks, logos, rubber stamping or self-adhesive stickers onto the article copies.

Additionally, article copies must be a freestanding part of any information package (i.e. media kit) into which they are inserted. They may not be physically attached to anything, such as an advertising insert, or have anything attached to them, such as a sample product. Article copies must be easily removable from any kits or informational packages in which they are used. The only exception is that article copies may be inserted into three-ring binders.

FOR CORPORATE INTERNAL USE:

The AAAS material covered by this permission may not be altered in any way. No

additional printing may be set onto an article copy other than the required credit line. Any alterations must be approved in advance and in writing by AAAS. This includes, but is not limited to the placement of sponsorship identifiers, trademarks, logos, rubber stamping or self-adhesive stickers onto article copies.

If you are making article copies, copies are restricted to the number indicated in your request and must be distributed only to internal employees for internal use.

If you are using AAAS Material in Presentation Slides, the required credit line must be visible on the slide where the AAAS material will be reprinted

If you are using AAAS Material on a CD, DVD, Flash Drive, or the World Wide Web, you must include the following notice in any electronic versions, either adjacent to the reprinted AAAS material or in the terms and conditions for use of your electronic products: "Readers may view, browse, and/or download material for temporary copying purposes only, provided these uses are for noncommercial personal purposes. Except as provided by law, this material may not be further reproduced, distributed, transmitted, modified, adapted, performed, displayed, published, or sold in whole or in part, without prior written permission from the publisher." Access to any such CD, DVD, Flash Drive or Web page must be restricted to your organization's employees only.

FOR CME COURSE and SCIENTIFIC SOCIETY MEETINGS:

Permission is restricted to the particular Course, Seminar, Conference, or Meeting indicated in your request. If this license covers a text excerpt or a Full Text Article, access to the reprinted AAAS material must be restricted to attendees of your event only (if you have been granted electronic rights for use of a full text article on your website, your website must be password protected, or access restricted so that only attendees can access the content on your site).

If you are using AAAS Material on a CD, DVD, Flash Drive, or the World Wide Web, you must include the following notice in any electronic versions, either adjacent to the reprinted AAAS material or in the terms and conditions for use of your electronic products: "Readers may view, browse, and/or download material for temporary copying purposes only, provided these uses are for noncommercial personal purposes. Except as provided by law, this material may not be further reproduced, distributed, transmitted, modified, adapted, performed, displayed, published, or sold in whole or in part, without prior written permission from the publisher."

FOR POLICY REPORTS:

These rights are granted only to non-profit organizations and/or government agencies. Permission covers print and electronic versions of a report, provided the required credit line appears in both versions and provided the AAAS material reproduced as permitted herein remains in situ and is not exploited separately.

FOR CLASSROOM PHOTOCOPIES:

Permission covers distribution in print copy format only. Article copies must be freestanding and not part of a course pack. They may not be physically attached to anything or have anything attached to them.

FOR COURSEPACKS OR COURSE WEBSITES:

These rights cover use of the AAAS material in one class at one institution. Permission is valid only for a single semester after which the AAAS material must be removed from the Electronic Course website, unless new permission is obtained for an additional semester. If the material is to be distributed online, access must be restricted to students and instructors enrolled in that particular course by some means of password or access control.

FOR WEBSITES:

You must include the following notice in any electronic versions, either adjacent to the reprinted AAAS material or in the terms and conditions for use of your electronic products: "Readers may view, browse, and/or download material for temporary copying purposes only, provided these uses are for noncommercial personal purposes. Except as provided by law, this material may not be further reproduced, distributed, transmitted, modified, adapted, performed, displayed, published, or sold in whole or in part, without prior written permission from the publisher."

Permissions for the use of Full Text articles on third party websites are granted on a case by case basis and only in cases where access to the AAAS Material is restricted by some means of password or access control. Alternately, an E-Print may be purchased through our reprints department (brocheleau@rockwaterinc.com).

REGARDING FULL TEXT ARTICLE USE ON THE WORLD WIDE WEB IF YOU ARE AN 'ORIGINAL AUTHOR' OF A SCIENCE PAPER

If you chose "Original Author" as the Requestor Type, you are warranting that you are one of authors listed on the License Agreement as a "Licensed content author" or that you are acting on that author's behalf to use the Licensed content in a new work that one of the authors listed on the License Agreement as a "Licensed content author" has written.

Original Authors may post the 'Accepted Version' of their full text article on their personal or on their University website and not on any other website. The 'Accepted Version' is the version of the paper accepted for publication by AAAS including changes resulting from peer review but prior to AAAS's copy editing and production (in other words not the AAAS published version).

FOR MOVIES / FILM / TELEVISION:

Permission is granted to use, record, film, photograph, and/or tape the AAAS material in connection with your program/film and in any medium your program/film may be shown or heard, including but not limited to broadcast and cable television, radio, print, world wide web, and videocassette.

The required credit line should run in the program/film's end credits.

FOR MUSEUM EXHIBITIONS:

Permission is granted to use the AAAS material as part of a single exhibition for the duration of that exhibit. Permission for use of the material in promotional materials for the exhibit must be cleared separately with AAAS (please contact us at permissions@aaas.org).

FOR TRANSLATIONS:

Translation rights apply only to the language identified in your request summary above. The following disclaimer must appear with your translation, on the first page of the article, after the credit line: "This translation is not an official translation by AAAS staff, nor is it endorsed by AAAS as accurate. In crucial matters, please refer to the official English-language version originally published by AAAS."

FOR USE ON A COVER:

Permission is granted to use the AAAS material on the cover of a journal issue, newsletter issue, book, textbook, or annual report in print and electronic formats provided the AAAS material reproduced as permitted herein remains in situ and is not exploited separately

By using the AAAS Material identified in your request, you agree to abide by all the terms and conditions herein.

Questions about these terms can be directed to the AAAS Permissions department permissions@aaas.org.

Other Terms and Conditions:
v 2

Questions? customercare@copyright.com or +1-855-239-3415 (toll free in the US) or +1-978-646-2777.

SPRINGER NATURE LICENSE TERMS AND CONDITIONS

Feb 27, 2018

This Agreement between Kevin J Kruse ("You") and Springer Nature ("Springer Nature") consists of your license details and the terms and conditions provided by Springer Nature and Copyright Clearance Center.

License Number	4297231076379
License date	Feb 27, 2018
Licensed Content Publisher	Springer Nature
Licensed Content Publication	Nature
Licensed Content Title	Spatiotemporal dynamics of RhoA activity in migrating cells
Licensed Content Author	Olivier Pertz, Louis Hodgson, Richard L. Klemke, Klaus M. Hahn
Licensed Content Date	Mar 19, 2006
Licensed Content Volume	440
Licensed Content Issue	7087
Type of Use	Thesis/Dissertation
Requestor type	academic/university or research institute
Format	print
Portion	figures/tables/illustrations
Number of figures/tables /illustrations	1
High-res required	no
Will you be translating?	no
Circulation/distribution	<501
Author of this Springer Nature content	no
Title	N-Cadherin Juxtacrine Signaling Regulates the Endothelial Barrier
Instructor name	n/a
Institution name	n/a
Expected presentation date	May 2018
Portions	1A
Requestor Location	Kevin J Kruse 835 S Wolcott Ave MSB E403 CHICAGO, IL 60612 United States Attn: Kevin J Kruse
Billing Type	Invoice

Billing Address	Kevin J Kruse 835 S Wolcott Ave MSB E403 CHICAGO, IL 60612 United States Attn: Kevin J Kruse
Total	0.00 USD

Terms and Conditions

Springer Nature Terms and Conditions for RightsLink Permissions

Springer Customer Service Centre GmbH (the Licensor) hereby grants you a non-exclusive, world-wide licence to reproduce the material and for the purpose and requirements specified in the attached copy of your order form, and for no other use, subject to the conditions below:

1. The Licensor warrants that it has, to the best of its knowledge, the rights to license reuse of this material. However, you should ensure that the material you are requesting is original to the Licensor and does not carry the copyright of another entity (as credited in the published version).

   If the credit line on any part of the material you have requested indicates that it was reprinted or adapted with permission from another source, then you should also seek permission from that source to reuse the material.

2. Where **print only** permission has been granted for a fee, separate permission must be obtained for any additional electronic re-use.

3. Permission granted **free of charge** for material in print is also usually granted for any electronic version of that work, provided that the material is incidental to your work as a whole and that the electronic version is essentially equivalent to, or substitutes for, the print version.

4. A licence for 'post on a website' is valid for 12 months from the licence date. This licence does not cover use of full text articles on websites.

5. Where **'reuse in a dissertation / thesis'** has been selected the following terms apply: Print rights for up to 100 copies, electronic rights for use only on a personal website or institutional repository as defined by the Sherpa guideline (www.sherpa.ac.uk/romeo/).

6. Permission granted for books and journals is granted for the lifetime of the first edition and does not apply to second and subsequent editions (except where the first edition permission was granted free of charge or for signatories to the STM Permissions Guidelines http://www.stm-assoc.org/copyright-legal-affairs/permissions/permissions-guidelines/), and does not apply for editions in other languages unless additional translation rights have been granted separately in the licence.

7. Rights for additional components such as custom editions and derivatives require additional permission and may be subject to an additional fee. Please apply to Journalpermissions@springernature.com/bookpermissions@springernature.com for these rights.

8. The Licensor's permission must be acknowledged next to the licensed material in print. In electronic form, this acknowledgement must be visible at the same time as the figures/tables/illustrations or abstract, and must be hyperlinked to the journal/book's homepage. Our required acknowledgement format is in the Appendix below.

9. Use of the material for incidental promotional use, minor editing privileges (this does not include cropping, adapting, omitting material or any other changes that affect the meaning,

intention or moral rights of the author) and copies for the disabled are permitted under this licence.

10. Minor adaptations of single figures (changes of format, colour and style) do not require the Licensor's approval. However, the adaptation should be credited as shown in Appendix below.

Appendix — Acknowledgements:

For Journal Content:
Reprinted by permission from [**the Licensor**]: [**Journal Publisher** (e.g. Nature/Springer/Palgrave)] [**JOURNAL NAME**] [**REFERENCE CITATION** (Article name, Author(s) Name), [**COPYRIGHT**] (year of publication)

For **Advance Online Publication papers:**
Reprinted by permission from [**the Licensor**]: [**Journal Publisher** (e.g. Nature/Springer/Palgrave)] [**JOURNAL NAME**] [**REFERENCE CITATION** (Article name, Author(s) Name), [**COPYRIGHT**] (year of publication), advance online publication, day month year (doi: 10.1038/sj.[JOURNAL ACRONYM].)

For Adaptations/Translations:
Adapted/Translated by permission from [**the Licensor**]: [**Journal Publisher** (e.g. Nature/Springer/Palgrave)] [**JOURNAL NAME**] [**REFERENCE CITATION** (Article name, Author(s) Name), [**COPYRIGHT**] (year of publication)

Note: For any republication from the British Journal of Cancer, the following credit line style applies:

Reprinted/adapted/translated by permission from [**the Licensor**]: on behalf of Cancer Research UK: : [**Journal Publisher** (e.g. Nature/Springer/Palgrave)] [**JOURNAL NAME**] [**REFERENCE CITATION** (Article name, Author(s) Name), [**COPYRIGHT]** (year of publication)

For **Advance Online Publication** papers:
Reprinted by permission from The [**the Licensor**]: on behalf of Cancer Research UK: [**Journal Publisher** (e.g. Nature/Springer/Palgrave)] [**JOURNAL NAME**] [**REFERENCE CITATION** (Article name, Author(s) Name), [**COPYRIGHT**] (year of publication), advance online publication, day month year (doi: 10.1038/sj.[JOURNAL ACRONYM])

For Book content:
Reprinted/adapted by permission from [**the Licensor**]: [**Book Publisher** (e.g. Palgrave Macmillan, Springer etc) [**Book Title**] by [**Book author**(s)] [**COPYRIGHT**] (year of publication)

Other Conditions:

Version 1.0

ELSEVIER LICENSE
TERMS AND CONDITIONS

Feb 27, 2018

This Agreement between Kevin J Kruse ("You") and Elsevier ("Elsevier") consists of your license details and the terms and conditions provided by Elsevier and Copyright Clearance Center.

License Number	4297231177575
License date	Feb 27, 2018
Licensed Content Publisher	Elsevier
Licensed Content Publication	Current Biology
Licensed Content Title	Fluid Shear Stress on Endothelial Cells Modulates Mechanical Tension across VE-Cadherin and PECAM-1
Licensed Content Author	Daniel E. Conway,Mark T. Breckenridge,Elizabeth Hinde,Enrico Gratton,Christopher S. Chen,Martin A. Schwartz
Licensed Content Date	Jun 3, 2013
Licensed Content Volume	23
Licensed Content Issue	11
Licensed Content Pages	7
Start Page	1024
End Page	1030
Type of Use	reuse in a thesis/dissertation
Intended publisher of new work	other
Portion	figures/tables/illustrations
Number of figures/tables /illustrations	1
Format	print
Are you the author of this Elsevier article?	No
Will you be translating?	No
Original figure numbers	1A
Title of your thesis/dissertation	N-Cadherin Juxtacrine Signaling Regulates the Endothelial Barrier
Expected completion date	May 2018
Estimated size (number of pages)	160
Requestor Location	Kevin J Kruse 835 S Wolcott Ave MSB E403 CHICAGO, IL 60612 United States

	Attn: Kevin J Kruse
Publisher Tax ID	98-0397604
Total	0.00 USD

Terms and Conditions

INTRODUCTION

1. The publisher for this copyrighted material is Elsevier. By clicking "accept" in connection with completing this licensing transaction, you agree that the following terms and conditions apply to this transaction (along with the Billing and Payment terms and conditions established by Copyright Clearance Center, Inc. ("CCC"), at the time that you opened your Rightslink account and that are available at any time at http://myaccount.copyright.com).

GENERAL TERMS

2. Elsevier hereby grants you permission to reproduce the aforementioned material subject to the terms and conditions indicated.

3. Acknowledgement: If any part of the material to be used (for example, figures) has appeared in our publication with credit or acknowledgement to another source, permission must also be sought from that source. If such permission is not obtained then that material may not be included in your publication/copies. Suitable acknowledgement to the source must be made, either as a footnote or in a reference list at the end of your publication, as follows:

"Reprinted from Publication title, Vol /edition number, Author(s), Title of article / title of chapter, Pages No., Copyright (Year), with permission from Elsevier [OR APPLICABLE SOCIETY COPYRIGHT OWNER]." Also Lancet special credit - "Reprinted from The Lancet, Vol. number, Author(s), Title of article, Pages No., Copyright (Year), with permission from Elsevier."

4. Reproduction of this material is confined to the purpose and/or media for which permission is hereby given.

5. Altering/Modifying Material: Not Permitted. However figures and illustrations may be altered/adapted minimally to serve your work. Any other abbreviations, additions, deletions and/or any other alterations shall be made only with prior written authorization of Elsevier Ltd. (Please contact Elsevier at permissions@elsevier.com). No modifications can be made to any Lancet figures/tables and they must be reproduced in full.

6. If the permission fee for the requested use of our material is waived in this instance, please be advised that your future requests for Elsevier materials may attract a fee.

7. Reservation of Rights: Publisher reserves all rights not specifically granted in the combination of (i) the license details provided by you and accepted in the course of this licensing transaction, (ii) these terms and conditions and (iii) CCC's Billing and Payment terms and conditions.

8. License Contingent Upon Payment: While you may exercise the rights licensed immediately upon issuance of the license at the end of the licensing process for the transaction, provided that you have disclosed complete and accurate details of your proposed use, no license is finally effective unless and until full payment is received from you (either by publisher or by CCC) as provided in CCC's Billing and Payment terms and conditions. If full payment is not received on a timely basis, then any license preliminarily granted shall be deemed automatically revoked and shall be void as if never granted. Further, in the event that you breach any of these terms and conditions or any of CCC's Billing and Payment

terms and conditions, the license is automatically revoked and shall be void as if never granted. Use of materials as described in a revoked license, as well as any use of the materials beyond the scope of an unrevoked license, may constitute copyright infringement and publisher reserves the right to take any and all action to protect its copyright in the materials.

9. Warranties: Publisher makes no representations or warranties with respect to the licensed material.

10. Indemnity: You hereby indemnify and agree to hold harmless publisher and CCC, and their respective officers, directors, employees and agents, from and against any and all claims arising out of your use of the licensed material other than as specifically authorized pursuant to this license.

11. No Transfer of License: This license is personal to you and may not be sublicensed, assigned, or transferred by you to any other person without publisher's written permission.

12. No Amendment Except in Writing: This license may not be amended except in a writing signed by both parties (or, in the case of publisher, by CCC on publisher's behalf).

13. Objection to Contrary Terms: Publisher hereby objects to any terms contained in any purchase order, acknowledgment, check endorsement or other writing prepared by you, which terms are inconsistent with these terms and conditions or CCC's Billing and Payment terms and conditions. These terms and conditions, together with CCC's Billing and Payment terms and conditions (which are incorporated herein), comprise the entire agreement between you and publisher (and CCC) concerning this licensing transaction. In the event of any conflict between your obligations established by these terms and conditions and those established by CCC's Billing and Payment terms and conditions, these terms and conditions shall control.

14. Revocation: Elsevier or Copyright Clearance Center may deny the permissions described in this License at their sole discretion, for any reason or no reason, with a full refund payable to you. Notice of such denial will be made using the contact information provided by you. Failure to receive such notice will not alter or invalidate the denial. In no event will Elsevier or Copyright Clearance Center be responsible or liable for any costs, expenses or damage incurred by you as a result of a denial of your permission request, other than a refund of the amount(s) paid by you to Elsevier and/or Copyright Clearance Center for denied permissions.

LIMITED LICENSE

The following terms and conditions apply only to specific license types:

15. **Translation**: This permission is granted for non-exclusive world **English** rights only unless your license was granted for translation rights. If you licensed translation rights you may only translate this content into the languages you requested. A professional translator must perform all translations and reproduce the content word for word preserving the integrity of the article.

16. **Posting licensed content on any Website**: The following terms and conditions apply as follows: Licensing material from an Elsevier journal: All content posted to the web site must maintain the copyright information line on the bottom of each image; A hyper-text must be included to the Homepage of the journal from which you are licensing at http://www.sciencedirect.com/science/journal/xxxxx or the Elsevier homepage for books at http://www.elsevier.com; Central Storage: This license does not include permission for a scanned version of the material to be stored in a central repository such as that provided by Heron/XanEdu.

Licensing material from an Elsevier book: A hyper-text link must be included to the Elsevier homepage at http://www.elsevier.com . All content posted to the web site must maintain the copyright information line on the bottom of each image.

Posting licensed content on Electronic reserve: In addition to the above the following clauses are applicable: The web site must be password-protected and made available only to bona fide students registered on a relevant course. This permission is granted for 1 year only. You may obtain a new license for future website posting.
17. **For journal authors:** the following clauses are applicable in addition to the above:
Preprints:
A preprint is an author's own write-up of research results and analysis, it has not been peer-reviewed, nor has it had any other value added to it by a publisher (such as formatting, copyright, technical enhancement etc.).
Authors can share their preprints anywhere at any time. Preprints should not be added to or enhanced in any way in order to appear more like, or to substitute for, the final versions of articles however authors can update their preprints on arXiv or RePEc with their Accepted Author Manuscript (see below).
If accepted for publication, we encourage authors to link from the preprint to their formal publication via its DOI. Millions of researchers have access to the formal publications on ScienceDirect, and so links will help users to find, access, cite and use the best available version. Please note that Cell Press, The Lancet and some society-owned have different preprint policies. Information on these policies is available on the journal homepage.
Accepted Author Manuscripts: An accepted author manuscript is the manuscript of an article that has been accepted for publication and which typically includes author-incorporated changes suggested during submission, peer review and editor-author communications.
Authors can share their accepted author manuscript:

- immediately
  - via their non-commercial person homepage or blog
  - by updating a preprint in arXiv or RePEc with the accepted manuscript
  - via their research institute or institutional repository for internal institutional uses or as part of an invitation-only research collaboration work-group
  - directly by providing copies to their students or to research collaborators for their personal use
  - for private scholarly sharing as part of an invitation-only work group on commercial sites with which Elsevier has an agreement
- After the embargo period
  - via non-commercial hosting platforms such as their institutional repository
  - via commercial sites with which Elsevier has an agreement

In all cases accepted manuscripts should:

- link to the formal publication via its DOI
- bear a CC-BY-NC-ND license - this is easy to do
- if aggregated with other manuscripts, for example in a repository or other site, be shared in alignment with our hosting policy not be added to or enhanced in any way to appear more like, or to substitute for, the published journal article.

Published journal article (JPA): A published journal article (PJA) is the definitive final record of published research that appears or will appear in the journal and embodies all value-adding publishing activities including peer review co-ordination, copy-editing, formatting, (if relevant) pagination and online enrichment.
Policies for sharing publishing journal articles differ for subscription and gold open access articles:
Subscription Articles: If you are an author, please share a link to your article rather than the full-text. Millions of researchers have access to the formal publications on ScienceDirect, and so links will help your users to find, access, cite, and use the best available version.
Theses and dissertations which contain embedded PJAs as part of the formal submission can be posted publicly by the awarding institution with DOI links back to the formal publications on ScienceDirect.
If you are affiliated with a library that subscribes to ScienceDirect you have additional private sharing rights for others' research accessed under that agreement. This includes use for classroom teaching and internal training at the institution (including use in course packs and courseware programs), and inclusion of the article for grant funding purposes.
Gold Open Access Articles: May be shared according to the author-selected end-user license and should contain a CrossMark logo, the end user license, and a DOI link to the formal publication on ScienceDirect.
Please refer to Elsevier's posting policy for further information.
18. **For book authors** the following clauses are applicable in addition to the above:
Authors are permitted to place a brief summary of their work online only. You are not allowed to download and post the published electronic version of your chapter, nor may you scan the printed edition to create an electronic version. **Posting to a repository:** Authors are permitted to post a summary of their chapter only in their institution's repository.
19. **Thesis/Dissertation**: If your license is for use in a thesis/dissertation your thesis may be submitted to your institution in either print or electronic form. Should your thesis be published commercially, please reapply for permission. These requirements include permission for the Library and Archives of Canada to supply single copies, on demand, of the complete thesis and include permission for Proquest/UMI to supply single copies, on demand, of the complete thesis. Should your thesis be published commercially, please reapply for permission. Theses and dissertations which contain embedded PJAs as part of the formal submission can be posted publicly by the awarding institution with DOI links back to the formal publications on ScienceDirect.

Elsevier Open Access Terms and Conditions
You can publish open access with Elsevier in hundreds of open access journals or in nearly 2000 established subscription journals that support open access publishing. Permitted third party re-use of these open access articles is defined by the author's choice of Creative Commons user license. See our open access license policy for more information.
Terms & Conditions applicable to all Open Access articles published with Elsevier:
Any reuse of the article must not represent the author as endorsing the adaptation of the article nor should the article be modified in such a way as to damage the author's honour or reputation. If any changes have been made, such changes must be clearly indicated.
The author(s) must be appropriately credited and we ask that you include the end user license and a DOI link to the formal publication on ScienceDirect.
If any part of the material to be used (for example, figures) has appeared in our publication

with credit or acknowledgement to another source it is the responsibility of the user to ensure their reuse complies with the terms and conditions determined by the rights holder.
Additional Terms & Conditions applicable to each Creative Commons user license:
CC BY: The CC-BY license allows users to copy, to create extracts, abstracts and new works from the Article, to alter and revise the Article and to make commercial use of the Article (including reuse and/or resale of the Article by commercial entities), provided the user gives appropriate credit (with a link to the formal publication through the relevant DOI), provides a link to the license, indicates if changes were made and the licensor is not represented as endorsing the use made of the work. The full details of the license are available at http://creativecommons.org/licenses/by/4.0.
CC BY NC SA: The CC BY-NC-SA license allows users to copy, to create extracts, abstracts and new works from the Article, to alter and revise the Article, provided this is not done for commercial purposes, and that the user gives appropriate credit (with a link to the formal publication through the relevant DOI), provides a link to the license, indicates if changes were made and the licensor is not represented as endorsing the use made of the work. Further, any new works must be made available on the same conditions. The full details of the license are available at http://creativecommons.org/licenses/by-nc-sa/4.0.
CC BY NC ND: The CC BY-NC-ND license allows users to copy and distribute the Article, provided this is not done for commercial purposes and further does not permit distribution of the Article if it is changed or edited in any way, and provided the user gives appropriate credit (with a link to the formal publication through the relevant DOI), provides a link to the license, and that the licensor is not represented as endorsing the use made of the work. The full details of the license are available at http://creativecommons.org/licenses/by-nc-nd/4.0.
Any commercial reuse of Open Access articles published with a CC BY NC SA or CC BY NC ND license requires permission from Elsevier and will be subject to a fee.
Commercial reuse includes:

- Associating advertising with the full text of the Article
- Charging fees for document delivery or access
- Article aggregation
- Systematic distribution via e-mail lists or share buttons

Posting or linking by commercial companies for use by customers of those companies.

20. **Other Conditions**:

v1.9

Questions? customercare@copyright.com or +1-855-239-3415 (toll free in the US) or +1-978-646-2777.